DOE/JPL-1060-58
(DE83011247)

PROCEEDINGS—FOURTH PARABOLIC DISH SOLAR THERMAL POWER PROGRAM REVIEW

November 30—December 2, 1982

February 1, 1983

Work Performed Under Contract No. AT04-80AL13137

California Institute of Technology
Jet Propulsion Laboratory
Pasadena, California

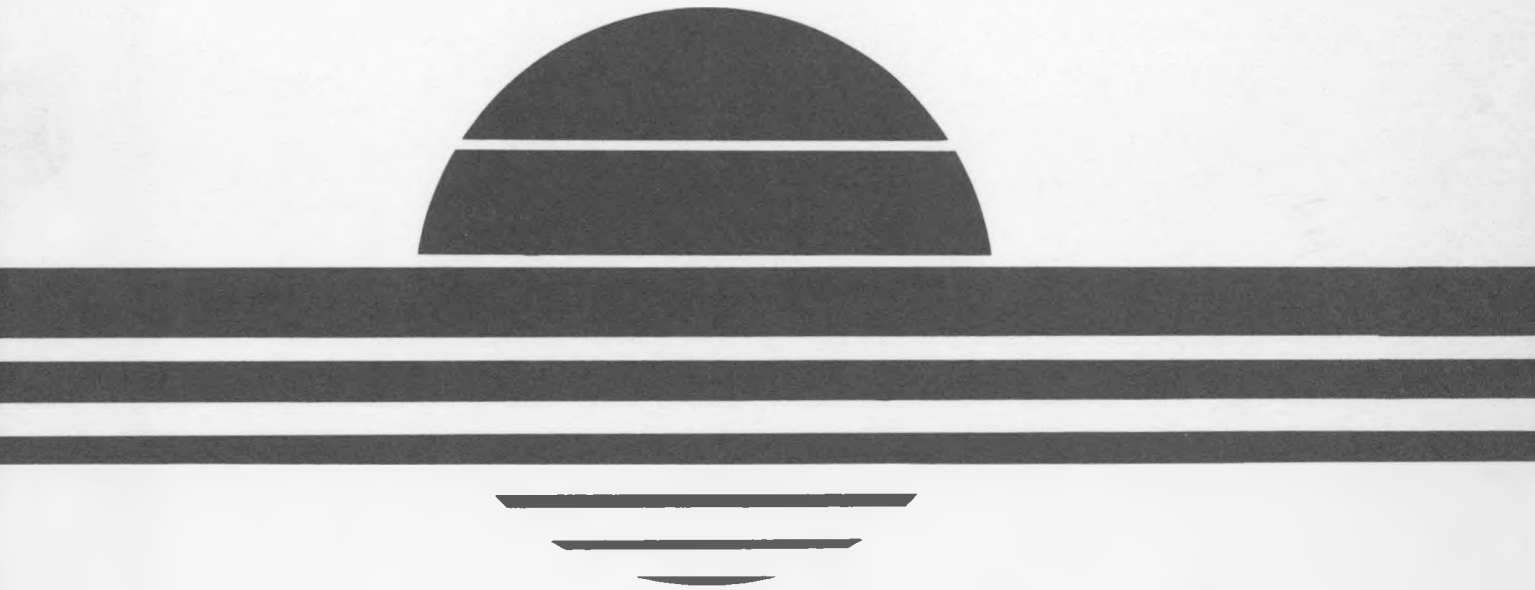

U.S. Department of Energy

Solar Energy

5105-122
Solar Thermal Power Systems Project
Parabolic Dish Systems Development

DOE/JPL--1060-58

DE83 011247

Proceedings, Fourth Parabolic-Dish Solar-Thermal Power Program Review

November 30 - December 2, 1982
Pasadena, California

February 1, 1983

Prepared for
U.S. Department of Energy
Through an Agreement with
National Aeronautics and Space Administration
by
Jet Propulsion Laboratory
California Institute of Technology
Pasadena, California

JPL Publication 83-2

ABSTRACT

The Fourth Parabolic Dish Solar Thermal Power Annual Program Review was held on November 30 - December 2, 1982, at the Huntington-Sheraton Hotel, Pasadena, California, under the sponsorship of the U.S. Department of Energy, and conducted by the Jet Propulsion Laboratory.

The primary objective of the Review was to present the results of activities within the Parabolic Dish Technology and Applications Development element of the Department of Energy's Solar Thermal Energy Systems Program. The Review consisted of 6 technical sessions, covering Stirling, Organic Rankine and Brayton module technologies, associated hardware and test results to date; concentrator development and progress; economic analyses; and current international dish development activities. Two panel discussions, concerning industry issues affecting solar thermal dish development and dish technology from a utility/user perspective, were also held.

These Proceedings contain the texts of presentations made at the Review, as submitted by their authors at the beginning of the Review; therefore, they may vary slightly from the actual presentations in the technical sessions.

ACKNOWLEDGMENT

This conference was conducted by the Jet Propulsion Laboratory and was sponsored by the U.S. Department of Energy through Interagency Agreement DE-AM04-80AL13137 (NASA/JPL TASK RE-152, Amendment No. 327).

Blank Page

CONTENTS

OPENING REMARKS

C. K. Stein - General Chairman

Jet Propulsion Laboratory

Pasadena, CA 91109

Good morning!

I'm very pleased to welcome you to the Department of Energy's Fourth Annual Review of the Parabolic Dish Solar Thermal Project.

I am Chuck Stein, JPL Parabolic Dish Project Technical Staff and General Chairman of this Review.

We are happy to see all of you in attendance and I think we have a very interesting and informative program for you over the next three days. It's also a very full program as you can see from the program in the abstract handout.

I'm sure by now you are very well aware that William R. Gould, Chairman of the Board of the Southern California Edison Company, is our luncheon speaker on Wednesday. As you may know, Southern California Edison is one of the largest investor-owned public utility companies and a leader in the development and support of alternate energy sources.

We also have two outstanding panels. Today's panel has been assembled by its moderator, John Wilson, Executive Director of the Renewable Energy Institute, which I'm sure he will describe this afternoon. His panel deals with industrial issues affecting solar thermal dish commercialization. His panelists include Gene Frankel, Science Consultant of the House Subcommittee on Energy Development, and Byron Washom, President of Advanco Corporation which is responsible for Dish-Stirling Development Projects. On the financial side, we have Ed Blum of Merrill-Lynch and Phil Huyck, Consultant to First Boston Financial, who are experts in small and large alternate energy financing; and Lee Goodwin, an attorney with Goodwin and Schwartzstein and a PURDA expert. Lee also supports the Renewable Energy Institute.

This morning we have Jim Rannels of DOE who will provide an overview of the DOE Program. Jim will be followed by a review of the Dish Project by Vince Truscello, JPL's Parabolic Dish Solar Thermal Project Manager.

Following a coffee break, we will have papers on the successful testing of the Stirling Module and its latest development plans.

After lunch, the Organic Rankine Module progress will be discussed including the recent testing and plans for its use in a small communities solar experiment.

After the aforementioned panel and before a reception, there will be a short "Solar Thermal Energy Association" (STEA) meeting that will be announced formally after lunch. The reception will be here in the Viennese Room Foyer starting about 45 minutes to an hour after the conclusion of the panel session.

Tomorrow, Wednesday, progress reports on the Dish-Brayton Module will be reviewed followed by a number of excellent progress reports on concentrators. We then have two economic papers leading to our second panel of experts, assembled with the support of Dave Martin, Applied Energy Research and Public Service Director, at the University of Kansas Center for Research. His panel on dish technology from a user/utility perspective should shed much light on our customers' needs. His panel includes: John Bigger, Electric Power Research Institute, better known as EPRI; Mark Anderson, Sacramento Municipal Utility District; John Stolpe, Southern California Edison, an investor owned utility, heavily involved in alternate energy; Peter Steitz from Burns and McConnell, consultants, architects and engineers, Kansas City, who perform energy studies and designs; and Bob Pottoff of the San Diego Gas and Electric, an investor-owned utility.

We also have an outstanding day planned for Thursday - starting with an International Dish System Development Session, followed by a visit to the Parabolic Dish Test Site in the Mojave Desert.

Advances in dish technology outside the United States will be discussed in our "formal session" Thursday morning from 8 to 10:15. We are very fortunate to have a broad representation of foreign participants including speakers from Switzerland, France, Israel, Australia and West Germany.

The specific topics and speakers are not listed in your handout; however, they will be posted later in the foyer.

Following the international session, we will be departing from the main entrance to the hotel on our field trip to view the Parabolic Dish Test Site and its ongoing activities located on the Edwards Air Force Base.

Although this field trip and lunch was included as part of the registration as well as the other two lunches and tonight's reception, you must indicate your intention to participate. A list of participants will be posted in the lobby later this afternoon. You also should have received a ticket in your registration package if you indicated that you planned to attend the field trip. If you have any questions, please let us know.

We will be publishing a proceedings which should be available approximately 60 days following the meeting. One copy is included in the registration fee. Additional copies are available at $20 each and can be ordered now at the registration desk.

Pat McLane is our Conference Coordinator here at JPL. She and her staff are located at the registration desk if you have any questions or problems.

In summary, we are delighted to see all of you here this morning and look forward to a very informative and productive three days.

And now it is my pleasure to introduce Jim Rannels, Program Manager from the Department of Energy. Jim -

DOE SOLAR THERMAL PROGRAM OVERVIEW

PRESENTED TO

FOURTH PARABOLIC DISH SOLAR THERMAL POWER ANNUAL REVIEW

DIVISION OF SOLAR THERMAL TECHNOLOGY

JAMES E. RANNELS

SOLAR THERMAL TECHNOLOGY

INTRODUCTION

OBJECTIVE: TO PROVIDE TECHNICAL AND COST DATA FOR THE ENERGY R&D AND MANUFACTURING INDUSTRIES TO DEVELOP SOLAR THERMAL TECHNOLOGIES TO A POINT WHERE MARKET FORCES DOMINATE THEIR DEVELOPMENT.

STATUS: PROGRAM HAS PURSUED RESEARCH IN EACH OF THE RELEVANT AREAS SPECIFIED BY AUTHORIZING LEGISLATION. SIGNIFICANT COST REDUCTIONS HAVE BEEN REALIZED IN TWO MAJOR SYSTEM TYPES (TROUGHS AND HELIOSTATS). ALTHOUGH ALL CONCEPTS HAVE FOLLOWED SIMILAR DEVELOPMENT PATHS, THEY ARE AT SOMEWHAT DIFFERENT LEVELS OF TECHNICAL MATURITY AND READINESS FOR COMMERCIALIZATION.

COST GOALS: ESTABLISHED AS FRAMEWORK TO PRIORITIZE AND EVALUATE PROPOSED R&D -

ELECTRICITY - 80-100 MILLS/kWh (1990 PROJECTIONS, IN 1980$)

HEAT - $5-7/MM BTU

SOLAR THERMAL TECHNOLOGY

AUTHORIZATION

P.L. 93-473 SOLAR ENERGY RESEARCH, DEVELOPMENT, AND DEMONSTRATION ACT OF 1974

SEC. 6.(c) THE SPECIFIC SOLAR ENERGY TECHNOLOGIES TO BE ADDRESSED OR DEALT WITHIN THE PROGRAM SHALL INCLUDE --

☑ (1) DIRECT SOLAR HEAT AS A SOURCE FOR INDUSTRIAL PROCESSES, INCLUDING THE UTILIZATION OF LOW-LEVEL HEAT FOR PROCESS AND OTHER INDUSTRIAL PURPOSES;

☑ (2) THERMAL ENERGY CONVERSION, AND OTHER METHODS, FOR THE GENERATION OF ELECTRICITY AND THE PRODUCTION OF CHEMICAL FUELS;

(3) THE CONVERSION OF CELLULOSE AND OTHER ORGANIC MATERIALS (INCLUDING WASTES) TO USEFUL ENERGY OR FUELS;

(4) PHOTOVOLTAIC AND OTHER DIRECT CONVERSION PROCESSES;

(5) SEA THERMAL GRADIENT CONVERSION;

(6) WINDPOWER CONVERSION;

(7) SOLAR HEATING AND COOLING OF HOUSING AND OF COMMERCIAL AND PUBLIC BUILDINGS; AND

(8) ENERGY STORAGE.

SOLAR THERMAL TECHNOLOGY

AUTHORIZATION (CONT'D.)

P.L. 93-473 SOLAR ENERGY RESEARCH, DEVELOPMENT, AND DEMONSTRATION ACT OF 1974

SEC. 7.(a) THE CHAIRMAN IS AUTHORIZED TO INITIATE A PROGRAM TO DESIGN AND CONSTRUCT, IN SPECIFIC SOLAR ENERGY TECHNOLOGIES (INCLUDING BUT NOT LIMITED TO, THOSE LISTED IN SECTION (6)(c), FACILITIES OR POWERPLANTS OF SUFFICIENT SIZE TO DEMONSTRATE THE TECHNICAL AND ECONOMIC FEASIBILITY OF UTILIZING THE VARIOUS FORMS OF SOLAR ENERGY. THE SPECIFIC GOALS OF SUCH PROGRAMS SHALL INCLUDE --

- ☑ (1) PRODUCTION OF ELECTRICITY FROM A NUMBER OF POWERPLANTS, ON THE ORDER OF ONE TO TEN MEGAWATTS EACH;
- ☑ (2) PRODUCTION OF SYNTHETIC FUELS IN COMMERCIAL QUANTITIES;
- ☑ (3) LARGE-SCALE UTILIZATION OF SOLAR ENERGY IN THE FORM OF DIRECT HEAT;
- ☑ (4) UTILIZATION OF THERMAL AND ALL OTHER BYPRODUCTS OF THE SOLAR FACILITIES;
- ☑ (5) DESIGN AND DEVELOPMENT OF HYBRID SYSTEMS INVOLVING THE CONCOMITANT UTILIZATION OF SOLAR AND OTHER ENERGY SOURCES; AND
- ☑ (6) THE CONTINUOUS OPERATION OF SUCH PLANTS AND FACILITIES FOR A PERIOD OF TIME.

SOLAR COLLECTOR TECHNOLOGIES AND HEAT APPLICATIONS

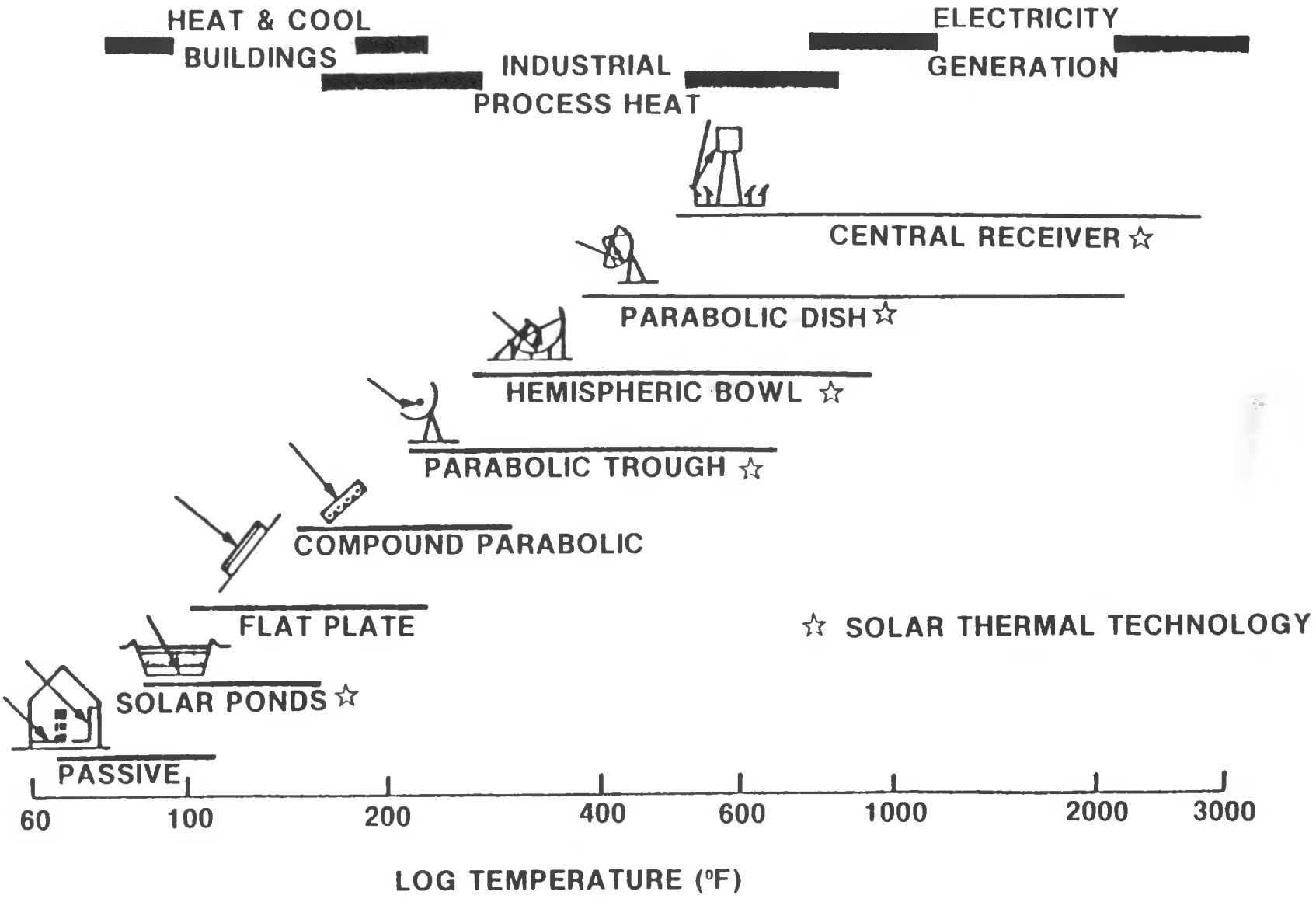

SOLAR THERMAL TECHNOLOGY ORGANIZATION CHART

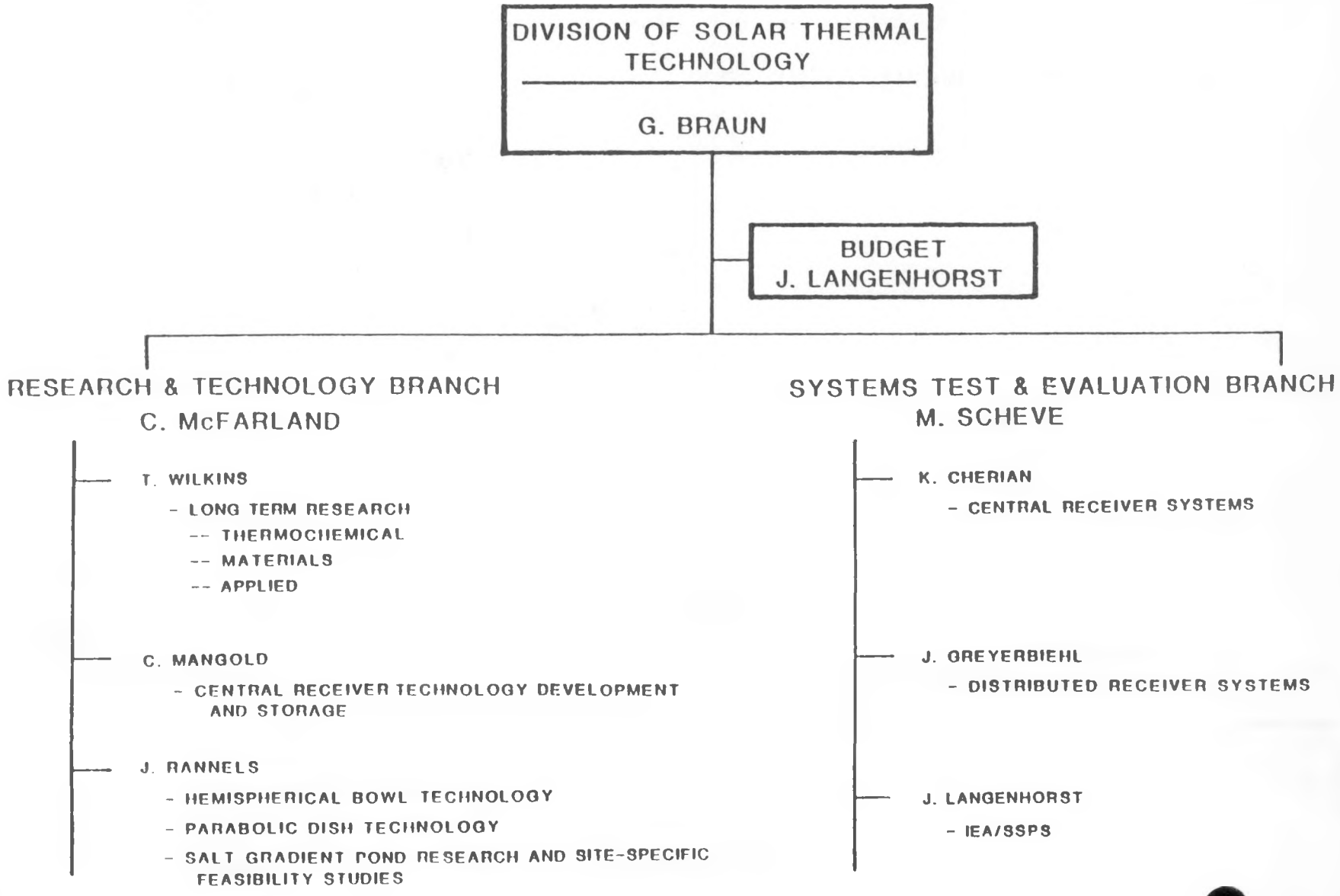

SOLAR THERMAL TECHNOLOGY

MAJOR PROGRAM ELEMENTS

- RESEARCH AND TECHNOLOGY DEVELOPMENT
  - MATERIALS DEVELOPMENT
  - APPLIED RESEARCH
  - CENTRAL RECEIVER TECHNOLOGY
  - PARABOLIC DISH TECHNOLOGY
  - HEMISPHERICAL BOWL TECHNOLOGY
  - SOLAR FUELS AND CHEMICALS
  - SOLAR SALT GRADIENT POND TECHNOLOGY

- SYSTEMS TEST AND EVALUATION
  - 10 MWe CENTRAL RECEIVER PILOT PLANT (BARSTOW, CA)
  - SOLAR TOTAL ENERGY PROJECT (SHENANDOAH, GA)
  - REPOWERING
  - DISTRIBUTED RECEIVER TECHNOLOGY
  - IEA SMALL SOLAR POWER SYSTEMS PROJECT (ALMERIA, SPAIN)

RESEARCH AND TECHNOLOGY

- MATERIALS
  - COMPLETED MATRIX APPROACH TO TESTING MIRRORS (MATM) REPORT DEALING WITH OPTICAL MATERIALS FOR MIRRORS. BEGAN TESTING SELECTED WINDOW MATERIALS (FUSED QUARTZ, VYCOR, PYREX, SAPPHIRE, VISTAL, IRTRAN 1/3/5, AND SPINEL)

- APPLIED RESEARCH
  - REDIRECTING PROGRAM TO CONCENTRATE ON POLYMER BASED CONCEPTS FOR ENCLOSURES AND PROTECTIVE COATINGS. CONDUCTING ENGINEERING TESTS OF GAS ENTRAINMENT REACTOR.

- CENTRAL RECEIVER TECHNOLOGY
  - CONSTRUCTING A COST SHARED SYSTEMS-LEVEL MOLTEN SALT EXPERIMENT WITH INDUSTRY AND UTILITIES. COMPLETED MOLTEN SALT STORAGE EXPERIMENT. COMPLETED SODIUM RECEIVER TEST AT THE CENTRAL RECEIVER TEST FACILITY.

RESEARCH AND TECHNOLOGY (CONT'D)

- PARABOLIC DISH TECHNOLOGY
  - OSAGE CITY, KANSAS SELECTED AS SITE FOR SMALL COMMUNITY EXPERIMENT. TESTING RANKINE AND STIRLING MODULES ON THE TEST BED CONCENTRATORS AT THE PARABOLIC DISH TEST SITE (PDTS). PREPARING SOLARIZED ADVANCED GAS TURBINE (SAGT-1) BRAYTON ENGINE FOR TEST AT PDTS. INITIATED EVALUATION OF THE PARABOLIC DISH CONCENTRATOR-1 (PDC-1) AT PDTS.

- HEMISPHERICAL BOWL TECHNOLOGY
  - FUTURE STATUS OF CROSBYTON PROJECT TO BE DETERMINED.

- FUELS AND CHEMICALS
  - REVIEW OF CANDIDATE CHEMICAL PROCESS APPLICATIONS AND TECHNOLOGY REQUIREMENTS IS UNDERWAY WITH EMPHASIS ON HYDROGEN. COMPLETED REQUEST FOR PROPOSAL FOR DIRECT FLUX SOLAR REACTOR STUDY. CONDUCTING SOLID REACTION ZINC SULFATE ($ZNSO_4$) TESTS AT WHITE SANDS SOLAR FURNACE.

- SALT GRADIENT PONDS
  - TEST TANK BUILT AT SERI FOR HEAT AND MASS EXTRACTION EXPERIMENTS. COMPLETED JOINT FEASIBILITY STUDY WITH ARMY CORPS OF ENGINEERS. PREPARING REPORT TO CONGRESS ON TRUSCOTT BRINE LAKE. INITIATED SALTON SEA PRELIMINARY DESIGN PHASE.

SOLAR THERMAL TECHNOLOGY

SYSTEMS TEST AND EVALUATION

- BARSTOW
  - PROJECT DEDICATED AND OPERATING AS EXPECTED. CONDUCTING EXPERIMENTAL TEST AND EVALUATION PHASE. PLANT USED FOR WEEKEND POWER BY SOUTHERN CALIFORNIA EDISON COMPANY.

- SHENANDOAH
  - PROJECT DEDICATED. ENTERING EXPERIMENTAL TEST AND OPERATIONS PHASE; PREPARING TO TRANSFER OWNERSHIP TO GEORGIA POWER COMPANY.

- REPOWERING
  - INITIATED FOUR PRELIMINARY DESIGNS FOR REPOWERING APPLICATIONS.

SOLAR THERMAL TECHNOLOGY

SYSTEMS TEST AND EVALUATION (CONT'D)

- DISTRIBUTED RECEIVER SYSTEMS
  - INITIATED OPERATION OF U.S. STEEL CHEMICAL, HOME LAUNDRY, AND CATERPILLAR TRACTOR IPH SYSTEMS. THREE IPH SYSTEM UPGRADES COMPLETED. FOURTH UPGRADE NEARING COMPLETION. TESTING MODULAR INDUSTRIAL RETROFIT-QUALIFICATION TEST SYSTEMS (MISR-QTS). COMPLETED TESTING OF PERFORMANCE PROTOTYPE TROUGH.

- IEA-SSPS
  - BOTH CENTRAL AND DISTRIBUTED SYSTEMS IN OPERATIONAL PHASE.

SOLAR THERMAL TECHNOLOGY

LIST OF PHOTOGRAPHS

FIGURE

1. Examples of stable (top) and unstable (bottom) black chrome plating for parabolic trough receiver tubes.

2. Design of entrainment reactor.

3. Martin Marietta molten salt receiver undergoing refurbishment for the Molten Salt Electric Experiment at the Central Receiver Test Facility (CRTF) - Albuquerque, New Mexico.

4. Artists concept of the Small Community Solar Thermal Experiment - Osage City, Kansas.

5. Organic Rankine and Stirling Power Conversion Units under test at the Parabolic Dish Test Site (PDTS)- Edwards AFB - California.

6. Hemispherical Bowl Solar Hybrid Project - Crosbyton, Texas.

7. White Sands Solar Furnace, New Mexico - Site of planned $ZnSO_4$ tests.

8. Solar salt gradient pond test tank experiment for heat and mass extraction at the Solar Energy Research Institute (SERI)

9. Proposed salt gradient pond sites - Great Salt Lake and Salton Sea.

10. Barstow 10MWe Power Plant - near Barstow, California

11. Shenandoah Total Energy Project - Shenandoah, Georgia.

12. Artist concept of proposed "Solar 100" central receiver project.

13. Industrial Process Heat Project at United States Steel Chemical - Haverhill, Ohio.

14. Modular Industrial Solar Retrofit - Qualification Test Systems (MISR-QTS) being installed at eht CRTF.

15. International Energy Agency (IEA) Project - Almeria, Spain.

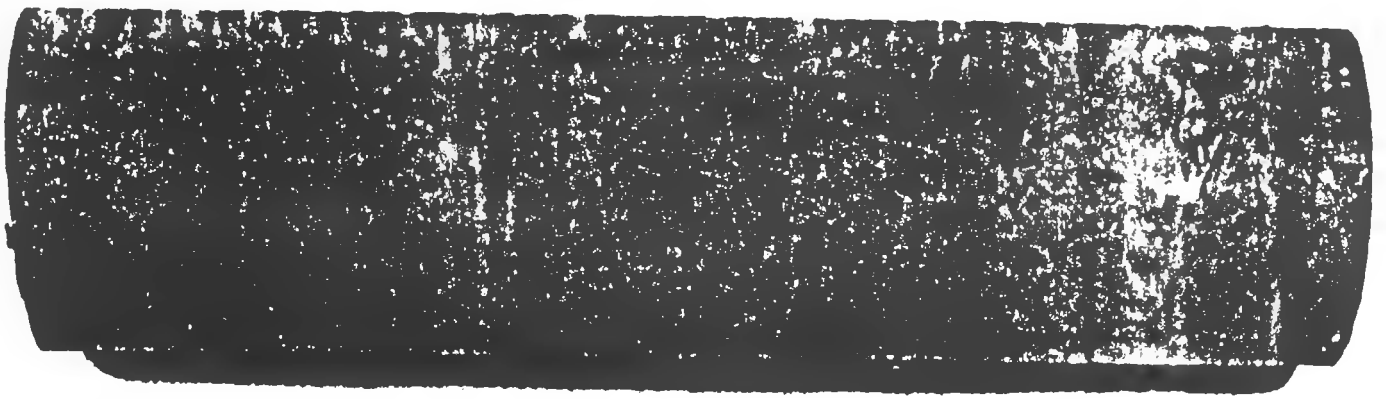

ENTRAINMENT REACTOR

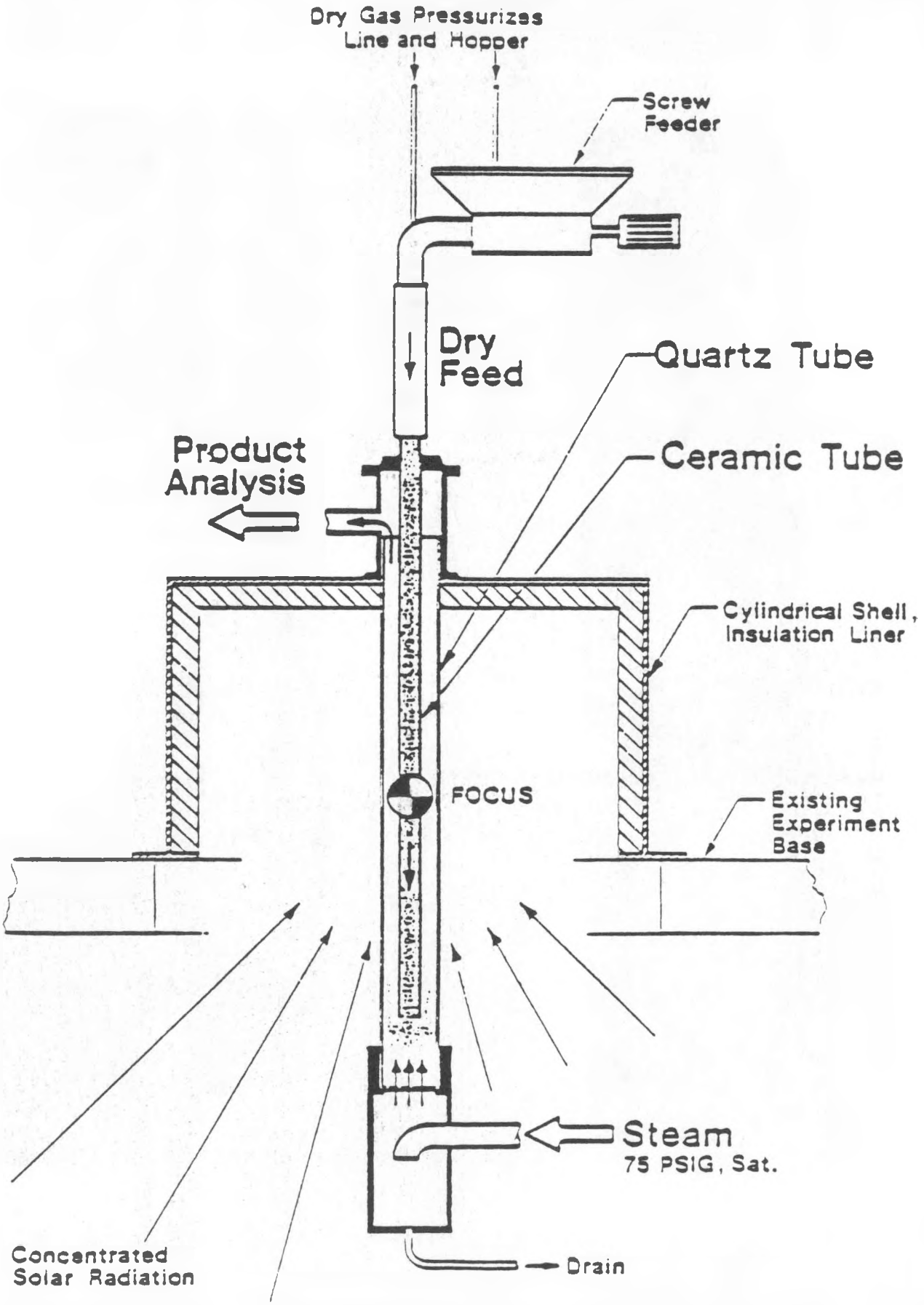

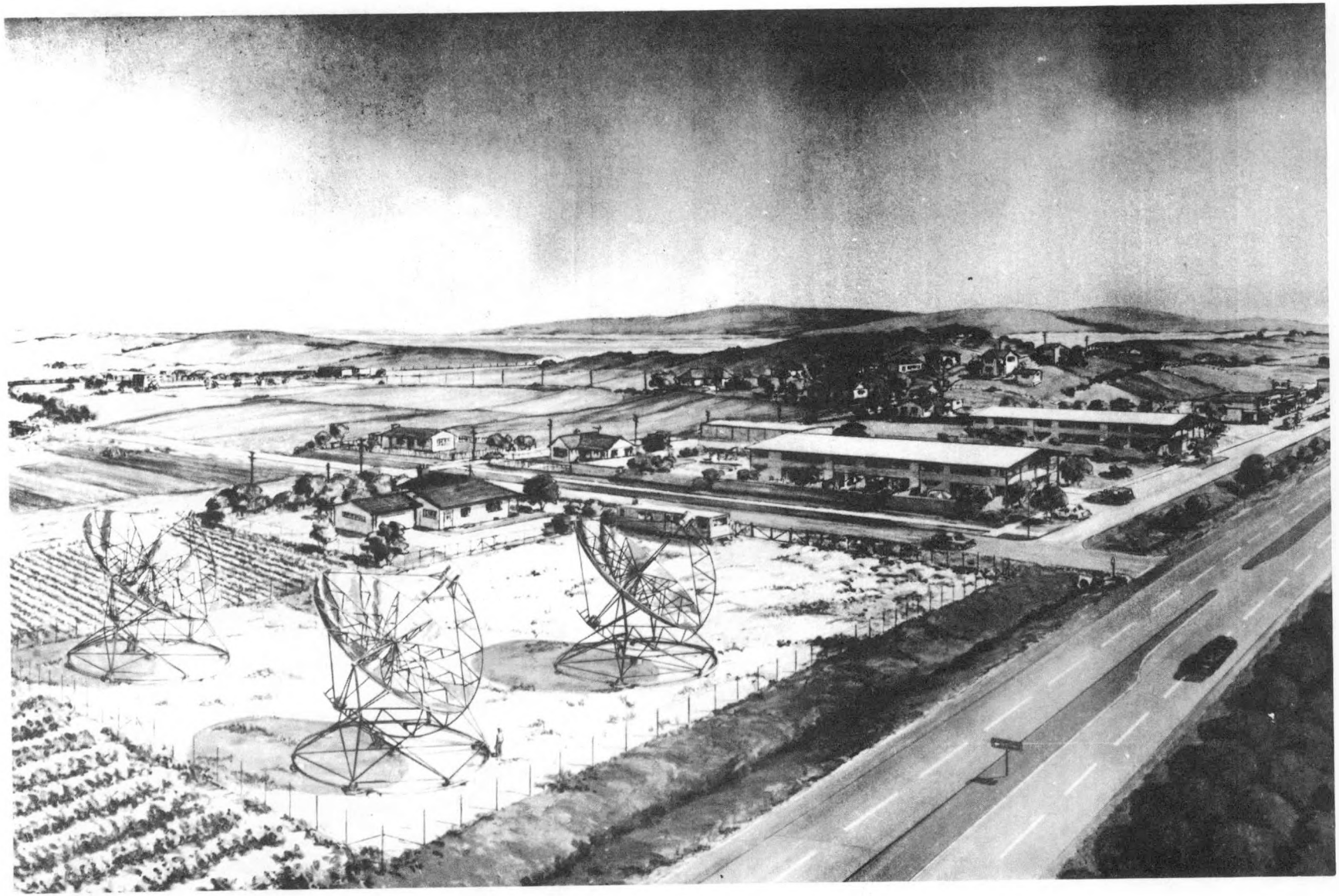

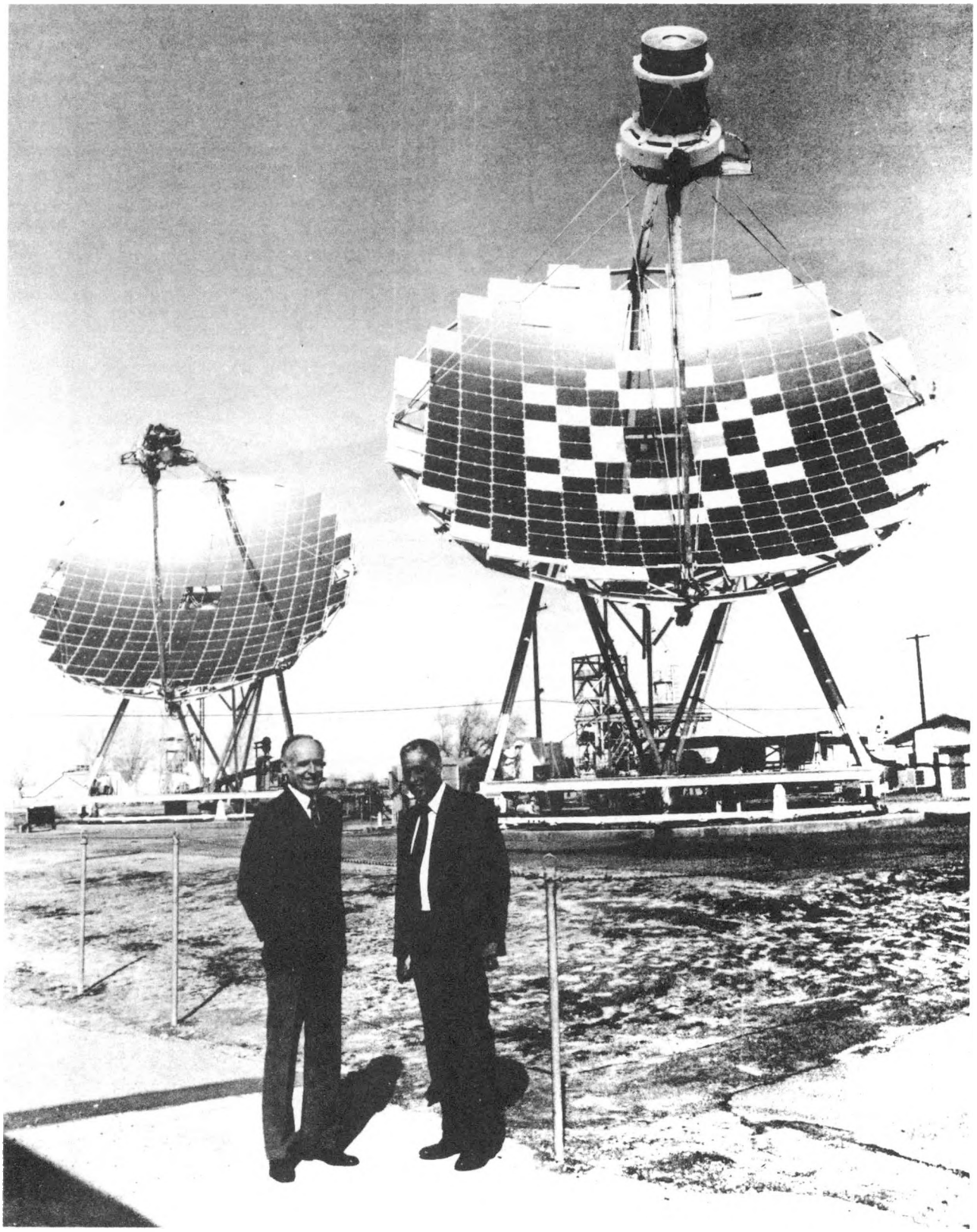


DANGER
DO NOT
ENTER

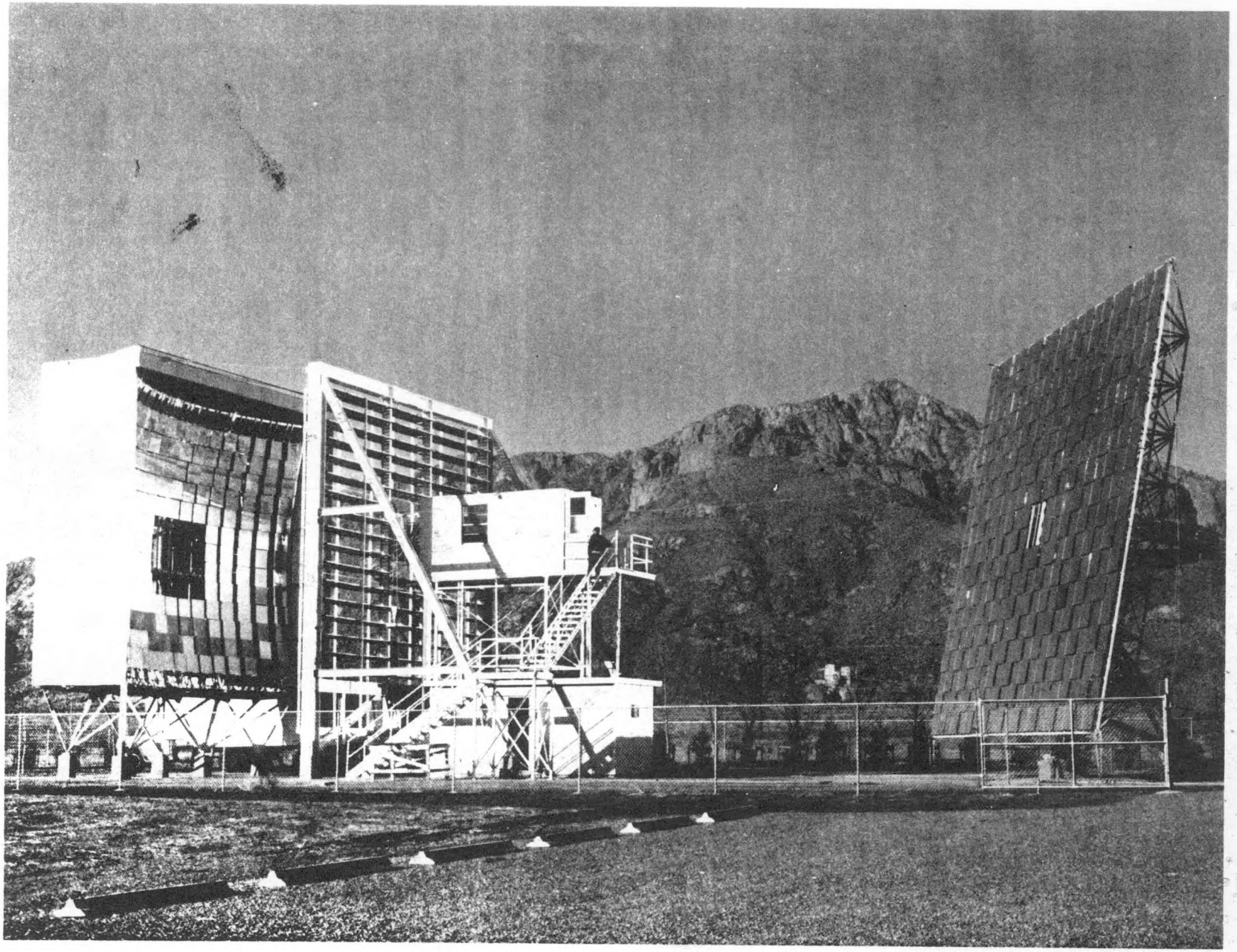

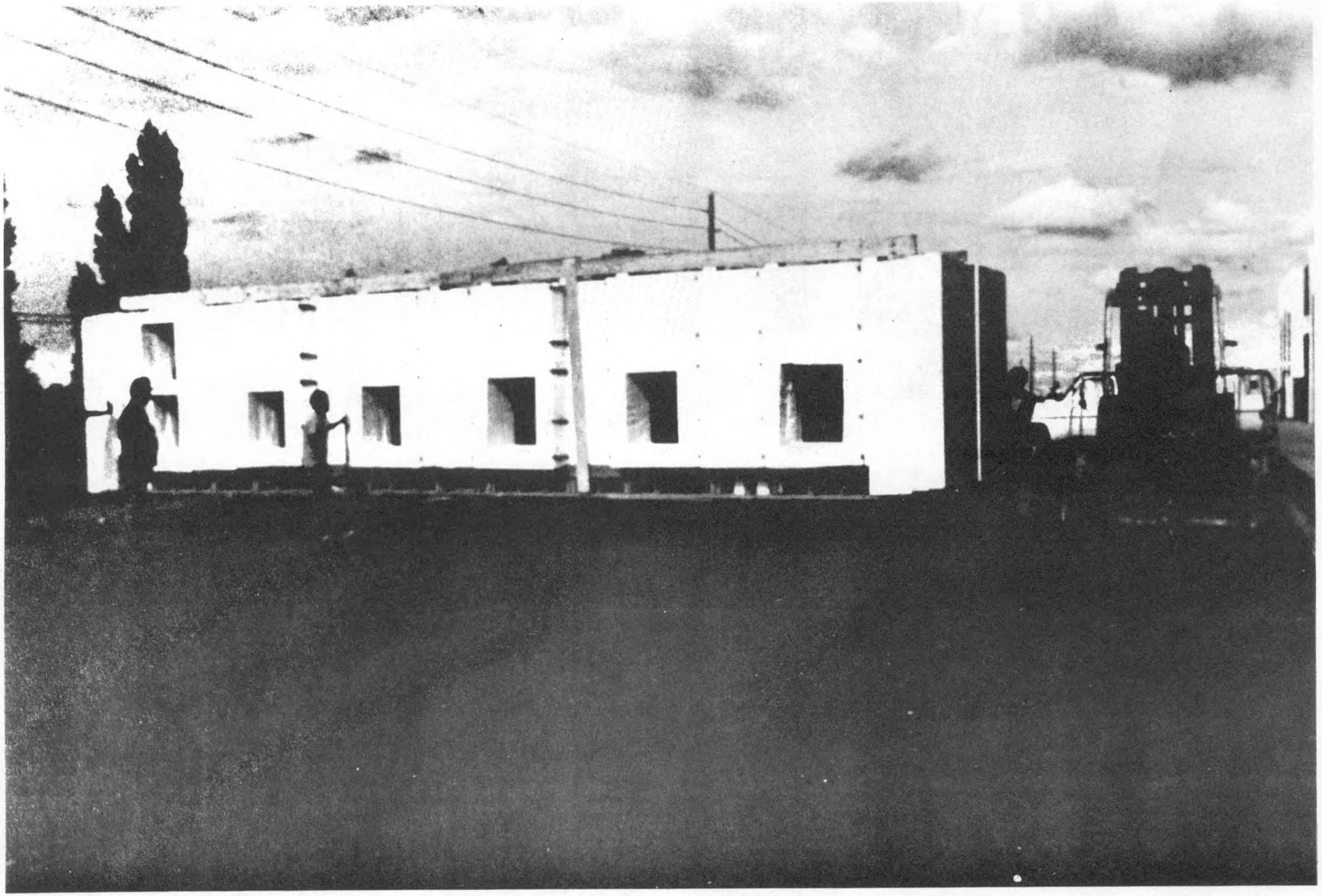

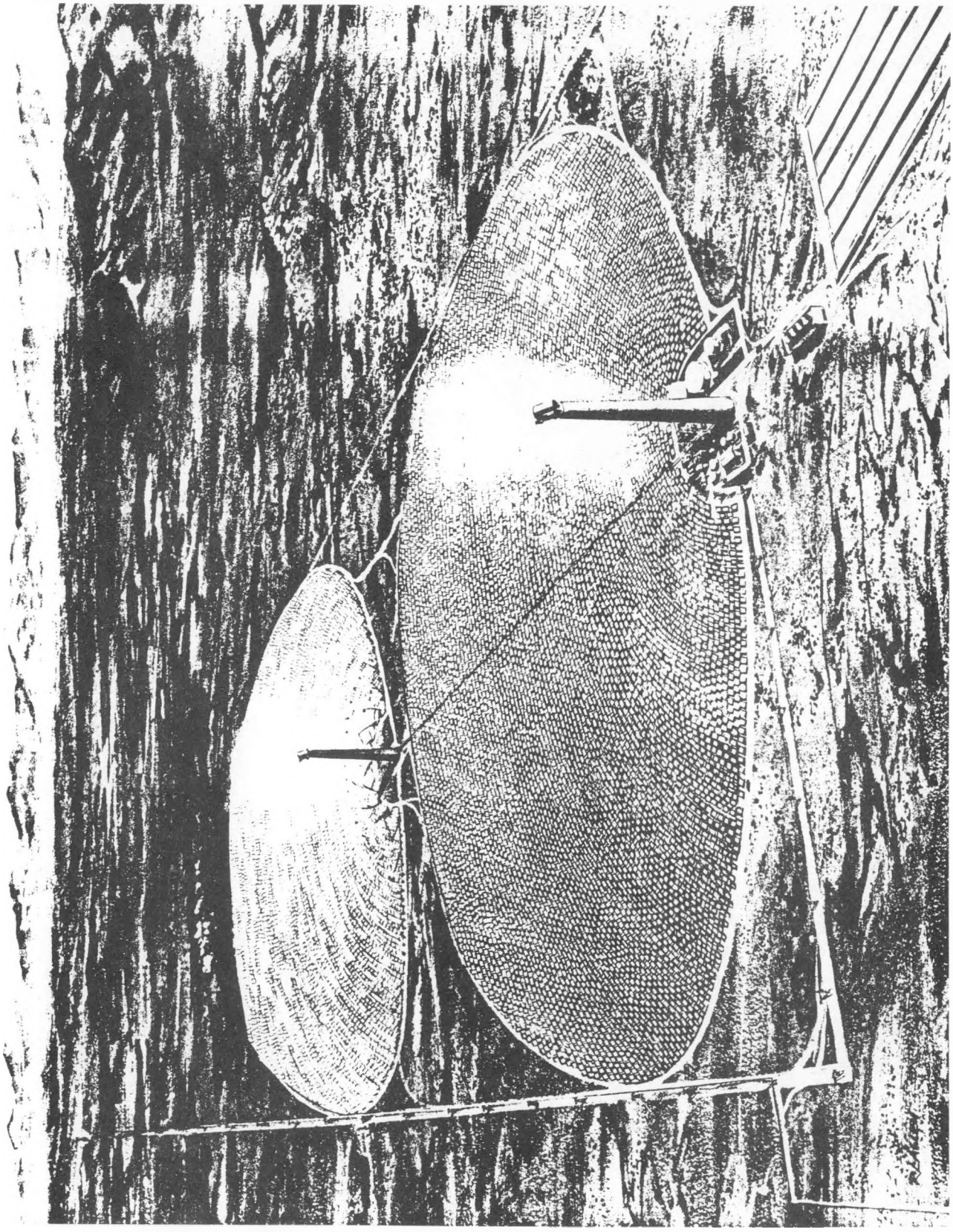

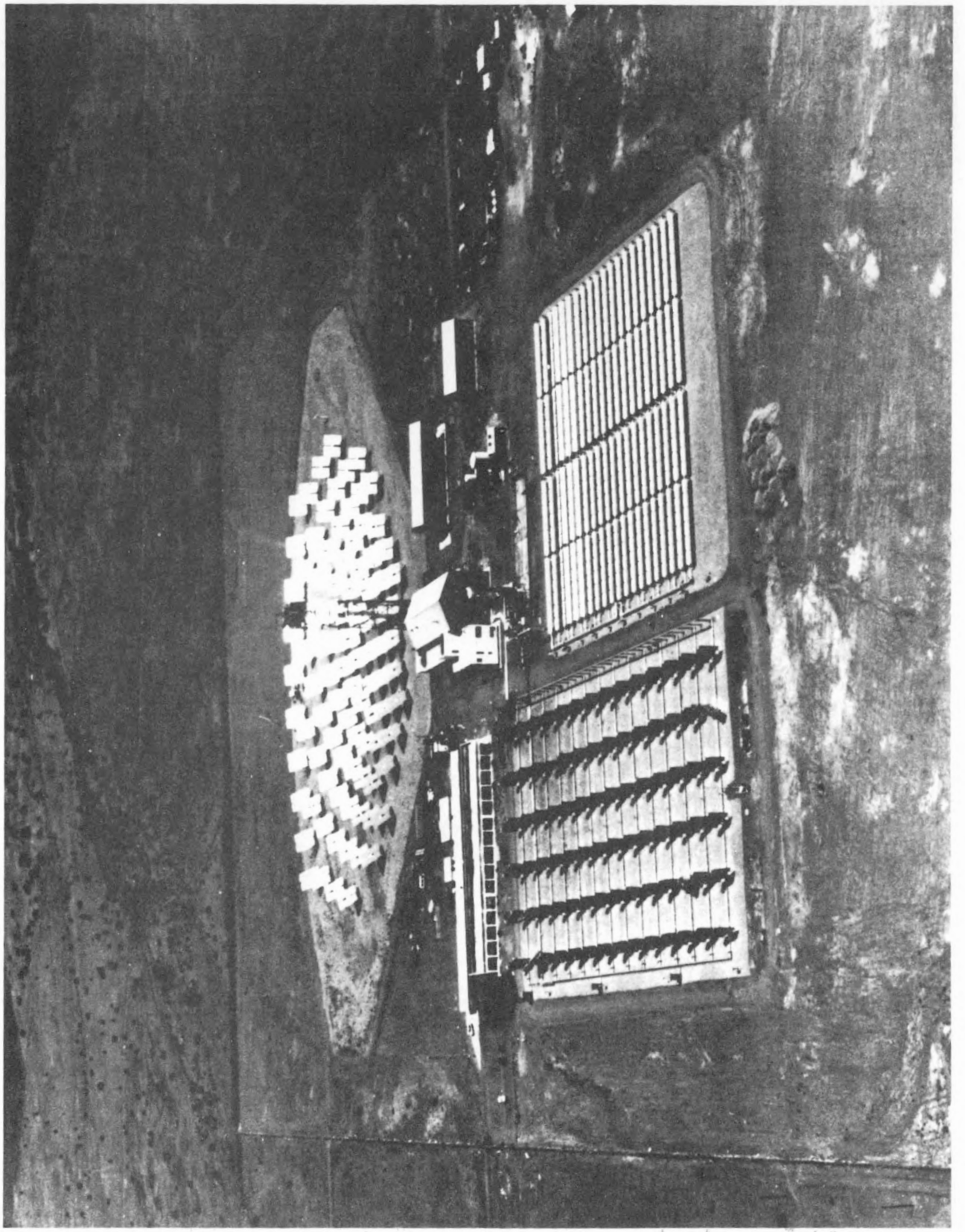

SOLAR THERMAL TECHNOLOGY

LONG-RANGE EMPHASIS

- THERMOCHEMICAL RESEARCH
  - FUEL PROCESSES
- CENTRAL RECEIVER TECHNOLOGY
  - HIGH-TEMPERATURE COMPONENTS
- MATERIALS RESEARCH
  - THERMAL MATERIALS RESEARCH
- CONCENTRATOR RESEARCH
  - LIGHTWEIGHT, LOW-COST CONCENTRATORS

SOLAR THERMAL TECHNOLOGY PROGRAM FUNDING

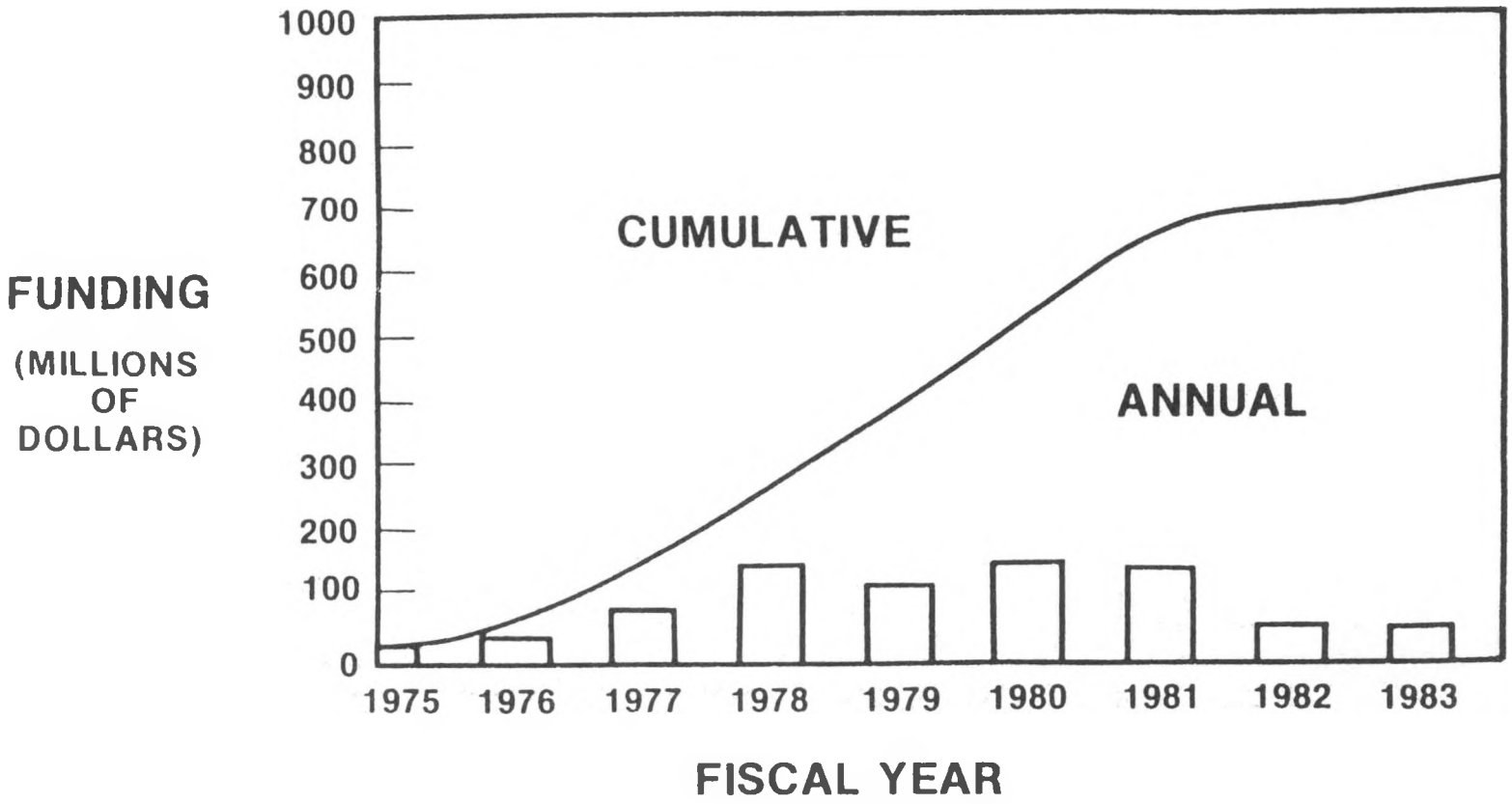

Blank Page

PARABOLIC DISH PROJECT
OVERVIEW

Vincent C. Truscello
Jet Propulsion Laboratory
Pasadena, CA 91109

1982 was one of significant hardware accomplishments for the parabolic dish-electric project. Two different heat engine technology modules provided the Southern California Edison Company (SCE) utility grid with electricity and the first pre-production parabolic dish concentrator was fabricated, assembled and is under test at the Parabolic Dish Test Site (PDTS) in California's Mojave Desert.

A number of Stirling cycle power conversion assembly (PCA) configurations operated at the focus of a parabolic test bed concentrator. One configuration using a hybrid receiver and a Stirling engine, successfully operated in both a hybrid and non-hybrid mode using solar and natural gas heat inputs. Three different versions of a receiver, using only solar energy, successfully operated with a Stirling engine on a test bed concentrator (TBC). Noteworthy accomplishments included a number of successive sunrise-to-sunset operation days that provided the SCE grid 20 kWe at a normalized solar insolation level of 1000 w/m^2. During one test, 25 kWe was generated by the PCA corresponding to a solar-to-electric conversion efficiency of nearly 30% (from sunlite incident on the concentrator to electricity out of the generator).

In response to a DOE Program Opportunity Notice (PON), a team of industrial and university contractors entered into a Cooperative Agreement with DOE to design, build and test a parabolic dish-Stirling module based on the above PCA.

An organic Rankine cycle (ORC) PCA consisting of a receiver, an ORC engine and an integral permanent magnet alternator (PMA), was operated on a TBC at the PDTS and produced nearly 16 kWe when the insolation level was 920 w/m^2. Throughout low, intermittent and high insolation levels, the ORC PCA operated smoothly and the control system performed flawlessly during engine start-up, operation, and shutdown; the PCA ran without incident during simulated and actual cloud passages. Work is continuing to improve the engine bearing design to meet long life objectives.

The unit tested is a prototype to a solar thermal electric generating system that will be combined with a parabolic dish concentrator and deployed in the field as an autonomous energy-producing module working in conjunction with other replicated modules.

A prototype parabolic dish concentrator called the PDC-1 was fabricated and erected at the PDTS during FY 1982. The 12 m (39 ft) dish was designed for ORC temperatures of about 400°C (750°F). Initial tests indicate that the performance of the PDC-1 may exceed design specifications.

The Brayton cycle FY 1982 effort, although greatly reduced in scope because of budget constraints, also provided significant hardware and system progress. An engine and receiver package using a solarized version of an automotive gas turbine has been fabricated and will be tested early in 1983.

Contractor trade studies recommended developing an early Brayton module using a small Brayton cycle subatmospheric gas turbine engine coupled to one of a number of independently developed small dishes for the 1980's. It further recommended an 11 m (36 ft) dish coupled to an engine developed from the production automobile engine program for the 1990's.

The Small Community Solar Experiment (SCSE) was initiated in 1977 when Congress appropriated funds to build an experimental solar power plant that would be a first step in addressing the needs of the small community sector. An organic Rankine cycle (ORC) based technology was selected for this experiment. In FY 1982, Congress appropriated $4.0 M to construct the experiment. During the course of the year DOE directed the construction of a 100 kWe plant, a size considered sufficiently large to satisfy most of the technical requirements of the experiment while meeting the intent of the Congress to minimize the cost. Concurrent with the development of the organic Rankine module, DOE has been involved in the selection of a site for the experiment. During FY 1982 DOE selected Osage City, Kansas, for the SCSE plant with Molokai, Hawaii, selected as the alternate site. This decision culminated the selection process in which 44 communities across the country competed.

Osage City is an ideal setting for the experiment because it is representative of a large number of small cities throughout the country. It has its own generation capability, but also purchases power when economically advantageous. Insolation at Osage City is about average for the nation. DOE has entered into negotiations with Osage City with the objective of signing a cooperative agreement in FY 1983 for site participation.

STIRLING MODULE COOPERATIVE AGREEMENT

(VANGUARD I)

BYRON WASHOM

ADVANCO CORPORATION

"This paper is based on work sponsored in part by the Department of Energy under Cooperative Agreement No. DE-FCO4-82AL16333."

1.0 EXECUTIVE SUMMARY

1.1 BACKGROUND

The report is a compilation of the results achieved by the Vanguard team during the performance of Task 1 of DOE cooperative agreement number DE-FC04-82AL16333. The objectives of the program performed under this agreement are to design, fabricate, and evaluate the performance of an autonomous solar parabolic dish-Stirling module suitable for sale in specific markets. The program consists of four tasks: Market Assessment and Conceptual Design, Detailed Design, Fabrication and Assembly, and Testing. Phase I of the program, comprising the first two tasks, commenced May 28, 1982, and is scheduled for completion on April 28, 1982. It is the goal of this program to successfully test the Vanguard Dish-Stirling Module and to independently engage the Vanguard team in the business of selling these modules in the specific markets identified in Section 2.1 of this report.

The Vanguard team organization is illustrated along with team member responsibilities in Figure 1.

Task 1 of this program consisted of three major activities: a privately funded market study to identify an early market for a dish-Stirling module and assess its commercial potential, preparation of a conceptual system and subsystem design to address this market, and preparation of an early sales implementation plan involving team corporate commitment. The main body of this report, Section 2, contains a detailed description of these activities and their results and is organized accordingly. Section 1 contains introductory material, a summary of major findings and conclusions, and the results of the first Utility Research Advisory Panel (URAP). Extremely detailed information supplementing several of the studies performed during Task 1 is contained in the appendices.

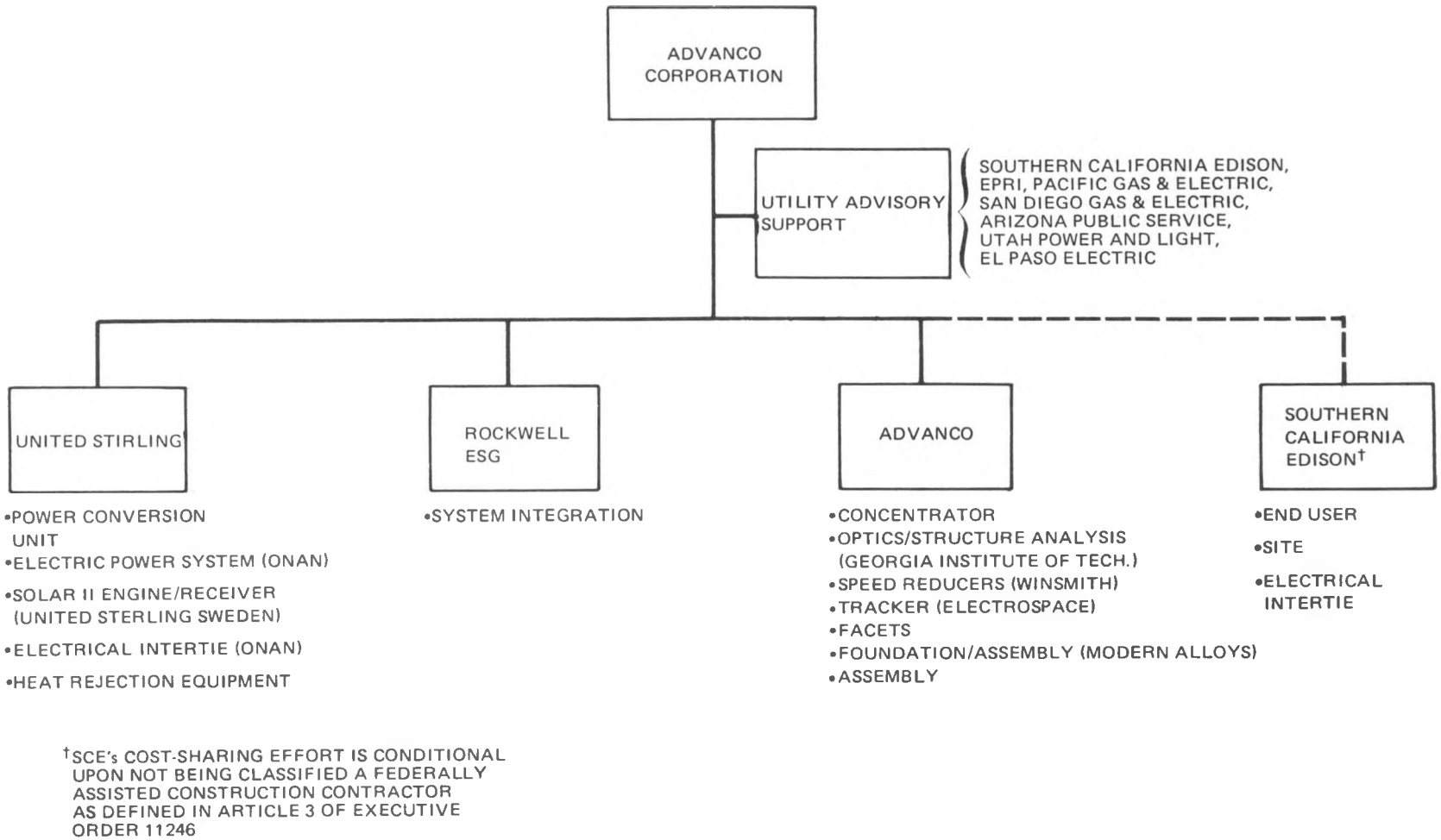

Figure 1. Vanguard Program Organization

1.2 MAJOR FINDINGS, CONCLUSIONS, AND DECISIONS

The 4-month conceptual design and market analysis period has resulted in a number of significant findings, conclusions, and decisions. Foremost among these are the following, determined by the Vanguard team:

- The pre-1986 period will be characterized as having a production limitation of approximately 1000 units. This market can be adequately generated by the utilization of federal and state energy tax credits through Limited Partnerships.

- The grid-connected, solar-only operation represents the most economical and opportunistic market for parabolic dish-Stirling systems in the pre-1986 market.

- The sales implementation plan should be accelerated to satisfy any possible future requirements regarding grandfathering of a project in regard to eligibility of the federal and state tax credits.

- The post-1986 market is extremely large and diverse if production costs can be lowered to $1,900/kW for a unit that produces 59,750 kWhe per year.

- A record conversion efficiency of 29.5% net solar energy to electricity from the July 1982 tests positively indicates that a Stirling engine coupled with a parabolic concentrator is technically ready for commercialization.

- The six critical issues identified in the proposal have been addressed, and significant progress has been made toward their resolution.

- The technical excellence of the Stirling engine/parabolic dish combination along with the inherent modularity of the technology are the key to early penetration of the selected markets.

- Significant system capital and lifetime cost savings over previous module designs will result from improvements in locating the heat rejection unit at the focal point, utilizing a conventional electricity collection and transmission system, using an optimum cluster sizing of 32 units based on O&M and controls, and modifying the hydrogen supply system to the Stirling engine.

- The induction generator selected for this module best matches the performance, cost and safety requirements for efficient conversion of Stirling engine torque to AC electrical output.

- Major progress has been made in solving the optical problems associated with the concentrator/receiver interface.

- Several inexpensive, simple methods have been identified to prevent the most severe accident (a solar image walk-off of the receiver) from occurring.

- Finally, the Vanguard team remains convinced that there are no major technical and few financial obstacles to the early commercialization of the Vanguard Module.

1.3 SUMMARY DATA

This section contains a selection of figures and tables from the main body of the report, Section 2, which taken as a whole gives a good overview of the report.

Table I illustrates the addressable market for parabolic dish power systems based on our assessment of insolation, avoided cost, and projected demands for electricity. Also shown in this table is our time-phased sales implementation goal.

TABLE I

PARABOLIC DISH POWER SYSTEM ADDRESSABLE MARKET
AND VANGUARD SALES IMPLEMENTATION PLAN

Pre-1986			Post-1985	
Market: Third Party Ownership and Operation with Direct Electricity Sales to Utilities			Domestic Market: Municipalities Military Bases, Utility Owned and Operated Foreign Market: Desalinization	
Year	Addressable Market	Sales Goal	Addressable Market	Sales Goal
1983	3	3		
1984	32	32		
1985	500	500		
1986			3,000	3,000
1987			8,000	6,000
1988			13,000	9,800
1989			19,000	14,300
1990			25,000	18,800
1995	and onward		≥50,000	≥37,500

Figure 2 is a histogram of Stirling engine/JPL Test Bed Concentrator performance for July 15, 1982, the day the Stirling engine set a record for overall net conversion efficiency of sunlight to electricity of over 29%.

Figure 3 is an arrangement drawing depicting the overall conceptual design of the Vanguard parabolic dish-Stirling module. The improvements made in this design over the design introduced in the proposal* are summarized in Table II.

*DE-PN04-81 AL16333, "Solar Parabolic Dish-Stirling Engine System Module - A Technical and Management Proposal to DOE Albuquerque," August 24, 1981, Advanco Corporation

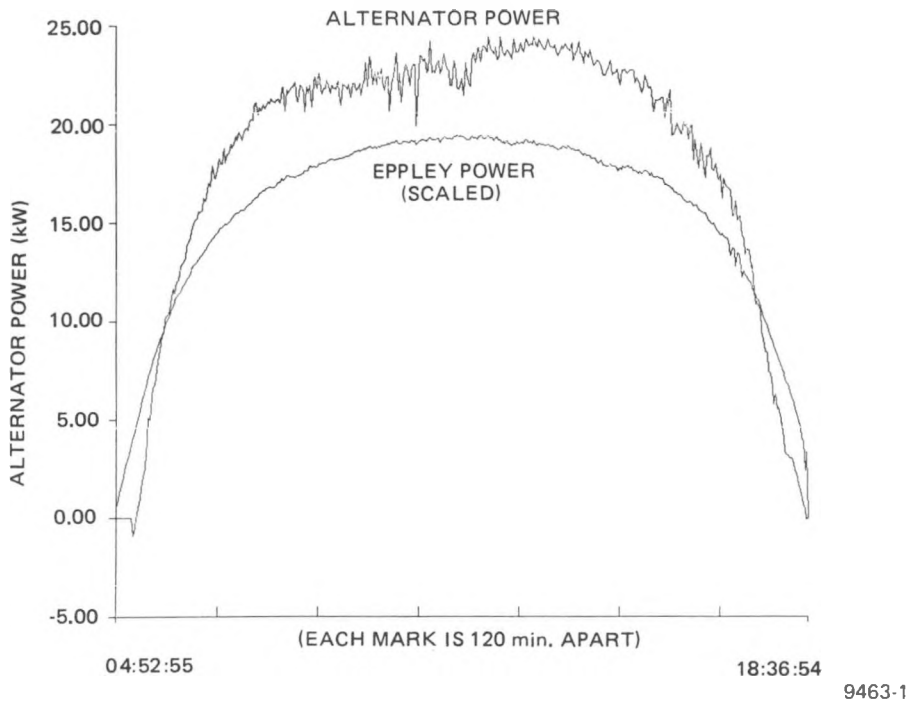

Figure 2. Insolation and Output of Record-Breaking Stirling Solar Power System - July 15, 1982

TABLE II

SUMMARY OF VANGUARD DESIGN IMPROVEMENTS

Improvement	Result
1. Drives mounted internally in gimbal	Improved drive reliability
2. Adoption of steel as dish structure	Decreased capital cost
3. Centralized hydrogen supply system	Decreased capital and O&M cost
4. Relocated waste heat radiator to dish focal area	Decreased capital cost, parasitic power, and improved reliability
5. Miscellaneous minor Stirling engine improvement	Decreased capital cost, improved reliability, increased engine life
6. Added walk-off protection	Reduced probability of accidental solar image walk-off
7. Rerouted utility and control cabling through gimbal	Increased life of cabling, reduction of cabling exposure

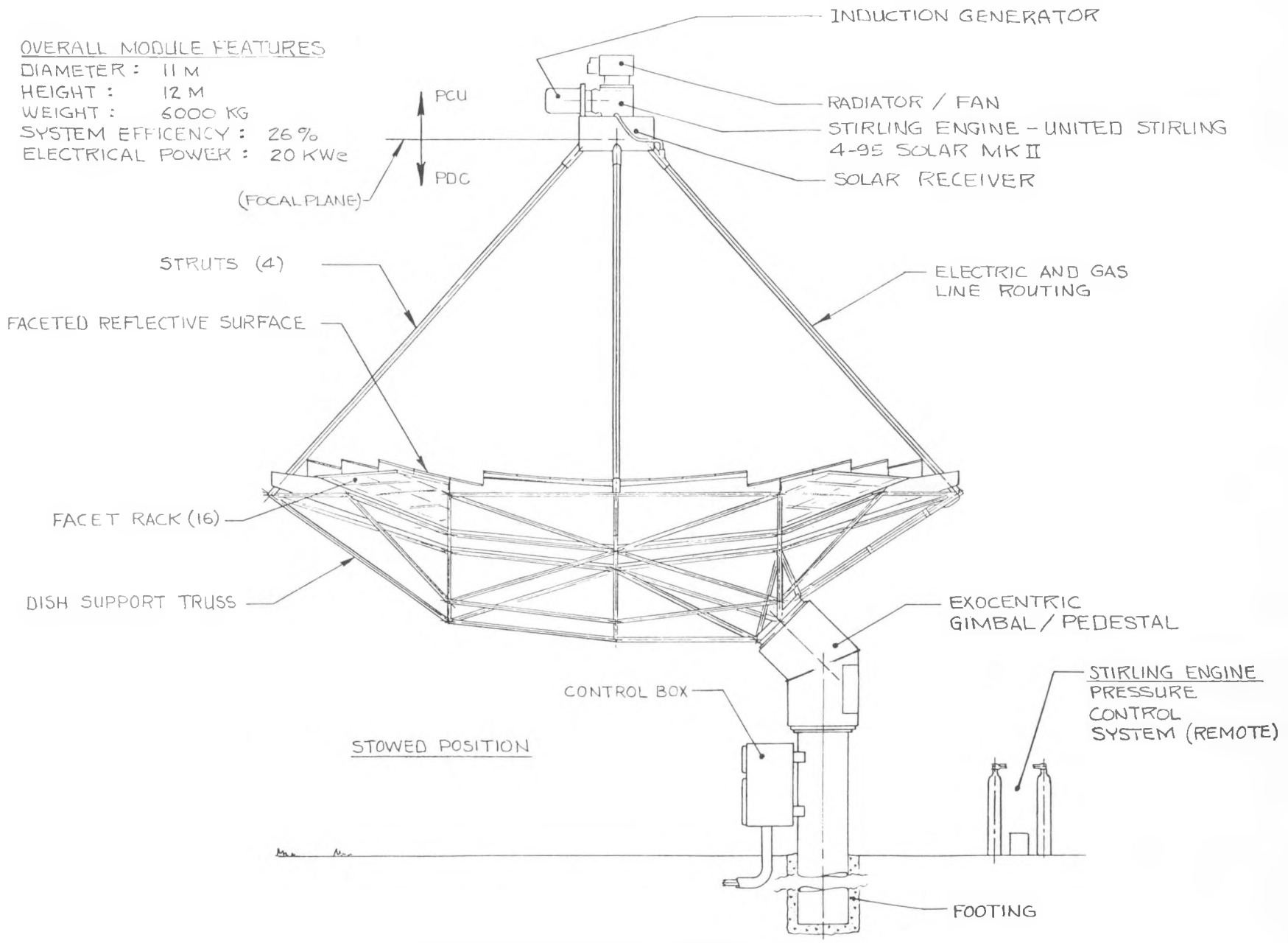

Figure 3. Vanguard Dish-Stirling Module

As a result of a trade study involving operating and maintenance as well as electrical interconnection considerations, 32-module groups were selected as the fundamental autonomous building blocks for the Vanguard system. These groups can be installed singly or assembled into larger blocks of up to 16 groups, which constitute a cluster. A typical cluster is illustrated in Figure 4.

Another trade study selected an induction generator as the baseline torque-to-electricity converter for the Vanguard module. This study is summarized in Figure 5.

The Georgia Institute of Technology has been involved in analyzing the structural and optical characteristics of the collector. Figure 6 shows their latest projection of the optical receiver pattern.

Six critical issues were identified in the Vanguard proposal to DOE that was originally submitted in July 1981. Substantial progress has been achieved in resolving these issues. Table III identifies the original six critical issues and the status of each one.

Finally, the team has, as a result of our marketing and technical investigation, acquired a renewed appreciation for the concept of solar power system modularity. Table IV is a sampling of the benefits of modularity.

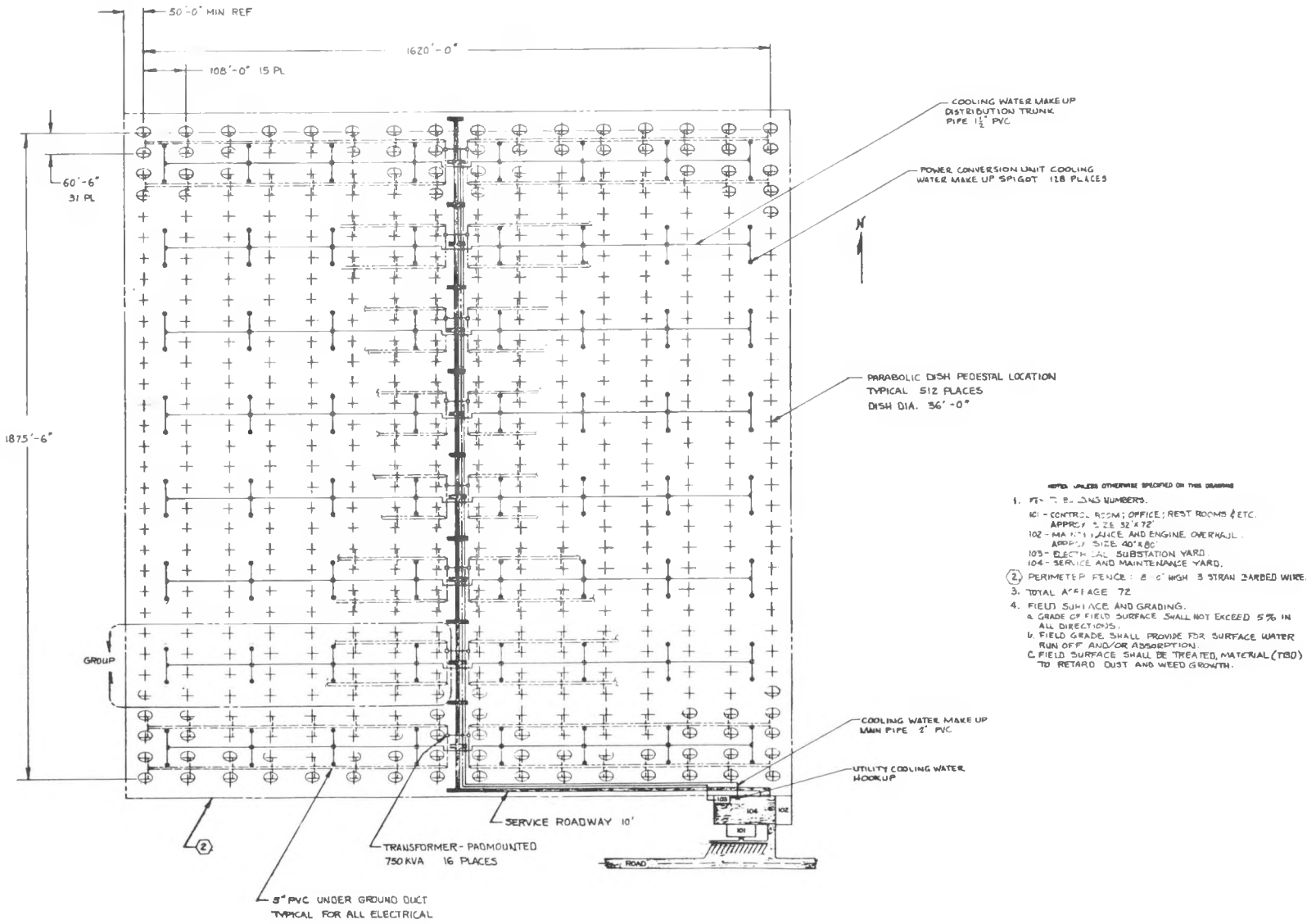

Figure 4. Typical Cluster Layout, 10-MWe Nominal Output

TABLE III

PROGRESS ON VANGUARD CRITICAL DESIGN ISSUES

Critical Issue July 1981	Report Status October 1982
1. Design of Solar-Only Receiver	1. Experimental Solar-Only Receiver has operated at Edwards AFB without failure for over 300 hours of scheduled test at temperatures up to 700°C and pressures of 15 MPa (mean gas pressure).
2. Induction vs synchronous generators set in a multi-module system	2. Onan Inc. has concluded and Southern California Edison has concurred that an induction generator best fulfills the eight-point criteria established. Similar induction generator testing at ETS has technically confirmed this conclusion.
3. Avoidance of critical materials	3. The amount of cobalt used in the manufacture of the 4-95 Stirling engine has been reduced from 20% to negligible.
4. Domestic production of solar glass	4. Corning Glass Works has announced a new product line (code 8503) that has a plentiful supply due to a large nonsolar application. Foreign suppliers (Schott, Flaberg, and Glauerbel) have increased the attractiveness of importing their products.
5. Low-cost alignment of the reflective surface	5. With the assistance of JPL personnel and on-going realignment experiences at ETS, three low-cost alignment techniques are being investigated.
6. Cost and frequency of O&M	6. By extrapolating field and factory testing, scheduled maintenance on the concentrator and Stirling engine has been reduced to 72 hr/yr and 150 hr/yr, respectively.

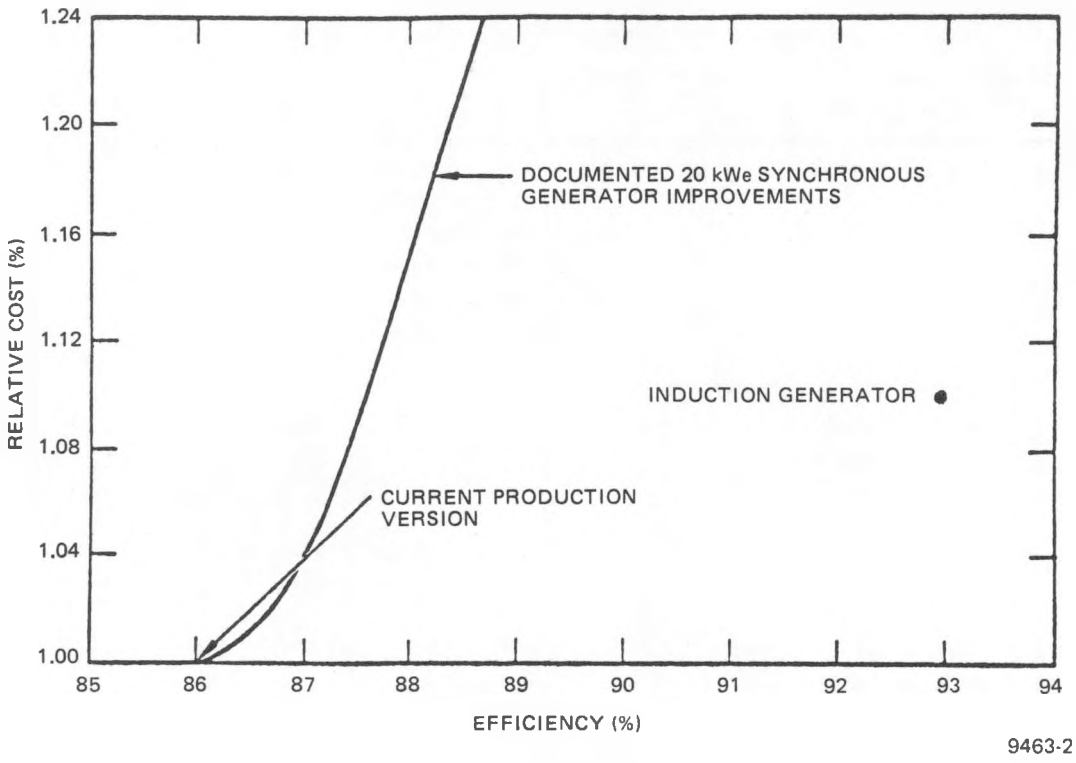

Figure 5. The Induction Generator Offers Higher Efficiency Than a Synchronous Generator of Equivalent Cost at 20 kWe

TABLE IV

THE ADVANTAGES OF MODULARITY TO UTILITIES

1.	Little or no debt service prior to operation
2.	Project "off ramps" are available
3.	Immediate placement of modules in rate base for capital recovery
4.	Essentially instant additions to capacity with little lead time required
5.	Increased electricity source reliability through redundancy
6.	Modest investment required to prove viability

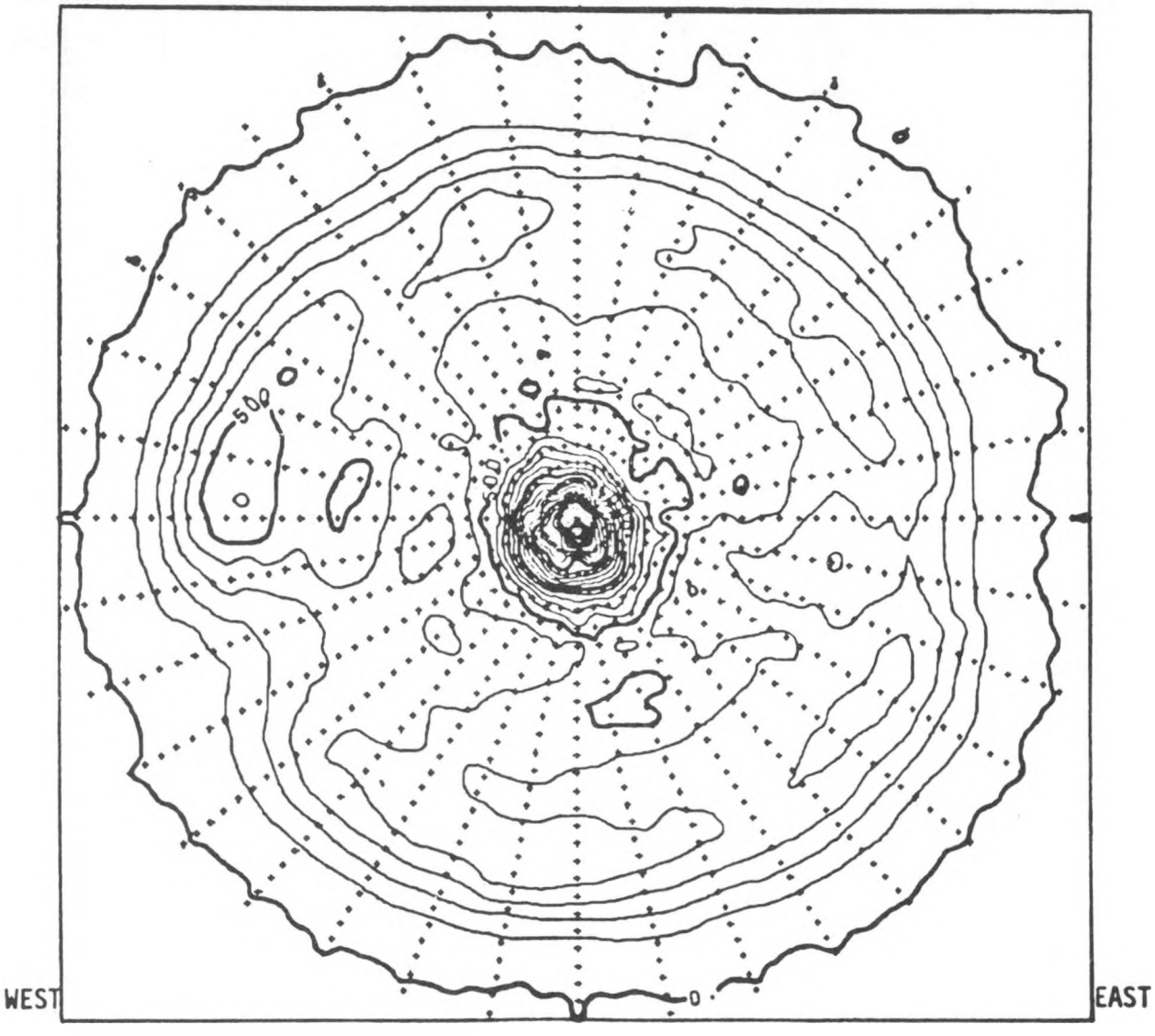

Figure 6. Cone Flux-Stiffened Structure, 30 mph

1.4 UTILITY RESEARCH ADVISORY PANEL

On September 15, 1982, the first meeting of the Utility Research Advisory Panel (URAP) was convened by Southern California Edison. The URAP consists of a group of utilities and two utility associations, and includes Southern California Edison, Pacific Gas & Electric, San Diego Gas & Electric, Arizona Public Service, El Paso Electric, Utah Power & Light, Electric Power Research Institute, and the American Public Power Association. The purpose of this panel is to meet periodically to evaluate the Vanguard team's technical and cost goals in relation to the public utility market. This process assures that the research effort is properly addressing the true needs of the primary market. Twenty-one comments were offered by URAP following an all day presentation by the Vanguard team. The team then met on September 16, 1982, to assign each comment to an individual for attention and response during the balance of the Task 1 and Task 2 efforts. Table V presents the major comments provided by URAP on September 15, 1982.

TABLE V

URAP COMMENTS
SEPTEMBER 15, 1982 MEETING

1. Design Issues

   a. The team should firmly establish the basis of the detailed design effort, particularly the typical number of units that would be installed at any one location.

   b. Is the 32 units per group truly optimal? Confirm this figure during Task 2.

   c. Has there been enough thermal cycling investigation on the receiver?

   d. The field assembly must be optimized and tight tolerances by field laborers should not be anticipated.

   e. What is the contribution of 32 units to the fault duty?

TABLE V

URAP COMMENTS
SEPTEMBER 15, 1982 MEETING
(continued)

f. Software rather than hardware is the greatest concern as a source of failure.

g. The technology presently appears to be of the frail, "hi-tech" variety that will not withstand environmental punishment. Endurance testing is a must.

h. Cost attainment is paramount.

i. Confirm Cal-OSHA standards for hydrogen use.

2. Manufacturing Issues

a. Indicate the efforts that will be taken to produce a large and dependable supply of units.

b. Articulate the rationale that increased reliability and economics will be achieved through redundancy, vis a vis, the utility trend of economies of scale.

c. Establish a basis for quality assurance on the PCU.

3. Operations and Maintenance

a. There must be a visually confirmed disconnection of the system and each module to the grid to provide for personnel protection.

b. Enlarge the use of maintenance classified personnel and minimize, if not eliminate, operator classified personnel.

c. Design to maximize unmanned operation and best utilize scheduled maintenance.

4. Data Gathering

a. The presently planned number of data points is inadequate and needs to be substantially enlarged.

b. Sequential event recording is desirable during failure modes.

Blank Page

Testing of 4-95 Solar Stirling Engine in Test Bed Concentrator at Edwards Air Force Base.

Author: Hans-Göran Nelving
Deputy Program Manager Solar Systems
United Stirling AB-Sweden

Abstract

This paper discusses the 4-95 solar Stirling engine tests in the test bed concentrator at the JPL test site, Edwards Air Force Base. The design of the power conversion unit, available hardware and advanced technology efforts are presented, with a special emphasis on the receiver system. The flux distribution and temperature distribution of the receiver are important parameters influencing the system performance.

The test result evaluation shows maximum module performance, daily performance as well as a break down of component performance. Characteristics of transient operation are also shown.

The highlights from the testing-24 kW module power output, 27 % overall efficiency, 33 % Stirling power conversion unit efficiency-indicate the excellent module performance. Consequently the solar Stirling engine used in a parabolic dish results in a module, competitive to other power generating systems, and especially other solar systems.

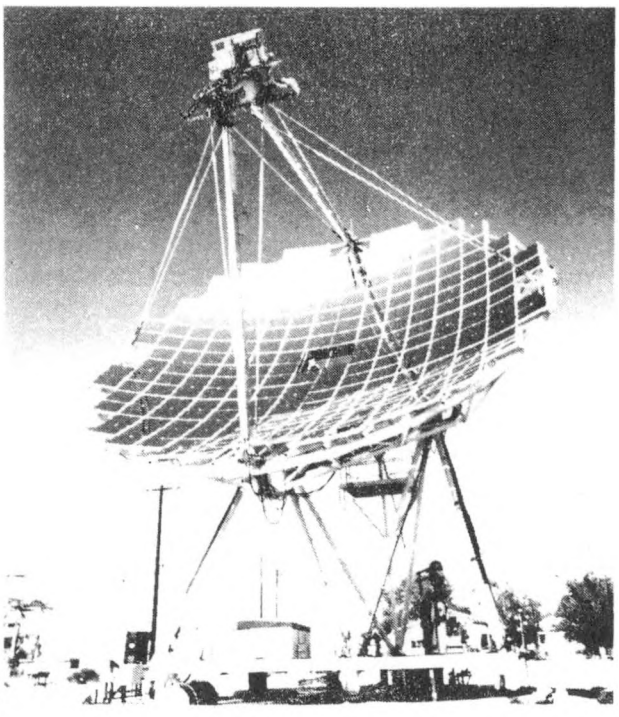

Introduction

The Stirling Parabolic Dish Program was initiated by JPL in 1979 and United Stirling AB of Sweden was selected as the supplier to JPL of the basic Stirling engine. The engine chosen was the USAB model 4-95, which was compatible with an 11 m concentrator developed and fabricated by JPL. The engine had, however, to be modified for use in the solar application.

The receiver system for the first generation of solar Stirling engines was designed, fabricated and tested by JPL. Further development at USAB of the solar Stirling engine, the receiver and control systems lead to a testing activity in the JPL test bed concentrator at Edwards Air Force Base which started early 1982.

The USAB developed "solar only" receiver and a solar digital engine control are being tested under a mutual contract between United Stirling AB and JPL. United Stirling AB has supplied and operated the power conversion unit while JPL has operated the concentrator and the electrical support system.

System description

The base for the power conversion unit has been the United Stirling 4-95 engine. It is a well proven reliable engine used in laboratory testing and field demonstrations, with combustion system, for over 29.000 accumulated running hours in 25 different engines.

To be able to use this engine in the solar application the engine had to be modified in three different areas:

1) lubrication system-to use the engine for operation in an inverted position a redesign of the lubrication system, including a separate external oil tank and oil pump, was necessary.

FIG 1. PARABOLIC DISH STIRLING SYSTEM.

2) receiver system-to use the engine with insolation as the sole supplied energy source, a specially formed receiver was designed for collecting the insolation and transferring the heat to the Stirling cycle,

3) control system-to use the engine with insolation as energy input a specially designed digital control system was made, which modulates engine power to follow variations of the insolation.

During the testing a standard induction alternator directly connected to the grid without additional devices has been used for electric power output generation. The other systems used, are the JPL test site installed equipment:

- the 11 m test bed concentrator
- the electric high voltage connections from concentrator to grid including all breakers and safety equipment
- radiator system for heat engine cooling located on the base of the concentrator structure
- data aquisition system for output data

The above auxiliary systems have not been optimized for the ongoing development tests.

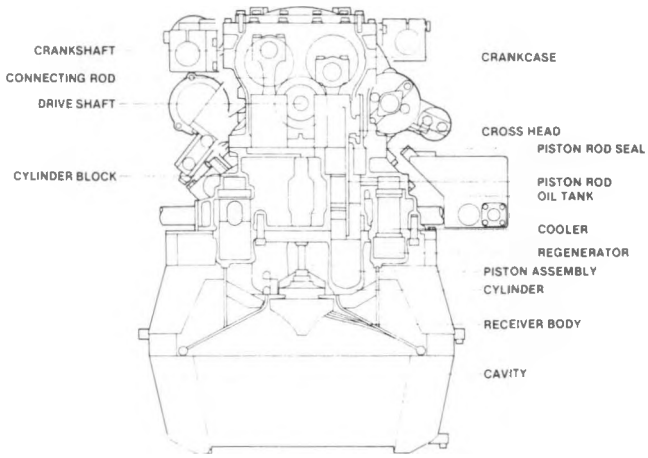

FIG 2. SOLAR STIRLING ENGINE CROSS SECTION

Control system

The complete control system consists of two major parts:

1) dish tracking control system,
2) solar Stirling engine control system.

The dish tracking control system is not included in the USAB responsible work and is not described here.

The control system for the solar Stirling engine has been designed for automatic, totally remote (unattended) operation. Manual control capability has been provided for installation, check-out, testing and maintenance.

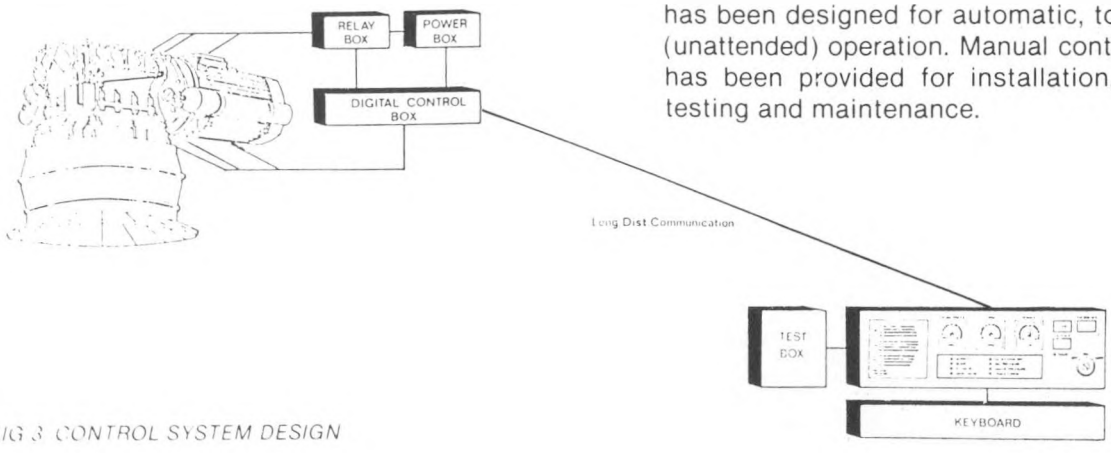

FIG 3. CONTROL SYSTEM DESIGN

The control equipment consists of one unit located near the engine in the focal mount of the parabolic dish and one monitor unit in the control room for the capability of start up, shut down, manual operation and recording/display of data (fig 3). The engine control unit consists of both electronic control equipment – a digital control unit – and electric equipment such as solenoid valves and high voltage relays and meters for grid connection of the alternator.

The digital control unit includes all operational modes as well as guard and emergency functions. The monitor unit for manual operation and recording and display of data includes the same digital control unit for communication as the digital engine control unit. The monitor also includes a cathode ray tube, meters for data display and a key-board for manual operation such as value change of a constant for different types of operations or control modes.

The operating modes for the engine can be separated in two parts:

- normal operation including start up, shut down, transients, stand by, restart, temporary stop, etc.
- detrack/emergency operation.

The control system is designed to operate the engine at its highest efficiency points during various insolation levels.

Following assumptions are involved in the control logics:

- no insolation control
- all output power delivered to grid
- engine receiver temperature kept constant at varying insolation levels
- induction alternator connected to grid to keep engine speed constant
- engine pressure varied to keep temperature constant at varying insolation levels
- grid/alternator used for start up of engine

During an increase of insolation a receiver temperature up to 600°C is allowed for a non-rotating engine. When temperature exceeds this level cranking of the engine is done by connecting the alternator to the grid for a short time period (alternator is used as starter motor). If engine can sustain operation, the engine speed is allowed to increase with disconnected alternator to 1800 rpm providing the receiver temperature does not exceed 700°C.
When speed reaches 1800 rpm the alternator is connected to the grid and engine produces electrical power to the grid. If insolation increases, working gas pressure in the engine is increased to maintain constant receiver temperature.

During decrease of insolation the receiver temperature is kept constant by pumping working gas (back to storage bottle). When engine no longer produces positive power, alternator is disconnected from grid and continues to rotate as long as the cycle is self-sustaining with continuously decreasing receiver temperature and with working gas pressure at its minimum level.

System performance

During the test period very successful system performance has been attained. Especially during testing in July the ambient conditions were superior for evaluation purposes and gave the highest engine performance recorded so far.

The highlights from the testing are

- 24.9 kW output from alternator at normalized 1000 W/m² insolation level
- 33 % energy converter efficiency
- 13.5 hours of operation with positive power output over a day
- generation of more than 250 kWh over a day.

The figures show insolation level and corresponding output power over a full day of testing. Also shown is the near constant receiver temperature during the test period (fig 4).

A break down of the system component power levels and efficiencies is shown in figure 5. The results show a conversion efficiency level from insolation input power to net system electric power delivered to grid of 27% for a 25 kW system.

Some more interesting results from the recent testing include:

- start rotation of engine at sunrise when insolation equals about 80 W/m²
- generation of positive power to grid at sunrise when insolation reaches 240 W/m²
- positive power to grid at sunset down to 180 W/m² insolation level.

The mean daily efficiency for the module performance according to curves presented in figure 4, is calculated to equal 95% of the maximum efficiency level during the day, which gives a mean daily conversion efficiency level around 26%.

The receiver temperature shown in figure 4 shows a control stability of ± 6°C. To keep the temperature within this band the pressure is varied as described earlier. This control principle results in anomalies in the output power characteristics shown in graph. The cause is belived to be wind effects in the receiver system which influences the temperature. As gas pressure has to be changed to compensate for temperature variations the power output also varies.

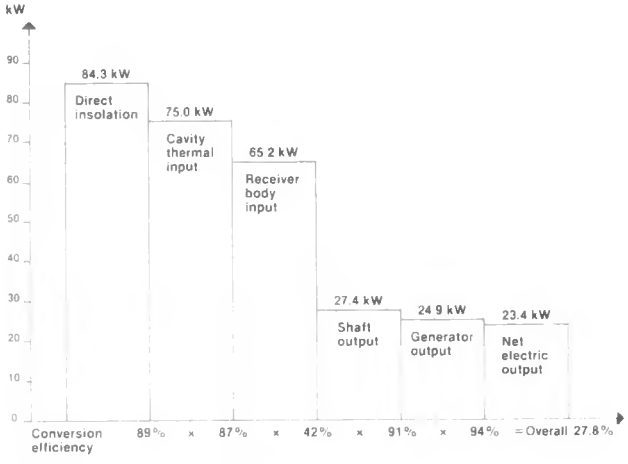

FIG 5. SYSTEM POWER LEVELS AND EFFICIENCY BREAK DOWN.

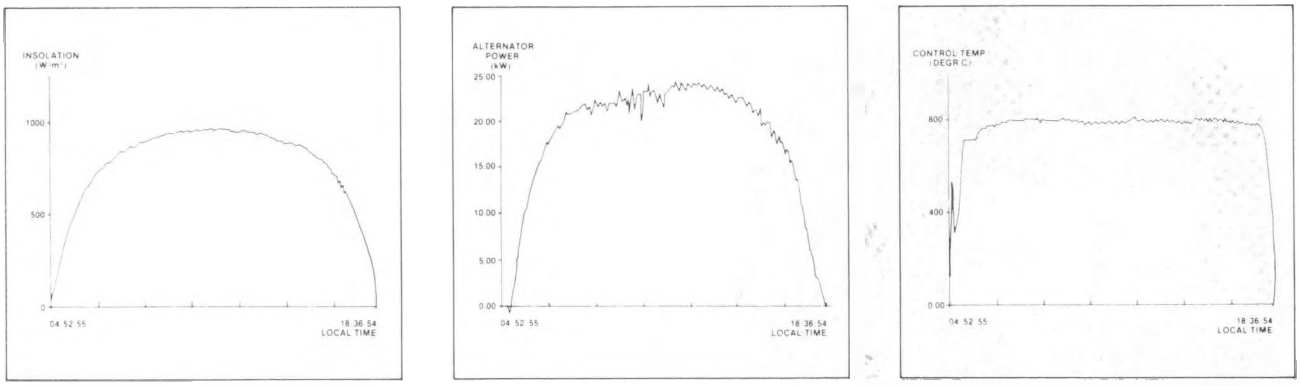

FIG 4. INSOLATION, ELECTRIC POWER OUTPUT AND TEMPERATURE FROM A DAILY TEST.

Receiver system

The receiver is the key component in the solar parabolic dish system. During the testing this component has proven to be the most interesting one to observe.

The receiver is identified as the interface between the concentrator and the Stirling engine. The concentrator on one hand and the Stirling engine on the other hand have their requirements for optimum performance. The flux pattern from the concentrator and the tube lay out of the solar heater have to be integrated.

The solar heater is a conical shaped heat exchanger formed by tubes which connect the cylinder and regenerator of the Stirling engine. Geometrical restrictions are involved in the lay out of the tubes. The most important restriction is the length of the tubes which has to be matched to the insolation flux pattern. To get reasonable flux levels and somewhat uniform flux distribution on the conical tube area, the solar heater cage diameter is made larger than desirable. This results in relatively long tubes and decreasing engine performance. Other restrictions include the requirement to cover the heat receiving surface completely with tubes and to avoid high temperature levels on uncooled surfaces. To acheive minimum spacing between the tubes especially near the outer diameter, results in a complex tube lay out which influences the optimum design. Also the center plug of the receiver cannot be covered with tubes.

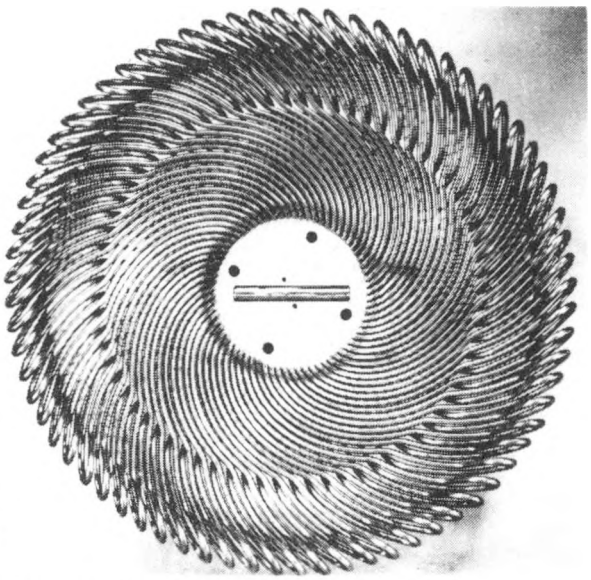

FIG 6. RECEIVER TUBE LAY OUT - TOP VIEW.

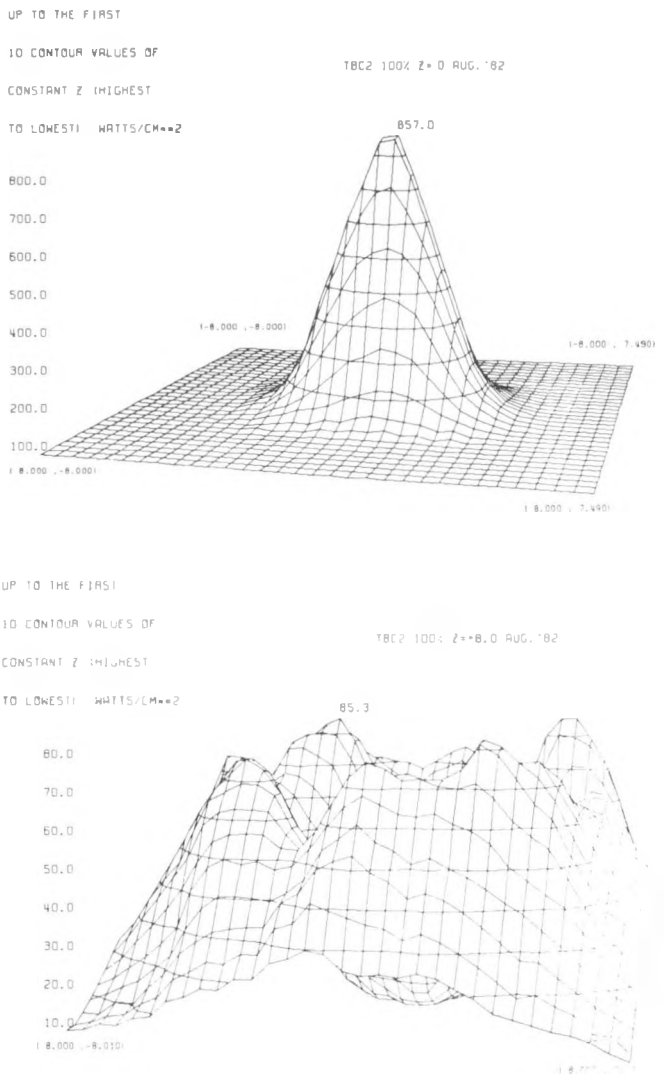

FIG 7. INSOLATION FLUX DISTRIBUTION - 3 DIMENSIONAL FIGURES SHOWING DISTRIBUTION IN FOCAL PLANE AND RECEIVER PLANE.

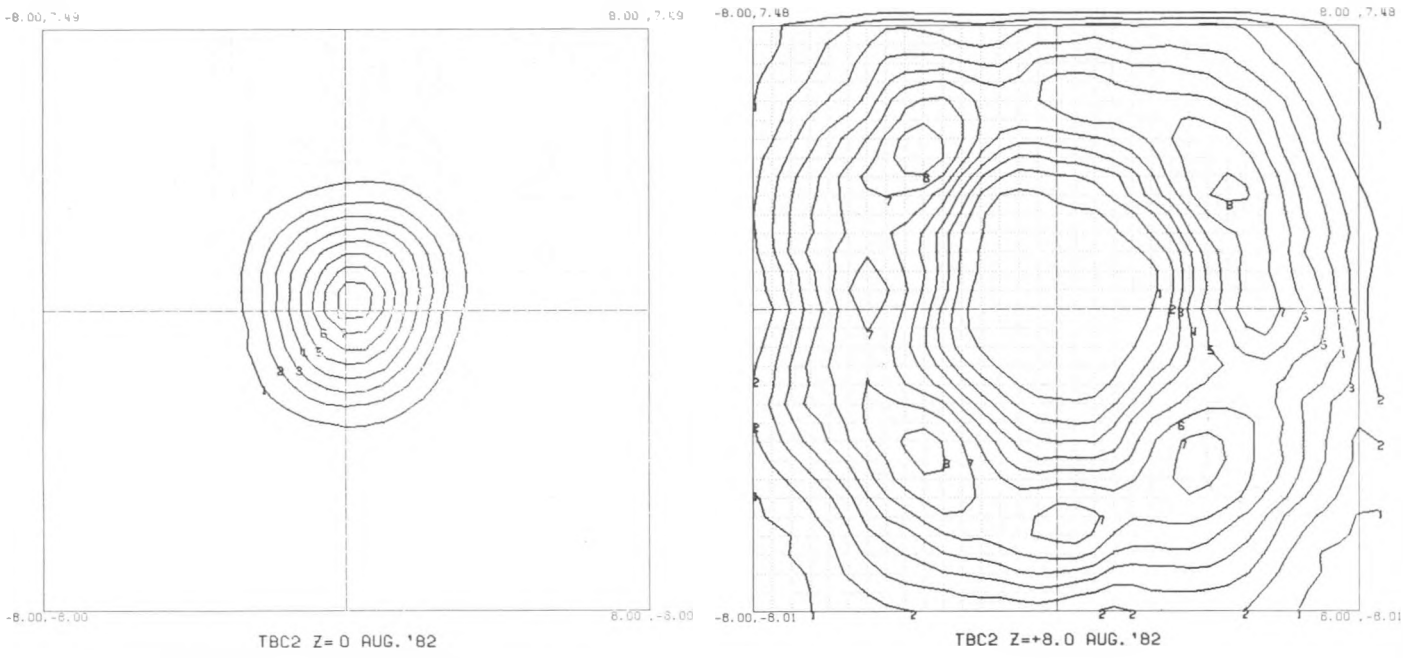

FIG 8. INSOLATION FLUX DISTRIBUTION IN X-Y PLANE-FOCAL PLANE AND RECEIVER PLANE.

The concentrator which appears to best match the Stirling engine requirements is the adjustable facet type. When using different types of alignment strategies almost any type of flux pattern can be achived, both for optimum flux distribution on the solar heater surface and on the aperture cone. One strategy used in the realignment of the concentrator can avoid insolation on the center plug as well as outside the heater maximum diameter. This means lower temperature levels on uncooled surfaces thus decreasing heat losses which results in a higher conversion efficiency.

During testing in early 1982 one realignment strategy caused temperatures above 1000° C on uncooled surfaces on center plug and cavity walls. After realignment of concentrator in May, further testing has shown cavity temperatures of the same level as the solar heater surfaces – 700°C. Cavity efficiency has therefore been improved approximately 8%. The flux pattern after this realignment is of dounut shape. The concentrator has also been flux mapped by JPL to get detailed information when evaluating the system. Figure 7 shows a three-dimensional picture of the flux distribution at the focal plane and at a plane where the solar heater is located. Figure 8 shows the corresponding two-dimensional x-y flux distribution and figure 9 shows the two-dimensional distribution in the x-z plane. Also indicated is the location of the solar heater. These figures show the uniformity in flux levels as well as the absolute levels. The maximum flux level near the focal plane is around 13000 suns and on the heater surface it is around 1000 suns.

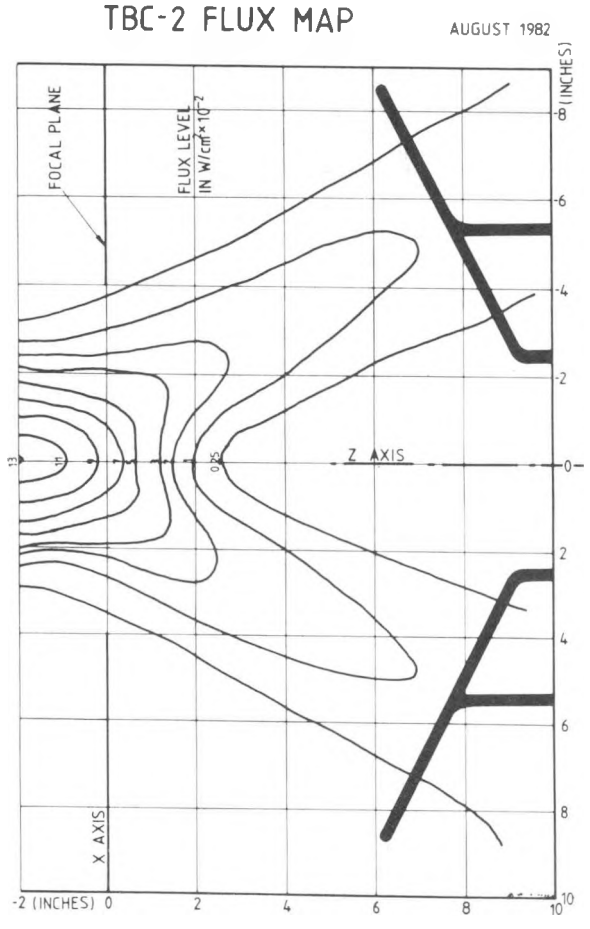

FIG 9. INSOLATION FLUX DISTRIBUTION IN X-Z PLANE. RECEIVER AND FOCAL PLANE SHOWN.

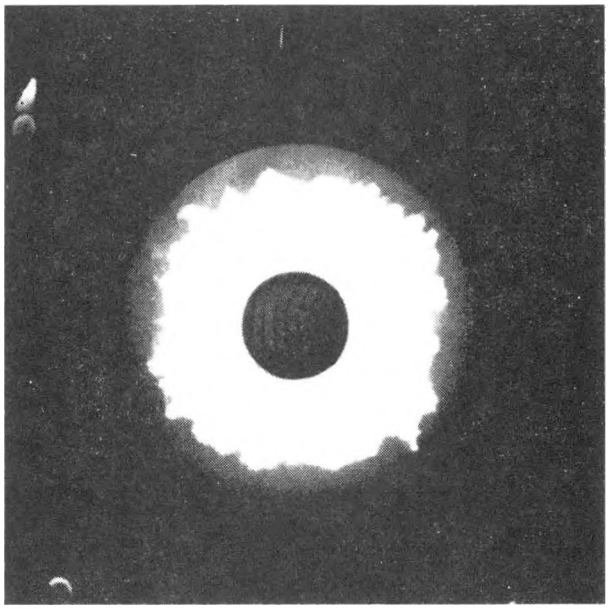

FIG 10. PHOTO OF FLUX DISTRIBUTION.

STIRLING ENGINE CERAMIC HEATER HEAD DEVELOPMENT

Valerie J. Van Griethuysen
Energy Conversion Branch-Air Force Wright Aeronautical Laboratories
Wright-Patterson AFB, OH

ABSTRACT

This paper presents the results of a program sponsored by the Aero Propulsion Laboratory (APL) of the Air Force Wright Aeronautical Laboratories (AFWAL) to develop a ceramic solar receiver/heater head for a kinematic Stirling engine. Ceramic heat receivers promise to alleviate several limitations characteristic of metallic heat receivers, namely high temperature creep, life and high cost strategic materials. Also, ceramic receivers may allow higher operating temperatures than their metallic counterparts with increased system efficiencies.

The objectives of the Ceramic Heater Head Development (CHHD) program were to determine ceramic types and fabrication processes capable of meeting design requirements and to formulate further ceramic development requirements. The paper presents engine load requirements, material coefficients of thermal expansion compatability, ceramic utilization for different heater and housing components and how the Stirling engine ceramic heater head power system will depend on the integration of Stirling engine, ceramic, heat transfer and structural requirements and limitations during further design efforts.

Areas identified for further development include low conductivity ceramic materials that have approximately the same coefficients of thermal expansion as silicon carbide, silicon carbides with high and low conductivities, and joining technology of ceramic to ceramic and ceramic to metal combinations.

INTRODUCTION

This program was initiated as a joint effort between the JPL Advanced Subsystem Development Group of the Thermal Power Systems Project and the Energy Conversion Branch of AFWAL (APL). The overall objective of the joint effort was to design, develop, fabricate, test and evaluate a ceramic solar-gas fired hybrid heater head for the 4-95 Stirling engine.

BACKGROUND

Work on the Fairchild Industries, Stratos Division metallic Stirling solar-gas fired hybrid receiver demonstrated the feasibility of the hybrid

concept. Subsequent testing of the metallic hybrid receiver revealed that the maximum operating temperature of the receiver is limited by the metal's high temperature creep characteristics[1]. The substitution of metals with ceramics, in combination with either new or modified heater head designs, offers the potential of higher operating temperature. This in turn increases engine efficiencies. In addition, ceramics will facilitate operation at the higher temperatures for longer time periods.

In 1979, Fairchild developed a concept for a ceramic hybrid receiver heater head as shown in Figure 1. Modifications of this design to decrease stresses and improve heat transfer to the working fluid took place at JPL during 1981. This modified design (Figure 2) was originally part of the CHHD program. During the initial stages of the program, it was determined that existing ceramic processes would have difficulty in meeting fabrication requirements and that there would be a low probability for successfully fabricating such a heater head. During this same time period, a hybrid receiver heater head with a simpler configuration was undergoing preliminary development at United Stirling of Sweden (USSw). The decision was made to direct the CHHD program toward the USSw design. A discussion of the JPL/Fairchild and USSw design configurations follows.

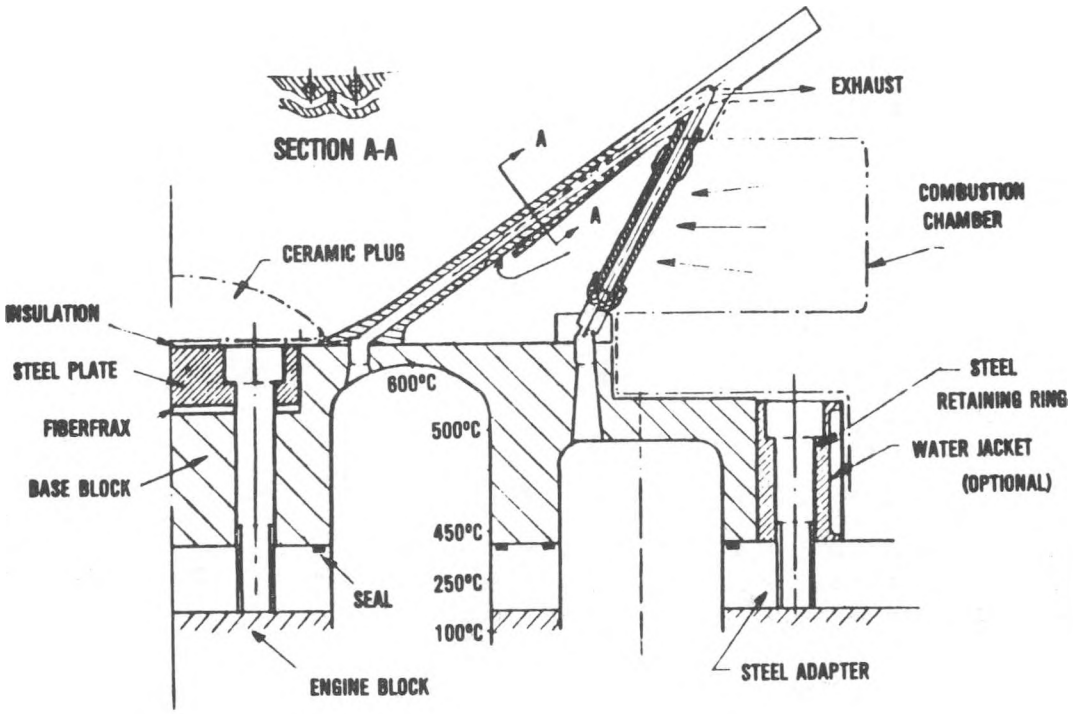

FIG. 1. FAIRCHILD CERAMIC DESIGN CONCEPT

The JPL/Fairchild solar hybrid receiver design consists of a solar receiver with internal passages to connect the piston cylinders to the heater tubes (regenerator tubes) and a base block. This design (Figure 2) is similar in configuration to the metallic hybrid solar receiver designed by Fairchild as shown in Figure 3.

The United Stirling hybrid receiver design differs radically from the JPL/Fairchild design. The USSw design is based on a proprietary solar only receiver design for a Stirling engine with annular regenerators. Figures 4 and 5 show a cross section and top view of a design concept that is similar in configuration to the hybrid design developed during this program. This design, because of its piston cylinder position and dimensions, cannot be adapted to the 4-95 engine. However, the MOD I Stirling engine, (developed under the Department of Energy's Automotive Technology Development Program) because of its cylinder spacing, can be used after some modifications with the USSw hybrid receiver design.

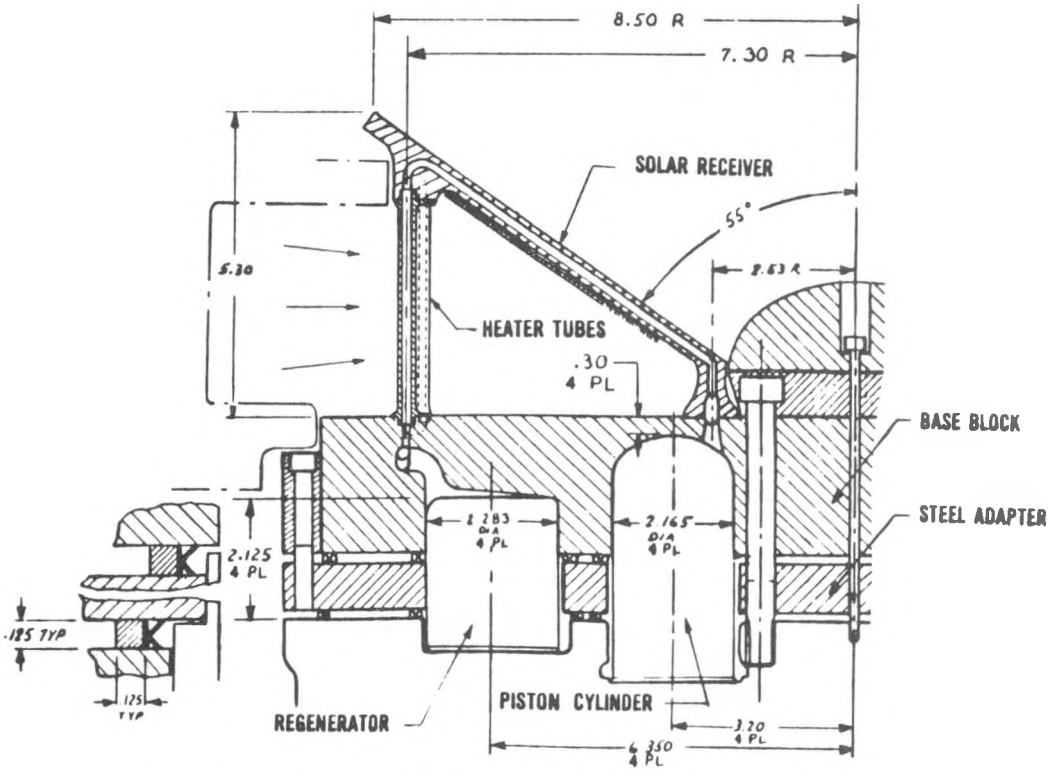

FIG. 2. JPL/FAIRCHILD CERAMIC DESIGN CONCEPT

The USSw design eliminates the tubes prevalent in the JPL/Fairchild design. Instead, channels are incorporated in the ceramic receiver plate to satisfy the flow and heat transfer requirements. Since there are no tubes, there are fewer parts in the USSw design. For example, the JPL/Fairchild design has 52 parts per quadrant whereas the USSw design has 7 parts. The

number of joints per quadrant associated with each of these designs are 98 and 6 respectively. When considering an entire heater head this corresponds to 208 parts and 392 joints for the JPL/Fairchild design and 28 parts and 24 joints in the USSw design. In the long run, the differences in the numbers of parts and joints will impact not only production costs but also the reliability of the units.

Minimizing the number of joints is particulary important since the probability of failure increases as the number of joints increase. For example, the number of joints required in the current JPL/Fairchild design suggests a high probability of leaky joints and a corresponding decrease in system reliability.

Analyses conducted at the Carborundum Resistant Materials Company, Advanced Materials Division indicate that in addition to the fewer parts, the USSw design will require nine to ten pounds less material per quadrant. Not only will this reduce system weight, but also system cost. In addition, cost reductions are expected due to a decrease in fabrication time associated with the fewer parts. Furthermore, less grinding of surfaces will be required in the USSw design.[2]

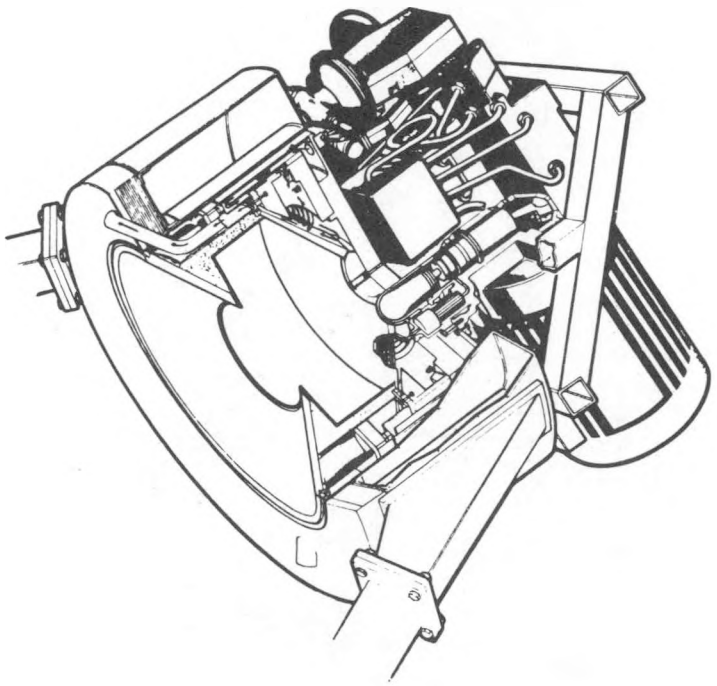

FIG. 3 FAIRCHILD METALLIC HYBRID RECEIVER[3]

Stress analyses have been conducted on the JPL/Fairchild design, but not on the USSw design. Before a stress analysis can be accomplished on the USSw design, a thermal analysis is needed to identify methods (i.e. fin configurations) for improving heat transfer from the combustor gases to the back surface of the collector cone plate. Once this has been accomplished, a stress analysis will be needed.

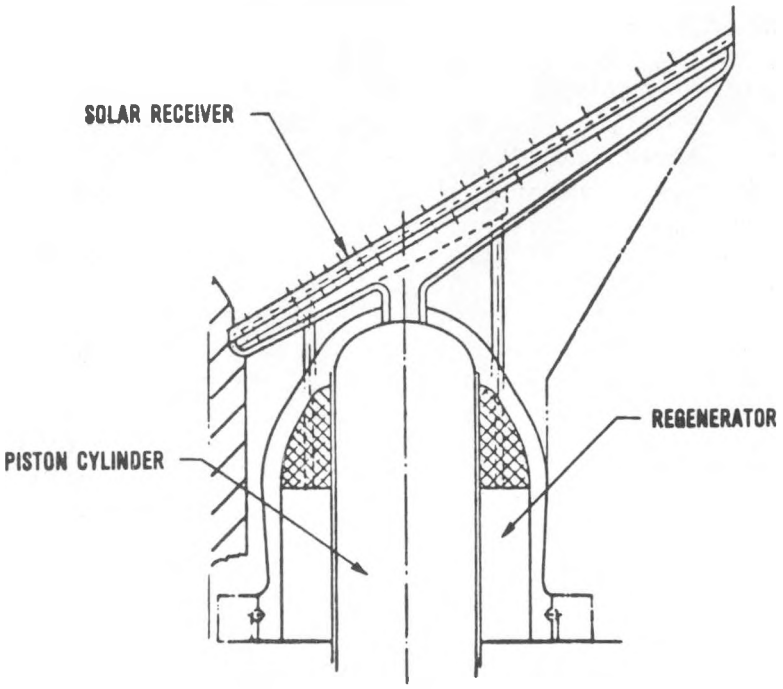

FIG. 4 USSw CERAMIC DESIGN CONCEPT - CROSS SECTION[4]

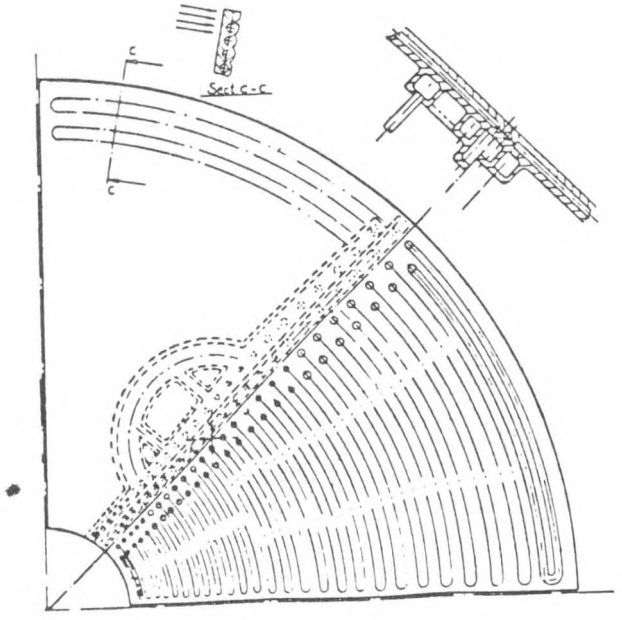

FIG. 5 USSw CERAMIC DESIGN CONCEPT - TOP VIEW[4]

MATERIAL TRADE OFF ANALYSIS

An important part of this program was the trade-off analysis of various ceramics to determine the optimum combination of usage in the heater head. A key consideration in the selection of ceramics for a Stirling engine is the need for a high thermal conductivity material in the heater portion and a low thermal conductivity material in the regenerator housing region.[2] In addition, thermal expansion compatibility of materials in the two regions is important.

A United Stirling analysis showed the effects of using different materials for the heater and housing regions on the power output and thermal efficiency of the 4-95 engine, combustion only design. Although this engine differs from the annular regenerator engine in configuration and performance, the results should apply to both. The analysis was run for two operating pressures, 11MPa (1595 psi) and 15 MPa (2175 psi) and was based on using hydrogen as the working fluid and the engine operating at 1800 RPM. The results are shown in Table 1. The differences in thermal conductivities for the same materials is due to a non linear difference in conductivities at different temperatures.[2]

Comparing B and D in Table 1 shows that if only one material is to be used for both the heater and housing, it is more beneficial to use a material with a lower conductivity. Comparing C and D shows that, although the metal and silicon nitride (Si_3N_4) have approximately the same thermal conductivities, a higher maximum temperature does raise the engine output power and efficiency. A third observation from the table shows that, in the case of A, the best theoretical performance occurs with silicon carbide (SiC) for the heater and SI_3N_4 for the housing.

TABLE 1 MATERIAL AND EFFICIENCY COMPARISONS[2]

CASE	MAXIMUM TEMPERATURE °C	HEATER	HOUSING	THERMAL CONDUCTIVITY W/mK	PRESSURE, MPa	POWER OUTPUT, kW	EFFICIENCY, %
A	1120	SiC	Si_3N_4	40 20	11 15	29.2 40.0	47.6 49.8
B	1120	SiC	SiC	40 50	11 15	29.2 40.0	42.5 45.8
C	720	METAL	METAL	20	11 15	20.0 28.4	40.7 42.0
D	1120	Si_3N_4	Si_3N_4	20 15	11 15	28.7 39.2	47.1 49.3

Without an analysis directed specifically toward the performance of an engine with an annular regenerator, it is unknown to what magnitude the results presented in Table 1 will vary. If using two materials, as in case A, produces only a minimal increase in performance, it would not be worthwhile to use such a combination. If, on the other hand, there is a significant improvement in performance then the problems associated with using materials with vastly different coefficients of thermal expansion (CTE) should be addressed. This problem cannot be under emphasized and will be discussed in the next paragraph. If an analysis for the annular regenerator design demonstrates that Si_3N_4 will produce a significant performance increase over SiC then its utility value should also be assessed on other factors.

A finite element analysis was conducted to investigate the stresses that might arise when the hot end of the cylinder is constructed with SiC and the regenerator housing is made with Si_3N_4. The results revealed that stresses as high as 90ksi would occur in the Si_3N_4 and 70ksi in the SiC during a cool down from 1100°C to room temperature during fabrication.[2] These stresses are due to the large differences in thermal expansions and elastic moduli between the two ceramics.

To reduce the stresses when two materials are joined, their CTE's should be approximately the same. In addition, reducing the elastic moduli of the materials without reducing their strength or drastically changing their thermal conductivities will have to be determined. An alternative to using two different ceramics is to use one material. The thermal conductivity of Hexaloy SA SiC (single phase sintered) can be varied by either using dopants or by using different processing methods, such as hot pressing, chemical vapor deposition (CVD) and sintering[2]. Table 2 shows the processing effects on thermal conductivity for SiC. The thermal conductivity of the hot pressed SiC and sintered SiC is three and a half to six times greater than CVD SiC. There is minimal difference in the CTE's.

TABLE 2
SiC PROCESSING EFFECTS ON THERMAL PROPERTIES

Temperature	Thermal Conductivities, Cal/sec-cm-C°		
	Hot Pressed	Sintered	Chemical Vapor Deposition
100°C	0.186	0.187	0.0327
1000°C	0.086	0.1	0.0238
	Coefficients of Thermal Expansion, cm/cm-C° x 10^{-6}		
20°C-1250°C	4.73	4.72	4.78

In addition to the Hexaloy SA SiC, other silicon carbides such as reaction bonded silicon carbide (RBSiC) materials have properties that are conducive to the heater head. RBSiC materials can be used for the regenerator housing and the partition wall which separates the cylinder and regenerator. As the Hexaloy SA SiC and RBSiC have similar CTE's, they can be used together to take advantage of their different thermal conductivities. However, the RBSiC has a process difficulty which prevents it from being a prime candidate material. During its siliconization step, free silicon is left on the surface which could plug the internal passages.[2]

MANUFACTURING PROCESS ANALYSIS

There are seven parts per quadrant (upper and lower plates, inner plate flow passages, manifold, regenerator housing and two parts in the partition wall) to be fabricated in the USSw design. All of these parts can be fabricated by injection molding. While in the green state, the parts can be joined by a number of plastic welding techniques, such as ultrasonic welding, hot gun welding, solvent welding, etc.[2]

After the parts are joined, the assembly can be leak tested to assure quality of the joints. Minor leaks can be repaired, whereas more seriously defective assemblies can be crushed and reused for injection molding.[2] With additional design work, it would be possible to reduce the number of parts to be fabricated. For example, the regenerator housing and partition wall could be fabricated as one piece.

Further design iterations are required before a final manufacturing process can be selected. Additional trade-off analyses are needed to determine the optimum combination in molding time reduction, joint elimination and tooling costs.

An analysis was conducted, using the existing USSw design, to determine the cost of producing numbers of quadrants per year. The graph in Figure 6 gives the results of that analysis and shows that the cost is reduced significantly with increased production. For low production, tooling cost is the dominant parameter in the total cost. As production increases, labor and manufacturing yields are the dominant costs. Within this area, molding and joining costs contribute about one third of the total labor cost for the 500 quadrant case.[2]

CONCLUSION

Further design iterations are required on both the JPL/Fairchild and USSw solar-gas fired hybrid heater heads before they can be constructed with ceramics and have a high probability of success. In conjuction with the design effort, thermal and stress analyses and ceramic properties and manufacturing process considerations must play an integral part in the overall design of the heater head. Ceramic process development has advanced considerably in the last two years. Many limitations that were originally incorporated into the heater head designs no longer exist. Complex shapes and thin walled tubes can now be fabricated with ceramics.

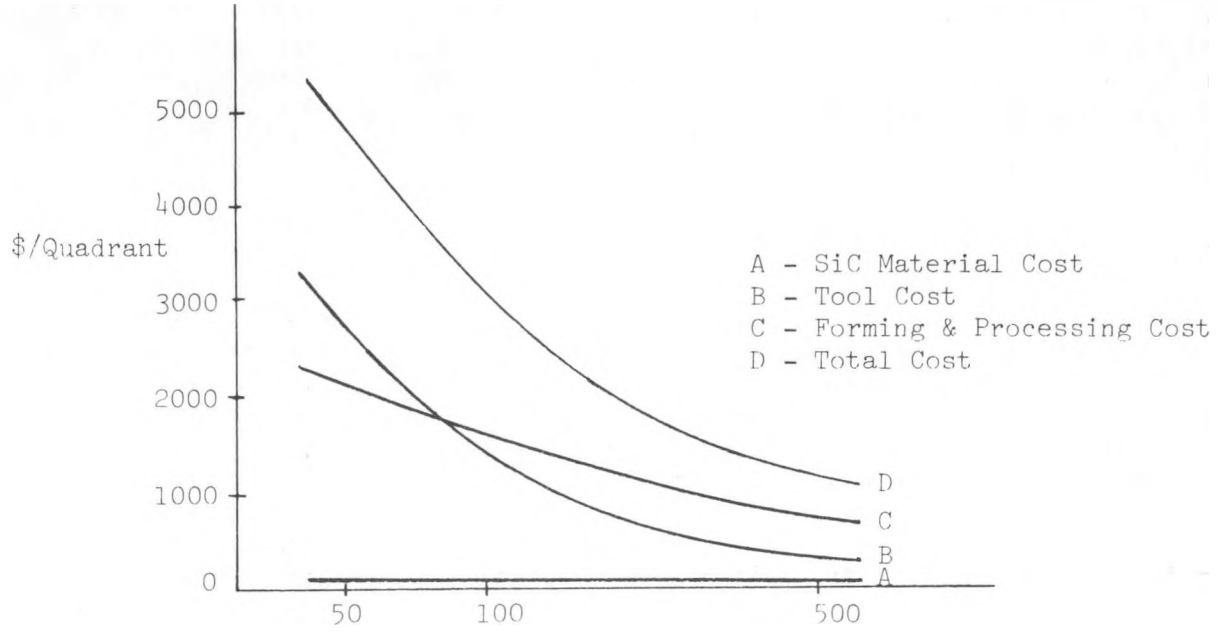

FIG. 6 PRODUCTION ANALYSIS[2]

Prior to fabrication of an actual ceramic heater head, several ceramic and design development tasks must be completed. Fin configuration for the backside portion of the USSw solar receiver must be determined. A complete finite element stress analysis of the entire heater head must be completed to determine survivability potential of the head during various heating situations, particularly during transient conditions such as start up and shut-down. If unfavorable results occur, further design and finite element analysis iterations will be required until an acceptable design is obtained. The development of high and low thermal conductivity SiC materials is needed to eliminate the material CTE mismatch problem.[2] Engine efficiency predictions are needed with computer simulations of the actual engine type with various combinations of materials. Further development of joining and bonding techniques are also needed.

REFERENCES

1. R. Haglund, et al, "Technical Feasibility of a Ceramic Dish Solar Stirling Receiver", Document Number ER78911-4-6, JPL Contract #955400 pg. 1, February 1980.

2. M. Kasprzyk, "Ceramic Heater Head Development", Draft Technical Report under AF Contract F33615-81-C-2072, November 1982.

3. R. Haglund, "Dish Stirling System Integration and Test Progress Report", Third Parabolic Dish Thermal Power Annual Review, Atlanta, Georgia, December 1981.

4. United Stirling (Sweden), "Design Study of a Kinematic Stirling Engine for Dispersed Solar Electric Power Systems", DOE/NASA/0056-79/2, NASA Cr-159588, pp 62-63, 1980.

STATUS OF THE SMALL COMMUNITY SOLAR POWER SYSTEM

R. H. Babbe
Ford Aerospace & Communications Corp., Aeronutronic Division
Newport Beach, CA 92663

ABSTRACT

This paper presents a summary of the Small Community Solar Thermal Power Experiment (SCSE). Emphasis is placed on the single power module being tested at the JPL Parabolic Dish Test Site, Edwards AFB, California. The power module consists of a regenerative, air-cooled 20-25 kW_e organic Rankine cycle (ORC) engine/generator unit and a cavity receiver mounted at the focus of the solar concentrator. Toluene is the working fluid and is heated in the receiver to 750°F before expanding across a single-stage axial flow turbine direct-coupled to a permanent magnet alternator (PMA). Other equipment includes a control subsystem designed for unattended operation and an energy transport subsystem utilizing a special inverter for voltage (load) control and conversion of dc to grid compatible ac power. The typical power output of the module for the Edwards tests was about 16 kW_e at 950 W/m^2 direct solar insolation; the net module efficiency at these conditions was 19.5%. Receiver efficiency was greater than 95% and the net ORC power conversion unit efficiency (engine/alternator/rectifier) was approximately 22%. The Edwards tests were the first demonstration of a control system designed for an unattended plant. The computers maintained stable operation under the most severe transients caused by commanding the closing and opening of a water-cooled plate at the entrance of the receiver.

Multiple modules will be joined together electrically to form a Small Community Power Plant. The plans for this phase of the program are decribed.

Companion papers give further information on the results from the Edwards tests and the status of the control subsystem. References cited in this paper provide additional information on the SCSE program and hardware.

INTRODUCTION

Ford Aerospace is currently completing the second phase of the Small Community Solar Thermal Power Experiment (SCSE) under contract 955637 to JPL. This effort comprises the development and integration of a single prototype power module consisting of a parabolic dish concentrator, power conversion hardware, plus central equipment for control and power conditioning/distribution.

Figure 1 is a simplified schematic of the equipment used in the initial tests at the JPL Parabolic Dish Test Site (PDTS) at Edwards AFB. The power conversion assembly (PCA) is located at the focal point of the solar concentrator and is comprised of a Ford Aerospace cavity receiver and an organic Rankine cycle (ORC) engine built by Barber-Nichols Engineering Company,

Arvada, Colorado. A cut-away view of the PCA is shown in Figure 2. The heart of the engine is the turbine/alternator/pump (TAP) in which the turbine is direct-coupled to the permanent magnet alternator (PMA) and the main feed pump. The variable frequency 3-phase ac power generated by the PMA is converted to dc by a rectifier mounted at the base of the concentrator. Hence, it goes to a nearby switchboard and to an inverter which changes dc to 3-phase, 480 V 60 Hz power. This power is fed into a local grid, or into a load bank during the initial test runs at Edwards. Engine control is achieved using a microprocessor, and a minicomputer is used for overall control. The minicomputer also logs test data, monitors the status of the various components, sounds warnings if key parameters are outside normal ranges and automatically shuts down the engine if conditions warrant.

The SCSE is designed to supply a portion of the electrical power requirements of a small community. A specified rated power level is reached by adding power modules and connecting the dc output from each module to a common dc bus in the central switchboard. The major components which are dependent on the size of the plant are the switchboard, inverter and grid interface equipment. The central minicomputer called the MPC or master power controller, has the capability of providing overall control of a plant up to a power range of approximately 1 MW_e. Each power module has its own microprocessor for control of the engine and concentrator. These microprocessors, called the remote control interface assemblies or RCIAs, make each power module virtually independent of all the other modules.

SYSTEM DESCRIPTION

Receiver

The organic Rankine cycle receiver is a cavity formed by a cylindrical shell of copper with stainless steel tubes brazed to the outside of the side and back walls. The unit is classified as a direct-heated, once-through, monotube boiler. It operates at either sub- or super-critical pressure regimes of the heat transfer fluid, toluene ($C_6H_5CH_3$). The copper core is 1.9 cm (0.75 in.) thickness supported by struts and insulated with a ceramic blanket of Cerawool®. A protective sluminum casing covers the insulation. The interior dimensions of the cavity are 0.61 m (24 in) diameter and 0.48 m (19 in) deep. The 1.95 cm (0.625 in) diameter 347-type stainless steel tubing fits into a matching groove machined in the exterior surface of the copper. The tubing and copper core are brazed together to form a good thermal contact, and nickel plated to prevent oxidation. The cavity is painted with high temperature black paint (Pyromark 2500®) to obtain a high solar absorptivity. The overall weight is 234 kg (516 lb). A copper aperture plate is attached to the front of the receiver; a hole 37.95 cm (14.95 in) in diameter provides a geometric concentration ratio of ~1000 when used with the 12 m PDC-1 concentrator.

Design requirements include a rated input thermal power of 95 kW_t, an efficiency at rated conditions greater than 96 percent, toluene flow from 0.9 to 9.1 kg/min, a nominal toluene outlet temperature of 399°C (750°F), and operating pressures up to 5862 kPa (850 psi), although the unit is normally operated at subcritical pressures in the range of 3450-4140 kPa (500-600 psi).

The receiver has been thoroughly tested in both ground and solar tests and has met or exceeded all specified requirements, including efficiency. Additional information on the receiver is included in Reference 1; typical test data are provided in References 2 and 3 for the initial ground tests and References 4 and 5 for the solar tests.

Engine

The engine , also called the power conversion subsystem (PCS), utilizes the Rankine cycle with toluene as the working fluid. The PCS is a sealed, regenerative unit with a single-stage axial flow turbine approximately 13 cm (5 in) in diameter. The air-cooled condenser is packaged in a cylindrical shape surrounding the regenrator and the TAP; a total of 369 finned aluminum tubes in three concentric rows form the heat transfer surfaces. A two-speed electrically-driven fan provides cooling air at a maximum rate of 212 m^3/min (7500 cfm). The dimensions of the PCS are 1.1 m (44 in) diameter and 1.5 m (60 in) length. The PCS weight is approximately 418 kg (920 lb).

The turbine wheel is fabricated from Inconel 718 and the 110 blades (each 10.7 mm or 0.42 in. high) are electrochemically milled by a process developed by Barber-Nichols. Ten nozzles are used to drive the turbine at speeds in the range of 45,000 to 60,000 rpm. The PMA has six samarium-cobalt magnets on the rotor and a 9-tooth copper-wire wound, laminated-iron stator. It produces three-phase ac power with a frequency of 3000 Hz at 60 krpm.

The net power output of the PCS is rated at 20 kW_e at the output of the rectifier and a thermal input of 75.6 kW_e, and a peak output of approximately 25 kW_e at an input of 92.4 kW_t. The unit operates at all attitudes from 5° to 90° above the horizon, with the capability to stow at minus 90°.

A vapor throttling valve located between the receiver and PCS maintains a near-constant turbine inlet temperature of 399°C (750°F) by controlling the mass flow rate of toluene. The design uses a pintle valve operated by a hydraulic actuator which in turn is powered by high-pressure liquid toluene. Valve command signals are keyed to temperature sensors in the receiver shell and in the fluid at the outlet of the receiver.

Other components include a fin-tube regenerator, electrically powered boost pump and start pump, a rectifier and an overspeed brake. In the event of loss of control, the brake quickly brings the TAP to a stop by electrically shorting the windings in the PMA and closing the vapor control valve. Further information on the PCS design details is contained in References 6 and 7.

The test program at Edwards demonstrated that the performance of the unit was close to expected values (Reference 8), with a net efficiency of approximately 22 percent at an input power of 70.8 kW_t (gross efficiency of ~23 percent). Inspection of the TAP hardware after completion of the tests showed that further design improvements were needed to increase the life of the bearings in the TAP. Most of 1982 was spent in analysis, design and testing of improved bearings at Barber-Nichols. A new bearing design has now been developed and the delivery of the modified TAP is due in December 1982. Testing of this unit at the PDTS is scheduled to start immediately after being installed in the PCS at the test site.

Energy Transport Subsystem (ETS)

The ETS consists of: 1) the conventional electrical cabling (dc) which connects each power module to the switchboard, 2) a switchboard, 3) an inverter, and 4) grid interface equipment such as protective relays and, if required, a step-up transformer to boost the voltage to that of the local grid. The dc voltage is in the 500 to 600 V range (the exact value is set by an adjustment in the inverter), and the output of the inverter is 480 V, 3-phase ac as noted in Figure 1. Also included in the ETS is the hardware necessary to provide parasitic power (ac) to drive the concentrators, boost pumps, fans, computers, and similar equipment. Normally, parasitic power comes from the local grid, but if the grid fails, an uninterruptable power supply (UPS) is provided to operate the key components. A load bank is used to dissipate the generated power in the event the grid should fail.

The major benefit of using a dc electrical transport system is that it permits the speed of each ORC engine to be varied in proportion to its heat input in order to achieve high part-load efficiency and thus high annualized performance (Reference 9). The central inverter not only converts dc to ac, but performs a key control function of providing the load (voltage) control for the engine. Finally, the inverter provides grid synchronization at a single point, rather than having multiple synchronizations as would be required for an ac system.

The inverter load control function operates as follows. As input (dc) voltage increases--which corresponds to a power increase from one or more modules--the inverter increases its output power by increasing its SCR switching duty cycle, which reduces the input resistance of the inverter. This causes a greater voltage crop across the equivalent resistance of the alternator(s). A drop in inverter input voltage (i.e. a drop in input power) produces an opposite effect. The inverter is a self-commutating unit with a bridge type SCR power switching regulator. Capacitors and inductors are used for commutation of the SCRs and an ac filter is provided. The outputs from the square wave inverter and the ac filter are combined to provide a sinewave output. The utility voltage is sampled and fed back through an isolation transformer to a control circuit which synchronizes the inverter with the utility. Power factor control is also provided to maintain this parameter within specified limits.

The switchboard performs the function of routing power to and from the various components such as the PCAs, computers, inverter, UPS, load bank, and utility grid. It also provides mimic lights to indicate which components are operating and breakers to isolate each electrical circuit. The switchboard also contains the sensors to measure input (dc) voltage and current to the inverter and output (ac) voltage, current and power factor.

The inverter and switchboard for the Edwards tests are subscale units rated at only 30 kVA since they were designed to handle only one power module. However, the design and operating principles are the same as will be used for a multi-module plant in the next phase of the program. The test data demonstrated that the inverter will maintain the dc voltage within ±5 V of the predetermined setting (~500 Vdc) in the inverter except during periods of low power output ("idle mode"). It has also been shown that the inverter will control the voltage (load) from the simultaneous output of two sources: the

power module and the simulated output of another module using a dc power supply. The measured inverter efficiency is 83.3 percent at an input power of 16.2 kW_e and a voltage of 500 Vdc. Peak efficiency is 87 percent at 26.8 kW_e input when the unit is fed from both the power module and the dc power supply.

Plant Control Subsystem

The plant control subsystem is described in References 2, 10, and 11 and only a summary is included here. Two types of computers perform the control* and monitoring functions. A microprocessor in the RCIA controls each engine, of which there was only one for the Edwards PDTS tests. The RCIA also has the capability to control the concentrator, which is now being implemented for the next phase of the program. This digital unit performs data encoding for the PCS and receiver, PCA mode control, and control loop functions. A minicomputer (MPC) provides overall control, communicates with the RCIAs and displays/records data. A unit called the Central Control Interface Assembly (CCIA) provides the means of interfacing the MPC to external subsystems. A serial data link connects the MPC with each RCIA.

The solar tests demonstrated that the control subsystem achieves stable, controllable and safe operation of the SCSE hardware over a wide range of input conditions (References 4 and 12). This included severe transients caused by deliberately closing a water cooled door to shut off the solar input to the receiver or vice versa. The fluid temperature at the receiver outlet was normally controlled by the RCIA to 399 ±3°C (750 ±5°F) despite short periods of solar insolation variation of over 2:1. These tests constituted the first demonstration of a truly automatic control for a point focus, distributed receiver solar plant, and tests over the range of operating conditions were completely successful.

SYSTEM PERFORMANCE

The component and subsystem performance and efficiencies that were obtained during a typical solar test at Edwards have been combined to yield a "waterfall" chart with "module" and "overall" performance and efficiency values. The term "module" refers to the power out of the inverter.

Typical results are shown in Figure 3. The example selected was 12:00 noon during Run 13 (March 3, 1982). The solar insolation from the local Eppley pyrheliometer at this time was 983 W/m^2. The power available for focusing was 83.1 kW based on the projected area of the concentrator's reflective surface and a factor to account for the circumsolar effect, i.e. the wide field of view of the pyrheliometer compared to the size of the sun. The value of 74.4 kW shown the second step of Figure 3 and the corresponding efficiency of 89.6 percent was obtained from the reflectivity, average dust correction factor and blockage ratio for the concentrator (0.95, 0.975, and 0.967, respectively). The receiver performance ("RCVR" in Figure 3) was obtained by measuring the pressure and temperature of the toluene at the inlet and outlet of the receiver, determining the mass flow rate and change in enthalpy of the fluid and calculating the power. This was compared to an independent calculation accounting for the theoretical losses from the

*Note that the inverter performs voltage (load) control independently of the computers.

receiver due to conduction, reradiation, convection and reflection. For this particular example, the measured receiver efficiency was 95.2%; slightly higher efficiency will be obtained at higher input power.

The PCS efficiency and power shown in Figure 3 have two values, the one in parenthesis is the net value and has the measured fan and pump parasitic power subtracted. The PCS output power was obtained from the measured voltage and current from transducers in the switchboard.

The overall or system efficiency for this example case was 15.5 percent (net) or three points less than that for the module due to losses through the inverter (83.3 percent efficient). As previously mentioned, the inverter was a small unit sized for a rated input of 30 kVA and was operating at only 16.2 kW for this test. Also, the input voltage was set at 500 V compared to a design value of 600 V, thus increasing the I^2R losses.

The performance values shown in Figure 3 were calculated in real-time using the Ford Aerospace Power/Energy/Efficiency Program located in the MPC. Each of the 19 values output by the program were updated at one second intervals and could be displayed on the CRT as one of the display options. Also the values from the program, as well as the remaining 74 data channels, were stored on magnetic tape and could be plotted as a function of time. Typical plots are shown in the following paper and proved to be very valuable in evaluating component and subsystem performance.

The February-March tests at the PDTS were successful and satisfied all of the major objectives of the program. The performance and operating characteristics of all components were verified. These tests constituted the first demonstration of a truly automatic control for a point focus, distributed receiver solar plant.

FUTURE PLANS

The next test series for SCSE at the Edwards site will be the evaluation of improved TAP bearings using the concentrator (TBC-1) used for the Feb.-March 1982 tests. Then the equipment will be moved to the new 12m Parabolic Dish Concentrator No. 1 (PDC-1) which is now undergoing performance evaluation. PDC-1 was designed by General Electric and assembled by Ford Aerospace. It features a front-braced structure, plastic reflective surfaces and an inverted stow position. A paper on this concentrator is given in Session III.

The final phase of the program (Phase III) will address the design, fabrication, installation and checkout of the hardware and software elements required for a 100 kW_e plant to be located at Osage City, Kansas. Funding for this effort has been provided by Congress and the implementation of Phase III is awaiting certain programmatic decisions by the Department of Energy.

REFERENCES

1. Haskins, H. J., Taylor, R. M., and Osborn, D. B., "Development of a Solar Receiver for an Organic Rankine Cycle Engine", IECEC Paper No. 819750, Atlanta, GA, August 9-14, 1981.

2. Pons, R. L., "Development Status of the Small Community Solar Power System", Third Parabolic Dish Review, Atlanta, GA, December 7-10, 1981.

3. Osborn, D. B., Haskins, H. J., Conway, W. A. and Wan, C. C., "Design and Test of a Solar Receiver for an Organic Rankine Cycle Engine", ASME Solar Energy Conference, Albuquerque, NM, April 26-30, 1982.

4. Clark, T. B., "SCSE Power Conversion Assembly Verification Test on the TBC", SCSE Report No. 023, Ford Aerospace & Communications Corp., April, 1982.

5. Pons, R. L. and Boda, F. P., "Preliminary Test Results for the Small Community Solar Power System", ASME Paper 82-WA/Sol-30, November 1982.

6. Boda, F. P., "The SCSE Organic Rankine Engine," IECEC Paper No. 819610, Atlanta, GA, August 9-14, 1981.

7. Barber, R. E. and Boda, F. P., "Organic Rankine Power Conversion Subsystem Development for SCSE", Third Parabolic Dish Review, Atlanta, GA, December 7-10, 1981.

8. Boda, F. P., "Test Results for the Small Community Solar Power System", Fourth Parabolic Dish Solar Review", Pasadena, CA, November 30-December 2, 1982.

9. Pons, R. L. and Dugan, A. F., "A Small Community Solar Thermal Power System", Solar Sciences, Spring 1982 (pp. 15-35).

10. Bergthold, F. M., Fulton, D. G. and Haskins, H. J., "Control System Development for an Organic Rankine Cycle Engine", ASME 3rd Annual System Simulation Conference, Reno, Nevada, April 27-May 1, 1980.

11. Daubert, E. R., Bergthold, F. M. and Fulton, D. G., "Control System Development for a 1 MW_e Solar Thermal Power Plant", IECEC Paper No. 819751, Atlanta, GA, August 9-14, 1981.

12. Fulton, D. G., "Control System Development for SCSE", Fourth Parabolic Dish Solar Review", Pasadena, CA, November 30-December 2, 1982.

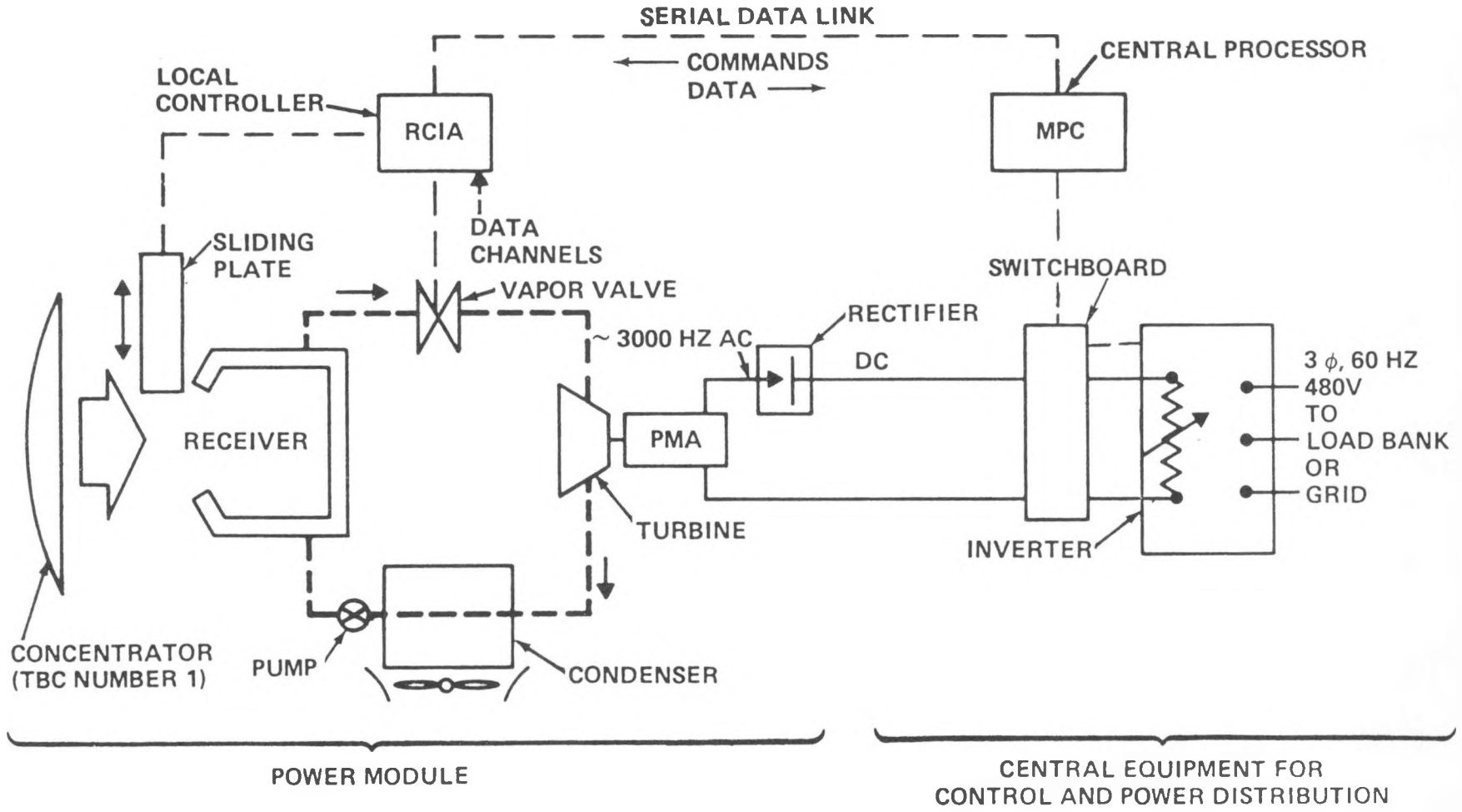

FIGURE 1. SIMPLIFIED SCHEMATIC OF PDTS EXPERIMENT HARDWARE

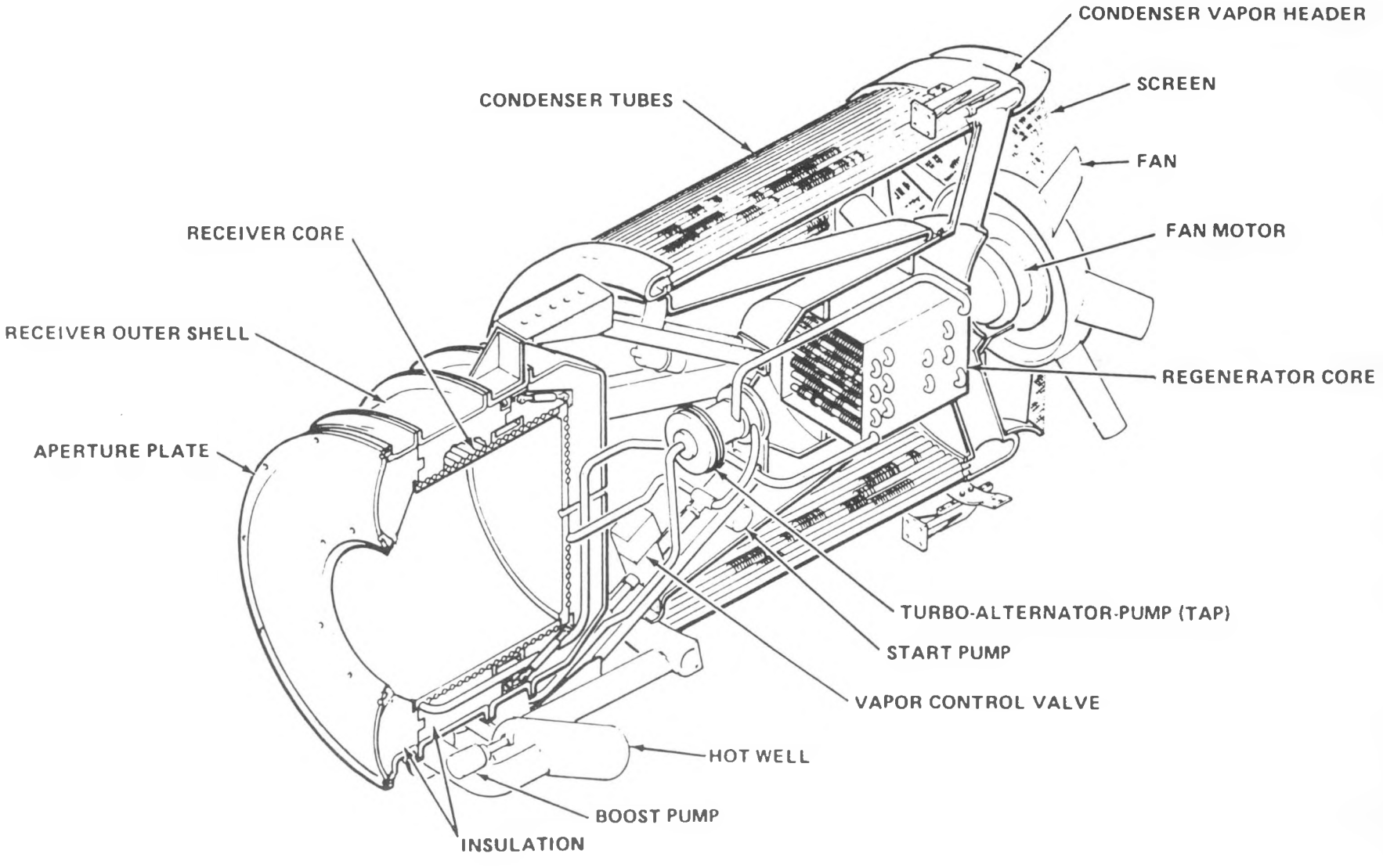

FIGURE 2. POWER CONVERSION ASSEMBLY (PCA)

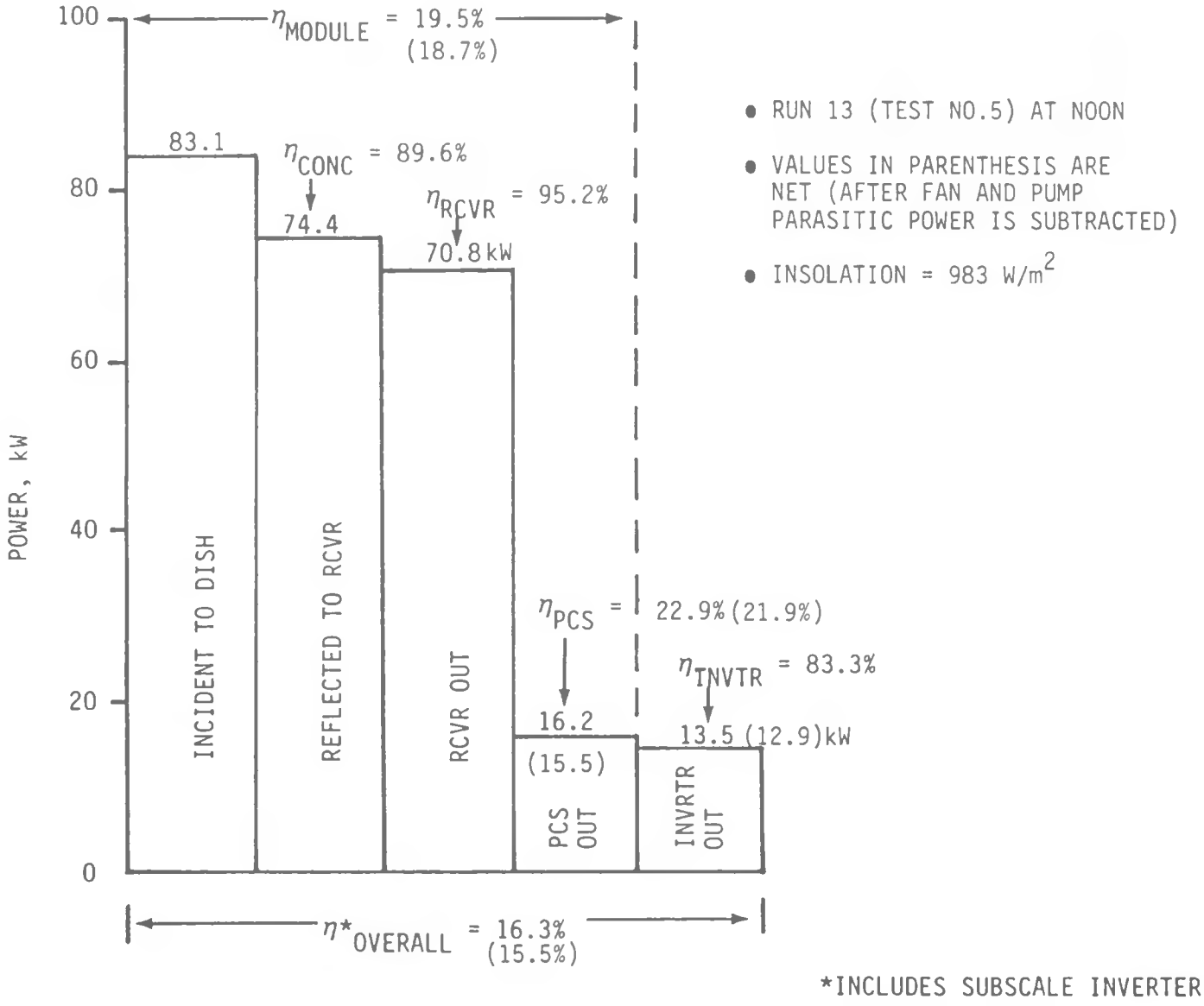

FIGURE 3. MEASURED COMPONENT, MODULE AND SYSTEM PERFORMANCE FOR A TYPICAL SOLAR TEST (MARCH 3, 1982)

CONTROL SYSTEM DEVELOPMENT FOR THE SMALL COMMUNITY SOLAR POWER SYSTEM

D. G. Fulton

Ford Aerospace & Communications Corp., Aeronutronic Division
Newport Beach, CA 92663

ABSTRACT

This paper describes the operation of the SCSE plant control system. Emphasis is on the computer control functions of a single module with test results obtained from the demonstration performed at the JPL Parabolic Dish Test Site at Edwards Air Force Base. The extension of the logic for the control of a multiple-module automatically-controlled plant is also described.

SYSTEM DESCRIPTION

The Small Community Solar Experiment (SCSE) plant consists of a number of power modules delivering power to a central collection point where the power is appropriately converted and delivered to the utility interface. Each power module consists of a parabolic dish concentrator with a receiver and a regenerative, air-cooled organic Rankine cycle (ORC) engine/alternator power conversion system (PCS) located at its focus. Three-phase ac power is transferred to a rectifier at the base of each concentrator and converted to 600 volts dc. The dc power is transported to the central collection site where it is supplied directly to the common dc bus which collects the dc power from all the other modules in the plant. This bus then drives the inverter, which produces utility grid-compatible ac power.

In addition to efficient collection of the sun's energy by the concentrator, the key elements of efficient power generation at all input power levels are control of the working fluid temperature and control of turbine speed to maximize the overall efficiency of the power conversion. These major control system tasks are:

1. Concentrator Pointing Control. The concentrator is provided with controls to allow it to perform all required functions, such a stow, acquire sun track by using ephemeris data, or sun track using sun sensors.

2. Fluid Temperature Control. The engine's cycle efficiency is maximized by maintaining the working fluid temperature at the receiver outlet at the maximum allowable value, thereby maximizing the turbine inlet

temperature. This is accomplished by varying the fluid flow rate by means of a controllable vapor valve at the receiver outlet, thereby varying the power delivered to the turbine as the solar insolation changes. During normal operation at either part or full load, the working fluid temperature at the receiver outlet is maintained at 399 degrees C (750 degrees F), which is dictated by the limitations of the working fluid (toluene).

3. Turbine Speed Control. At every input power level, the turbine has an optimum speed which maximizes efficiency. The technique of rectifying the generated power to dc removes the requirement that the alternator operate synchronously with the grid, and permits variation of the turbine speed for control purposes. It may be shown that by selecting the alternator characteristics properly, the torque balance of the turbine and alternator will result in very nearly the optimum turbine speed at all power levels if the alternator is driving a constant-voltage load. The constant-voltage load is produced by the central inverter, which varies its chopper duty cycle and hence its effective input impedance, keeping the input voltage nearly constant. All power modules are thus controlled to the optimum turbine speed at all power levels by the central inverter and the requirement for individual alternator field control is avoided.

The overall control of the plant requires implementation of the above tasks as well as many logic control functions at both the power module and the plant level. The computer hierarchy used to provide this control is designed to make each power module relatively self-sufficient by providing it with its own processor which is called the Remote Control Interface Assembly (RCIA). All of the RCIAs are then put under the control of the Master Power Controller (MPC) which performs the overall plant data and control functions. A two-way serial data link is provided to connect the MPC with all RCIAs. More complete descriptions and analyses of the control system components are contained in References 1-3.

The central plant control requirements are met by implementation of the MPC hardware and by its software program. The MPC is configured around a Data General Nova 4/X minicomputer. The unit includes 65K words of MOS semiconductor memory and a 6.25 M word Winchester disk. Operator interfaces are provided by a Cathode Ray Tube (CRT) display with a keyboard and a printer. Interface cards are mounted in the Nova chassis for A/D and D/A conversions, discrete I/O and serial digital data links. A magnetic tape recorder is provided for data recording. The primary functions of the MPC are:

- Read keyboard or remote entries from the plant operator.

- Send data to and receive data from the RCIA at each Power Module via the serial data link.
- Collect analog and discrete data from the Energy Transport Subsystem (ETS), and from the Weather Station.
- Display data on the operator's CRT.
- Print data in real time on the local printer.
- Record all data collected on magnetic tape for later playback.
- Perform specified logic functions relative to control of the ETS and the Power Modules.
- Compute ephemeris data for the concentrator and transmit to all RCIAs.

Each Power Module is controlled by an RCIA and its software program, the Remote Operational Program (ROP). The RCIA is a Z80-based microprocessor installed in a weather-proof NEMA enclosure located at the base of the concentrator. The processor and associated support and I/O circuitry are built on STD BUS boards by Pro-Log Corporation, and are designed to operate in a wide temperature range (-25 C to +49 C). The RCIA is under the high level supervision of the MPC by means of commands on the MPC/RCIA serial data link. The functions which the RCIA must perform are:

- Read any of the specified data messages from the MPC serial data link.
- Sync its one-second cycle to the MPC by receiving the SYNC command on the serial data link.
- Send a long or short data message or a circular buffer dump to the MPC on request.
- Perform debug functions as required.
- Perform Power Module automoding logic (see a later section of this paper).
- Perform detailed PCA control.
- Perform detailed concentrator control.

OPERATIONAL EXPERIENCE

Verification tests of the SCSE elements were conducted at the JPL Parabolic Dish Test Site (PDTS), at Edwards Air Force Base during the first

quarter of 1982. The test configuration utilized the complete control system including the MPC and RCIA, and the Electrical Transport Subsystem (ETS) consisting of the inverter, switchboard and cabling. Tests were conducted on the JPL Test Bed Concentrator (TBC) with a sliding water-cooled plate provided to open and close the aperture of the receiver. The following sections describe the control system configuration which was used for these tests and show some of the test results. These tests are described fully in Reference 4.

Operator Control

The MPC/RCIA software configuration provides manual control capability which gives the operator a high degree of flexibility over the PCS operation. The repertory of available mode commands was expanded as the testing progressed, and proved to be useful in dealing with abnormal or unexpected situations. In future tests the software will include logic to deal with all contingencies, and the manual mode control functions will be eliminated or rarely used.

The PCS mode control functions available to the operator are:

- PCA TEST ON/OFF. Initiate pump start procedure.
- PCA COOLDOWN ON/OFF. Flow fluid without spinning the turbine.
- SPEED CONTROL ON/OFF. Turbine speed control mode.
- HIGH POWER ON. Force wide open valve command.
- DETRACK. Close sliding plate.
- EMERGENCY SHUTDOWN. Close sliding plate and shut engine down.
- FAULT RESET. Clear faults and warning flags.
- START. Force turbine start.
- PCA ON/OFF. Enable startup sequence.

Startup Control Sequence

The RCIA software is programmed to automatically start and run the turbine when it has been enabled by the operator. During operation, the operator observes the sequences, but unless problems develop, is not required to take any action. During the tests which were conducted, the concentrator (TBC) was not under control of the SCSE computer; this capability is now being developed for future tests and for the Phase III

power plant. The RCIA is programmed to initiate a startup procedure when a rising receiver shell temperature is observed. The automatic sequence includes pump and fan start commands, valve command to start the turbine, and fluid temperature control at the receiver outlet. When the solar insolation is removed by moving the concentrator off-sun, or by a cloud passage, the temperature is controlled as long as possible, and the turbine is then shut down.

Vapor Valve Control Law

The primary task of the vapor valve control law is to control flow (power) to the turbine so as to keep the toluene temperature at the receiver outlet at a constant temperature of 750 degrees F. A simplified block diagram of the control law which was used to do this is shown in Figure 1. As shown in the figure, the inner loop controls the receiver shell temperature, and has a control time constant of about 10 seconds. This loop drives the shell temperature to a value, SETPT, which is determined by the outer loop which has a time constant of about 6 minutes.

A sample startup transient is shown in Figure 2. The sliding plate was opened at 13:06 and the turbine was started at 13:10. The receiver outlet temperature was above 700 degrees F within 3 minutes although the system was not well stabilized until about 20 minutes after the start.

As the input power decreases (i.e., cloud passage) the vapor valve closes to try to keep the receiver fluid exit temperature at 750 degrees F. If the input power drops too low, the output voltage will go below the control voltage of the inverter while the turbine speed continues to drop. The control law then changes to a speed control loop, controlling the turbine speed to about 35,000 rpm. When the input power returns, the temperature rises and the control law returns automatically to the temperature control mode. An example demonstrating this action is shown in Figure 3, where a cloud passage was simulated by closing the sliding plate for 4.5 minutes. During the time the valve command was on the minimum speed limit, the temperature dropped because energy was still being withdrawn and the heat input was zero. During this time the control variable SETPT was ramped down so as to prevent a temperature overshoot when the solar power returned. When the sliding plate was opened, the temperature began rising, and within about 5 minutes the major part of the transient was over. The receiver temperature and valve position for this same run are shown in Figure 4.

A typical record of cloud passages is shown in Figure 5. The figure shows that the valve position responded to the insolation level changes thereby changing the power delivered to the turbine. Throughout the run, however, the toluene temperature at the receiver outlet was kept within about 20 degrees F of the desired 750 degrees F, even when the insolation dropped to one-third of its normal level. Normally, the temperature is held to within ± 5 degrees F for short periods (approximately 1 minute) at insolation levels as low as one-half of the normal value.

The performance of the inverter voltage control may be observed on Figure 6, which is a plot of the same test run as Figure 5. Figure 6 shows the dc voltage (input to the inverter) and the turbine speed as the solar insolation is varying. During most of the time, the dc voltage is nearly constant and the turbine speed is held within a fairly narrow band even when the input power is varying widely. If the input power drops too low for too long (e.g. as shown at a time of 09:13 on Figures 5 and 6), the flow rate is reduced by the temperature-control law so much that the turbine stops producing positive output power, and the speed begins to drop. The inverter remains on-line, but goes to its highest input impedance state, and the alternator is only very lightly loaded. When the turbine speed drops, the valve control law reverts to the speed-control mode and holds the speed at 35,000 rpm. When the insolation returns, the temperature rises, the vapor valve opens, the dc voltage increases to the active control range of the inverter and the turbine speed again becomes controlled by its applied load.

AUTOMODING

Automoding refers to the computer logic which allows the plant and its sub-components to operate automatically, i.e. without operator action. To implement this automatic operation, the logic is structured in a hierarchy involving the plant, the ETS, the Power Modules, the PCAs and the concentrators. The logic structure is illustrated in Figure 7. Two major categories of logic are shown here: Plant Modes and ETS Modes are controlled by the MPC; and Power Module Modes, PCA Modes and Concentrator Modes are controlled by the RCIA.

The plant modes may be commanded by the plant operator or by logic within the MPC, and are implemented by sending Power Module mode commands to the RCIA at each power module by means of the serial data link. A brief description of the function of each of the plant modes is as follows:

- Manual Plant Mode. Allows the plant operator to input the Power Module Mode of individual modules.

- Out Of Service. Disables the operation of all Power Modules. This plant mode is provided to allow for maintenance or other intentional down time.

- Emergency Shutdown. Shuts the plant down in the normal manner, but sets the Emergency Shutdown Fault flag which prevents the plant from re-starting without operator intervention.

- Shutdown. Shuts all power modules down, waits until they have completed shutdown and are stowed, and then changes the Plant Mode to Ready. The plant will re-start if the appropriate conditions are met.

- Self Test. Commands all modules to Self Test mode.

- Standby. Commands all modules to Standby.

- Ready. The normal enabled mode of the plant while waiting for conditions suitable for generating power.

- Normal Power. The plant mode when power is being generated. Power generation will continue until some reason exists to stop. The mode will then be changed to Shutdown or Emergency Shutdown.

The Power Module modes may be commanded to the RCIA from the MPC, or may be determined by mode logic within the RCIA. The modes are implemented by generating mode commands to the PCA control and the concentrator control. A summary of the functions performed by the Power Module Modes is as follows:

- Power Module Manual. Allows processing of PCA mode and concentrator mode commands from the plant operator.

- Stow. Waits for PCA mode Poweroff and then commands the concentrator to stow.

- Standby. Commands the concentrator to Offset Track.

- Self Test. Performs a sequence of tests on the concentrator and PCA to determine that the module is healthy.

- Power On. First initiates Self Test mode. If the self test passes, the concentrator is brought on sun, the turbine is started and power is generated until a stop criterion is reached.

- Power Down. Takes the concentrator off sun, waits for the turbine to shut down and then commands Stow mode.

STATUS

The test program which has been completed successfully demonstrated the key elements of engine control including:

- Automatic startup and shutdown procedures.

- Fluid temperature control under varying insolation conditions.

- Turbine speed control by the inverter (constant input voltage).

- Automatic fault monitoring.

- Stable operation under all conditions.

Effort is currently under way to define the software requirements to complete the software development to provide completely automatic plant control.

REFERENCES

1. Daubert, E.R., Bergthold, F.M. Jr. and Fulton, D.G., "Control System Development For a 1 MW Solar Thermal Power Plant", Paper No. 819751, IECEC Conference Atlanta, GA, August, 1981.

2. Bergthold, F.M. Jr., Fulton, D.G. and Haskins, H.J., "Control System Development For an Organic Rankine Cycle Engine", ASME Solar Energy Division 3rd Annual Systems Simulation Conference, Reno, Nevada, May 1981.

3. Pons, R.L., "Development of the Small Community Solar Power System", Third Parabolic Dish Solar Thermal Power Annual Program Review, Atlanta, GA., Dec. 1981.

4. Clark, T.B., "Power Conversion Assembly Verification Test on the TBC and Energy Transport Subsystem Qualification", SCSE Report No. 023, Ford Aerospace and Communications Corp., April 1982.

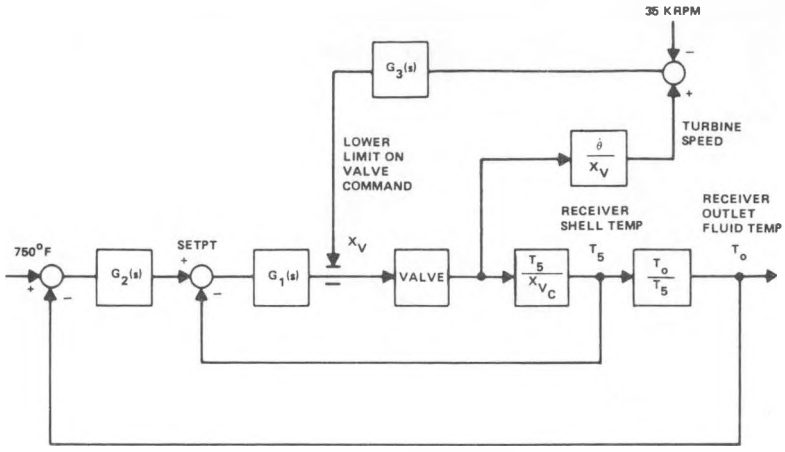

$$G_1(s) = \frac{1.6}{0.5s+1}, \quad \%\ \text{VALVE}/^{\circ}\text{F}$$

$$G_2(s) = .00153\ \frac{190s+1}{s}, \quad \frac{^{\circ}\text{F/SEC}}{^{\circ}\text{F}}$$

$$G_3(s) = 0.4\ \frac{10s+1}{s}, \quad \frac{\%/\text{SEC}}{\text{KRPM}}$$

FIGURE 1. VAPOR VALVE CONTROL LAW

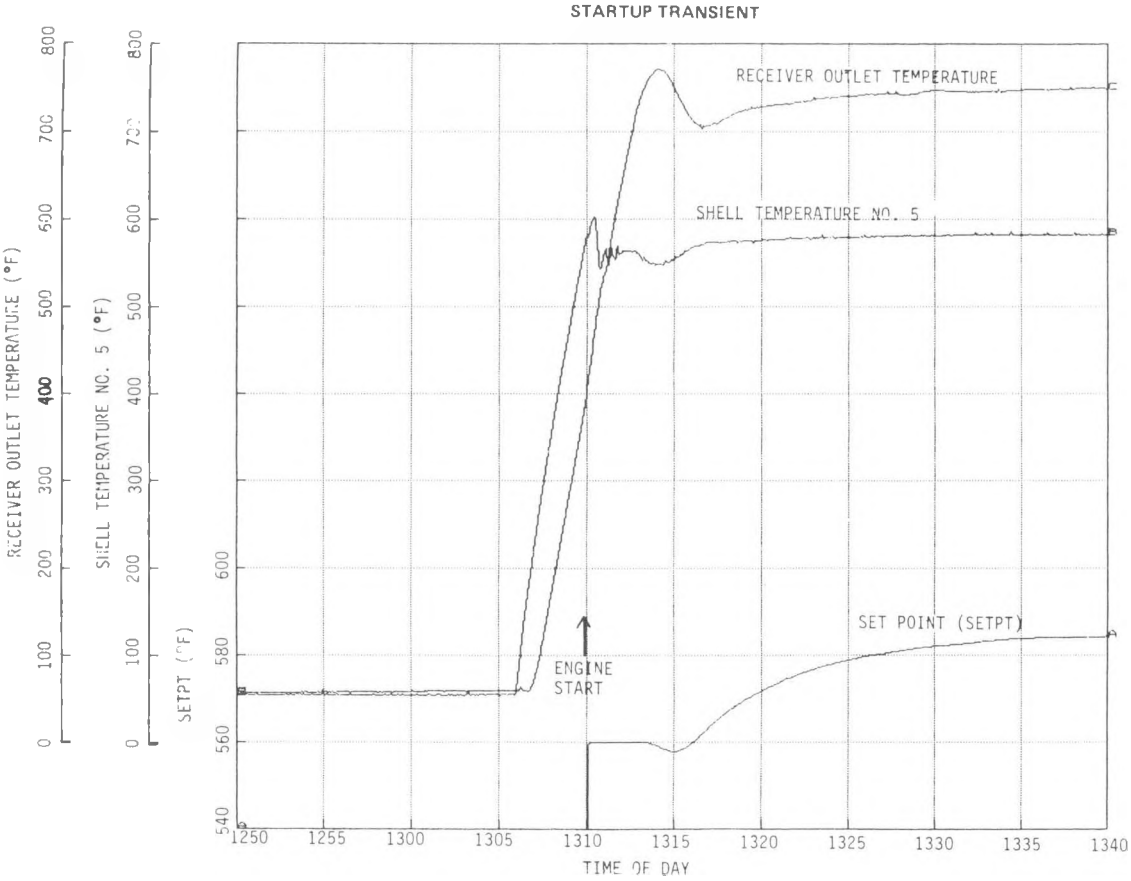

FIGURE 2. STARTUP TRANSIENT

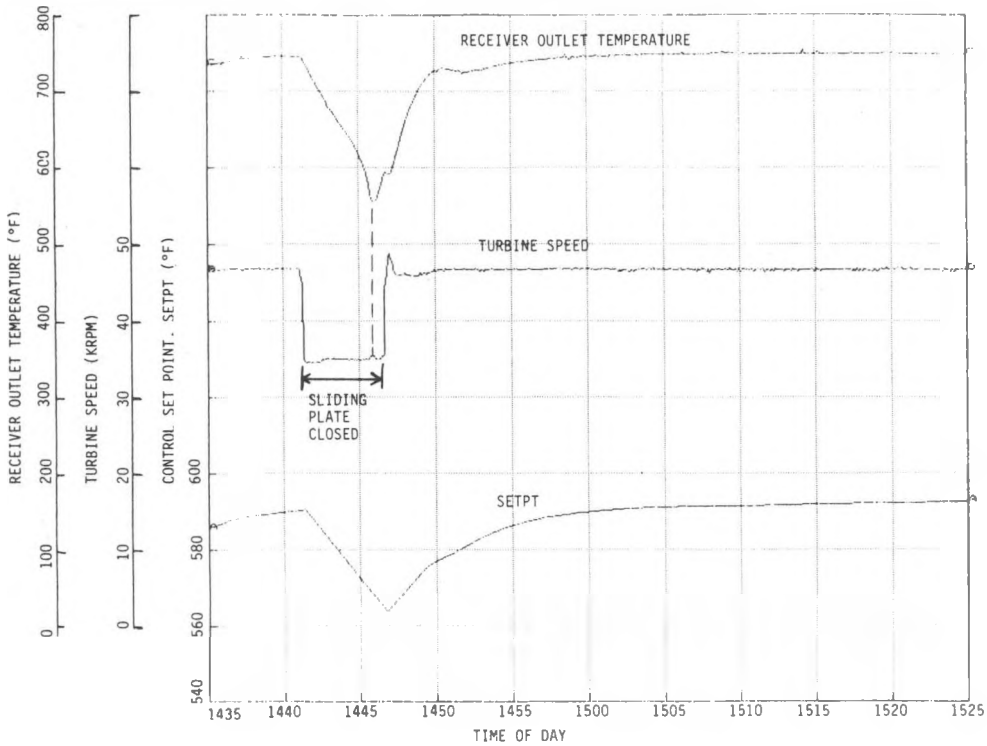

FIGURE 3. TRANSIENT INTRODUCED BY CLOSING THE SLIDING PLATE

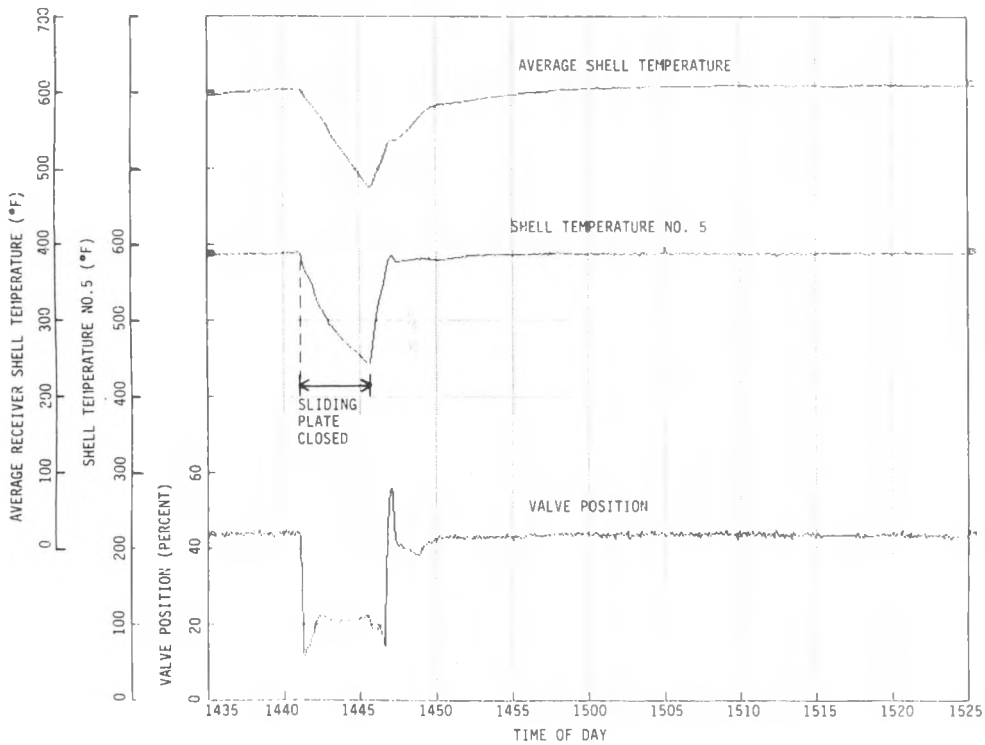

FIGURE 4. TRANSIENT RECEIVER TEMPERATURE AND VALVE POSITION CAUSED BY CLOSING THE SLIDING PLATE

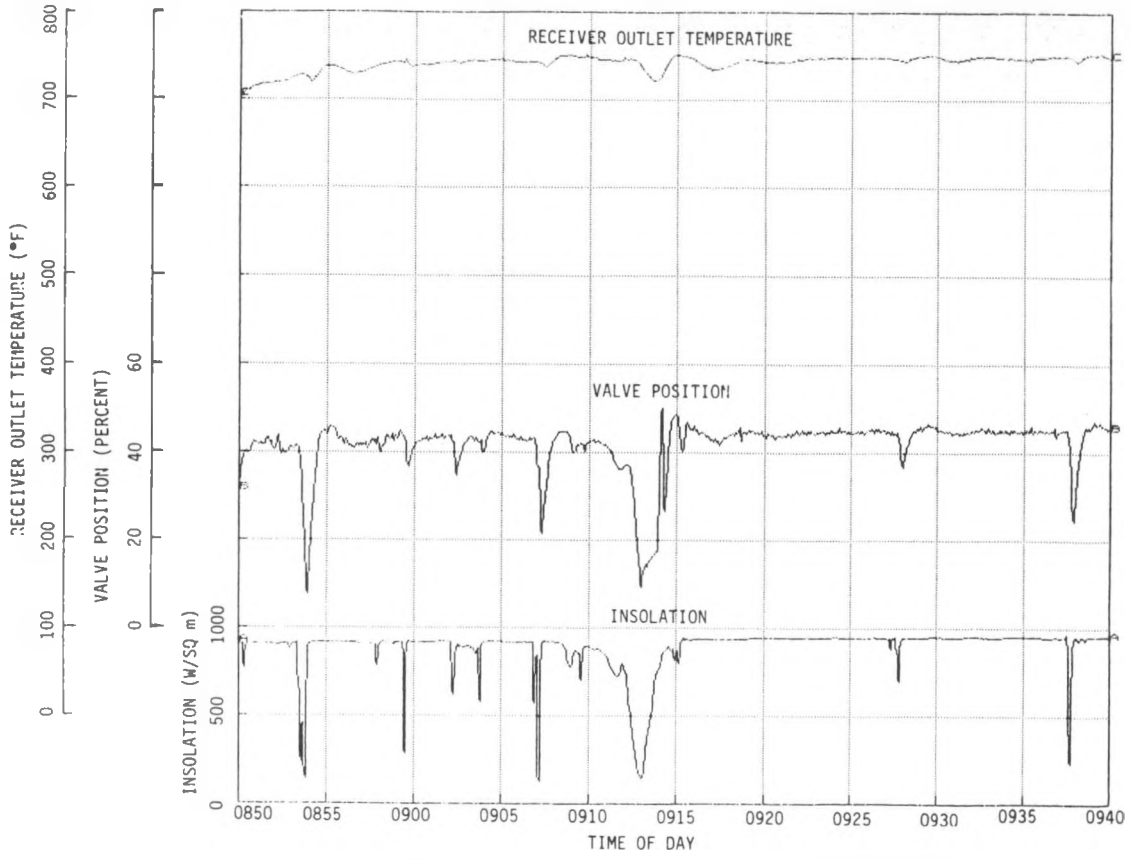

FIGURE 5. TEMPERATURE RESPONSE TO CLOUD PASSAGES

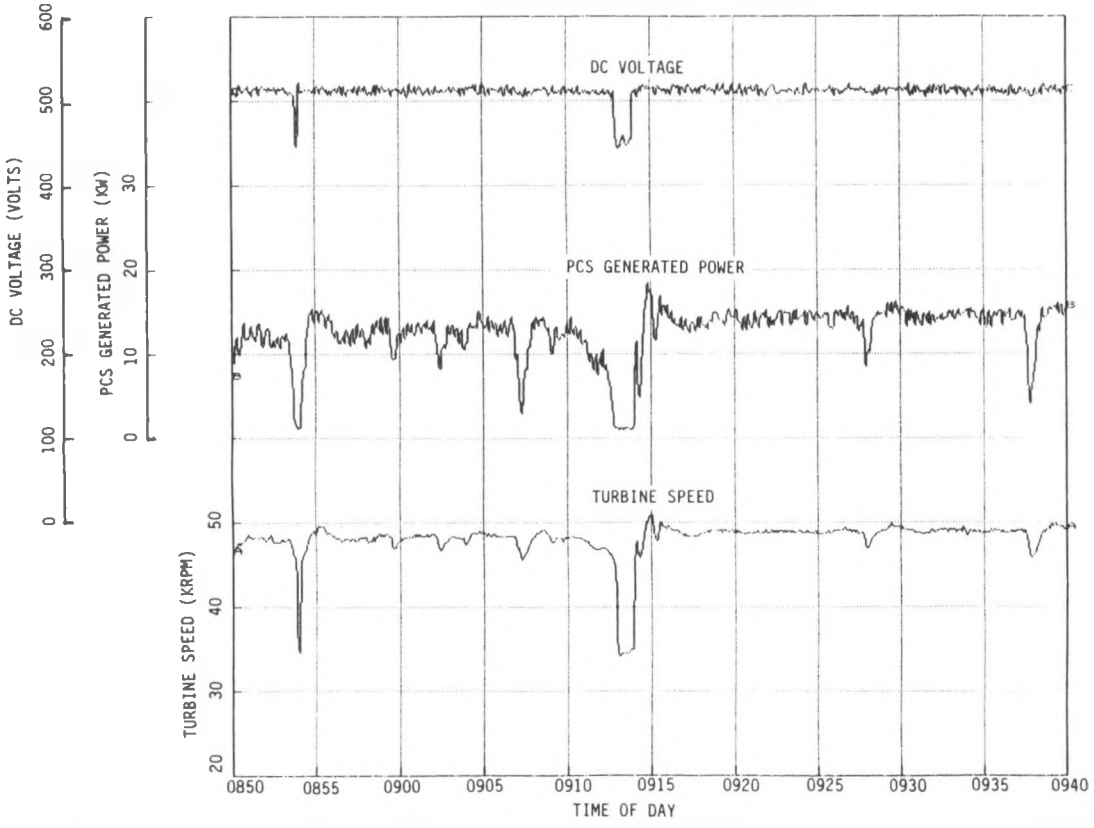

FIGURE 6. VOLTAGE/POWER/SPEED RELATIONSHIPS DURING A CLOUD PASSAGE

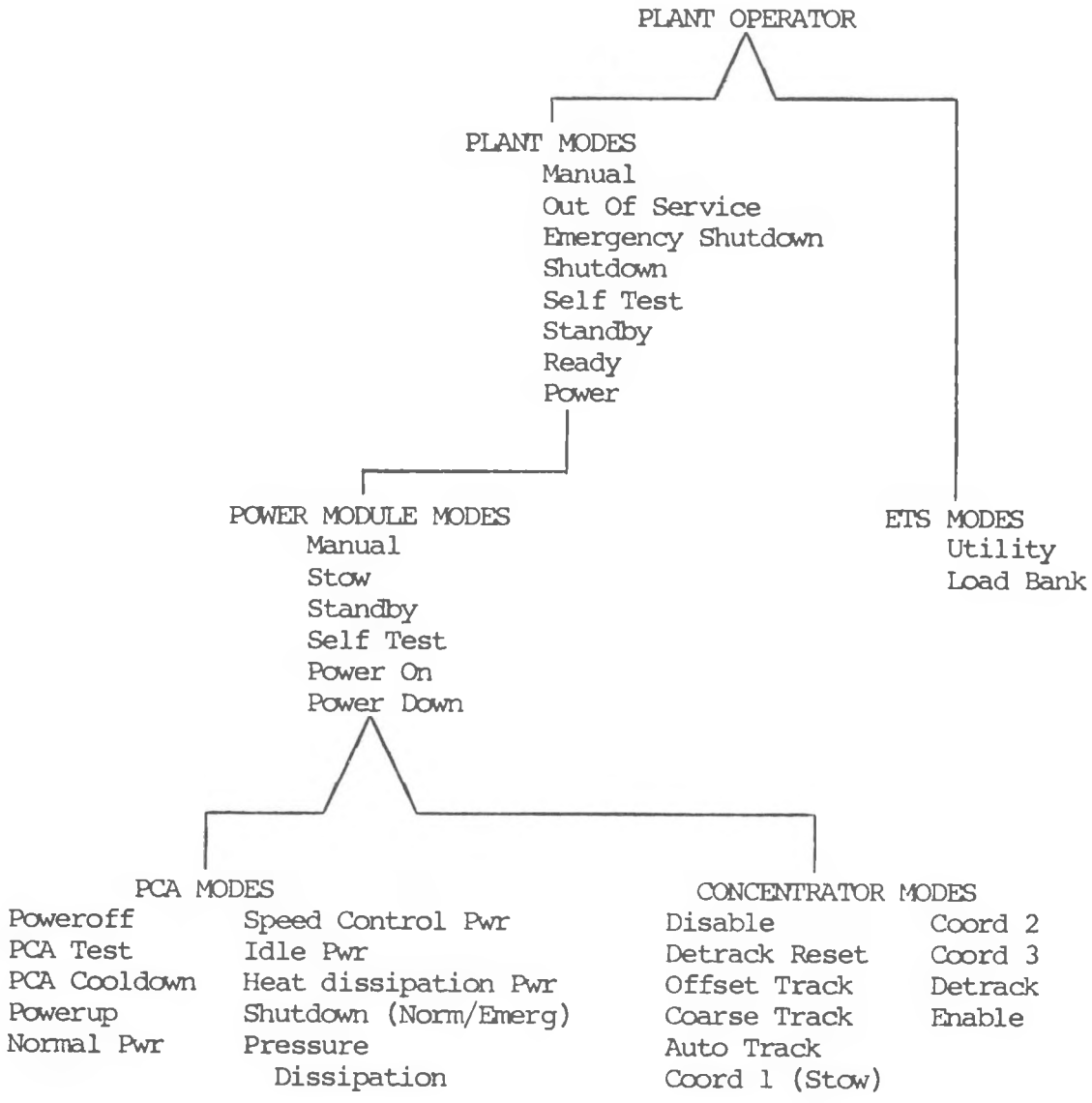

FIGURE 7. PLANT MODING HIERARCHY

TEST RESULTS FOR THE SMALL COMMUNITY SOLAR POWER SYSTEM

F. P. Boda
Ford Aerospace & Communications Corp., Aeronutronic Division
Newport Beach, CA 92660

ABSTRACT

This paper describes the testing which has been conducted to date on an organic Rankine cycle (ORC) power module and ancillary equipment as part of the Small Community Solar Thermal Power Experiment (SCSE) program (JPL Contract 955637). The power module consists of an air-cooled, regenerative 20 kW_e turbo-alternator system coupled to a cavity-type receiver (boiler), all mounted at the focus of a parabolic dish concentrator. The ancillary equipment includes a complete computer-based plant control subsystem and an electrical transport/conditioning subsystem with voltage control and grid interface capability.

Development testing of individual components and Qualification testing of major subsystems began in 1981. Full-up system testing "on the sun" was conducted in February and March of 1982 at the JPL Parabolic Dish Test Site (PDTS) utilizing the 11 meter Test Bed Concentrator (TBC). Computer plots of typical data from these tests are presented in graphical form. These data show the power module operation to be completely stable with excellent control of fluid temperature, pressure, flow, turbine speed and output voltage.

SYSTEM DESCRIPTION

The elements comprising the SCSE system tested at the JPL Parabolic Dish Test Site (PDTS) are described in a companion paper by R. H. Babbe. The "power module" is defined as the solar concentrator and the receiver/engine located at its focus. Ancillary equipment consists of a switchboard, inverter, power cabling and computer and is designed to be centrally located in order to interface with multiple modules which will comprise a typical power plant. The receiver/engine is called the Power Conversion Assembly (PCA), and performs the task of converting concentrated sunlight into electrical energy. It does this by boiling the toluene working fluid in a cavity-type receiver and using the 750°F vapor to drive a single-stage, axial-flow turbine which is directly coupled to a permanent magnet alternator. The turbo-alternator, shown in Figure 1, operates at speeds up to 60,000 rpm. The toluene circulates in a closed loop system and is pumped back to the receiver as a liquid after passing through a regenerator an an air-cooled condenser (see Figure 2).

The high-frequency ac power from the alternator is first rectified to dc so that it may be combined with outputs of other power modules. The dc electrical power is inverted to grid-compatible 3-phase ac. Unattended

plant operation is made possible by a computer-based control subsystem which provides dynamic control of all PCA functions, monitors safety functions, and records performance data.

TEST PROGRAM

The PCA and associated system components have been subjected to a series of development and qualification "ground" tests prior to installation and test on the Test Bed Concentrator (TBC) at Edwards AFB. These tests included:

1) Full functioning of the receiver and vapor control valve at Ford Aerospace using simulated solar flux provided by a 100 kW electrical radiant heater and a toluene test loop. The dynamic response of the receiver was evaluated by moving the heater in and out of the cavity. Receiver performance was completely stable over the design range of input flux and toluene mass flow, and for operation in both supercritical and subcritical pressure regimes.

2) Operation of the two types of computers used in the system was verified by means of a hardware-in-loop simulator. This simulation served to verify the plant-level control commands (control "modes") of the central minicomputer, and the engine control software programmed in the local microprocessor, called the RCIA.

3) The engine (called the Power Conversion Subsystem or PCS) was successfully tested at Barber-Nichols on a tilting test rig to map the performance at various attitudes. A typical test set-up is shown in Figure 3. These tests used an electrically heated toluene boiler and manual control of the engine. Measured net efficiency exceeded 23 percent at high power conditions.

4) Key electrical components were tested at the vendor's laboratories: The dc-ac inverter was tested by NOVA Electric Mfg. Corp., and the Permanent Magnet Alternator (PMA) by Simmonds Precision. The PMA had an efficiency of approximately 94%.

5) The PCA (consisting of the engine (PCS) and receiver) was assembled at Ford Aerospace and tested with the 100 kW electrical heater. The inverter was also used in these tests; it performs the key control function of maintaining a constant dc voltage which is equivalent to PCA load control. These tests were successful and complete functioning of the PCA was accomplished with computer control.

The PCA was installed on the TBC-1 dish at the PDTS in January of 1982. As shown in Figure 4, a water cooled sliding plate and shield were used to protect the receiver face plate from solar flux during the slow acquisition and de-track rate of the TBC. The sliding plate was also used to simulate dynamic events such as cloud passage and to block the flux to the receiver in the event of an emergency condition. (The water cooled units will not be employed when the PCA is tested on the PDC-1 dish; the PDC-1 slew rate is sufficiently fast that the receiver face plate can withstand the solar flux during all operating modes, including acquisition and de-track.)

The test set-up at Edwards included the complete power module with local microprocessor (RCIA), the central computer (MPC), the inverter, switchboard, uninterruptable power supply (UPS), load bank and grid interface protective devices. Weather permitting, on-sun testing was performed between 8 February and 26 March 1982. A total of 33.5 hours of run time was accumulated; sixteen (16) test runs were obtained, ranging from 5 minutes to 7 hours duration under all levels of solar insolation and cloud conditions. A portion of the tests used masking of some of the TBC mirror panels to obtain low power data. The emphasis for the early runs was placed on transient operation to permit evaluation of the control subsystem. This was accomplished by opening and closing the sliding plate for predetermined intervals.

TEST RESULTS

The system "ground" tests using the 100 kW electric heater demonstrated the high potential of the Small Community Solar Power concept. Operation was smooth, quiet and failsafe during all operating modes. A number of problems were detected and addressed, primarily related to excessive wear of the bearings in the turbine/alternator/pump (TAP) unit. The bearings were subsequently redesigned along with changes to the toluene feed system used to lubricate the bearings. Measured PCS efficiency over the complete load range was a few points below analytical predictions, primarily attributable to excessive pressure drop in the regenerator, feed pump losses and PMA losses. However, in view of the relatively good performance achieved and test schedule commitments, it was decided to proceed with solar testing without modification of the regenerator, pump or PMA. These modifications are planned for a subsequent test series.

SCSE System

The data collection technique used for the SCSE solar tests utilizes the central computer (MPC) for real-time processing and recording of performance and test data, and post-test printing or plotting of selected data channels. It is capable of recording, printing and plotting 103 test parameters per second (93 were used for the February-March, 1983 tests), and proved to be invaluable in presenting test results. The data that is permanently filed on magnetic tape for later printing or plotting by the computer includes:

- All key temperatures and pressures
- Voltage and current, both ac and dc
- Power factor
- Turbine speed
- Liquid reservoir level
- Vapor control valve position and commanded position
- Status of discrete events/commands
- Weather data, solar flux, wind speed
- Power, energy and efficiencies (calculated from data inputs)

Table I is a sample page of PCA performance data for data recorded on Run 13 of 3 March 1982. This is only one of 14 pages of print-out available; the complete list is documented in Reference 1.

Figures 5-10 are a representative sample of the actual computer printouts of test data for a time period of 08:30 to 15:30 recorded on 3 March 1982 (Run 13). These test results provide typical performance characteristics of the Small Community System during a 7-hour run under automatic computer control. Figure 5 shows normal, clear-sky operation interrupted only by one early cloud passage and five intentional closures of the water cooled plate. Figure 5 shows the position of the vapor valve (controlled by the RCIA computer) to maintain the desired 400°C (750°F) receiver outlet temperature. The first engine start and subsequent restarts were under the control of the RCIA computer which senses temperature and pressure in the receiver and commands startup (or other modes such as shutdown or idle) based on predetermined criteria. At noon, the measured insolation is 983 W/m^2, which results in an available insolation of 948 W/m^2 after correction for estimated circumsolar effects.

Figure 6 shows that dc voltage out of the rectifier is controlled by the inverter to a pre-set value of 500 ±5 V except during periods of very low power output ("idle mode"), while the output current varies directly with power level. As shown in the figure, turbine speed is also virtually constant at 48,000 rpm (indirectly controlled by the voltage set-point) except during periods of idle mode when the speed is ~35,000 rpm.

Figure 7 is a plot of the relative power levels into and out of the receiver and the PCS. Note that for each sliding plate re-opening there is a momentary overshoot in receiver output power; this is due to a short period surge in toluene flow rate (from the valve opening response) coupled with removal of stored energy in the copper core of the receiver. At noon, the receiver input power* was 74.4 kW, receiver output power was 70.8 kW and PCS power (dc) output was measured at 16.2 kW.

Figure 8 shows receiver efficiency and corresponding measured windspeed and insolation. For the aforementioned noon data point, receiver efficiency is not a strong function of wind speed, despite gusts up to 13-14 m/sec (30 mph).

Figure 9 shows key pressure data for Run 13. The pressure drop between the inlet to the receiver (approximately the same as pump outlet pressure) and the outlet is about 30 psi. The pressure drop between the receiver outlet and turbine inlet is primarily caused by the vapor valve.

PCS Performance

The gross PCS power output is 16.2 kW and the corresponding gross efficiency is 22.9% for the noon time period of Run 13 (Figure 10). Parasitic power consumption was measured at 688 W at high fan speed and is the grid power consumed in running the electrically-driven condenser fan, boost pump and valves. Net power output is therefore 15.5 kW and net efficiency is 21.9%. PCS performance over a wide power operating range is shown in Figure 11, and represents the results of testing carried out to date. Operation at low fan

*Receiver input power is a computed value (Ref. 1) and is based on insolation data and prior measurements which determine the ratio of reflected to incident energy for the TBC-1.

speed (corresponding to lower input power levels) results in better performance than with the high fan speed since the parasitic power is only 373 watts.

In general, the PCS performed smoothly and was quiet and easily controllable. The vapor control valve and the emergency shutdown system worked as planned under all modes of operation. After teardown of the system, some damage was detected with the axial thrust bearing. Barber-Nichols is currently conducting a bearing evaluation test program using the actual turbine/alternator/pump (TAP) assembly on a well-instrumented, laboratory test rig.

Receiver Performance

Figure 12 presents receiver wall temperature data for two steady-state runs compared to the original design predictions. The comparison is quite good considering: (1) the assumed fluid inlet temperature for the prediction was 20°F higher than for the tests, (2) the predictions were based on supercritical flow (600 psi fluid pressure) whereas all the tests at PDTS were conducted at subcritical conditions (480 to 550 psi fluid pressure), and (3) uncertainty in the flux distribution from the TBC. Note the data for the two runs are very close even though the input power to the receiver for Run 13 was 20 percent higher than for Run 17.

The receiver performed extremely well during all solar tests at the JPL PDTS and demonstrated excellent performance during all of the various test conditions (see Figure 8). Boiling and/or flow instabilities and local "hot spots" were not observed during any of these or previous tests, including the subcritical, two-phase flow regime in which the unit operated most of the time, but which was not the original design condition. No design deficiencies were found, and it was concluded that the basic receiver design meets or exceeds all performance requirements.

Inverter Performance

The unique requirement for the inverter is to control the input voltage, which is equivalent to controlling the load on the engine (Reference 3). As shown in Figure 6, voltage control is excellent with a variation of only about ±1 percent from the nominal input voltage during normal power output, that is, above idle conditions. The efficiency of the unit was measured at 83.3 percent for the conditions at noon for Run 13. This value is characteristic of the efficiency for units rated in the 30 kVA range. The fact that the unit was operating only at 16.2 kW for this test and had an input voltage of ~500 V compared to a design value of 600 V contributed to the loss in efficiency (Reference 3).

Control System Performance

The automatic or computer-controlled subsystem was used for the control of all the solar-powered tests. A brief description of the control subsystem and typical results are shown in a following companion paper (Reference 2). In summary, the solar tests for SCSE constituted the first demonstration of a truly automatic control for a point-focus, distributed receiver power plant,

and tests over the range of operating conditions showed complete stability and safe operation.

SYSTEM PERFORMANCE

The component and subsystem performance and efficiencies that were obtained during the typical solar test described above have been combined to form the "waterfall" chart shown in Figure 13. The following conditions apply:

- Time - 12:00 noon, Run 13 (March 3, 1982).
- Insolation - 983 W/m^2 (Eppley reading), 948 W/m^2 corrected for circumsolar effects.
- Performance values for TBC concentrator:
  --Reflectivity = 0.95
  --Dust correction factor = 0.975
  --Blockage ratio = 0.967
  --Projected reflective area of dish = 97.6 m^2

The component efficiency and performance values given in Figure 13 have been discussed above, and are also given in Reference 3. Receiver performance was obtained by using the measured fluid pressure and temperature data and a correlation of mass flow.

The overall or system efficiency for this example case was based on the power out of the inverter divided by the power available to the concentrator for focusing. This value was 15.5 percent (net) or three points less than that for the module due to losses through the inverter (83.3 percent efficient).

CONCLUSIONS

The February-March tests at the PDTS were successful and satisfied all of the major objectives of the program. The performance and operating characteristics of each component was verified and the dynamic response was excellent. Although some problems with bearing life and component efficiencies showed up, substantial progress has been made toward their solution. Planned modifications to the bearings, nozzles, pump and alternator should result in further increases in efficiency and a long life system. The operation of the computer-based plant control subsystem was excellent and we project a successful, fully automatic plant operation in later phases of the Small Community System.

REFERENCES

1. Clark, T. B., "SCSE Power Conversion Assembly Verification Test on the TBC", SCSE Report 023, Ford Aerospace & Communications Corp., April 1982.

2. Fulton, D. G., "Control System Development for SCSE", Fourth Parabolic Dish Solar Review, Pasadena, CA, Nov. 30-Dec. 2, 1982.

3. Babbe, R. H., "Status of the Small Community Solar Power System", Fourth Parabolic Dish Solar Review, Pasadena, CA, Nov. 30-Dec. 2, 1982.

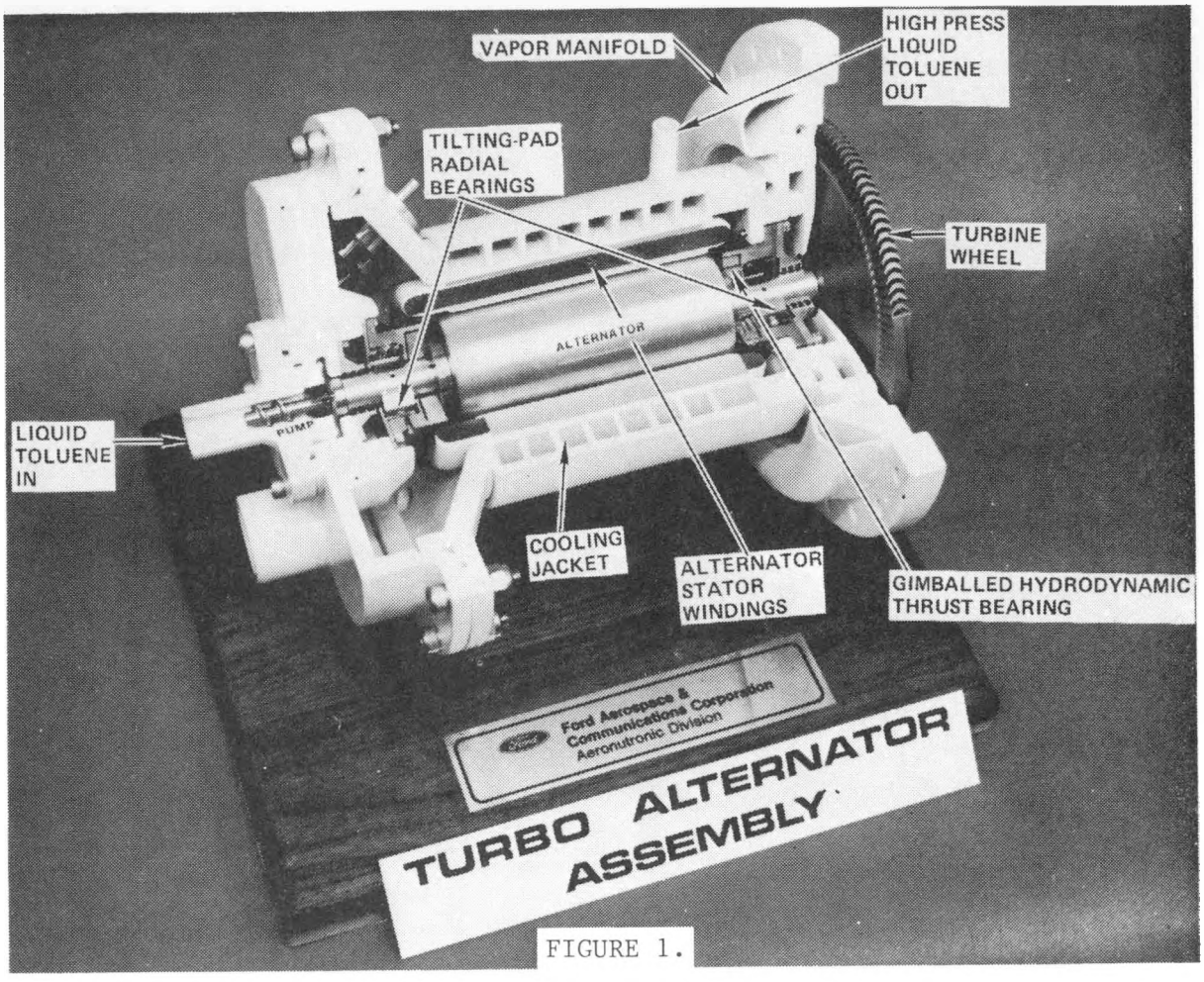

FIGURE 1.

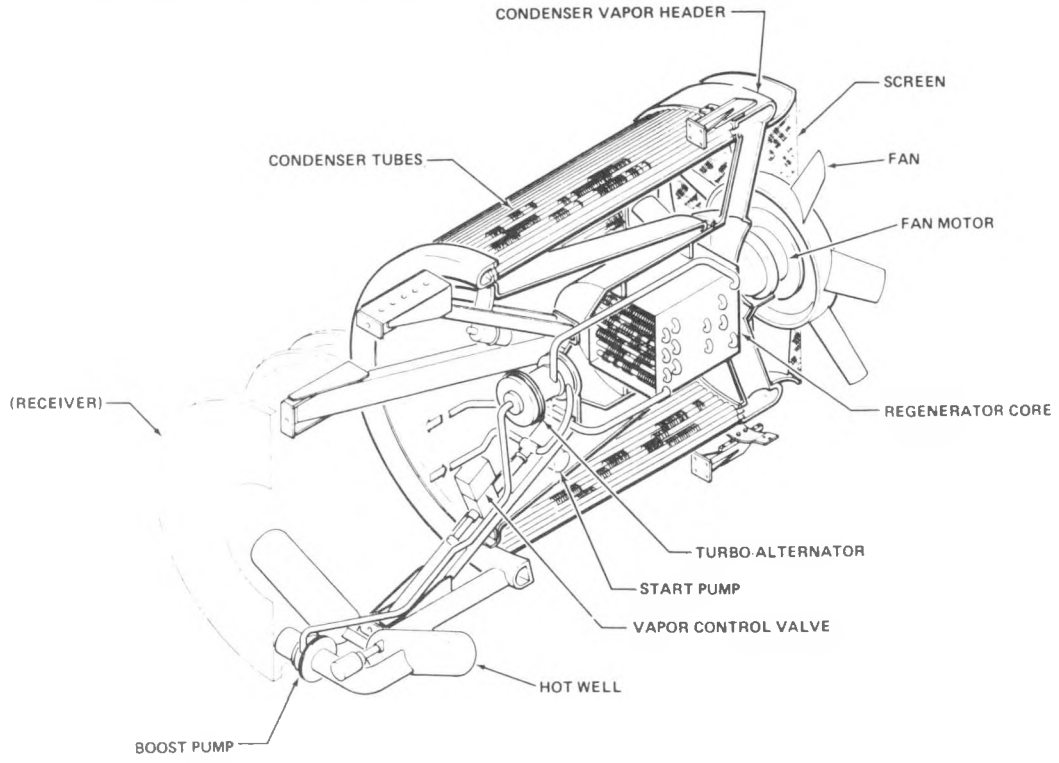

FIGURE 2. POWER CONVERSION SUBASSEMBLY (PCS)

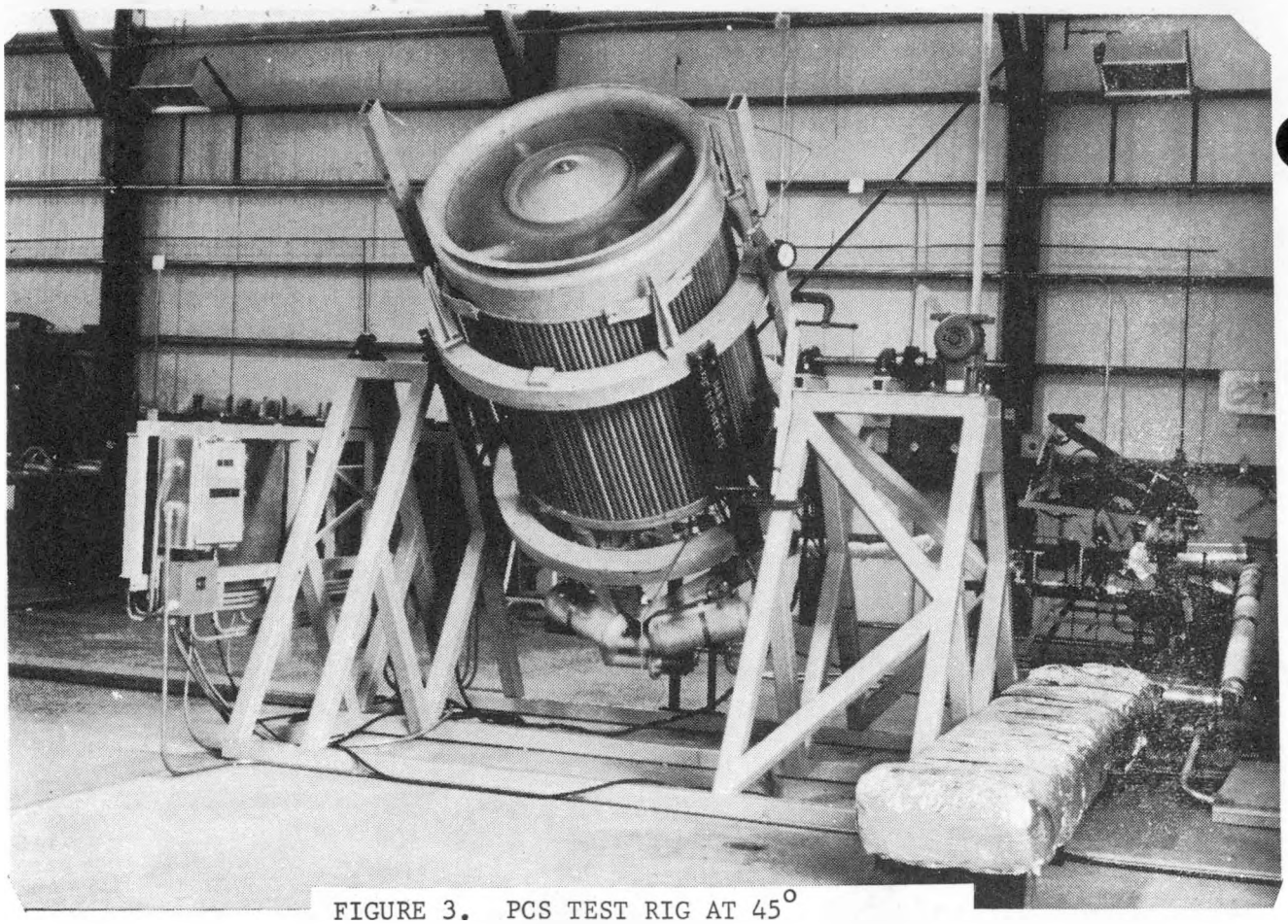

FIGURE 3. PCS TEST RIG AT 45° ELEVATION ANGLE

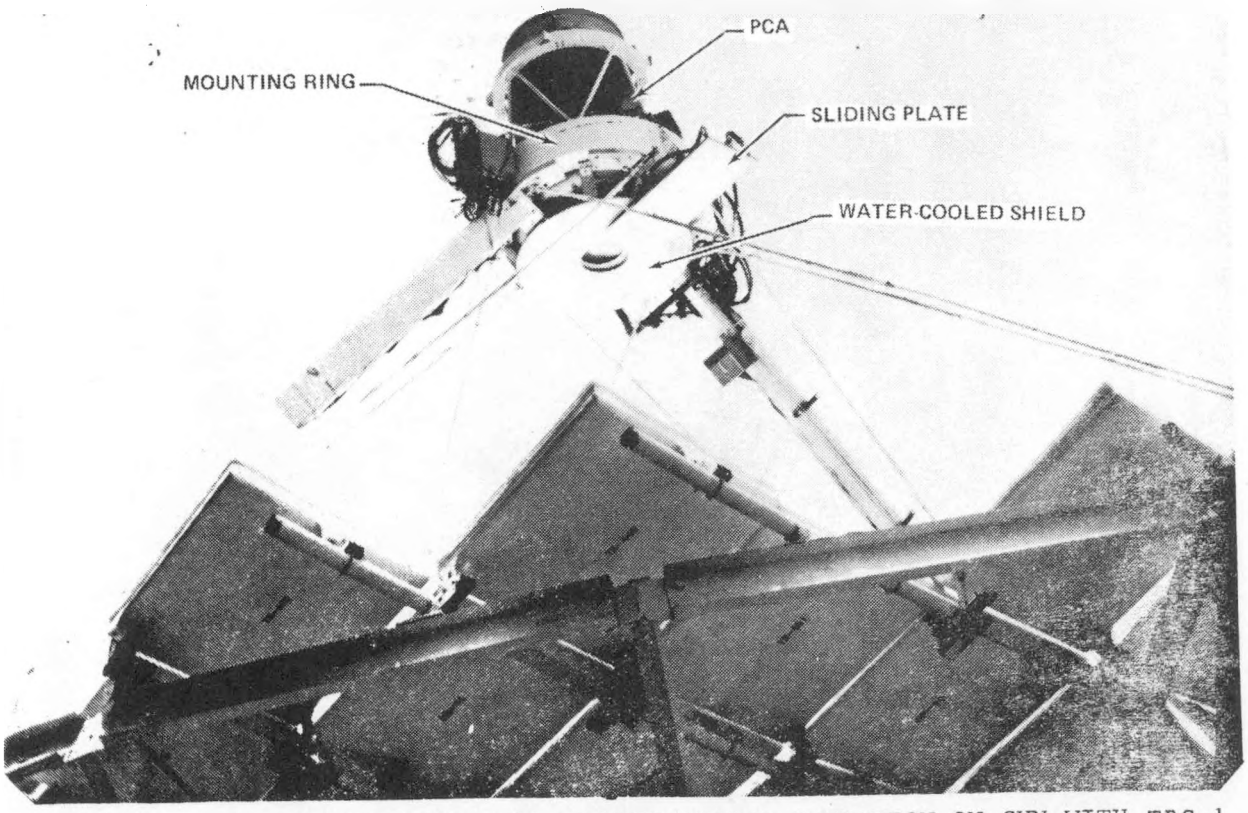

FIGURE 4. VIEW OF APERTURE END OF UNIT DURING OPERATION ON-SUN WITH TBC-1

TABLE I.

TYPICAL PCA PERFORMANCE DATA FOR RUN 13

DATE 03/03/82

PRINT 02R

TIME			CONDENSATE EXIT TEMP. DEG. F	REGEN LIQUID INLET TEMP. DEG. F	REGEN LIQUID EXIT TEMP. DEG. F	ALTERNATOR TEMP DEG. F	RECEIVER OUTLET PRESS PSIA	TURBINE INLET PRESSURE PSIA	TURBINE EXIT PRESSURE PSIA	CONDENSER EXIT PRESS PSIA	SYSTEM PUMP INLET PRESS PSIA	SYSTEM PUMP OUTLET PRESS PSIA
12:00:00	0	0	0082.8	0091.6	0380.4	0056.6	0494.0	0410.8	0001.5	0001.1	0027.8	0527.6
12:00:01	0	0	0082.8	0091.7	0378.4	0056.6	0494.0	0416.0	0001.5	0001.1	0027.4	0528.4
12:00:02	0	0	0082.6	0091.7	0378.4	0056.5	0493.6	0410.0	0001.5	0001.1	0027.8	0528.0
12:00:03	0	0	0082.7	0091.7	0378.8	0056.5	0494.4	0410.4	0001.5	0001.1	0027.7	0528.0
12:00:04	0	0	0082.6	0091.7	0377.6	0056.5	0494.4	0409.6	0001.5	0001.1	0027.8	0527.2
12:00:05	0	0	0082.7	0091.7	0378.4	0056.5	0494.4	0413.2	0001.5	0001.1	0027.4	0528.8
12:00:06	0	0	0082.6	0091.4	0378.4	0056.6	0494.4	0410.8	0001.5	0001.1	0027.6	0528.8
12:00:07	0	0	0082.6	0091.7	0376.8	0056.4	0494.4	0410.8	0001.5	0001.1	0027.7	0528.8
12:00:08	0	0	0082.6	0091.5	0378.0	0056.6	0494.4	0410.8	0001.5	0001.1	0027.8	0528.4
12:00:09	0	0	0082.6	0091.5	0378.8	0056.4	0494.4	0411.2	0001.5	0001.1	0027.5	0528.4
12:00:10	0	0	0082.6	0091.5	0378.8	0056.2	0493.6	0414.4	0001.5	0001.1	0027.5	0529.2
12:00:11	0	0	0082.5	0091.4	0378.4	0056.5	0493.6	0412.8	0001.5	0001.1	0027.6	0528.0
12:00:12	0	0	0082.5	0091.4	0378.4	0056.7	0494.0	0417.6	0001.5	0001.1	0027.7	0528.8
12:00:13	0	0	0082.4	0091.0	0378.4	0056.6	0494.8	0411.6	0001.5	0001.1	0027.9	0528.4
12:00:14	0	0	0082.4	0091.4	0378.4	0056.4	0494.8	0410.8	0001.5	0001.1	0027.7	0528.0
12:00:15	0	0	0082.5	0091.5	0378.4	0056.6	0494.4	0410.4	0001.5	0001.1	0027.8	0528.0
12:00:16	0	0	0082.7	0091.3	0378.4	0056.2	0494.8	0409.6	0001.5	0001.1	0027.8	0528.0
12:00:17	0	0	0082.4	0091.4	0379.2	0056.7	0494.0	0414.0	0001.5	0001.1	0027.7	0527.6
12:00:18	0	0	0082.2	0091.3	0378.4	0056.6	0492.0	0410.4	0001.5	0001.1	0027.8	0528.4
12:00:19	0	0	0082.3	0091.3	0378.4	0056.6	0495.6	0410.8	0001.5	0001.1	0027.8	0527.6
12:00:20	0	0	0082.3	0091.2	0378.4	0056.7	0495.2	0402.8	0001.5	0001.1	0028.0	0527.6
12:00:21	0	0	0082.3	0091.3	0379.2	0056.6	0495.6	0415.6	0001.5	0001.1	0027.7	0528.4
12:00:22	0	0	0082.1	0091.2	0378.4	0056.7	0494.4	0410.4	0001.5	0001.1	0027.8	0527.6
12:00:23	0	0	0082.1	0091.1	0378.4	0056.7	0494.0	0414.4	0001.5	0001.1	0027.6	0529.2
12:00:24	0	0	0082.2	0091.1	0379.6	0056.6	0494.4	0410.8	0001.5	0001.1	0027.6	0528.4
12:00:25	0	0	0082.3	0091.0	0378.4	0056.6	0494.4	0415.6	0001.5	0001.1	0027.8	0528.4
12:00:26	0	0	0082.1	0091.0	0378.0	0056.7	0494.4	0410.8	0001.5	0001.1	0027.8	0528.4
12:00:27	0	0	0082.1	0091.0	0378.4	0056.6	0494.4	0406.0	0001.5	0001.1	0027.8	0527.2
12:00:28	0	0	0082.0	0091.0	0379.2	0056.6	0494.4	0412.4	0001.5	0001.1	0027.7	0528.4
12:00:29	0	0	0082.1	0091.0	0378.4	0056.8	0494.4	0410.8	0001.5	0001.1	0027.7	0528.0
12:00:30	0	0	0082.1	0091.1	0376.8	0056.6	0495.6	0406.0	0001.5	0001.1	0027.8	0527.2

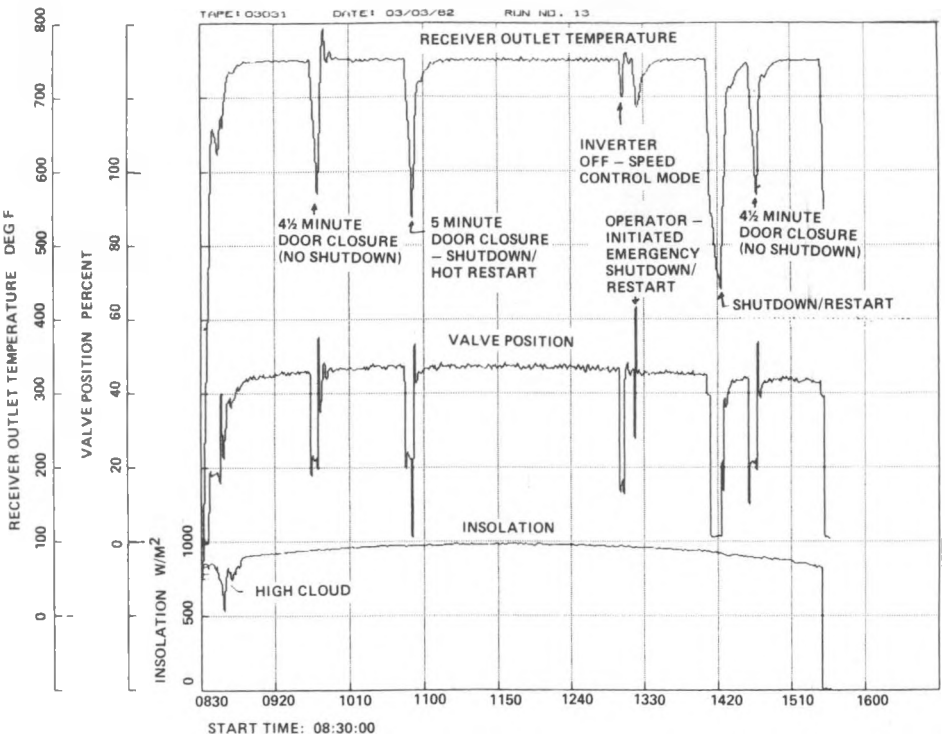

FIGURE 5. RECEIVER FLUID OUTLET TEMPERATURE vs. VALVE POSITION

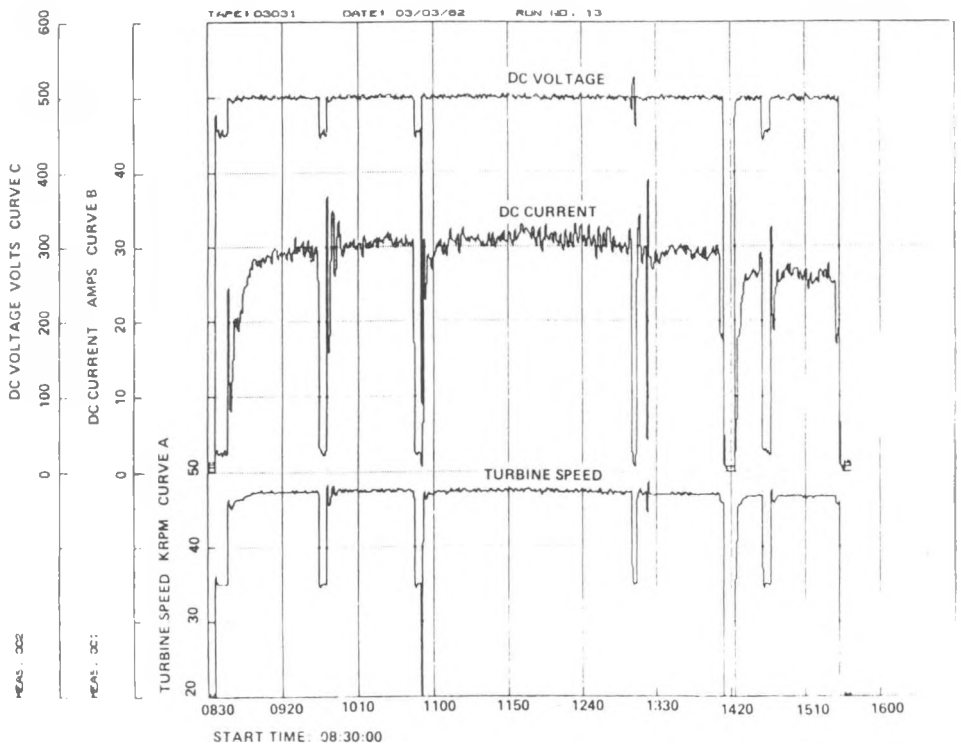

FIGURE 6. INVERTER VOLTAGE AND CURRENT vs. TURBINE SPEED

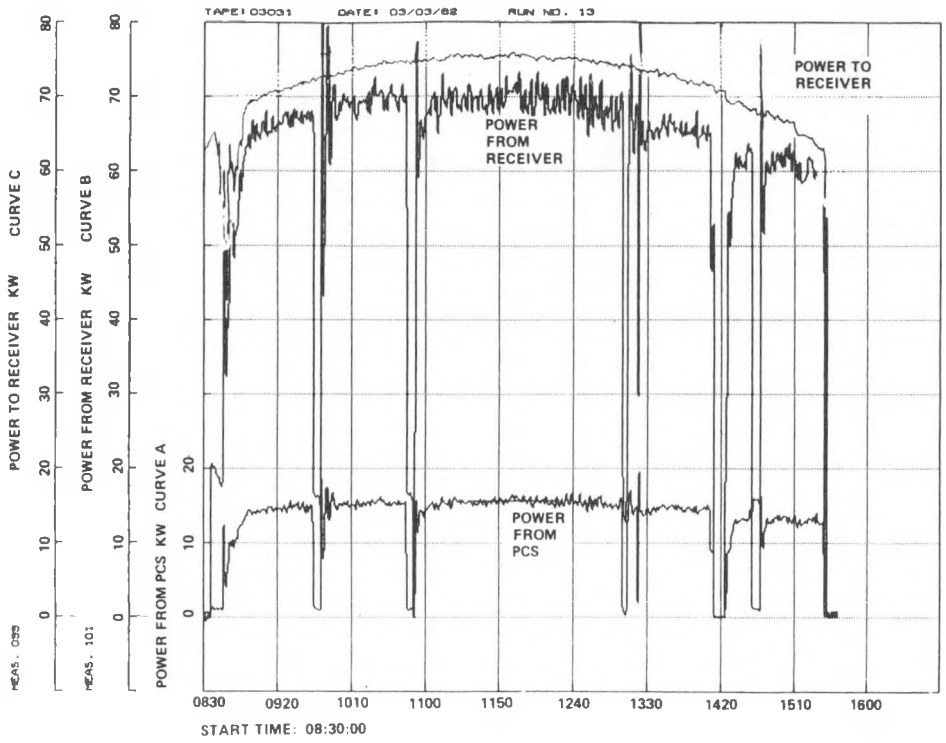

FIGURE 7. POWER LEVELS AT RECEIVER INLET AND OUTLET AND PCS OUTPUT

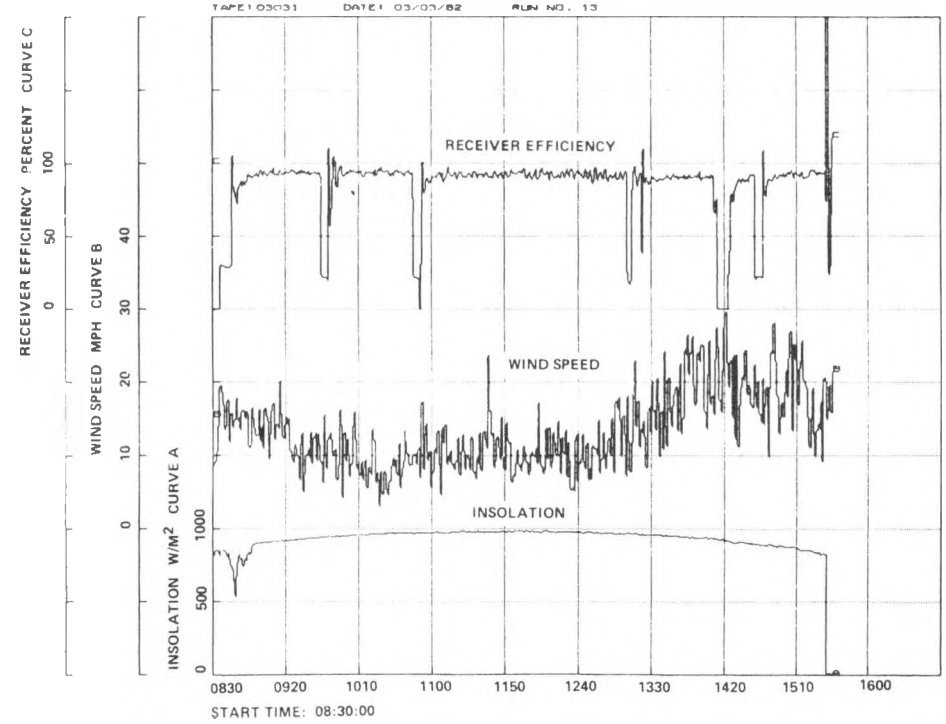

FIGURE 8. RECEIVER EFFICIENCY vs. WIND SPEED AND INSOLATION

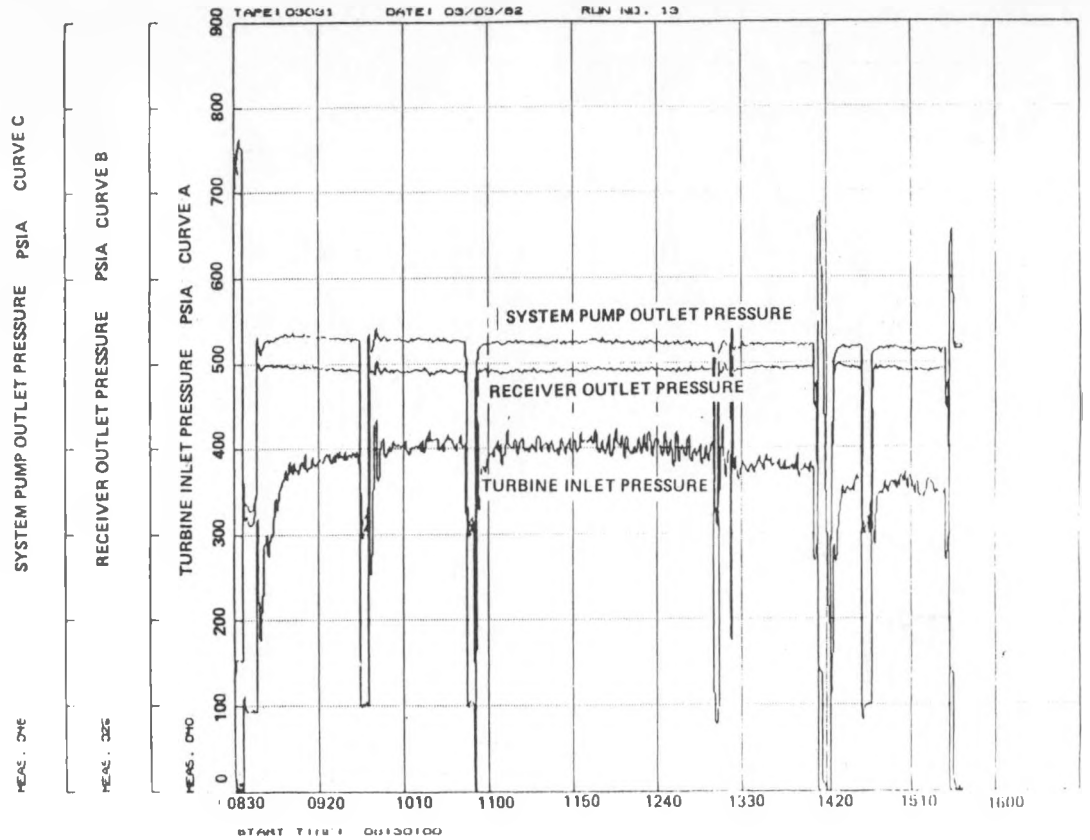

FIGURE 9. PRESSURE HISTORY AT KEY POINTS

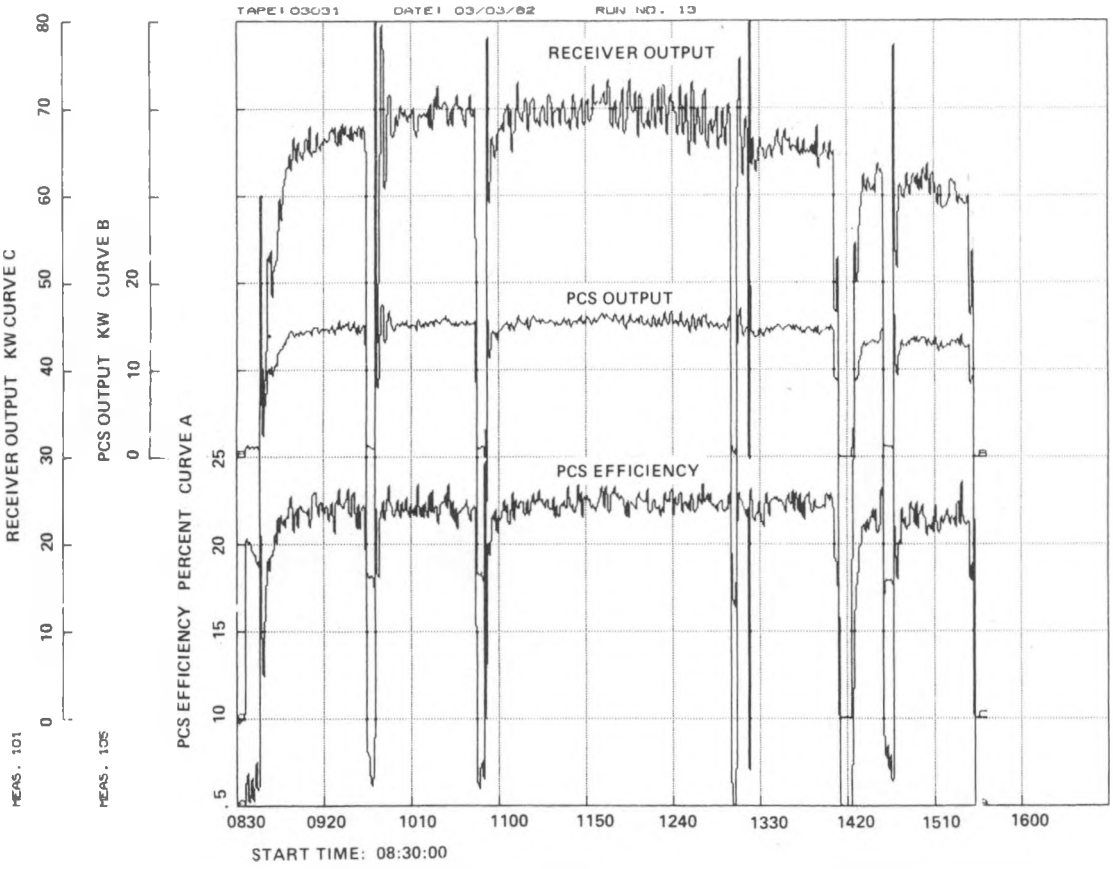

FIGURE 10. POWER OUTPUT OF RECEIVER AND PCS, AND PCS EFFICIENCY

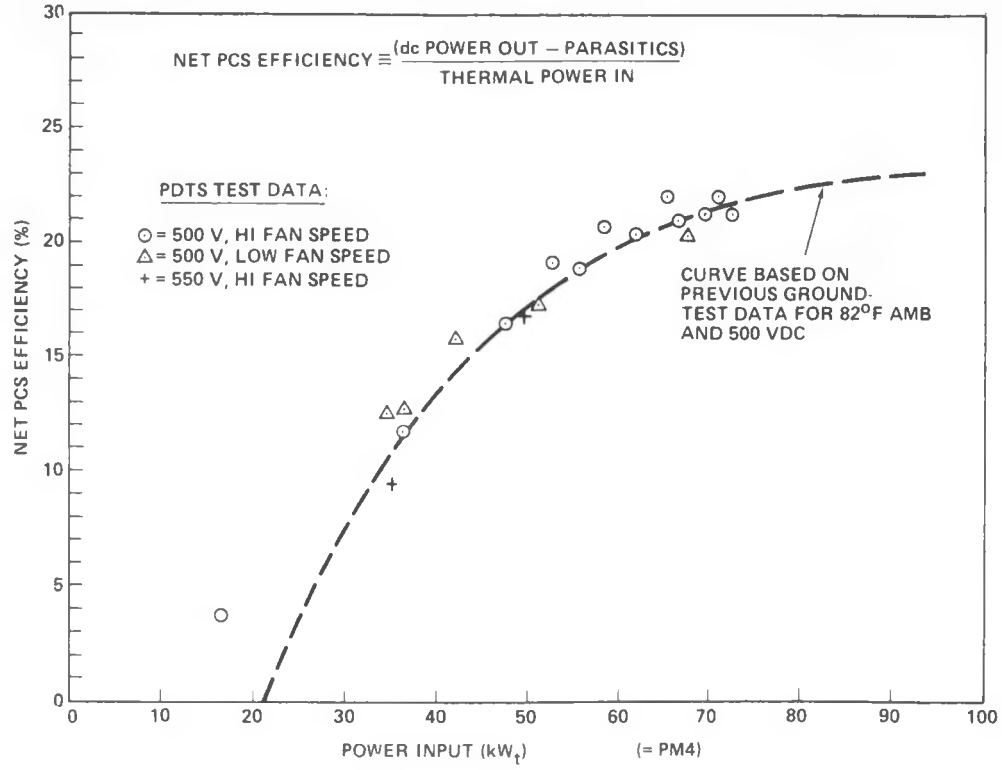

FIGURE 11. ORC ENGINE NET EFFICIENCY

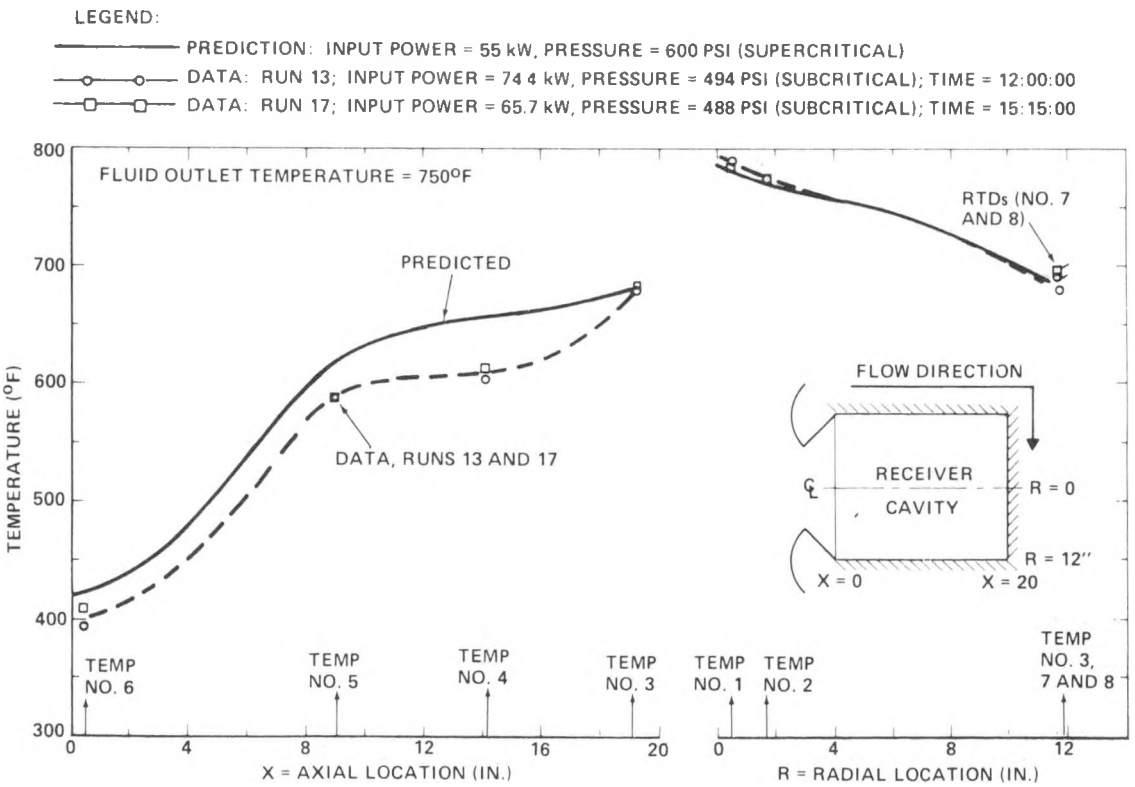

FIGURE 12. COMPARISON OF PREDICTED AND MEASURED RECEIVER TEMPERATURES

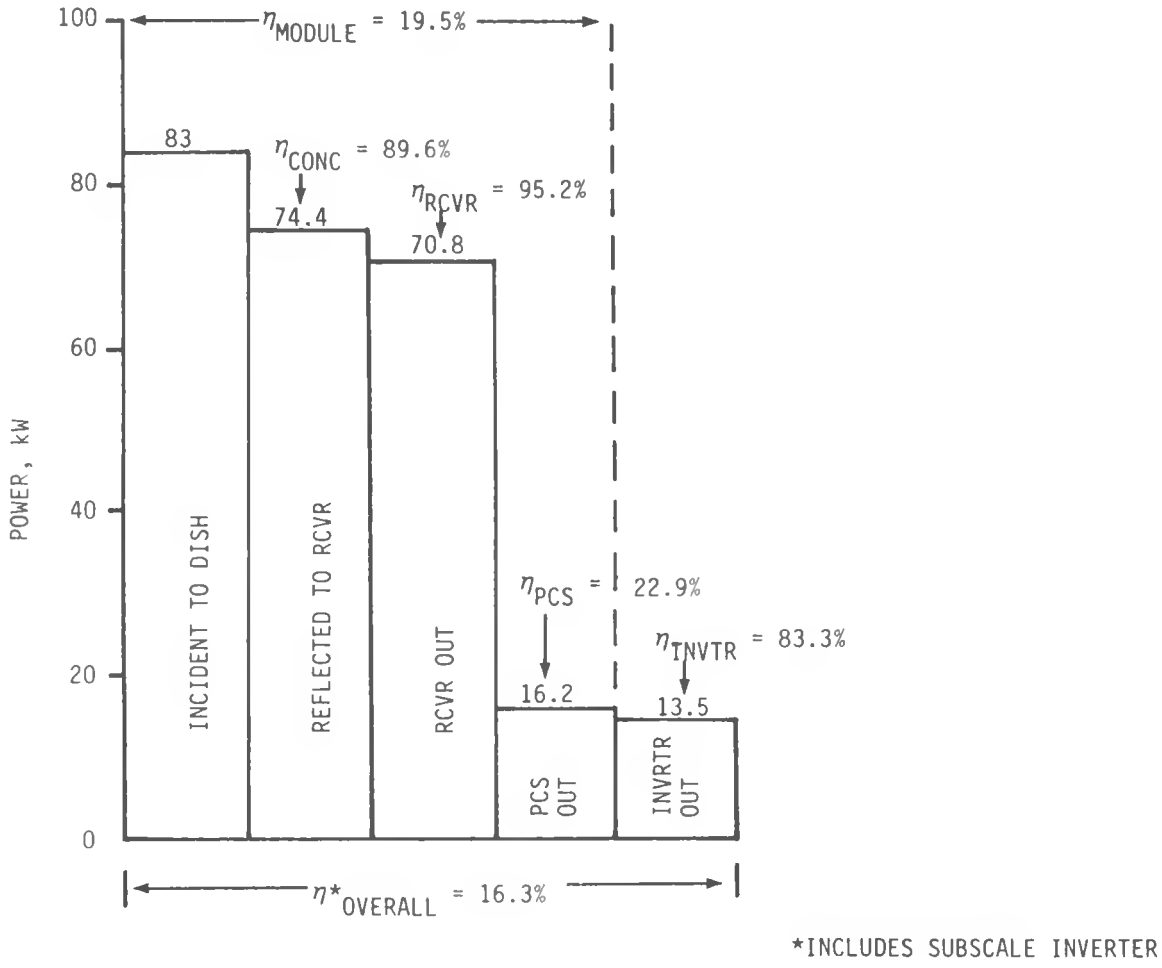

FIGURE 13. SCSE SYSTEM MEASURED PERFORMANCE FOR RUN 13 (3/3/'82)

SOLAR TESTS OF MATERIALS FOR PROTECTION FROM WALK-OFF DAMAGE

Leonard D. Jaffe
Jet Propulsion Laboratory
Pasadena, California

SUMMARY AND CONCLUSIONS

In parabolic dish solar concentrator systems, walk-off of the spot of concentrated sunlight can be a hazard in case of equipment or other malfunction that causes the concentrator to stop following the sun. The use of protective materials that can withstand exposure to walk-off conditions without active cooling provides certain advantages. A test program to evaluate possible materials was, therefore, carried out. Each test consisted of exposure to concentrated sunlight at a peak flux of about 7,000 kW/m^2 for a time of 15 minutes.

Types of materials tested included alumina, zirconia, mullite, silica, silicon carbide, graphite, aluminum, and copper. Of these, the only material that neither cracked nor melted was grade G-90 graphite, a premium grade. Grade CS graphite, a much cheaper commercial grade, cracked half-way across in each test, but did not fall apart. With proper design this grade should probably perform satisfactorily as a walk-off shield. Both of these grades are medium-grain extruded graphites.

The only other material tested which appeared promising was high-purity slip-cast silica. The one sample available survived four minutes before the test was terminated due to a deficiency in the test set-up. Further testing of similar material is probably worthwhile.

Other grades of graphite and silica tested, and all the samples of alumina, zirconia, mullite, silicon carbide, aluminum, and copper, either melted or fractured quickly during the test.

Coatings of white high temperature paint or boron nitride did not improve the performance of graphite samples. Immersion in water prior to test, simulating rain, did not affect their performance.

INTRODUCTION

If a malfunction occurs in a solar thermal dish-type power plant while a concentrator is pointed at the sun, motion of the concentrator may stop. As the sun moves relative to the Earth, the spot of concentrated sunlight then slowly "walks off" the receiver aperture and across the receiver face plate and the concentrator. Intense local heating by the concentrated sunlight may destroy these parts and put the unit out of service.

A wide variety of methods may be used for protection against damage by walk-off. They include materials that can withstand the concentrated sunlight, provision of water-cooling, shutters, emergency devices to point the concentrator away from the sun, provision of emergency power to turn the concentrator, etc. Advantages and disadvantages of various methods are discussed in Ref. 1. Many of the methods require use of emergency mechanisms, power or cooling supplies, and controls; these may add significant cost and may not function reliably when needed. Use of materials that can withstand the concentrated sunlight without active cooling has the advantage of providing passive protection, which should increase reliability, and may be less costly than alternative techniques. Moreover, a shutter, for example, must itself either be actively cooled during walk-off or must be made of material able to withstand walk-off heating.

Some work has been reported on the ability of uncooled materials to withstand concentrated sunlight for limited periods of time. This prior work was not, however, oriented toward dish concentrators and the flux densities used for testing have been considerably below those of interest for such concentrators. It therefore was considered worthwhile to undertake tests to evaluate candidate materials.

In particular, impetus for this work came from JPL interest in finding a suitable material for passive walk-off protection for the Organic Rankine system developed under contract with JPL by the Ford Aeronutronics and Communications Company. In this system, the peak flux at the receiver aperture, under design conditions, is expected to be about 7,000 kW/m^2.

An important constraint on this materials evaluation was cost, which was severely limited. This in turn limited the choice of materials to be tested and the measurements that could be made on them.

A more detailed account of this work is given in Ref. 2.

MATERIALS AND SAMPLES TESTED

Because of the limited budget for this work, most of the samples were provided cost-free by interested companies or obtained as surplus at JPL. The general types of materials tested included alumina, zirconia, mullite, silica, silicon carbide, and graphite. Also tested were aluminum and copper with temperature-resistant coatings, and graphite with temperature-resistant coatings. More information on each of the materials tested is given in the Ref. 2.

The preferred sample size selected was 200 x 200 x 25 mm (8 x 8 x 1 inch), to give samples not too small compared to the solar spot size and thick enough to provide reasonable protection. A few thicker specimens (about 35 mm, 1.4 inch) were tried to see if greater thickness improved performance. Because many samples were provided free rather than purchased, they were often smaller than preferred. Some were as thin as 0.4 mm (0.017 inch); these were provided more because of interest in using them for protection during normal acquisition and deacquisition than for walk-off protection.

TEST EQUIPMENT

Solar tests were made on Test Bed Concentrator 1 at JPL's Parabolic Dish Test Site. For the materials tests, a fixture was designed in the form of "window-frame" with outside dimensions 380 x 330 mm (15 x 13 inches), and an opening 230 mm (9 inches) square. The sample was placed in this opening. The fixture was 114 mm (4-1/2 inches) thick, and made from graphite, grade 3499. A key aim of the fixture design was to minimize conductive heat transfer from sample to test fixture and from test fixture to adjacent equipment. The sample was prevented from falling out toward or away from the concentrator mirrors by graphite rods 10 mm (3/8 inch) in diameter, made of graphite, grade 873S or HC. Rods were used to minimize thermal contact between support and sample. The support rods caused some local blockage of concentrated sunlight; this somewhat increased the thermal gradients and thermal stresses in the samples.

For tests of elements of the Organic Rankine module, the pointing of individual mirrors on the test bed concentrator and the distance between the mirrors and the receiver aperture were set to simulate the corresponding distribution of concentrated sunlight expected with Parabolic Dish Concentrator 1, the concentrator to be used with the Ford Organic Rankine module in the near future. The receiver is designed for a flux pattern peaking at 7,000 kW/m^2 at an insolation of 1 kW/m^2. In the materials testing, the side of the sample facing the mirrors was positioned 25 mm (1 inch) closer to the mirrors and to the waist of the concentrated pattern of sunlight than the position of the receiver aperture during module test. The distribution of solar flux in this materials test plane was measured with a flux-mapper. The peak measured flux in the materials test plane was 7,800 kW/m^2, but this is at an insolation of 1 kW/m^2. In the materials tests the actual insolation was somewhat lower than 1 kW/m^2, and the peak flux in these tests approximately matched that for the receiver design conditions.

TEST PROCEDURE

Solar Test

Tests were made at insolation of 580 to 960 W/m^2. The concentrator was pointed at the sun, with its shutter closed, and set to track the sun automatically. The shutter was then opened and the sample observed. Observations were by two means:

(1) An observer stationed in the shadow of the concentrator watched the sample throughout each test through an opening in the center of the mirror array, using binoculars and dark glasses.

(2) The concentrator operator observed the sample on television, utilizing a black-and-white TV camera mounted on a receiver support leg of the concentrator.

Tests were terminated by closing the shutter 15 minutes after it was opened, or when the sample failed, whichever occurred first. For this purpose, failure was initially defined as observation of cracking or of

melting and dripping. (To reduce the risk of damage to the concentrator mirrors from falling fragments or hot drops, tests were constrained to sun elevations below 45 degrees). It was found during testing that some samples cracked part-way, but did not fall apart; the procedure was later changed to continue the test despite such cracking. Also, some samples that survived the test without melting or cracking apart were retested for total exposure times up to 45 minutes.

A special test was run on a graphite sample to simulate repeated acquisition and deacquisition, rather than walk-off. The test consisted of 669 cycles of opening and closing the shutter (initially 1.1 s open, 19.2 s closed, soon changed to 1.1 s open, 9.2 s closed).

Several samples were tested wet to simulate exposure to rain followed by sunlight and walk-off. They were soaked in water at a depth of 15 to 30 cm (6 to 12 inches) prior to solar testing.

Temperature measurements, with minor exceptions, were not made on the samples during test because of the cost constraint.

During all tests, the television was recorded on a video cassette recorder. Insolation and weather data were also recorded digitally.

Measurements Before and After Solar Test

All samples were weighed, measured, observed visually, and photographed in color before and after solar test. Bulk densities prior to testing were calculated from the measured dimensions and weights.

To provide a rough measure of solar absorptivity at minimum cost, sample brightness was measured outdoors, in open shade, with a Pentax-type brightness meter designed for use in photography, and compared with the brightness of Kodak white and gray reflectance standards placed adjacent to the sample.

RESULTS AND DISCUSSION

Results of the solar tests are summarized in Table 1. More detailed results of these and other measurements are given in Ref. 2. The great majority of the samples melted or shattered in test, many of them within the first few seconds of solar exposure. The only materials tested that appeared promising for walk-off protection were graphite grades G-90 and CS and high-purity slip-cast silica.

Graphites

Grade G-90

Graphite, grade G-90, was the only material that survived 15-minutes without melting or cracking. A sample of G-90 survived two successive 15-minute tests without cracking. (Graphite cannot be melted at atmospheric pressure.) Another sample of this material was tested wet and did not crack.

Grade G-90 is an extruded material that is reimpregnated several times with coal-tar pitch and regraphitized to reduce its porosity and increase its bulk density. One application for this grade is as throats for solid-propellant rocket nozzles. G-90 is a premium grade and somewhat expensive for a graphite: about $45/kg ($20/lb). A typical protective shield for the Ford Organic Rankine module might have a mass of about 16 kg (weight 35 lb) if made of such graphite. The cost of about $700 for the material might be acceptable, but is probably higher than desirable for quantity use.

Grade CS

All five samples of uncoated graphite grade CS developed, during simulated walk-off test, a single crack extending from near the midpoint of an edge to near the center of the specimen. In some of these samples the crack was observed to advance gradually from edge to center. In no case did it advance farther, nor did any of these CS graphite specimens fall apart into two or more pieces. Two samples of CS graphite that cracked during initial exposure were retested to a total of 16 and (with occasional interruptions) 45 minutes, respectively, without further observed crack advance. With two other samples of this grade (one tested wet, one dry), the test was continued to 15 minutes despite the single crack that formed. After the usual post-test examination, these samples were retested another 15 minutes. No further advance of the crack was noted. Apparently the first crack, half-way across, was sufficient to relieve the thermal stresses and prevent further cracking. This suggests that with proper design, including segmenting, CS graphite should provide satisfactory walk-off protection.

CS is a commercial grade of extruded graphite and has medium grain size and bulk density. It costs about $4.50/kg ($2/lb); a protective shield for the Organic Rankine module would cost about $65 for the material.

Graphite grades G-90 and CS absorbed very little water on immersion and their subsequent test performance appeared unaffected by this wetting. Presumably rain would not impair their subsequent value for walk-off protection.

Within the limited range of thickness tested (24 to 37 mm, 0.95 to 1.5 inches), thickness had no obvious effect upon performance of graphite samples.

Other Graphite Grades

Other grades of graphite tested were 3499, 8826, and HLM-85. All samples of these grades cracked apart or shattered in test; the 3499 at exposure times of 1-1/2 to 8 minutes, the 8826 and HLM-85 in 1 to 1-1/2 minutes. The first two are fine-grained molded grades, the last a medium grain extruded grade that is reimpregnated and regraphitized.

The test fixture used was of grade 3499 graphite and survived 42 tests, with a total exposure time of 5.5 hours, without cracking. None of the 10 mm (3/8 inch) diameter support rods of 873S or HC graphite were observed to fracture in service.

Comparison of Graphite Grades

Graphite grades G-90 and CS, which performed well, are extruded grades with medium grain size (maximum particle size nominally 750 micrometers). 3499 and 8826 are fine-grained molded grades (maximum particle size nominally 75 micrometers); they shattered in test. This suggests that fine grain (and possibly molding) is less desirable than medium grain (and extrusion?) in graphites for walk-off protection. Such an interpretation of the grain size effect is consistent with the general belief in the graphite industry that coarse-grained graphites have better resistance to thermal shock than fine-grained.

Rather contrary to this suggested generalization is the behavior of the HLM-85 material, a medium-grained extruded material which shattered in test. Why this grade did not perform as well as G-90 and CS is not evident.

CS and G-90 were, respectively, the least dense and most dense grades tested, so bulk density (and the corresponding inverse variable, porosity), do not correlate well with good or poor performance in test. Only limited data were found on thermal expansion and thermal conductivity; perhaps the grades that behaved best had lower thermal expansion.

Many graphite grades are available besides those tested. Perhaps some further testing of grades with a wider range of characteristics would be worthwhile.

Coated Graphite

Three samples of graphite (grades CS and 3499) were coated with boron nitride, which is white, to evaluate the effect of reducing the solar absorptance of the material. The boron nitride was in the form of a fine powder dispersed in a water-based binder of aluminum phosphate and applied by spraying, followed by baking. In test, the white coating disappeared from the area of highest solar flux, and the bare region then spread outward uniformly to areas of lower flux. After this, the samples cracked like uncoated samples of the same grade except that one CS sample cracked all the way across, rather than half-way.

Two samples of graphite (grades 8826 and HLM-85) were painted with commercial high-temperature white paints. Their behavior in test was similar to that of samples coated with boron nitride.

Oxidation During Simulated Walk-Off

During testing, the graphite samples lost significant thickness at the center of their exposed faces, with a corresponding loss in mass. The loss in thickness due to oxidation for grades CS and G-90 varied from 0.2 mm (0.008 inch) to 8 mm (0.3 inch) per 15-minute exposure. The corresponding loss in mass, normalized, was 2 to 22% (normalized to 15-minutes exposure and a standard sample size of 25 x 200 x 200 mm, 1 x 8 x 8 inch). This may be acceptable for walk-off protection, since walk-off is expected to be an infrequent event and the test was probably more severe than the expected service. A protective shield could perhaps be replaced after a few walk-offs.

The effect of wind speed on the oxidation loss was significant and accounts for a large part of the variation in loss between samples. The mechanism of this effect appears straightforward: wind brings oxygen and removes carbon dioxide from the reacting surface. The mass loss rate for grade CS graphites was somewhat lower than that for grade G-90, under comparable conditions. Additional testing would be desirable.

Oxidation During Simulated Acquisition and De-Acquisition

More important than oxidation of graphite during walk-off may be oxidation during frequent normal sun acquisitions and deacquisitions. The repeated on-sun/off-sun cycles used for one sample of grade CS graphite were intended to give some indication of this. The sample lost 6.7 mm thickness, 4.7% of its weight, in 669 cycles, which might represent a year or so of service. The insolation in this test averaged 960 W/m^2; acquisition and deacquisition in service would probably be primarily at low sun, when insolation would be lower. Also, the test was severe in that the spot of concentrated sunlight remained at a fixed position on the sample; in acquisition-deacquisition the spot would traverse the material. The graphite in the spot reached a steady-state temperature of 650-700°C (1200-1300°F) when off the sun, whereas after a single acquisition or deacquisition it would cool to near ambient temperature. On the other hand, the wind speed during the simulated acquisition-deacquisition test was lower than desired (averaging 2 m/s, 4.5 miles/hour), so in this respect the test conditions were less severe than would often be encountered in service.

Silicon Carbide

Two samples of silicon carbide, from different sources, were tested. Both shattered within a second or so. It seems evident that silicon carbide, in the grades tested, is so sensitive to thermal shock failure that it is unsuitable for walk-off protection.

Silica

Two samples of slip-cast silica and one of fibrous, reaction-bonded silica were tested. The high purity sample of slip-cast silica, with fine particle size, survived four minutes and then began to melt where it was in contact with the graphite support rods. This is considered as an artifact of the test and not a fair evaluation of the sample: probably the melting, away from the area of peak solar flux, was caused by conductive heat transfer from the support rods to the sample. Because the support rods were black and the silica white, the rods absorbed a larger fraction of the flux incident upon them and probably became hotter than the sample.

The sample was therefore retested, turning it over to expose the other side and supporting it with rods which were placed farther from the area of highest solar flux and also were coated with boron nitride (as described above) to reduce the solar absorptance of the rods. This time the silica sample began to melt in the area of highest solar flux, after 1-1/2 minutes of exposure. The reason for more rapid melting in the retest is not clear. Perhaps the initial heating produced changes in the crystal

structure of the silica that affected its solar absorptivity or thermal emissivity. Testing of additional samples of similar material is clearly desirable.

If high-purity slip-cast silica does not melt, it may be the material of choice for walk-off protection since, unlike graphite, it will not oxidize. It has the disadvantages of possible changes in optical properties when heated in service and probable sensitivity to surface dirt and contamination, which may be hard to avoid in field service.

A sample of commercial grade slip-cast silica melted within 10 seconds. This suggests the importance of high purity and perhaps of crystal structure. This sample had a coarser and less uniform particle size than the high-purity sample and its reflectance was somewhat lower: 0.9 vs almost 1.0.

The fibrous reaction-bonded silica (similar to a proposed second-generation Space Shuttle tile) melted in less than 10 seconds. This sample had a black glazed surface toward the incident sunlight, which was intended to increase its emissivity at elevated temperatures, but also greatly increased its solar absorptance. (The reflectance was roughly 0.05.) Perhaps the material would be much better with a white exposed surface. It will probably be relatively expensive, however.

Zirconia, Alumina, Mullite

Samples of these materials all melted rather quickly. The sample that lasted the longest was of fibrous zirconia, about 25 mm (1 inch) thick, which melted in 2 minutes. A zirconia sample of similar thickness that was cast from a powder-vehicle mixture and then sintered melted in 30 seconds. A sample of zirconia cloth 0.5 mm (0.02 inch) thick developed slits in 8 seconds.

The alumina samples were in the form of "paper" (felt) 1.5 mm (0.06 inch) thick and less. All melted within 6 seconds.

The mullite samples were in the form of honeycomb, 30 to 38 mm (1.2 to 1.5 inch) thick. They melted in less than 5 seconds.

Since these refractory oxides have higher melting temperatures than silica but melted more rapidly, other characteristics must be important in determining behavior in these solar tests, perhaps the absorptance/emittance ratio, internal radiative heat transfer, etc.

Coated Copper and Aluminum

A copper sample 25 mm (1.0 inch) thick was nickel-plated and painted with a commercial high temperature white paint. It began to melt in 2 minutes. After this test, the paint was removed and the sample repainted with another brand of commercial high temperature paint, white on one side and black on the other. It was then tested twice more, once with the black side facing the concentrated sunlight and once with the white side facing the sunlight. The sample was so placed that the area of maximum solar flux fell on a different part of the sample in each of the three tests. With

the repainted white face exposed, melting started in 3 minutes; with the black face exposed, in 1 minute (Table 4). The shorter survival time with the black paint is presumably due to the difference in solar absorptance between black and white paints (reflectance 0.06 and 0.6 to 0.8, respectively). The difference in survival time with the two white paints may also be due to absorptance; the white giving longer survival had the higher reflectance.

A test was run on an aluminum alloy sample 1.8 mm (0.07 inch) thick coated on both sides with a laboratory-produced inorganic white paint developed for use on spacecraft. It melted in about 1/2 second.

REFERENCES

1. Jaffe, L. D., Levin, R. R., Moynihan, P. I., Nesmith, B. J., Owen, W. A., Roschke, E. J., Selcuk, M. K., Starkey, D. J., and Thostesen, T. O., "Systems Approach to Walk-Off Problems for Dish-Type Solar Thermal Power Systems," JPL Doc. 5105-97, Aug. 21, 1981.

2. Jaffe, L. D., "Solar Tests of Materials for Protection from Walk-Off Damage," JPL Doc. 5105-121.

Table 1
Summary of Results

Material Type		Thickness (mm)	Result
Graphite CS			
3499		26	Shattered, 1-8 m
8826		26	Shattered, 1-1½ m
HLM-85		24-26	Shattered, 1-1½ m
CS		28-37	Cracked halfway, 3-14 m
G-90		24-25	Survived 30 m
SiC		6-32	Shattered, 1 s
SiO_2	Slipcast, High Purity	18	Melted, 4 m (under rods)
	Slipcast, Commercial	20	Melted, 10 s
	Fibrous, Glazed	41	Melted, 7 s
Mullite		32-38	Melted, 1-4 s
Al_2O_3	Paper	0.4-1.4	Melted, 2-6 s
ZrO_2	Pressed & sintered	29	Melted, 20 s
	Fibrous board	25	Melted, 1 m
	Cloth	0.5	Melted, 8 s
Copper		26	Melted, 1-3 m
Aluminum		1.8	Melted, 1 s

Blank Page

RESULTS OF BRAYTON MODULE SYSTEM TRADE STUDIES

Theodore J. Nussdorfer, James B. Kesseli
Sanders Associates, Inc.
Nashua, N.H. 03060

Abstract

Sanders Associates, Inc. (S/A) has been selected to fulfill the systems integrator role for this program, with the responsibility of configuring and testing a Parabolic Dish Module (PDM) for the purpose of converting solar energy to electric power. The PDM consists of a solar concentrator, receiver, Brayton cycle gas turbine, generator or alternator, recuperator, hybrid combustor and any additional subsystem necessary to complete the integration of the power module and meet the JPL/PDM specifications.

An initial phase of this work recently completed involves Tradeoff studies and Performance Analyses of various system configurations. As presented here, this work has culminated in an integrated recommended program that utilizes for its initial experiments, components that are available, or soon to be available. The AiResearch subatmospheric gas turbine has been designated as an interim power plant to be interfaced with one of several competitive collector designs. This first experiment is a vital step toward the long term goal of utilizing the DOE/NASA Advanced Gas Turbine with its predicted high temperature/high efficiency performance for low cost Solar Brayton electric power.

RESULTS OF BRAYTON MODULE SYSTEM TRADE STUDIES

Theodore J. Nussdorfer, James B. Kesseli
Sanders Associates, Inc.
Nashua, N.H. 03060

INTRODUCTION

Sanders Associates has been selected by the Jet Propulsion Laboratory to perform the role of system integrator for the development of the Point Focus Brayton Module. This portion of the program is dedicated to the evaluation and selection of the available components. These principle components were classified in the four major categories: 1) solar receiver, 2) Brayton engine, 3) parabolic concentrator, and 4) generator/alternator.

Each of the candidates have been evaluated on the basis of efficiency, durability and life, system compatibility, as well as estimates of their ultimate production cost. The evaluation of the module centers around a custom optimization study for the solar receiver. This design incorporates the unique cycle characteristics of each engine candidate and the optical focusing quality of the concentrator to maximize module efficiency.

RECEIVER

The Sanders receiver performs the function of capturing the concentrated solar radiation. The proper design of this process will allow the energy to be efficiently conveyed to a working fluid. The concept, as applied to a small Brayton cycle, is illustrated in Figure 1. The energy transmitted through the aperture is absorbed on a "honeycomb" matrix and convected to the gas entering the turbine. A transparent material is required for the receiver aperture to contain the cycle fluid. Results from three design and test programs[1,2,3] conducted on Sanders' solar receivers concluded that a quartz aperture and a silicon carbide absorber are the most viable material selections at the temperature required for this application.

An outline of the receiver thermal efficiency modelling procedure is presented in Appendix 1. Figure 1 features the descriptive parameters of the model. This conception of the loss mechanisms has been used to develop a quantitative prediction of receiver dimensions and performance.

Many geometries have been investigated in the design phase of the original Sanders/JPL solar Brayton receiver[4]. In this study, the critical parameters which govern the heat transfer effectiveness of the absorber have been analyzed using finite element techniques (ANSYS). The determination of absorber temperature profile for various configurations could then be combined with the efficiency prediction model. The optimum receiver geometry, given by the maximum collection efficiency, could then be derived for each set of concentrators and engine conditions.

An example of the relative magnitudes of the six receiver thermal loss factors is presented in figure 2. The trends exhibit the dominating effect of the absorber radiation at elevated receiver discharge temperatures. Thermal conduction through the insulated vessel walls is also significant but is only a nearly linearly function of temperature. The best uncooled super-alloy turbines are capable of accepting receiver discharge temperatures or approximately 1600^{0}F. Lower temperatures are characteristic of less advanced rotors, or hybrid operating conditions. Temperatures in excess of 2300^{0}F are projected for the next generation of gas turbine components.

The selection procedure for the aperture diameter trades off the receiver efficiency with that of the concentrator. For example, improvements in receiver efficiency at decreasing aperture sizes are offset by an increased amount of spilled power. This optimization of solar collection efficiency requires a set of characterization parameters which describe the focusing quality of the concentrator.

The receiver efficiency, as described in figure 3, is defined as the power delivered to the Brayton cycle divided by the power incident on the receiver aperture plane. The concentration ratio represents the ratio of concentrator to receiver aperture areas. Furthermore, each point on these curves represents the selection of the optimum receiver aperture and absorber sizes necessary to maximize collection efficiency for the given set of engine and concentrator specifications.

Figure 4 describes the performance of a hypothetical Brayton engine and generator. The trend of increasing efficiency with increasing turbine inlet temperature is exhibited as an example of typical or projected open cycle recuperated (or regenerated) engine performance. These characteristics can then be combined with the results from the previous figure to describe the overall conversion efficiency. The combination of the solar receiver, the Brayton engine and the electrical generator is termed the Power Conversion Assembly (PCA).

Some of the results of this multi-dimensional optimization analysis are presented in figure 5. From this set of curves it is possible to evaluate the overall power conversion assembly performance for the various component combinations. Further, the impact of adjustments in individual component efficiencies may be weighed against economic factors.

BRAYTON ENGINES

The output power required for Brayton engines suitable for incorporation in Parabolic Dish Solar Brayton/Electric Systems is largely driven by the economics of the concentrator since approximately 50% of the overall system cost can be attributed to the concentrator. Various studies have been conducted (e.g. JPL/reference 5) that predict optimum collector diameters as large as the 11M-12M size. The thermal energy collected by such a dish translates to a nominal 20KW of electrical power for existing metal engine technology.

Both recuperated and unrecuperated cycles in this power range were assessed in the initial stages of this program. Following an economic assessment

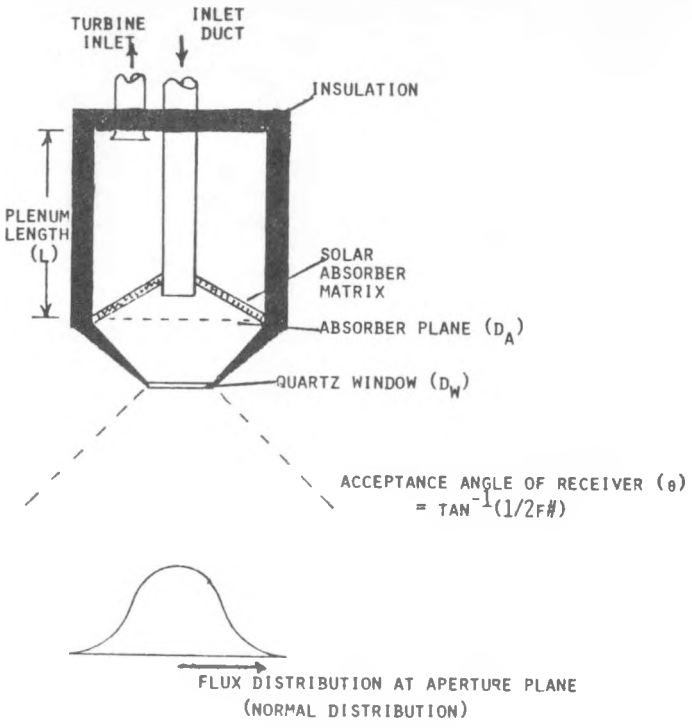

Fig.1:RECEIVER THERMAL MODEL

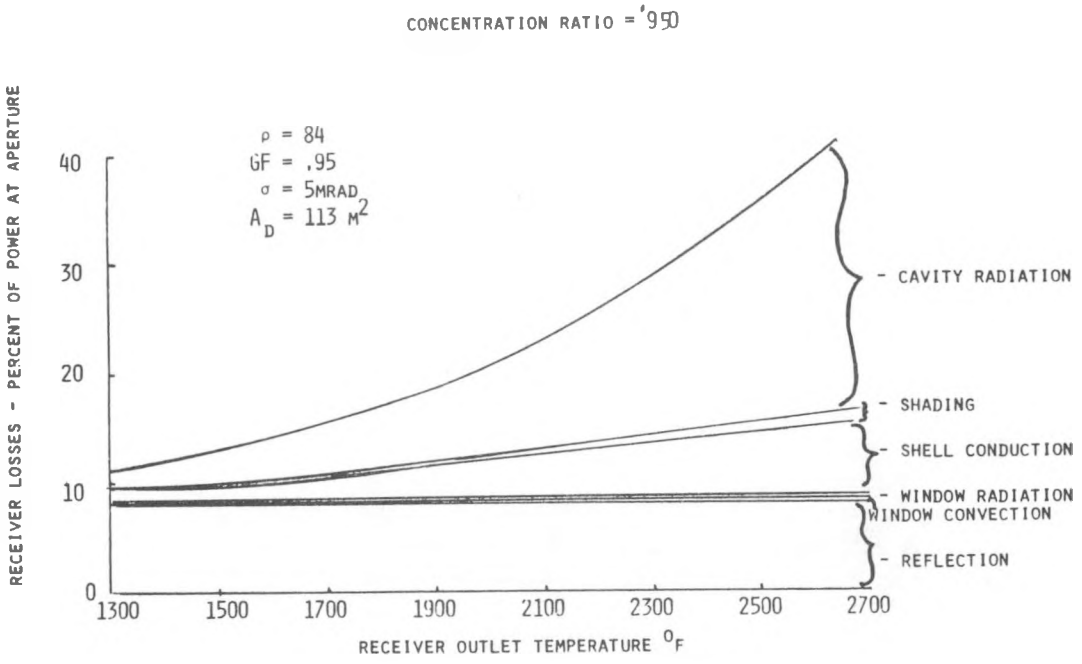

Fig.2:SUMMATION OF RECEIVER LOSSES

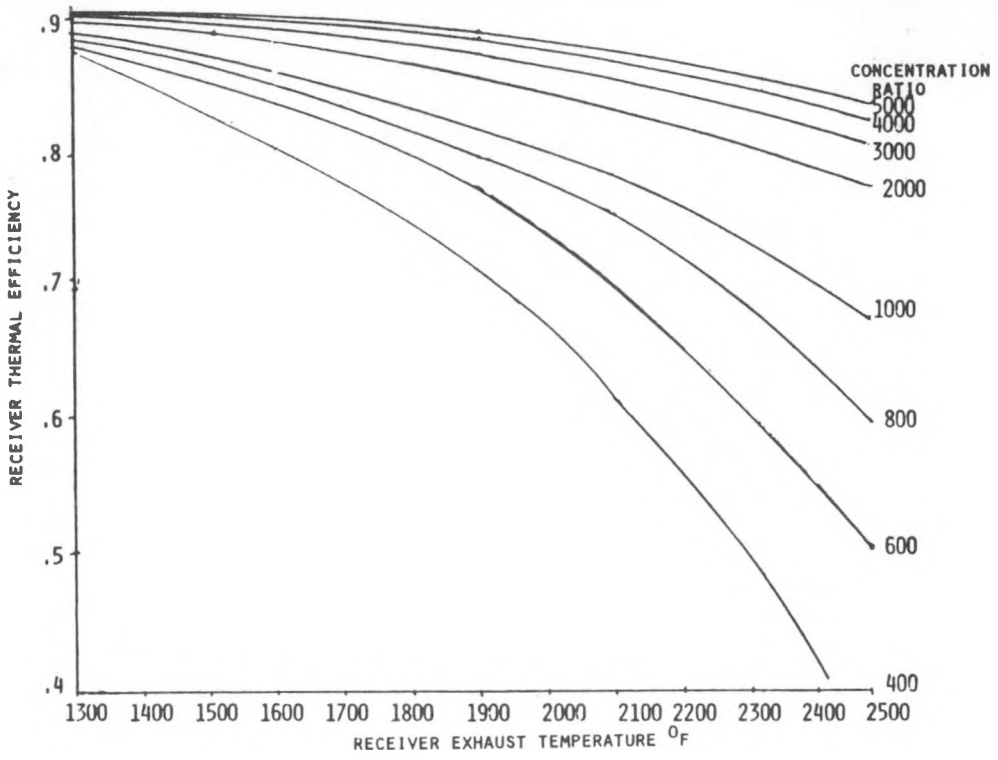

Fig. 3:SENSITIVITY OF RECEIVER EFFICIENCY TO RECEIVER EXHAUST TEMPERATURE

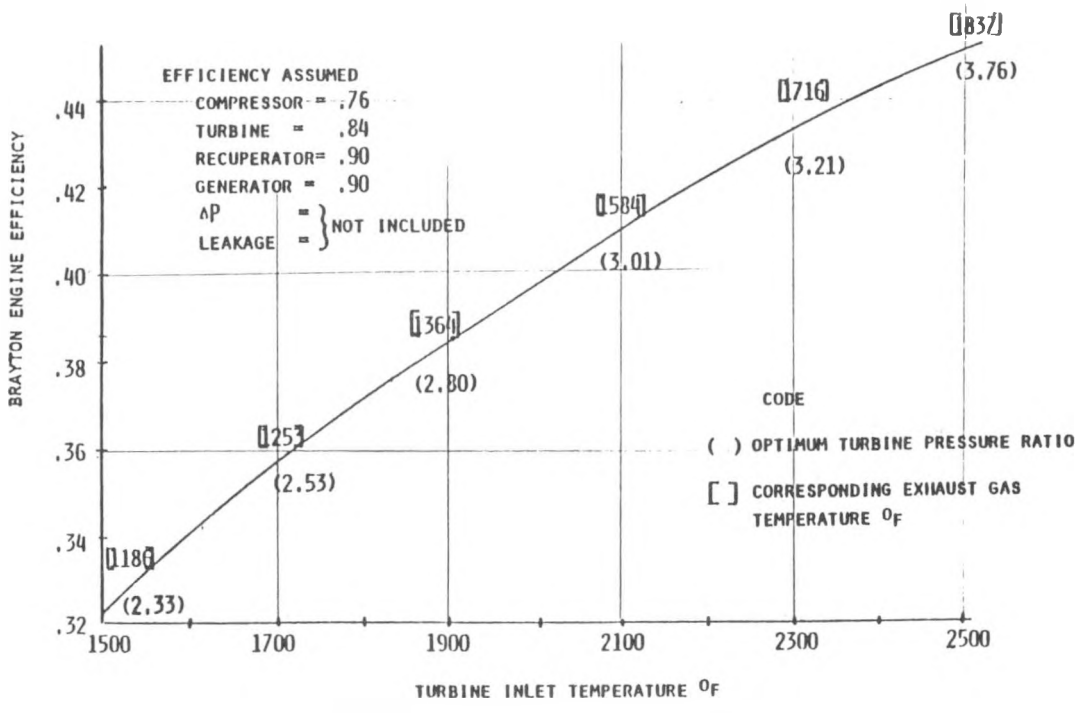

Fig.4:BRAYTON ENGINE GENERATOR EFFICIENCY

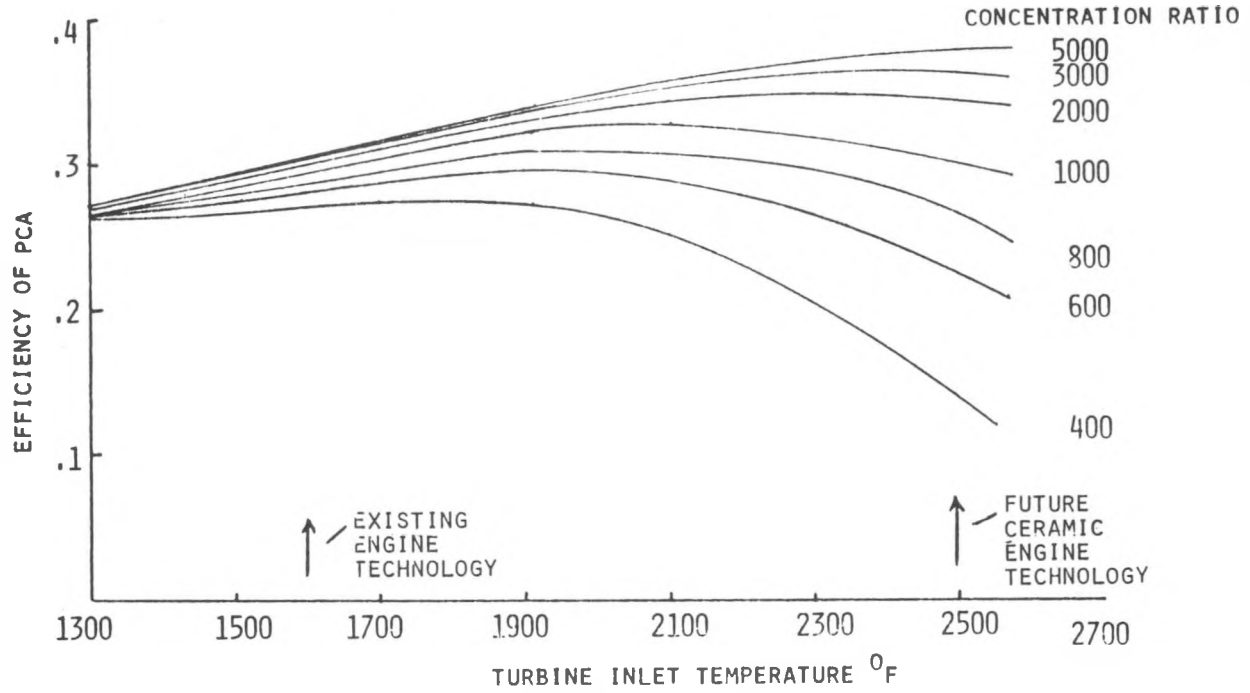

Fig.5:EFFICIENCY OF PCA IMPROVES WITH INCREASED TURBINE INLET TEMPERATURE

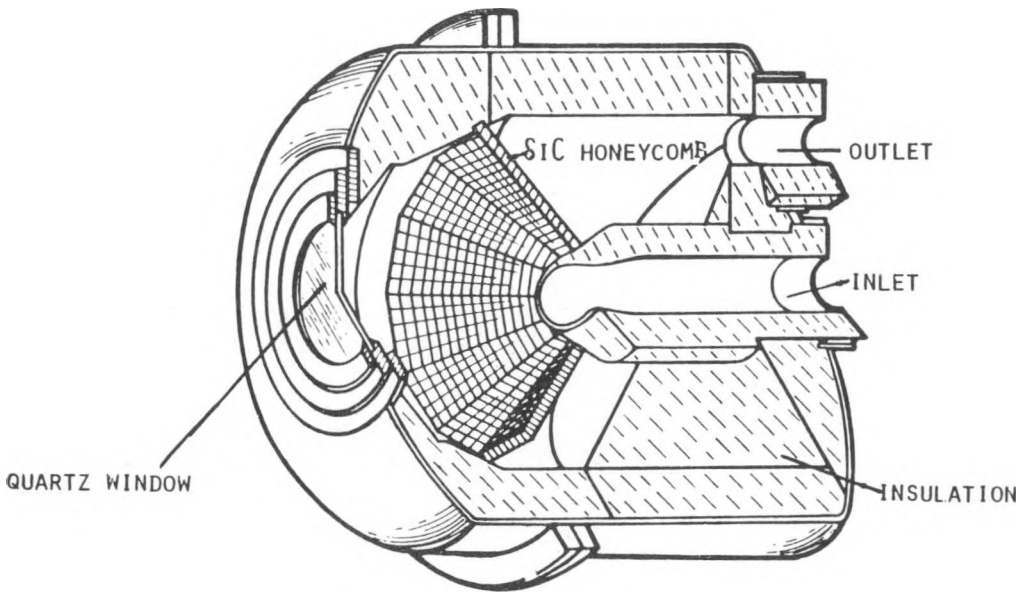

Fig. 6:SANDERS'HIGH TEMPERATURE SOLAR RECEIVER (CERAMIC MATRIX TYPE)

of projected power costs for both types of engines, it was concluded that the addition of a recuperative heat exchanger was cost effective. The small simple cycle was defeated primarily due to the inherently low potential efficiency. These small rotors face a serious degradation in efficiency for the high pressure ratios necessary to attain the good unrecuperated cycle efficiencies, due primarily to clearance leakages. However, the optimization of the recuperated Brayton cycle occurs at relatively low compression ratios, thus reasonable compressor and turbine efficiencies can be realized.

Four recuperative engines have been identified in this power range. AiResearch (Phoenix Division), and Detroit Diesel Allison (GM) are presently engaged in a competitive program sponsored by DOT/NASA to develop a Brayton engine for automotive use. These companies are pursuing similar paths toward ultra high efficiencies. The emphasis in this program is on the development of ceramic turbines, regenerators, and all hot section parts to permit turbine inlet temperatures approaching 2500°F. Shaft efficiencies on the order of 40 to 45% are projected. Although these engines are designed to deliver a peak power of 75KWs, their most efficient operating region corresponds to an automotive highway cruise condition at approximately 20KWs.

A solarized early version of this advanced gas turbine (SAGT-1A) engine has been assembled as an intermediate step in the engineering development. This prototype demonstrates the advanced design configuration with metal components. This engine does not promise high efficiencies at this stage of development but will provide the means for a solarized module test program at the JPL Parabolic Dish Test Site in January 1983.

Another small Brayton is under development at AiResearch (Torrance, CA) for use in commercial air conditioning units. This engine, fabricated from low cost metal castings, is attempting to enter this very cost competitive market within the next few years. The design incorporates elements necessary for a high reliability long life system. It is capable of providing a Mean Time Between Failure (MTBF) comparable to that of large scale utility generating Braytons, which are among the most reliable power plants operating today. The shaft efficiency is expected to reach the practical state-of-the-art limit for metallic components. At 30% efficiency, approximately 8KW of electrical power is available.

This 8KWe engine utilizes a configuration termed a subatmospheric Brayton cycle (SABC). It is essentially a closed cycle Brayton configuration in which a portion of the compressor exhaust air is vented at atmospheric pressure. The gas passing through the turbine, therefore, expands from nominally atmospheric pressure (14.7 psia) to the compressor suction pressure of approximately 7psia. One consequence of this configuration is the alleviation of the pressure load on the solar receiver. Through the elimination of the pressure vessel codes, a reduction of cost and a simplification of the design will occur.

CONCENTRATORS

Several concentrators, in the required power range, are under development. Some of their characteristics are listed in figure 8. The quantities

	GARRETT SABC	GARRETT SAGT-1A	DDA SAGT-100 MOD 1	GARRETT SAGT-MOD 2
TIT°F	1600	1600	1975-2350	2500
RPM OF OUTPUT TURBINE SHAFT AT MAX POWER	80,000	80,000	68,000	100,000
M LB/SEC	.25	.56	.76	.76
MAX SHAFT POWER OUT,KWs	9.3	17	75	75
WEIGHT, LB	750	450	300	300
TYPE OF RECUPERATOR/ REGENERATOR	METAL PLATE FIN	CERAMIC WHEEL	CERAMIC WHEEL	CERAMIC WHEEL
DERIVATIVE FROM:	AIR CONDI-TIONING & TURBO SUPER-CHARGER	ADVANCE AUTOMOTIVE	ADVANCE AUTOMOTIVE	ADVANCE AUTOMOTIVE

Fig.7:BRAYTON ENGINE CANDIDATES

DESIGNATION	CONCENTRATION RATIO	REFLECTIVE SURFACE	MANUFACTURER	STATUS
TBC	2600	2ND SURFACE GLASS + FOAMGLASS BACKING	E-SYSTEMS	2 IN USE AT PDTS
PDC-1	950	COATED FIBERGLASS MOLDED PANELS	GE DESIGN FAAC CONSTRUCTION	1 IN DEVELOPMENT
PDC-2	2600	2ND SURFACE GLASS + FOAMGLASS PANELS	ACUREX	DESIGN ONLY
ADVANCO	2000	2ND SURFACE GLASS ON FOAMGLASS PANELS	ADVANCO	1 IN DEVELOPMENT
PKI	250 - 800	2ND SURFACE GLASS PANELS ON CURVED STRUCTURE	POWER KINETICS	3 IN USE
ESSCO	1500	PLASTIC COATING ON ALUMINUM	ELECTRONIC SPACE SYSTEMS CORP.	1 IN TEST
SKI	290	PLASTIC COATING ON ALUMINUM	SOLAR KINETICS	100+ IN OPERATION
LaJET	1500	PLASTIC FILM OVER EVACUATED DRUM	LaJET ENERGY	3 IN TEST

Fig.8:CONCENTRATOR CANDIDATES

of available reflected power are suitable for two engine categories. The concentrators in the 11 to 12 meter diameter range will be considered for integration with the advanced automotive gas turbines. The smaller concentrators, Essco, LaJet, SKI and PKI, are well suited to the 8KWe SABC engine.

A performance comparison is normally accomplished on the basis of reflector surface quality. Structural integrity is also important to assure that the optical quality does not deteriorate due to thermal expansion and wind loading. The column in figure 8 entitled "Concentration Ratio" is presented solely for the purpose of comparison of the various candidates. It lists the ratio of the concentrator collection area to a near optimum receiver aperture area appropriate for use with a 1600^{o}F Brayton engine. Few concentrators have been satisfactorily characterized to date. Only the TBC (Test Bed Concentrator) and SKI (Solar Kinetics, Inc.) have been tested to the extent necessary to conduct the PCA optimization analysis previously discussed.

Large Concentrators

Two TBC's have been built for the JPL by E-Systems, Inc. and installed at Edwards Air Force Base. These concentrators have demonstrated excellent focusing characteristics. The glass on foam glass panels are highly accurate and a rigid back structure is provided. However, these units were not designed and constructed with a strong emphasis on cost reduction techniques.

Much of the technology developed from the TBC program has been applied to the PDC-2 (Parabolic Dish Concentrator). Acurex, as a prime contractor, seeks to duplicate the performance of the TBC while providing a feasible cost effective approach. Two types of reflector panels have been tested. Glass on a laminate plastic backing was originally viewed optimistically because of the significant cost advantage in production. The individual panels did not perform up to expectations in the test phase of the program. The glass on foam glass panels are again being reviewed but plans for manufacturing the concentrator are still on hold. The size of the concentrator, and the goals of this development program are well suited for the advanced automotive gas turbine derivatives.

The Advanco concentrator is presently in the design phase for use in the Stirling PDM program. Their approach utilizes the JPL/TBC panel design. The performance of this unit is expected to be close to that of the TBC and a significant reduction in cost is anticipated. Characterization is at least a year away.

The PDC-1 was delivered to the JPL Edwards Test Site in the summer of 1982. This concentrator was designed by General Electric and built under the direction of Ford Aerospace and Communications Corp. (FACC). Characterization has not yet been completed but is expected by January of 1983. Prior to delivery, individual gores were tested by the JPL. Based on these projections, the receiver optimization model indicates that a concentration ratio of about 950 is appropriate for the 1600^{o}F Brayton PCA. The gores feature a mylar film bonded to a glass reinforced plastic sandwich panel. This fabrication process is expected to yield a low cost production unit. The 12 meter diameter PDC-1 is approximately 19% larger than the PDC-2 design. Although

its optical performance and hence the collection efficiency is lower than that projected for the PDC-2, analysis indicates that the power available to the engine is about the same in either case.

Small Concentrators

SKI has produced more parabolic concentrators than any other manufacturer. As the principle supplier for the Shenandoah program, they delivered 120 units complete with tracker and a focal mounted liquid heat exchanger. The surface quality is only adequate for very low temperature Brayton cycles. Moreover, the design employed does not appear to lend itself to future improvements without extensive changes. The pressed panels are low cost but relatively crude. The overall structure also is quite massive, yet the panels are visibly distorted by wind gusts. The unit is presently available at a relatively low cost but does not appear to have the performance needed to compete with the higher performance designs.

Essco (Electronic Space Systems Company) is aggressively pursuing a private venture to manufacture their 7.3m diameter concentrator in large volume. The reflector panels, like SKI, utilize a mylar film on a molded aluminum panel. A box beam back structure provides the basis for a very rigid structure. Through Essco's vast experience in the ratio telescope field, they have devised a very precise and accurate method of panel fabrication. Their first unit has been on test for over a year but no characterization data has been made available. It has recently been moved to the University of New Mexico for evaluation and some data is expected in the near future.

Power Kinetics, Inc. (PKI) is marketing an innovative concentrator which employs a fresnel concept. One foot square panels are arranged in 12 groups of 72 panels each. This design incorporates low cost commercially available components and is easy to transport and assemble. Additional cost savings have been realized due to the low overall structure weight. An advantage of this segmented paraboloid is that wind loading is reduced. Thus, adequate rigidity is obtained with a minimized structure weight. One shortcoming of this design is that the use of the one foot square plane panels limits the overall concentrating ability. In its present configuration, the PKI performance is comparable to that of the SKI concentrator. A future effort is under consideration to introduce a one dimensional contour to the individual panels. Also, due to the relatively long focal length of this unit, a preliminary analysis has indicated that a terminal concentrator would improve the performance. Efforts in these areas could increase the concentration ratio of system from about 300 to 800 and consequently greatly enhance its commericial viability for use with the Brayton module.

Another promising concentrator candidate is under development at LaJet Energy. A lightweight space frame is used to support a cluster of 60 inch diameter parabolic dishes. The contour of each dish is obtained by stretching a mylar film over a partially evacuated drum. The surface quality of individual reflectors appears to be quite good, however, adequate characterization has not yet been completed.

The modular construction of this design provides the capability for expansion. The range of power available from this unit is well suited for the SABC engine. Three LaJet concentrators are presently undergoing field testing and characterization data is expected in the near future.

In conclusion, four concentrator candidates compatible with the 8KWe SABC engine will be available for the Parabolic Dish Module (PDM) Development Program scheduled for 1983. The three most advanced designs, Essco, PKI, and LaJet offer the most near term potential.

The Essco design relies on a precision fabrication process with proven accuracy, but the cost effectiveness of this process in the solar PDM market has not yet been demonstrated. The PKI approach, on the other hand, utilizes low cost prefabricated components as well as a simple fabrication process. If characterization of the LaJet unit confirms predictions it becomes the likely choice.

CONCLUSIONS AND RECOMMENDATIONS

The long term goal of this Solar Brayton/Electric Development Program is to utilize a high efficiency, low cost, advanced production Brayton engine. The current short range program recommendation is to design, build, and test a smaller 1600^{0}F T.I.T. unit (SABC) utilizing nearer term technology. The technical system challenges for a Solar Brayton Electric System are similar with both the SABC and the SAGT candidates, but only the small concentrator and engine is available to this program in the proper time frame. Problems associated with the system operation will be understood and economic solutions obtained in anticipation of the 2nd Generation development utilizing an adaptation of the automotive turbine.

REFERENCES

1. 1/4 Megawatt Solar Receiver, Final Report, Department of Energy, San Francisco Operations Office, Contract No. EG-77-C-03-1555, 10/79.

2. Final Report for a 10KWt Solar Energy Receiver, for Department of Energy, Chicago Operations Office, Contract # E(11-1)-2823, 11/78.

3. High Temperature Solar Thermal Receiver Final Report, JPL Contract # 955454, 11/79.

4. Parametric Analysis Report, High Temperature Solar Thermal Receiver, JPL Contract #955454, 7/79.

5. Projections of Distributed Collector Solar-Thermal Electric Power Plant Economics to Years 1990 - 2000, DOE/JPL/1060-1, Work Performed Under Contract No. EX-76-A-29-1060, December 1977.

APPENDIX 1

RECEIVER OPTIMUM EFFICIENCY DESIGN MODEL

- REFLECTION BY WINDOW = 8% OF INCIDENT ENERGY

- THERMAL LOSS FROM RECEIVER SHELL = $UA_0 (T_0 - T_\infty)$

  WHERE U = OVERALL HEAT TRANSFER COEFFICIENT
  AND FREE CONVECTION COEFFICIENT = 1 BTU/FT^{2}HR ^{0}F
  THERMAL CONDUCTIVITY OF CERAFORM INSULATION

  T_0 = TURBINE EXHAUST TEMPERATURE

  T_∞ = 60^{0}F

  A_0 = SHELL SURFACE AREA

  $= 2\pi(R_A + \delta)\,(L'(R_A/R')^{1/4} + X) + \pi(R_A + \delta)^2$

  δ = INSULATION THICKNESS

  L', R' = PLENUM DESIGN PARAMETERS

  X = DISTANCE BETWEEN ABSORBER AND WINDOW

- CONVECTION FROM WINDOW SURFACE = $HA_W(T_W - T_\infty)$

  WHERE H = FREE CONVECTION COEFFICIENT

  T_W = WINDOW TEMPERATURE = EGT/2 (FROM ANSYS MODEL)

  A_W = WINDOW APERTURE AREA

- RADIATION FROM WINDOW SURFACE

  $= A\sigma\varepsilon\,(T_W^4 - T_\infty^4)$

  WHERE ε = EMISSIVITY OF QUARTZ AT T_W

  σ = BOLTZMAN CONSTANT

- INTERCEPT FACTOR OF INCIDENT ENERGY DISTRIBUTION ON WINDOW

  $= 1 - E^{R_A^2/2\sigma^2}$

  WHERE σ = STANDARD DEVIATION OF ENERGY DISTRIBUTION

- SHADING OF CONCENTRATOR BY PCU

  $= \pi(R_R + F\alpha)^2/A_D$

  WHERE: R_R = RECEIVER OUTSIDE RADIUS

  F = CONCENTRATOR FOCAL LENGTH

  α = SUN ANGLE

  A_D = CONCENTRATOR COLLECTION AREA

- RERADIATION FROM RECEIVER ABSORBER

  $= A_A\sigma\varepsilon\tau F_V\,(T^4 - T_\infty^4)$

  WHERE: A_A = ABSORBER AREA

  ABSORBER RADIUS = X TAN θ + R_W

  $\theta = \tan^{-1}(1/2F\#)$

  ε = EMISSIVITY OF SIC MATRIX FUNCTION OF T_A

  τ = TRANSMISSIVITY OF QUARTZ WINDOW (OVER EMISSION SPECTRUM OF ABSORBER)

  T_A = ABSORBER TEMPERATURE = TURBINE INLET TEMPERATURE + ΔT

  WHERE: ΔT = EMPIRICAL FUNCTION OF SOLAR IRRADIANCE (BASED ON ANSYS MODEL)

  AND F_V = GEOMETRICAL VIEW FACTOR FROM ABSORBER THROUGH WINDOW

GARRETT TURBINE ENGINE COMPANY
A DIVISION OF THE GARRETT CORPORATION
PHOENIX, ARIZONA

SOLAR ADVANCE GAS TURBINE BRAYTON POWER CONVERSION ASSEMBLY

B. Anson

ABSTRACT

The solar advanced gas turbine Brayton power conversion assembly, SAGT-1A, is being developed by The Garrett Turbine Engine Company and Sanders Associates, Inc. Garrett has designed, fabricated and assembled the engine, generator and solar receiver under DOE/JPL/NASA Contract DEN3-181. Further, all necessary ancillary equipment required for the feasibility tests at the JPL parabolic dish test facility has been completed and verified operational.

The Brayton engine, SAGT-1, which will be used in the power conversion assembly, is approaching completion of required development for use in SAGT-1A. The engine is derived from the Advanced Gas Turbine, AGT101, now under technology development by Garrett and Ford Motor Company for automotive use under DOE/NASA Contract DEN3-167. To date, the engine has demonstrated operation over its entire speed range to 100,000 rpm and has produced 22 horsepower during initial performance testing.

SAGT-1A power conversion assembly testing at the JPL parabolic dish test site is planned for early 1983 with initial system operation in late 1982 at Garrett in Phoenix Arizona.

1.0 INTRODUCTION

A solarized advance gas turbine brayton power conversion assembly, SAGT-1A, is being developed by Garrett and Sanders Associates for feasibility testing at the JPL Parabolic Dish Test Site. Garrett is performing this effort under DOE/JPL/NASA Contract DEN3-181. This contract was amended in 1982 from the original task of developing a solar powered version of the Advanced Gas Turbine AGT101 (SAGT-1) to include design, fabrication and testing of a power conversion assembly utilizing the SAGT-1. This task required design of a power takeoff for the SAGT-1 to drive an induction generator, a structure on which the induction generator and solar receiver could be assembled, interconnecting ducting to the Sanders Solar receiver and all necessary support equipment required to conduct the feasibility tests at JPL.

This paper provides a report on the design and present status of the SAGT-1A and the AGT101 technology development status, from which the SAGT-1 is derived. The planned SAGT-1A testing also is discussed.

2.0 SAGT-1A DESIGN

The SAGT-1A power conversion assembly has been designed to demonstrate the feasibility of a Brayton engine operation with either solar energy or fossil fuel. The three major assembly components are the Brayton engine (SAGT-1), the Sanders Solar receiver and the induction motor/generator.

Figures 1 and 2 show the SAGT-1A assembly with several design features outlined below:

- The SAGT engine has the same internal configuration as the AGT101 (Figure 3) now in technology development--only the ducts providing engine through-flow air diversion to the solar receiver, differentiates the two engines--the engine output speed is reduced via a 38-inch gear system into a timing belt drive to the generator--the gearbox output also drives the engine regenerator--the belt drive is designed to accommodate several different pulley ratios so that engine speed may be optimized during the feasibility tests
- Engine control components also are obtained from the AGT101 program--this system utilizes a microprocessor control with a readily reprogrammable feature--this system was easily modified to perform the necessary solar operational requirements
- When operating on fossil fuel, the engine will use the unmodified AGT101 combustion system
- Engine air flow to and from the Sanders receiver is accomplished by two specially designed ducts that provide for thermal growth between the two components--internally reacted pressure loads in the flexible joints and a minimum pressure loss between the engine and reciever
- The selected induction generator is a commercially available high-efficiency, 60 Hertz machine and is directly connected

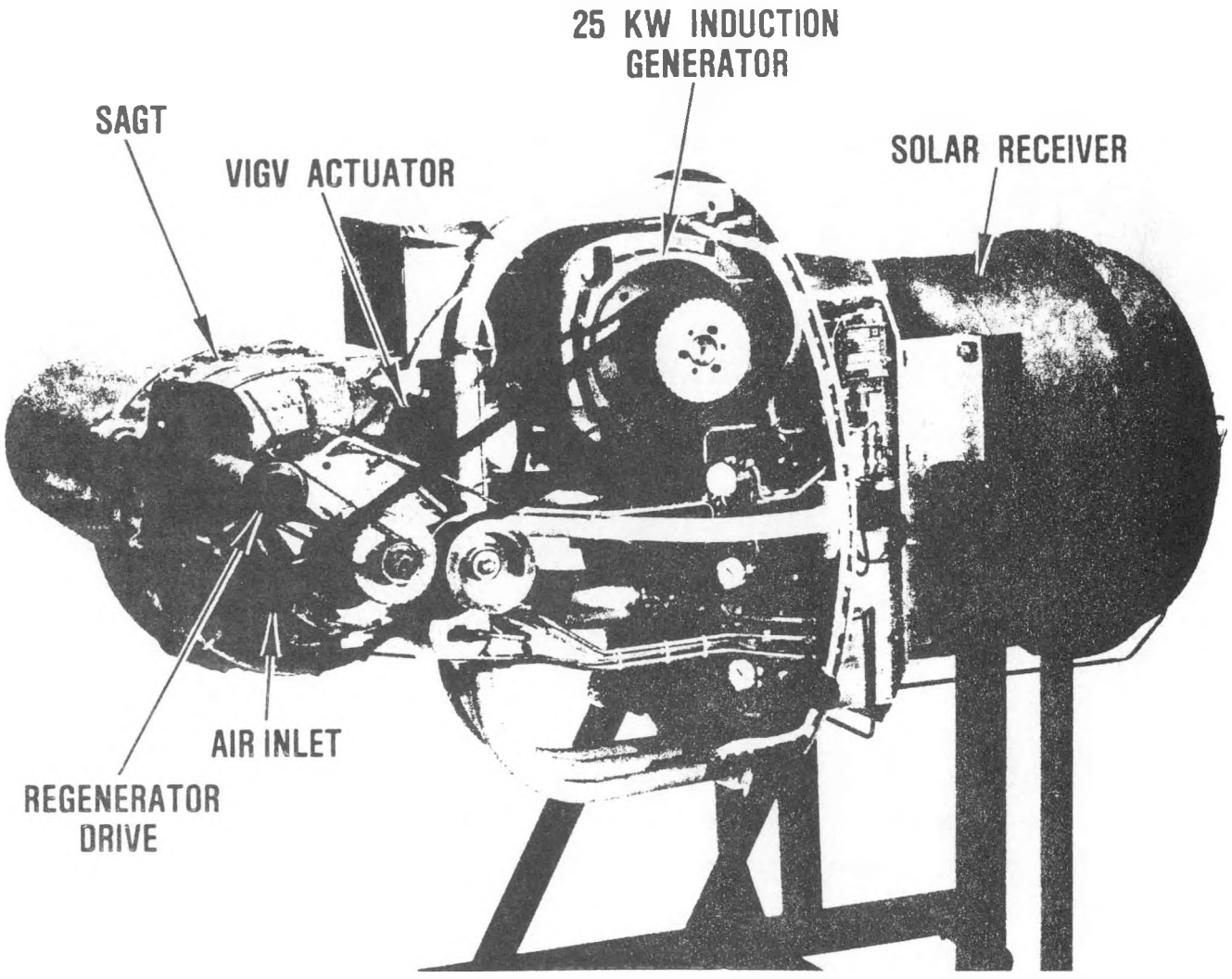

Figure 1. Power Conversion Unit.

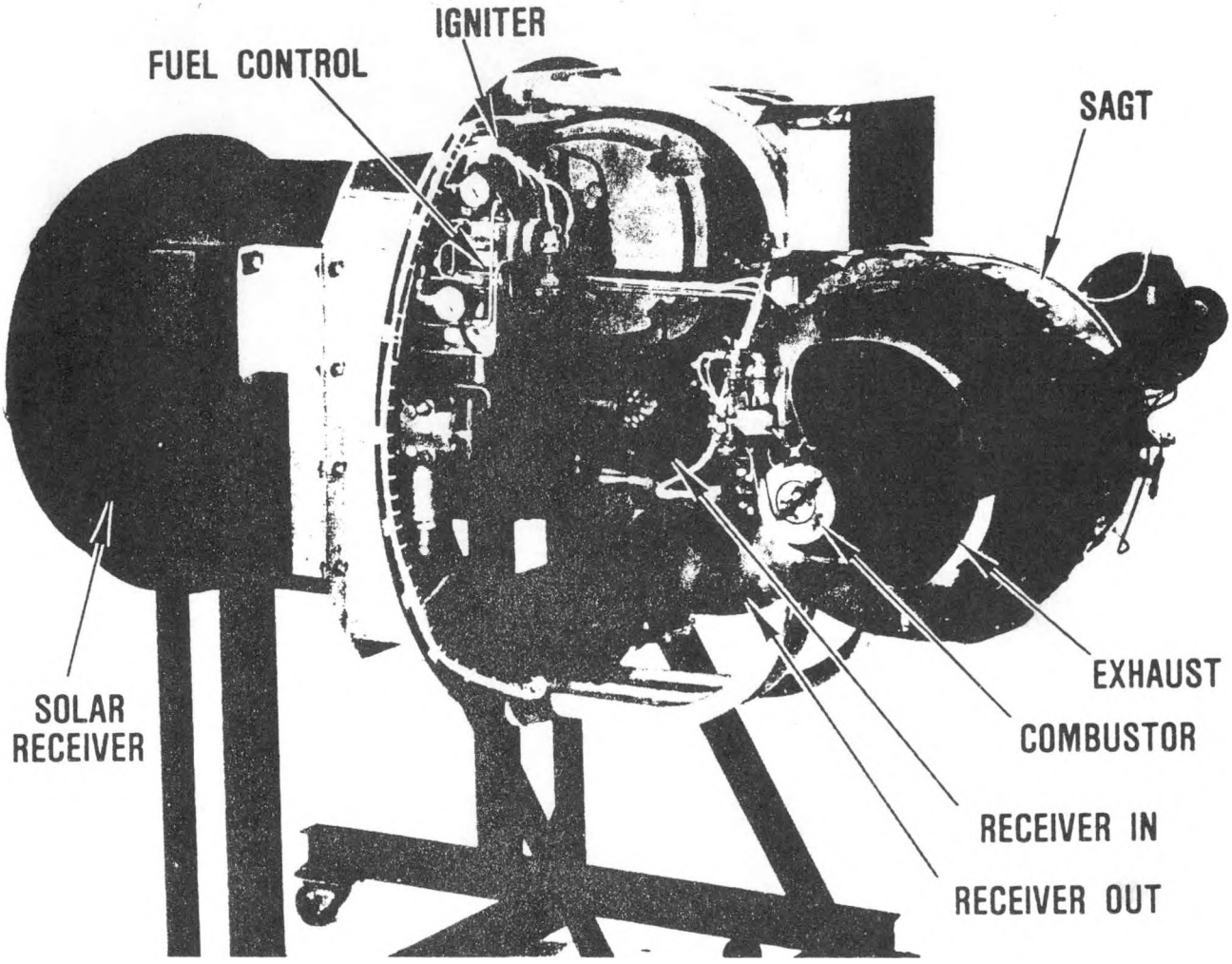

Figure 2. Power Conversion Unit.

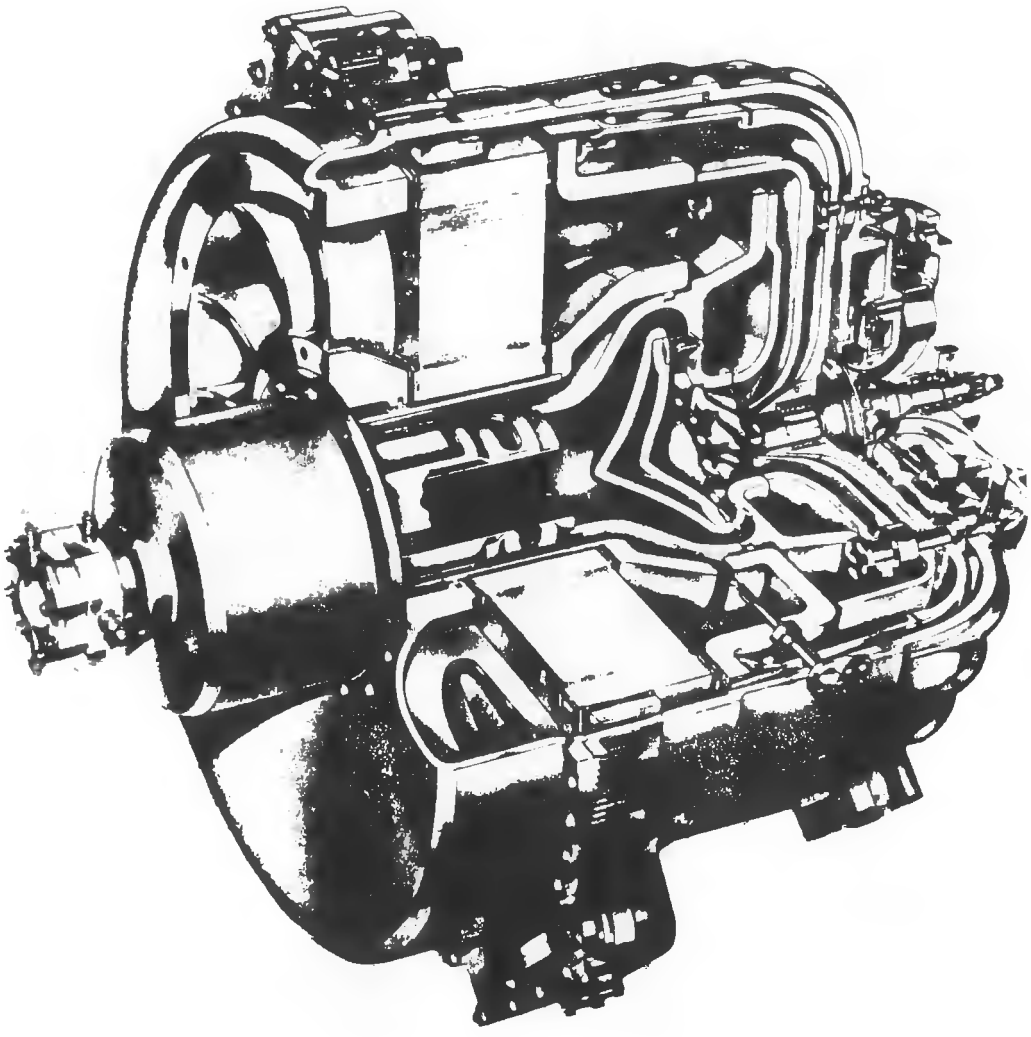

FIGURE 3. AGT101 Automotive Gas Turbine Engine.

to the ac grid--this eliminates the need for a separate power conditioning unit as well as an engine speed/load control--further, it serves as the SAGT-1 engine starting engine

- The SAGT-1A also is designed to mount directly to the JPL Test Bed Concentrator

Additional special equipment required to support the SAGT-1A tests are schematically shown in Figure 4--this equipment has been designed, fabricated, and operationally verified at Garrett.

The SAGT-1A, and related support equipment, was designed to be easily transportable and capable of operating with an ac power input, fossil fuel (DF_2) and/or solar energy. Tests at Garrett involve testing only with fossil fuel. The electrical equipment enclosure that will be located at the base of the parabolic mirror contains the following:

- Electronic microprocessor control and related power supply
- Relays necessary to activate the induction motor/generator
- Relays required to actuate several system valves required for the feasibilty tests

The instrument and control console will be located in the site control room--this console contains all necessary control functions and instrumentation required for SAGT-1A operation. The console receives power and inputs from the equipment cabinet through two specially fabricated electrical cables approximately 400 feet long. The console also provides for recording of pertinent engine operating parameters.

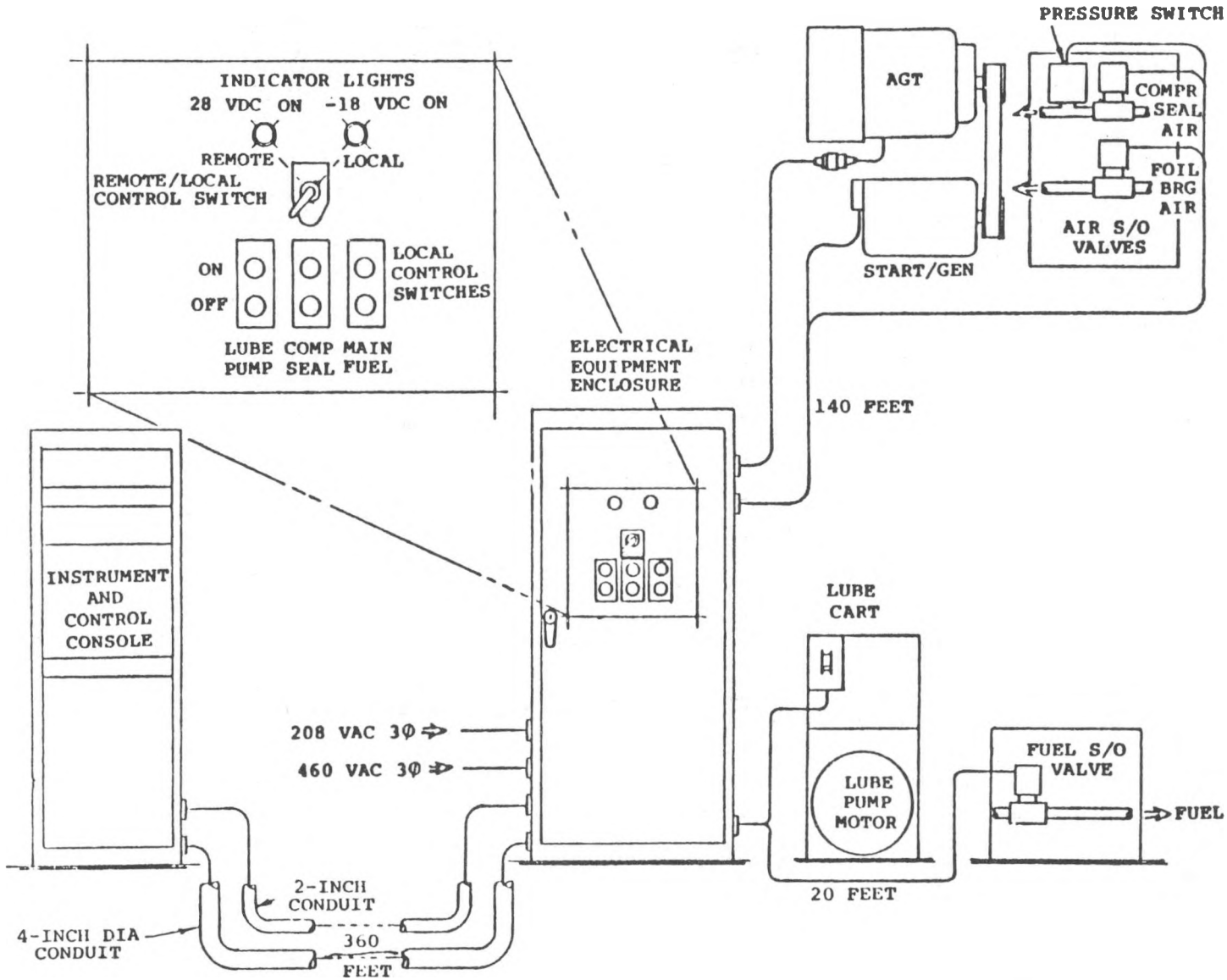

Figure 4. SAGT-1A Electrical Interconnect Diagram.

3.0 SAGT-1 STATUS

As previously mentioned, the SAGT-1 power section is the AGT101 engine except for the ducting required to interface the engine with the solar receiver. While the SAGT-1 has been checked out with the ducting, engine testing has been an integral part of the AGT101 technology development. During development testing, the engine is referred to as AGT101 S/N 003. A brief synopsis of the AGT101 development follows:

- First engine test was achieved in July 1981
- First self-sustaining engine operation occurred on December 15, 1981--the engine was operated at a speed of 50,000 rpm for 1 hour and 58 minutes
- Since that time three AGT101 engines have been tested--on September 28, 1982 S/N 001, Build 7 achieved full operational speed of 100,000 rpm--all three AGT engines have now achieved full speed--during initial performance testing in October 1982, Engine S/N 003 produced 22 horsepower--a summary of the engine testing to date is presented in Table 1.

Performance testing will continue. Engines S/N 001 and S/N 002 are test beds for ceramics and the other technologies being developed under the AGT101 program. The SAGT-1 will be mated with the Sanders Receiver and tested as an assembly at Phoenix before shipment to JPL's Parabolic Test Site.

TABLE 1. AGT101 TESTING THROUGH NOVEMBER 16, 1982

Power Section Serial Number	Starts	Operating Time
001	101	71 hrs 47 min
002	20	20 hrs 48 min
003	41	10 hrs 39 min
Total	212	103 hrs 14 min

4.0 SAGT-1A TEST PROGRAM

Garrett, under DOE/JPL/NASA-Lewis direction and in conjunction with Sanders Associates, has formulated a feasibility test program for the SAGT-1A. This program is comprised of three major elements as outlined below:

4.1 System Checkout and Calibration at the Garrett Phoenix Facilty

Testing in this phase will be accomplished only with fossil fuel. These tests will provide both a checkout for operation of the system and performance information at anticipated power conditions. After satisfactory completion of these tests, the system will be shipped to the JPL parabolic Dish Test Site.

4.2 Parabolic Dish Installation and Operation with Fossil Fuel

The system will be installed at the JPL facility and operated with fossil fuel to checkout the engine, receiver and dish. Several operating conditions similar with Phoenix test conditions will be conducted to verify proper system functioning and performance.

4.3 Solar Operation

In the third phase, the SAGT-1A will be operated using solar energy from the mirrored concentrator. A semi-automatic control system will provide constant turbine inlet temperature.

This test series is designed to demonstrate feasibility of the Brayton engine and solar receiver for solar power generating applications. Further, sufficient test information will be compiled to provide the necessary data for further Brayton system development.

The AGT101 and SAGT programs are providing a technology base for future gas turbine engines. Ceramics, low-emissions multi-fuel combustion, rotary regenerator, gas bearing, controls and high performance, aero, and thermal component development are all a part of these important programs.

Blank Page

Distributed Solar/Gas Brayton Engine Assessment

Jean Rousseau

AiResearch Manufacturing Company

Torrance, California 90509

BACKGROUND

A 10-ton gas-fired heat pump is under development at AiResearch under Gas Research Institute (GRI) sponsorship. This system, shown in Figure 1, features a highly efficient Brayton-cycle engine driving the centrifugal compressor of a reversible vapor-compression heat pump. The engine is subatmospheric and the natural gas fuel is combusted at atmospheric pressure. Pertinent performance data are listed in Figure 1 for the cooling mode of operation. The power delivered by the engine is estimated at 10.3 hp, at the conditions shown in the schematic.

The investigations described in this paper concern the commercial feasibility of solarizing this heat pump. As work progressed, the scope of the program was expanded to include other system configurations, which led to the evaluation of a hybrid cogeneration system.

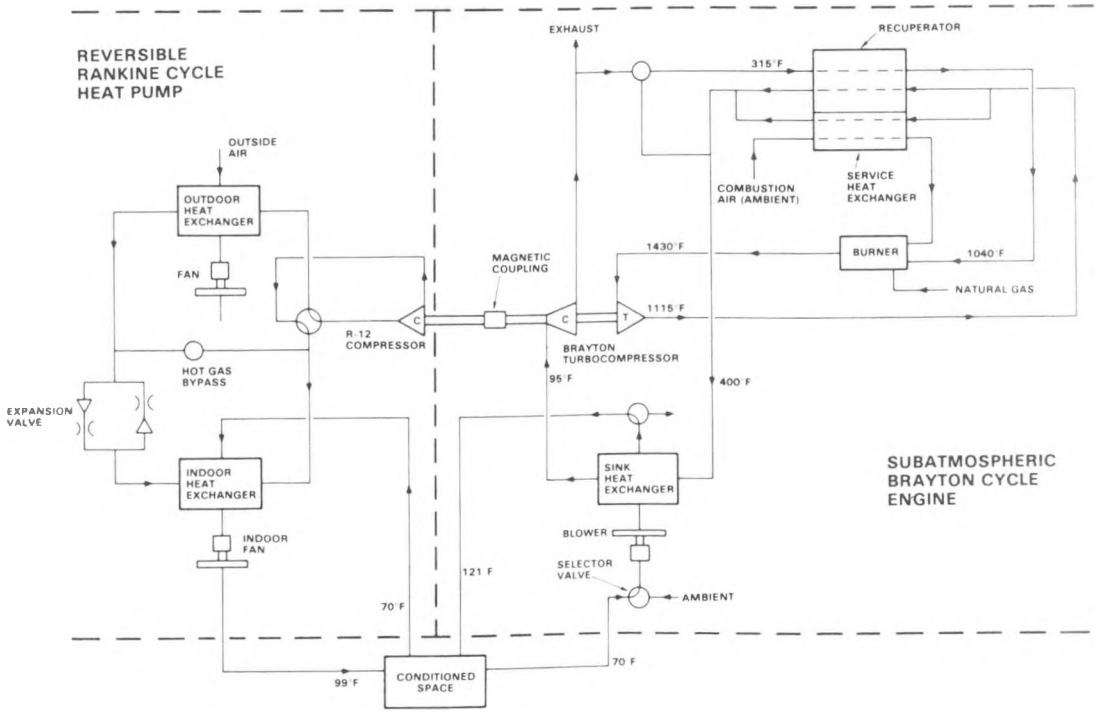

Fig. 1. Gas-fired Heat Pump Schematic Diagram

SOLARIZED GAS-FIRED HEAT PUMP

Description

Figure 2 illustrates the overall arrangement of the solarized heat pump and the location of the major components. The Brayton engine will be mounted at the focal point of the concentrator for close thermal coupling with the receiver. The Rankine vapor-cycle equipment will be on the ground to minimize weight at the focal point. This repackaging of the basic gas-fired heat pump has implications that affect the overall performance of the system:

- Incorporation of the solar receiver between the recuperator and the combustor
- Liquid and vapor lines between the engine-driven vapor compressor and the remainder of the refrigerant subsystem
- Liquid heat transport loop between the engine heat sink exchanger and the heat pump package

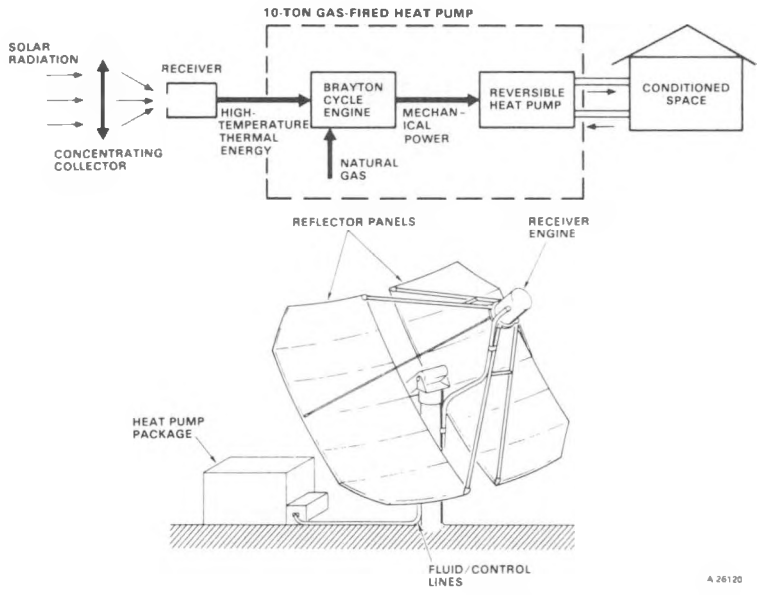

Fig. 2. Solarized Heat Pump System Concept

System Performance

In this type of heat pump system, the absence of thermal storage for solar energy makes it necessary to perform calculations on an hourly basis. This required the development of system/subsystem computer programs to mechanize the year-round performance calculations. Preliminary investigations showed that the optimum match occurred when the solar collector and receiver provide all engine energy requirements at the maximum insolation rate. With a combined collector/receiver efficiency of 0.79, this corresponds to a solar collector area of 385 sq ft.

All heat pump systems were analyzed in applications defined by three typical buildings and six representative geographic locations.

- Building Types

  Low-rise motel
  Small office building
  Small retail store

- Geographic Locations

  Madison, Wis.
  New York, N.Y.
  Nashville, Tenn.
  Dodge City, Kan.
  Fort Worth, Tex.
  Phoenix, Ariz.

In the applications considered, the building heating/cooling loads must be met whether solar energy is available or not. Conversely, excess solar energy over that required to satisfy building loads must be wasted. In such a demand system without storage, there is a fundamental mismatch between the heating/cooling demand and the availability of solar energy: 50 to 70 percent of the solar energy collected is wasted in this system arrangement. Figure 3 shows energy balance data for a typical application.

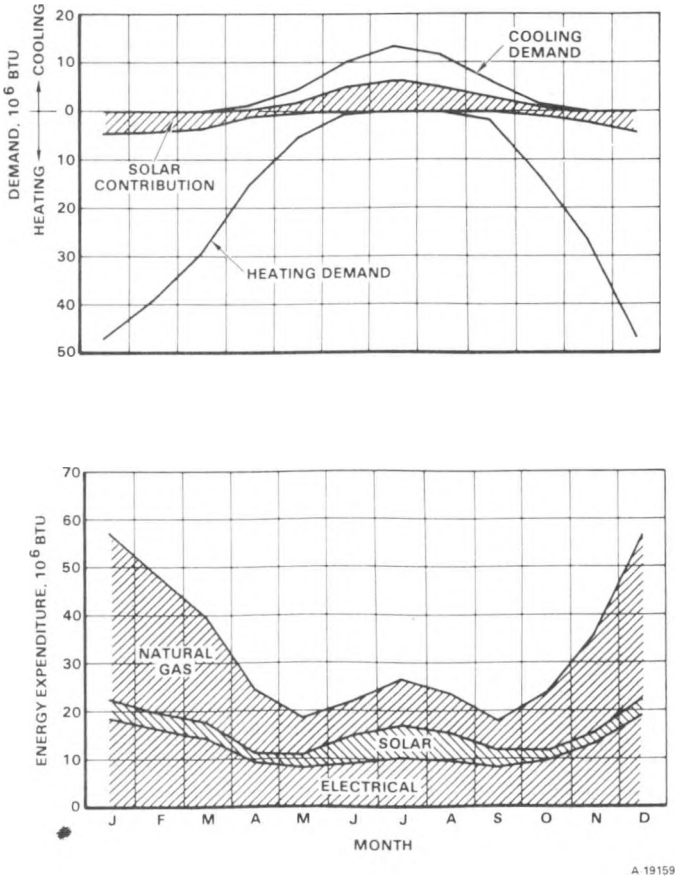

Fig. 3. System Performance for Nashville Low-Rise Motel With 385-sq-ft Collector

Table 1 summarizes yearly energy and economic data for a 10,000-sq-ft motel in the six locations considered. The energy savings through solarization are not sufficient to offset the high initial cost of the solar collector and receiver.

TABLE 1

ECONOMIC COMPARISON - 10,000-SQ-FT MOTEL

	Madison	New York	Dodge City	Nashville	Fort Worth	Phoenix
Solar-assisted gas-fired						
Yearly energy consumption						
• Natural gas, MMBtu	726	336	487	298	200	246
• Electricity, kw-hr	30,600	14,800	24,500	13,900	10,500	15,200
Operating cost, $/year	5,122	3,223	2,935	2,041	1,196	2,031
Initial cost, $	49,700	23,450	41,475	24,850	17,150	26,000
Gas-fired						
Yearly energy consumption						
• Natural gas, MMBtu	1,001	425	734	388	274	397
• Electricity, kw-hr	34,400	16,000	27,200	14,800	10,100	14,500
Operating cost, $/year	6,610	3,840	3,926	2,543	1,433	2,686
Initial cost, $	32,900	14,900	26,800	15,800	9,530	14,300
Equivalent energy savings, MMBtu/year	31.3	101	274	109	70	143
Simple payback, years	11.3	13.9	14.8	18.0	32.2	18.8

Conclusions

The conclusions reached with respect to the solar-assisted gas-fired heat pump are summarized as follows:

(a) The simple payback periods estimated for all buildings/locations considered are unacceptable

(b) Solar utilization efficiencies must be increased significantly for economic feasibility

Several approaches were considered to improve the system effectiveness in utilizing the collected solar energy:

(a) Storage of high-temperature solar energy was rejected as impractical because of the high weight necessary at the focal point. This presents technological problems and does not resolve the problem of long-term storage that is necessary for high solar utilization in spring and fall.

(b) Storage of heat pump effect in the cooling and heating modes becomes very complex considering the two sources of heat and also the possible requirements for heating and cooling on the same day. This approach also does not resolve the spring/fall waste of solar energy.

(c) Constant cooling load applications were investigated. In this situation all solar energy collected is used in the Brayton engine. As a result, much lower paybacks are estimated in comparison to the basic gas-fired heat pump.

However, the major performance advantage of the basic 10-ton gas-fired heat pump over conventional systems is in the heating mode, rather than the cooling mode. Consequently, the advantages of the solarized version of this machine in a constant cooling mode application are questionable. Furthermore, the market potential is limited by the constant base load application.

HYBRID COGENERATION SYSTEM

Description

The hybrid cogeneration system is shown in block diagram form in Figure 4. The system is hybrid with regard to energy input--solar, natural gas, or both--and will supply electrical power as well as thermal energy at temperature levels up to about 400°F. The system investigated utilizes the subatmospheric Brayton-cycle engine. In this arrangement the engine drives a permanent-magnet alternator at shaft speed. The high frequency power from that engine can be converted to any power quality desired, depending on the particular application.

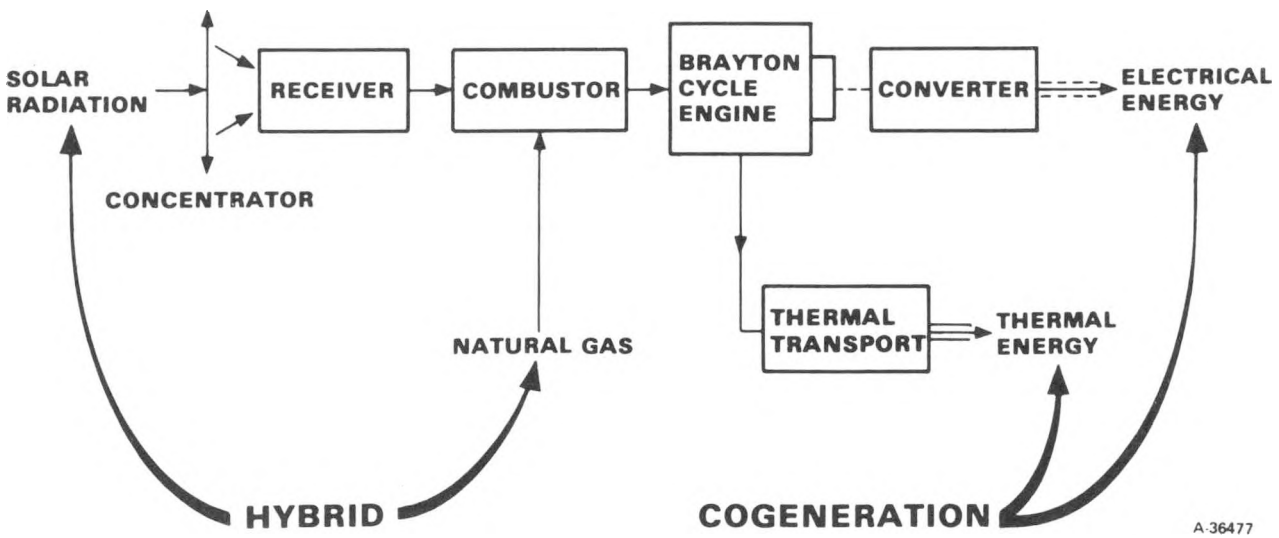

Fig. 4. Hybrid Cogeneration System Arrangement

The waste heat is from the engine heat sink heat exchanger and is obtained through an intermediary liquid loop between the engine and the ground. In this arrangement, engine operation is at constant speed (75,000 rpm) and constant turbine inlet temperature (1600°F). This is done by control of fuel flow to supplement solar thermal energy input.

Performance

The performance of the system was determined for the six locations considered in this study and covered a range of duty cycle and waste heat utilization. The lowest duty cycle considered in each case corresponds to system operation whenever solar energy is available at a rate higher than 10 percent of design. In this case, there is always a solar contribution and natural gas is used to make up the engine thermal input requirement. Expanding the duty cycle of the system for operation on natural gas alone will increase the electrical energy production of the system and also increase the availability of waste heat.

Baseline economic parameters are listed in Table 2. Figure 5 shows performance and economic data for the six locations considered. Figure 6 shows parametric data for Dodge City, Kansas.

TABLE 2

BASELINE ECONOMIC PARAMETERS

Initial equipment cost	$16,300	
Down payment	30 percent	
Salvage value	0	
Energy cost, 1982	Electrical, $/kw-hr	Natural Gas, $/MMBtu
Madison	0.058	4.61
New York	0.087	5.76
Nashville	0.051	4.61
Dodge City	0.051	3.46
Fort Worth	0.048	3.46
Phoenix	0.059	3.61
Energy Escalation rate	Natural gas: 15.6 percent to 1986, 10.3 percent after 1986 Electricity: 8.2 percent to 1986, 8.3 percent after 1986	
Elect. power buy-back	1.00 x average price	
Misc. operating cost	1.5 percent of cost	
Year of operation	1986	
Price year	1981	
Period of analysis	20 years	
Borrowing period	20 years	
Accounting lifetime	5 years	
Energy tax credit	10 percent	
Investment tax credit	10 percent	
Income tax at margin	50 percent	
Property tax	0 percent	
General inflation rate	7.1 percent	
Interest rate	10.1 percent	

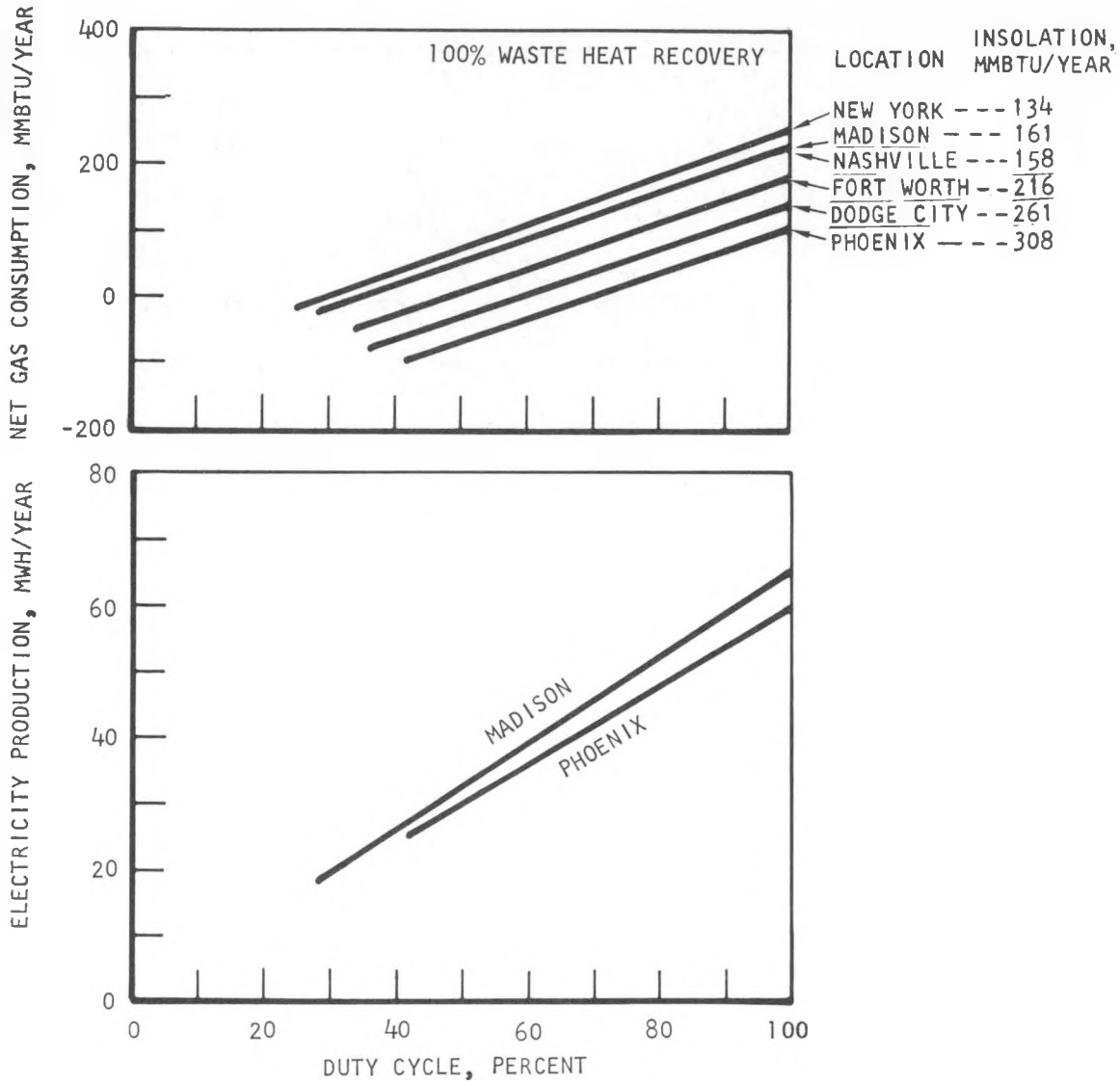

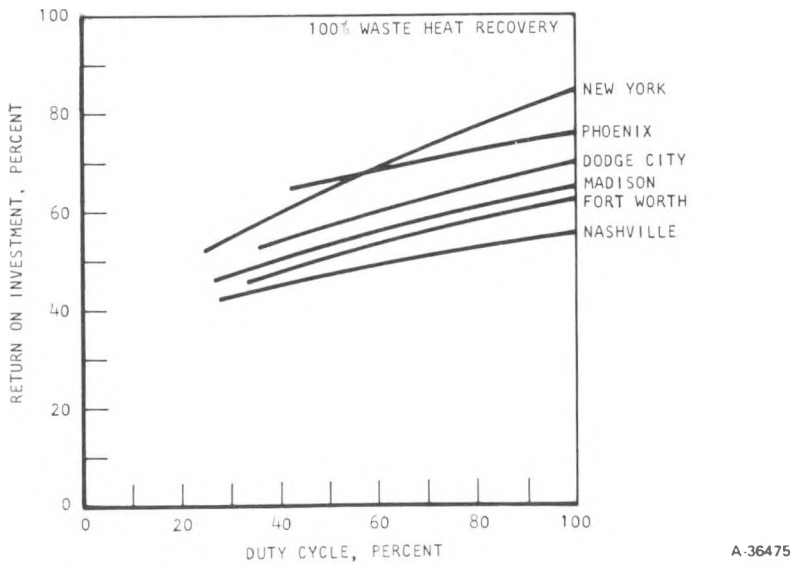

Fig. 5. Hybrid Cogeneration System Performance

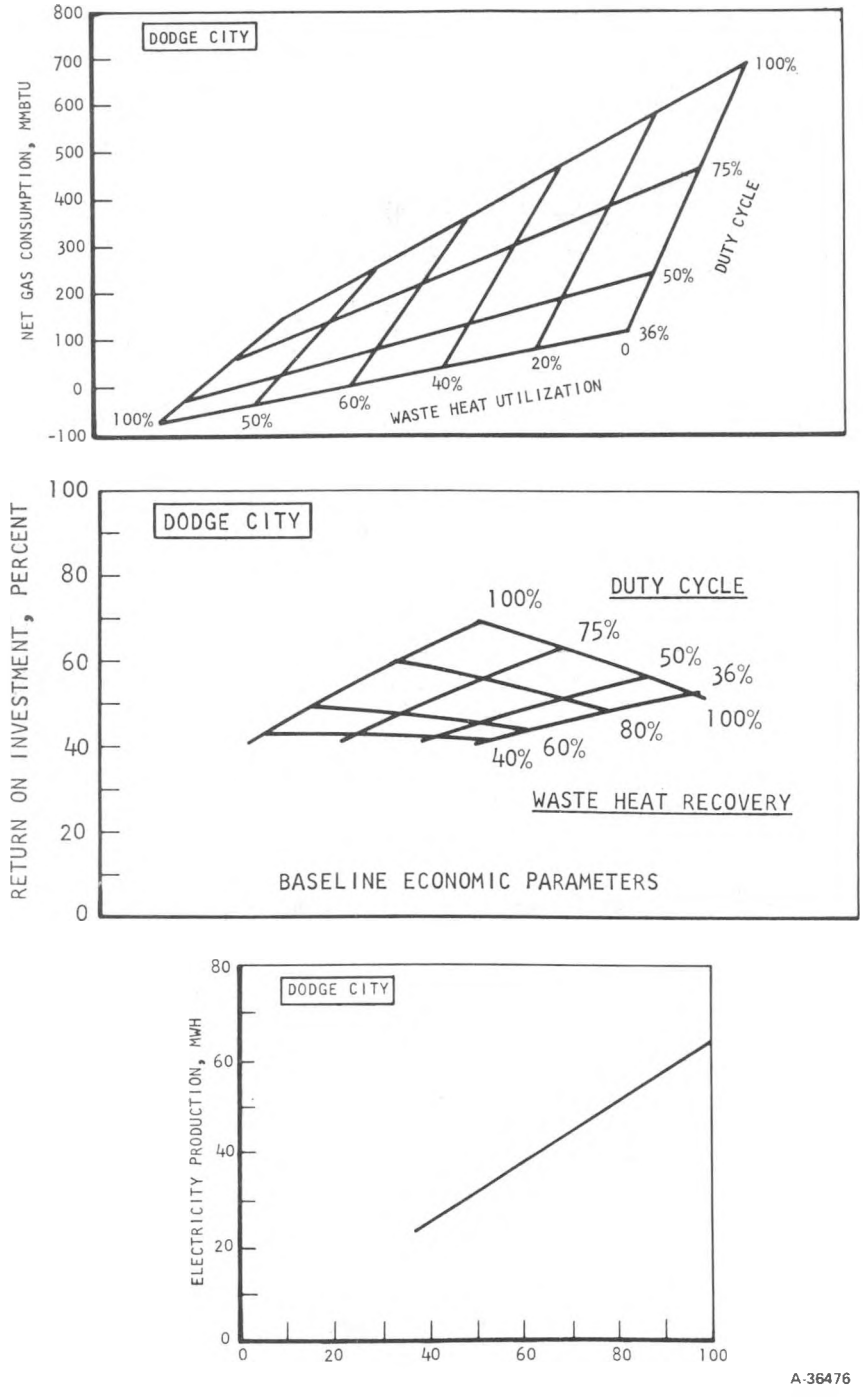

Fig. 6. Parametric Data for Dodge City, Kansas

The hybrid cogeneration system was found to yield a very attractive return on investment for all geographic areas considered over a range of duty cycles. Higher duty cycles and higher rates of waste heat utilization offer higher return on investment.

In addition to the economic benefits demonstrated for the hybrid cogeneration system module by itself, this system offers the general advantages of the distributed receiver concept for power generation.

Conclusions

The economic analyses performed have shown that the hybrid cogeneration system offers very attractive rates of return. The two major system features--solar/gas energy sources and waste heat utilization--contribute to the high potential return on investment.

The data generated over a range of duty cycles and utilization of waste heat available show that a higher duty cycle will result in higher economic benefit because of the better utilization of the equipment. Also, the higher the fraction of the available engine waste heat utilized, the higher the economic benefit.

DISCUSSION

The initial objective of the study program was to demonstrate the commercial feasibility of solarizing the basic 10-ton gas-fired heat pump. This proposed hybrid heat pump system was essentially a demand system where the heat pump is operated to satisfy a heating or cooling load in a conditioned space. Performance analysis of this system revealed that there is a mismatch between the heating and cooling demand and the availability of solar energy. Under these conditions, a large portion of the available solar energy is wasted and the initial cost of the equipment necessary to collect and process this solar energy cannot be justified economically.

These advantages are the result of (1) optimum use of the reflector surface, which is always pointed to the sun, and (2) a modular approach, which offers the following:

- Broad market potential--size can be matched to the application by addition of identical modules
- Potential for factory volume production techniques because of relatively small size
- Installation simplicity with minimum field work
- Operational flexibility whereby high efficiency is maintained over a wide range of loads
- High availability with minimum redundancy

This is made possible by (1) the high efficiency of the Brayton engine and (2) close coupling between the receiver and the engine.

A formal market survey was not conducted to determine the full commercial potential for the hybrid cogeneration system. However, a preliminary match of the major features of the system was made to the potential markets for such a device. This initial identification of markets is summarized in Figure 7.

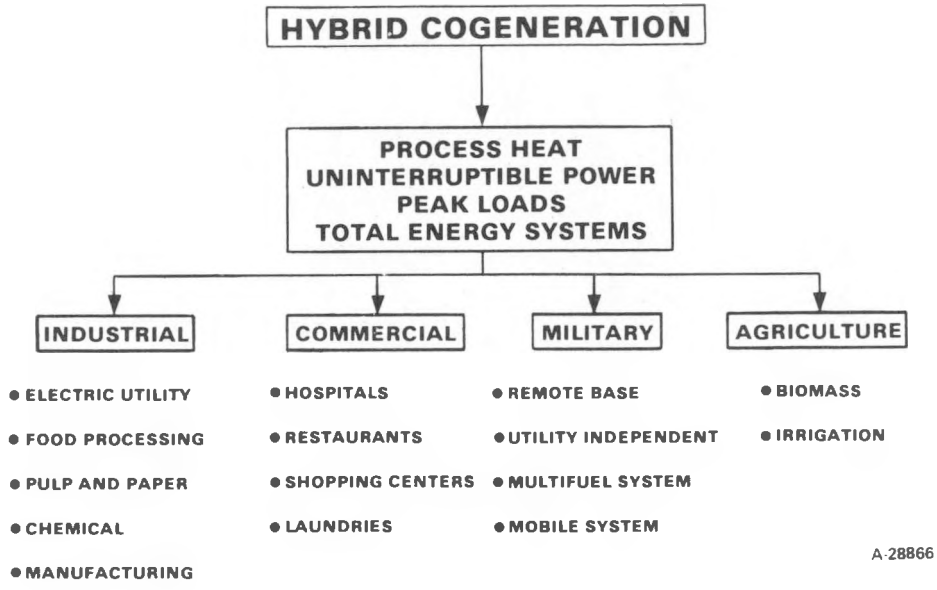

Fig. 7. Potential Markets

The basic cogeneration features (electrical power and thermal energy) will be attractive for a number of industrial, commercial, and military applications where waste heat is necessary either for processes, water heating, and space conditioning. The system can also be used as a total energy system.

As mentioned above, in a modular installation very high availability can be realized with minimum redundancy. Uninterruptible power systems can be integrated with such a modular arrangement at minimum cost. Numerous applications exist for such systems, including computer installations, hospitals, and military applications.

The heat-powered system, either solar or gas-fired, can be advantageously used by utilities, by industry, and in commercial applications to reduce or totally eliminate electric power peaks.

ACKNOWLEDGEMENTS

The data reported herein were generated in partial fulfillment of a study program sponsored by the Gas Research Institute; Mr. Keith Davidson and Mr. Doug Kosar provided able direction and advice throughout the program. Also, thanks are extended to the Jet Propulsion Laboratory personnel, namely Ab Davis, Fikry Lansing, and Bill Revere, who monitored the contract and supplied technical data in specialized areas.

Prospects for Enhanced Receiver Efficiency

William A. Owen
Jet Propulsion Laboratory
Pasadena, California

Solar receivers are the link between the concentrated solar energy and the engine or process that utilizes the energy. While much time and effort have been expended on developing concentrators and heat engines, comparatively little has been spent on receivers. This is probably due to the perception that they are inherently simple, low cost devices. Recent system studies however emphasize that receivers play just as important a role in system efficiency as the more complex components.

Until recently, receivers were designed using conventional heat exchanger techniques. But when these designs were converted into hardware, none performed as well as expected with losses exceeding calculations by 5% to 50%. In retrospect, these often substantial differences are not surprising when the complexity of the receiver as a thermal system is assessed. In any complex system, analysis is difficult especially in finding omissions in the model but this was especially true for receivers which had been given little overall system analysis. And, too, very little previous work, either analytical or experimental had been done on phenomena especially important to small cavities such as aperture convection or gray body radiation.

As more point focussing systems were constructed, a considerable body of data emerged. Table I lists a number of the earlier point focussing solar receivers for which good data was available. Examination of this data highlighted many of the special problems especially for higher temperature systems. It became clear that a number of design aspects including cavity shape, use of windows, coatings, surface condition, radiative properties, cavity convection effects, reflection, wind screens, lifetime, and other

TABLE I. EARLY RECEIVERS FOR WHICH PERFORMANCE DATA WAS AVAILABLE

- Garrett Steam Receiver
- Sanders High Temperature Solar Receiver
- Garrett Brayton Receiver
- GE Receiver-Shenandoah
- Omnium-G
- Organic Rankine-Ford
- Stirling

more secondary characteristics needed integration into a comprehensive design scheme. It also appeared likely that here was an opportunity to reduce system costs with only a relatively small R & D resource expenditure since even though the receiver was a critical link in the efficiency chain, there were many modes of improvement possible since not much optimization had been done previously compared to other major system elements.

Receiver efficiency depends on a multitude of thermal and hydrodynamic processes. Table II is a partial list of some of these. To reduce the receiver design problem to manageable size, one way is to examine each mode of heat loss, radiation, convection, and conduction, determine their importance in the overall receiver performance, and operate on each to reduce all losses to a minimum. From such an "ideal" receiver design, sensitivity analyses will permit each element of the receiver design to be examined for its overall system effect.

Table III shows typical loss data from medium temperature receivers under test on the 80 kWth Test Bed Concentrators at JPL's Parabolic Dish Test Site. In the 800°C to 1100°C (1500°F to 2000°F) temperature range, it can be seen that a typical 85% efficient receiver's losses are about one half from radiation, another quarter from cavity convection, and the remainder from other effects, largely conduction. While the absolute amounts are obviously a function of temperature, as can be seen in Figure 1, this distribution is an indication of the relative importance of the various loss mechanisms.

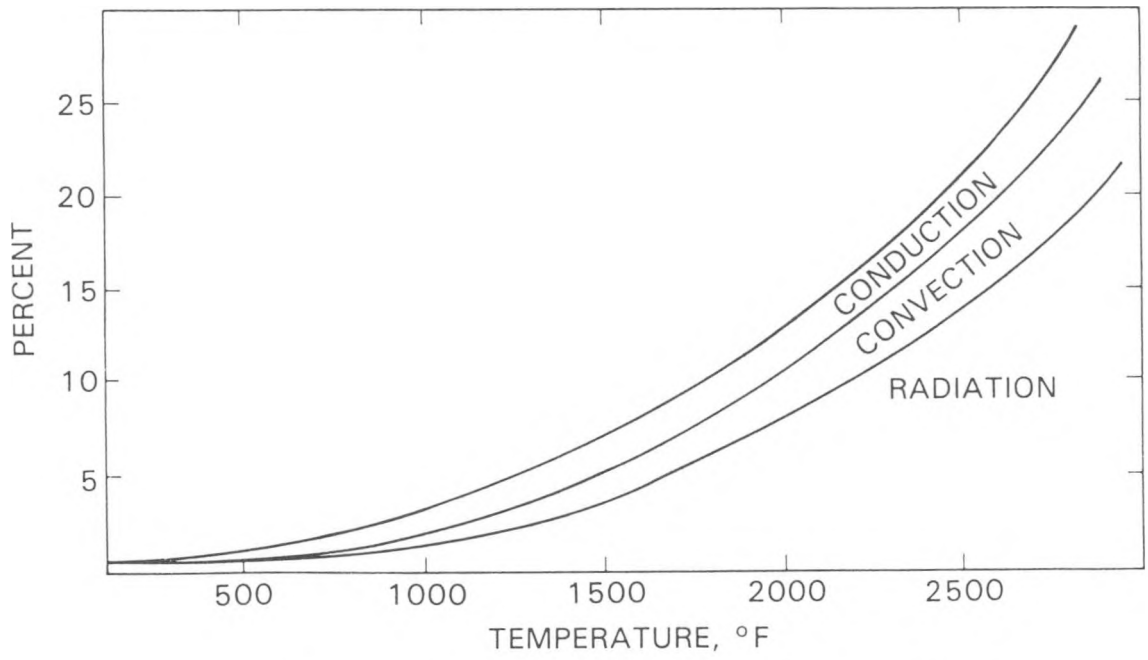

Fig. 1. Receiver Losses as a Function of Temperature

TABLE II. FACTORS CONTRIBUTING TO RECEIVER EFFICIENCY

- Operating Temperature
- Aperture Size
- Capture Geometry
- Absorbtivity of Surfaces
- Emissivity of Surfaces
- Aperture Convection Losses
- Aperture Radiation Losses
- External Radiation Losses
- Conduction Losses to Mount
- Spillage
- Heat Exchanger Characteristics
- Insulation Properties
- Attitude
- Definitions

TABLE III. LOSS DISTRIBUTION FROM 80 kWth RECEIVER IN 800 - 1100°C (1500 - 2000°F) RANGE. EFFICIENCY = 0.85.

	Loss in Watts	%
- Radiation	6000	50
- Cavity Convection	2500	25
- Conduction	2000	20
- External Convection	750	4
- Reflection	500	< 1
- External Radiation	250	< 1
	12000	

While radiation losses are largely determined by temperature, examination of the basic radiation equation does indicate several useful possibilities in reducing losses.

$$R_{Loss} = \sigma \times A \times F \times \varepsilon \times \Delta T^4$$

where R is total power lost due to radiation, σ is the Stefan-Boltymann constant, A the effective area, F the geometrical view factor, ε the effective emmissivity and T the absolute temperature.

The aperture area A is of prime importance in radiative losses. It obviously needs to be as small as possible. But this size is rarely under the control of the receiver designer but is usually dictated by the concentrator optics. And since the flux distribution at the aperture plane may not have a sharp boundary, a system level trade-off is often required to set the amount of allowable spillage.

The geometrical view factor F is next in importance once the aperture size is selected. The receiver designer has a number of options available to him to minimize the radiative view out the aperture. Important among these are cavity size, length to depth ratio, shape, location of heat exchanger surfaces, location of reflecting and reradiating elements, and the optical properties of each surface. Figure 2 illustrates how a cavity might be "tailored" to a given concentrator flux to insure minimum reradiation from the high temperature components of a receiver.

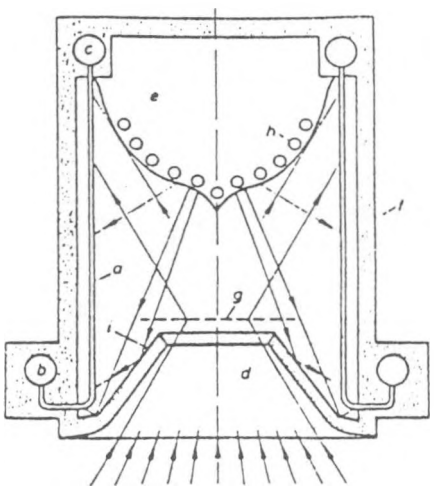

a	receiver tubing	e	radiation distribution cone
b	inlet header	f	receiver cage with insulation
c	outlet header	g	focal plane area
d	window	h	cooling tubes
		i	reflective wall

Fig. 2. Receiver Cavity Designed for Low Reradiation Loss (after Sutsch)

The final radiation factor ε is very often fixed when materials of construction are selected. However, even at high temperatures, the receiver designer has some choices in selecting materials with varying optical properties such as absorptivity α to emissivity ε ratios especially of coatings and special finishes are included. Also geometrical blackening via honeycombs, light traps and dispersive rulings may help.

In addition to the primary design elements, external optical methods may prove valuable in increasing cavity input without requiring aperture enlargement. Various reflecting surfaces on the concentrator structure may contributed. An especially attractive addition is a hyperbolic or "TRUMPET" secondary concentrator outside the aperture which can reduce the required aperture area by a factor of two.

The second largest receiver loss and, until recently, the most seriously underestimated, is cavity convection. Both natural convection and environmentally induced air currents carry considerable amounts of heat out of the receiver aperture. Due to the many inducing factors such as cavity shape and attitude, aperture size, wind speed and direction, cavity temperature, aperture configuration, and others, cavity convection experiences the largest variation in magnitude. In minutes, it can vary from near 0 to 50% of the receiver loss. Due to this variability it is often the most site specific loss also depending on winds. Recent studies of the flow characteristics of the cavity/aperture system do, however, offer clues as to how this flow may be disrupted. Some help can be gained from external collars and screens, internal baffles, and even by site enclosing wind screens or breaks. One obvious solution is to use an aperture window. While this does reduce input radiation by about 8%, some of this is recovered by less reradiation and by the lowered cavity convection. A system level analysis is required to determine the best solution.

The remaining loss mechanisms are those found conventionally in heat conversion systems. Included are convection and conduction from the external case of the receiver and in the usual thermal "short circuits" found in the mounting structures of the heat exchanger, apertures, and inlet and outlet process flow piping. However, since solar receivers tend to be high temperature, low power (< 100 kWth) devices, particular care should be taken to ensure optimum insulation thicknesses and placement as well as very low loss mounting structures since small heat leaks can represent significant loss percentages.

If all of the possible design improvements are incorporated into the next generation solar receiver, significant improvements in receiver efficiency should be possible. Table IV compares current technology with realistic improvements in the future. It should be possible to raise current receiver efficiencies by 10 percentage points to where the moderate temperature solar receiver should be well into the 90% regime and higher temperature systems correspondingly enhanced.

TABLE IV. POSSIBLE IMPROVEMENTS IN RECEIVER EFFICIENCY

	Previous Loss-Watts	Improved
Radiation	6000	1000 - 2000
Cavity Convection	2500	1000
Conduction	2000	500
External Convection	750	500
Reflection	500	200
External Radiation	250	200
	12000	3400 - 4400
Efficiency	85%	94 - 95%

Blank Page

PARABOLIC DISH CONCENTRATOR (PDC-1) DEVELOPMENT

I. F. Sobczak

Ford Aerospace & Communications Corp., Aeronutronic Division

Newport Beach, CA 92663

T. Thostesen

Jet Propulsion Laboratory

Pasadena, CA 91109

ABSTRACT

This paper summarizes the status of the 12 meter parabolic dish concentrator planned for use with the Small Community Solar Thermal Power System under concurrent development by Ford Aerospace for the Jet Propulsion Laboratory. The PDC-1 unit, designed by the General Electric Company, features a plastic reflector bonded to glass reinforced plastic sandwich gores. An elevation-over-azimuth mount fabricated of structural steel and thin-walled tubing is driven by a cable and drum arrangement powered by a pair of variable speed motors. The concentrator was fabricated and erected at the Parabolic Dish Test Site by Ford Aerospace under JPL contract. The reflective panels and the control/tracking subsystem were procured under separate contract by JPL.

INTRODUCTION

The PDC-1 unit is shown in Figure 1. Details of the General Electric design were reported at previous Parabolic Dish Solar Power Annual Reviews (Reference 1, 2 and 3). Since the last review the PDC-1 has been fabricated and erected under the direction of Ford Aerospace with the reflective panels and the control system supplied by JPL. ALCO Machine Company of Birmingham, Alabama was contracted to fabricate the structural components. Ashland Construction Company of Lancaster, CA prepared the site and poured the foundation. Valley Iron of Lancaster, CA did the assembly and erection of the structure, installation of electrical components including power and control cabling, and installation of the drive cable system. Valley Iron also assisted JPL in the installation of the GFE reflective panels. These panels were procured under separate contract from Design Evolution 4 of Lebanon, Ohio and optically tested by JPL in the space simulator facility (Reference 3).

The control system hardware was procured by General Electric under the design contract; however the software was extensively revised by JPL as will be described today in a subsequent paper.

The PDC-1 has experienced some problems which required hardware modifications. The completed PDC-1 has had tests to characterize the optical properties, which will be described in another paper today. Ford Aerospace coordinated and supervised the activities of ALCO, Ashland and Valley Iron

as a subtask of the Small Community Solar Experiment (SCSE) Contract.

FABRICATION AND ASSEMBLY

The concentrator is a 12 meter, front braced, parabolic dish suspended in an elevation-over-azimuth mount. The dish is divided into 36 reflective panels. Each panel is roughly 34 square feet in frontal area. The panels are constructed as a sandwich of polyester fiberglass skins over a balsa wood core. The reflective surface is an aluminized Llumar film laminated to a plexiglas sheet. The laminate is then bonded to the panel sandwich with contact cement. The front bracing ribs have caps formed to the parabolic shape of the reflector panels and are stiffened with corrugated steel webs. The tetrahedron mount-frame assembly consists of thin walled tubing joined at the intersections with welded fittings. Each tube is equipped with threaded clevis fittings that permit fine length adjustment by functioning as a turn-buckle. The entire mount is supported on four wheels and rotates about a central pintle bearing. Seven segments of twelve inch deep curved I-beams are bolted together to form a 41-foot diameter track supported by twenty-eight concrete piers. Variable speed dc motors operate two cable and drum arrangements of similar design to drive the dish in both azimuth and elevation. Fine tracking is controlled by a sun sensor. Coarse tracking is accomplished by computer via the Concentrator Control Unit (CCU) and two angular position resolvers. The CCU compares ephemeris predictions with resolver outputs and is capable of switching from fine track to coarse track or from coarse track to detrack as conditions may require. Several other programmed commands are available including STOW which drives the concentrator at a fast slew rate (currently 1.7°/sec) to the -90° elevation position.

Structure

ALCO Machine designed and fabricated an all-steel fixture for the assembly and dimensional inspection of the parabolic ribs. Figure 2 shows the buildup of a typical rib in the fixture. This fixture consists of heavy wall, square tubes forming a base and a vertical member. The vertical tube serves as the radial datum surface. A 0.25-inch thick steel strap, preformed to the desired parabolic shape, is supported from the base with angle iron braces at ten inch intervals. These brace members have slotted holes to permit fine adjustment of the parabolic strap at each support point. After optically verifying that the fixture conformed to the desired shape at each station, the cross member supports were tack welded to the angle iron braces. This prevented any subsequent slippage in the slotted holes. A complete set of twelve ribs plus two spares were produced in this fixture and the parabolic shape was reproduced within the required drawing tolerance.

A trial assembly of the mount frame, dish structure and elevation drive frame was performed at the factory. The mount frame consisted of the pintle bearing, truck assemblies and tubular tetrahedron sections. All parts were assembled and precisely adjusted to verify that the specified control dimensions were achievable. The entire assembly was checked with optical instruments to insure proper alignment.

In a similar fashion, the radial ribs, central hub and circumferential tie-rods of the dish assembly were optically aligned at the factory to insure proper rib positioning. Optical testing of the first article reflector panels was completed at JPL/Pasadena and the panels were shipped to ALCO for a fit check. The three segments were mated to the dish without difficulty. The contours and rib spacing matched satisfactorily. Absence of a full set of gore panels prevented assembly of the complete concentrator dish, and the structural stiffness of the ribs alone without the load carrying capability of the panels was not sufficient to allow lifting the partial dish. Any fit check of such an incomplete configuration would be inconclusive because the dish deformations would be different. Tape measurements were relied upon instead to make certain that (a) the shaft ends of the dish matched the elevation axis supports on the mount structure, and (b) the dish would swing through the mount without interference.

The elevation drive frame assembly was pinned together and an orthogonal set of centerlines was defined by means of taut wires stretched between end points of the assembly. The component sub-assemblies were adjusted until these centerlines were plumb and square relative to each other. Then the pilot holes at all the joints were drilled so that their relationships would be reproducible in the field.

All individual, separable piece parts were identified and marked using a scheme that would permit reassembly of each piece in the same location. Thus, a good fit-up at the site was anticipated with very little need for adjustment. Unfortunately, many of the turnbuckle fittings vibrated out of position during shipment so that the precision fit-up was lost. The assembly of parts, however, was greatly facilitated because of the careful marking of each piece.

Foundation

Site preparation at the JPL Parabolic Dish Test Site (PDTS) at Edwards AFB, California proceeded in parallel with the fabrication of the structure. Ashland Construction excavated and compacted the soil in preparation for the pintle foundation, track support piers and electrical and service line conduits. The completed piers and pintle foundation are shown in Figure 3. There are twenty-eight steel reinforced concrete piers equally spaced on a 41.33-foot diameter circle. Each pier is eighteen inches in diameter and is at least seven feet deep. The foundation for the pintle bearing is a thirty-inch diameter concrete cylinder expanding into a nine foot square block of reinforced concrete 2.5 feet below the surface. More than 8 cubic yards of concrete was used in the pintle foundation.

Base Support Erection and Dish Assembly

After the concrete foundation was cured Valley Iron installed the track, erected the mount frame and began assembling the dish structure (see Figure 4 and 5). Surveying transits were used to assure adequate reproduction of the trial assembly results. Meanwhile, JPL was testing the optical qualities of the thirty-six reflective panels produced by DE-4 of Lebanon, Ohio. Valley Iron assisted JPL in the installation of the reflective panels to the dish structure.

The dish structure was assembled on the ground adjacent to the foundation. The work proceeded reasonably on schedule until the dish assembly was completed. It was discovered that the panel restraint system originally designed (clamping the edges of the panels to the ribs by means of serrated clamp blocks) was inadequate to prevent panel movement during the daily temperature variations at the PDTS. A review of the structural analysis was performed by JPL and the structural model was updated to incorporate the latest design improvements. Completion of the loads analysis indicated large shear loads had to be reacted at each rib/panel interface. The panel attachment scheme was modified, as shown in Figure 6. In the original joint design, the lateral edges of adjacent panels were supported by a common rib. Every five or six inches along the rib a two-inch square of 1/4 inch thick plate clamps the back surface of each panel. This clamping force is produced by torqueing a 5/16 inch bolt into a rivnut installed in the rib cap material. The new design consists of a wider strap riveted to the rib cap to provide greater overlap with the panel edges. The panels were revised by installing metal inserts along the edges. The panels were then fastened to the new rib plates using 1/4 inch bolts loaded in shear. Bolt holes in the rib plates were match drilled to insure tight, close fitting joints between panels and ribs. JPL reworked the panels, and Valley Iron modified the rib caps under Ford Aerospace direction.

A second problem was uncovered during this panel rework period. Delamination of the reflective sheet was observed on several panels. JPL is now considering using an anaerobic contact cement on future panels.

The loads in the mount structure were reviewed at the same time the loads in the panels were recalculated. Two load conditions not included in the original analysis were added and were found to be the limiting cases. As a result, four members in the base frame were stiffened to prevent buckling during an earthquake and the quadripod tubing was replaced to increase the design margins.

Dish Installation

After completion of the panel rework, the dish was lifted into position on the base structure, see Figure 7. The elevation drive frame assembly was installed and a string was stretched between the engine mount and the counterweight cage passing through the center opening of the dish to provide a means of alignment. The engine and counterweight support tubes were adjusted until the elevation drive frame was aligned relative to the geometrical centerline of the dish assembly. Following this operation, the complete elevating mass was balanced by the addition of discrete cylindrical and rectangular weights at strategic locations.

Dish Rework

As will be described in a paper later today, the optical properties of the PDC-1, when first measured, were much poorer than expected. The panels were attached to the ribs after the rework of the mounting system in temperatures of up to 108°F. The shrinkage of the panels relative to the steel ribs in cooler weather, combined with the gravity sag when the panels were installed face down, resulted in the panels being flattened circumferentially

between the ribs. The result was a broadening of the reflected beam. The dish was taken down from the base frame, and the panels were removed and reinstalled. The bolt holes were redrilled while the panels were constrained in the proper parabolic contour between the ribs in a target temperature range of 55-60°F. The dial indicator tool used for positioning the panel contour is shown in Figure 8. These efforts resulted in a 3 fold reduction in the focal spot diameter.

Power and Control

All of the electrical power and control cabling was installed by Triangle Electric as a subcontractor to Valley Iron. Cables were pulled through the underground conduit from the above ground junction boxes located just outside the base track and routed through aluminum conduit clamped to the PDC-1 structural elements.

The flexible cable wrap around the azimuth axis is supported on the "GOR-TRAK" as shown in Figure 9. This is a commercially available device consisting of a series of hinged links that makes it very flexible, yet strong enough to support the weight of the cables and calorimeter water lines. One end is fastened to the concrete pad and the other end is attached to the rotating base structure. A pair of wheels support the weight at two intermediate points. The entire assembly forms a spiral loop that expands or contracts as the dish is moved in azimuth.

JPL provided the sun tracker, elevation and azimuth synchros, the CCU, a Central Computer (LSI 1123) and a manual control panel.

HARDWARE STATUS

Figure 10 shows the completed concentrator in a simulated tracking position. The unit is currently undergoing extensive optical and thermal characterization studies performed by JPL personnel. Upon completion of these tests, the Ford Aerospace Receiver/Engine Assembly will be integrated with the concentrator.

REFERENCES

1. Zimmerman, J. J., "First Generation Low Cost Point Focus Solar Concentrator", pages 63-67, DOE/JPL 1060-33 (Proceedings of First Semi-Annual Distributed Receivers Systems Review - Lubbock, Texas, January 22-24, 1980).

2. Zimmerman, J. J., "General Electric Point Focus Solar Concentrator Status", pages 143-147, DOE/JPL 1060-46, (Parabolic Dish Solar Thermal Power Annual Program Review Proceedings - Pasadena, California, January 13-15, 1981).

3. Sobczak, I. F., Pons, R. L., and Thostesen, T., "Development Status of the PDC-1 Parabolic Dish Concentrator", Third Parabolic Dish Review, Atlanta, Georgia, December 7-10, 1981.

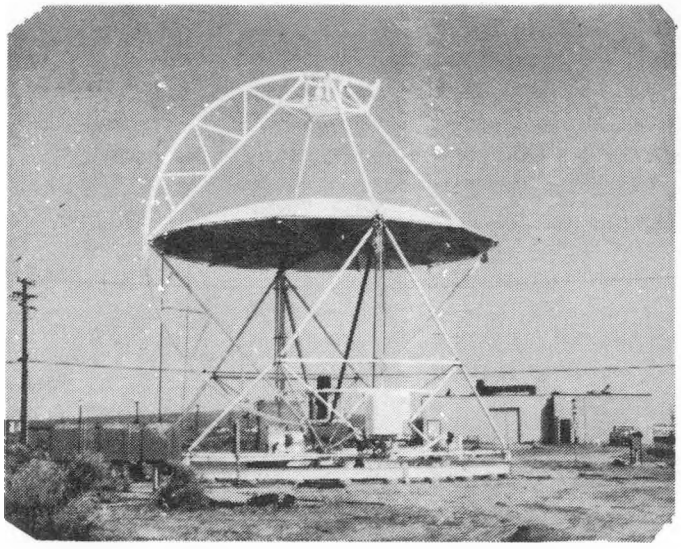

FIGURE 1. PDC-1 IN STOWED POSITION

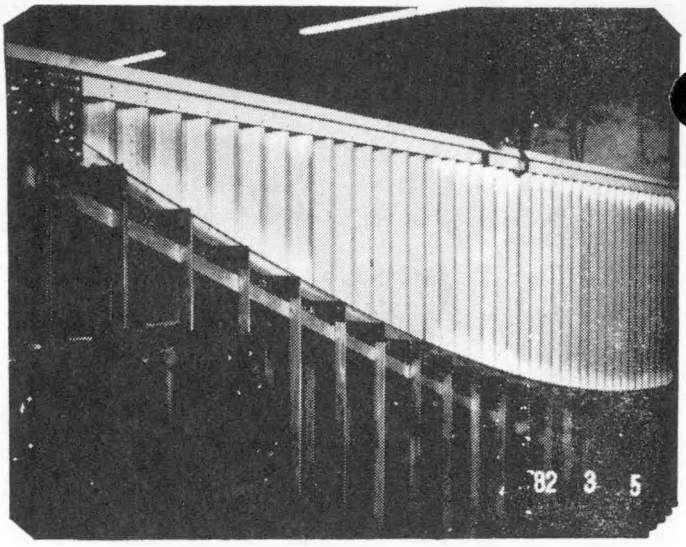

FIGURE 2. TYPICAL RIB IN THE ASSEMBLY/INSPECTION FIXTURE

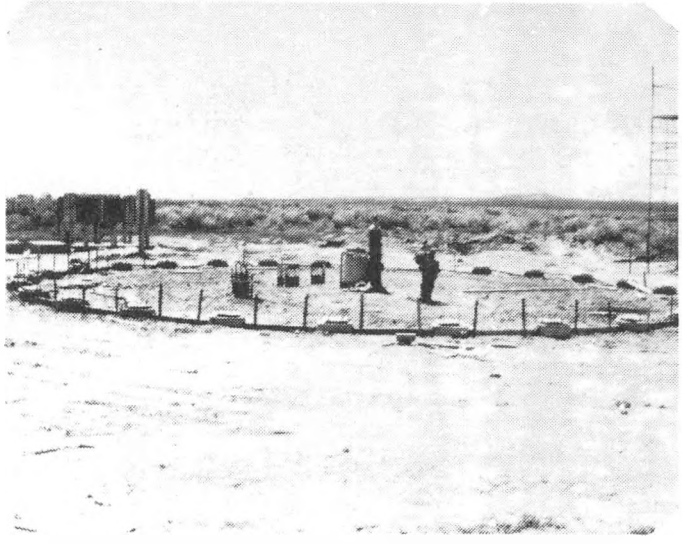

FIGURE 3. SUPPORT PIERS AND PINTLE BEARING FOUNDATION

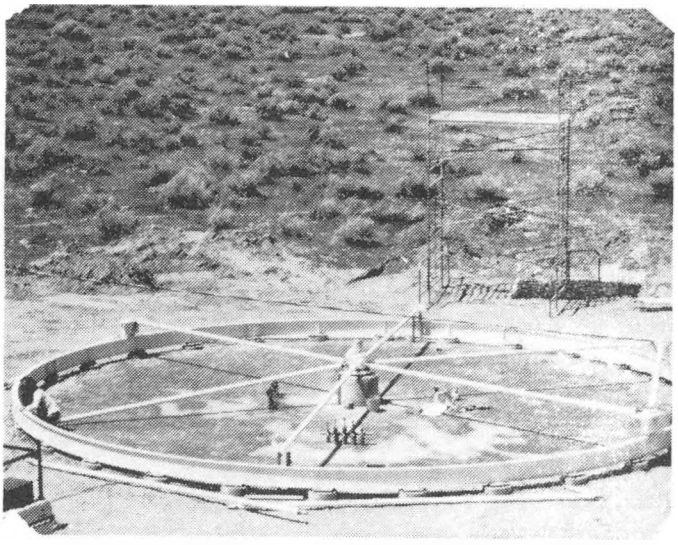

FIGURE 4. TRACK AND MOUNT BASE

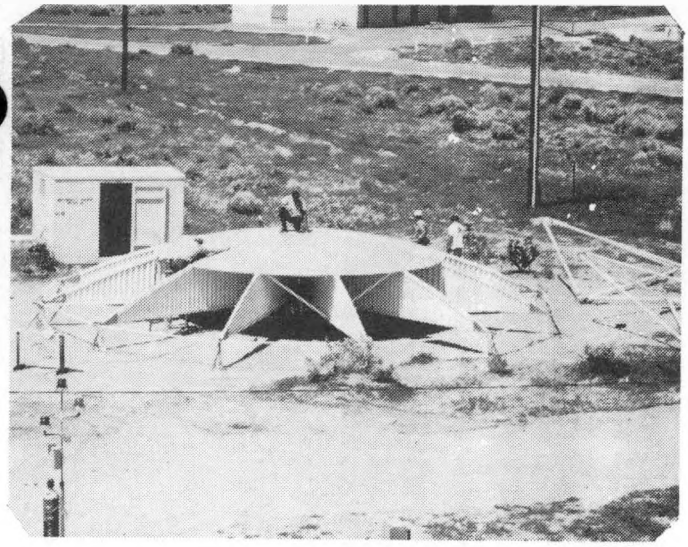

FIGURE 5. PARTIAL DISH ASSEMBLY

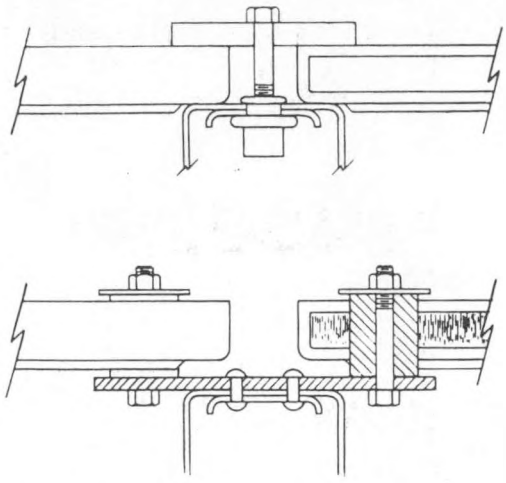

FIGURE 6. ORIGINAL AND REVISED PANEL ATTACHMENT DESIGN

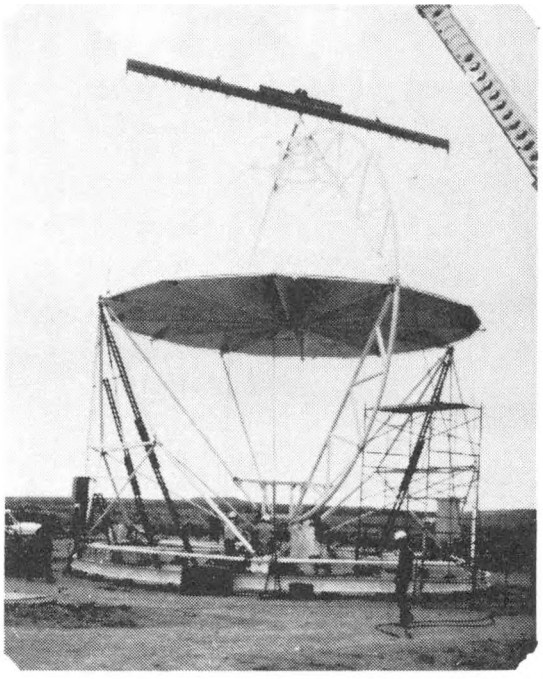

FIGURE 7. DISH INSTALLATION

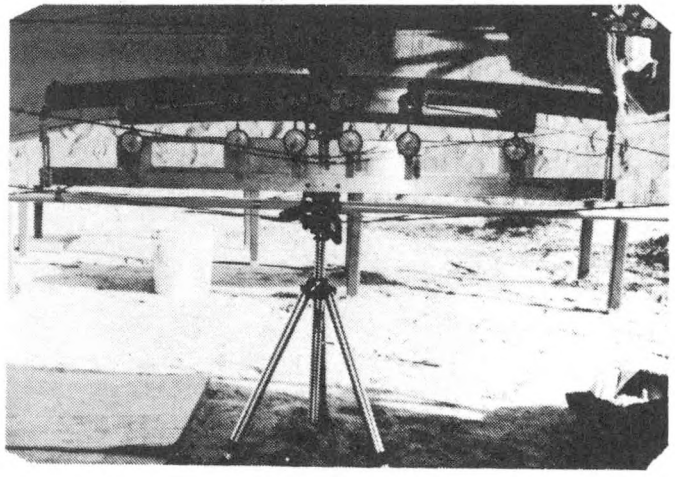

FIGURE 8. PANEL CONTOUR INSPECTION GAGE

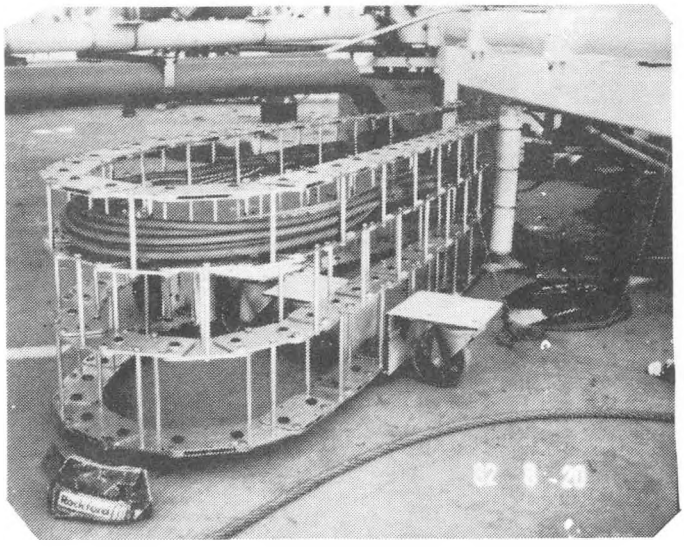

FIGURE 9. PINTLE WRAP SUPPORT

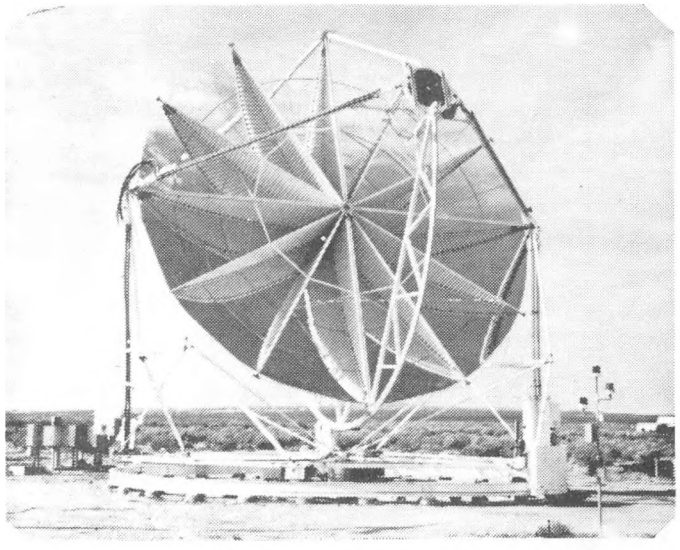

FIGURE 10. COMPLETE PDC-1 UNIT

PDC-1 CONTROL SYSTEM

Dr. John Stallkamp

Jet Propulsion Laboratory

Pasadena, California

This paper is a progress report and brief technical description of the control system for the Parabolic Dish Concentrator (PDC-1) currently being assembled at the test site at the JPL facility at Edwards Air Force Base, California.

The control system was designed by General Electric at Valley Forge, Pennsylvania. Originally there were to be three Concentrator Control Units (CCUs) operated from one master or host computer; however, only one set of hardware was eventually manufactured. This set of equipment was sent to JPL in the last months of 1981.

Checkout at JPL was started in January 1982. Numerous changes were made. Many were small and trivial and were the natural results of a checkout procedure independent of where or by whom the task was done. There were several significant changes; for example, in the way messages were handled between the host computer and the CCU micro-processor, the master speed and direction control relay interface, and the ephemeris calculation details. Capability for control of three units was not implemented, although this could be restored at a later time. In summary, with all the large and small changes, it is still the basic G.E. design; it would be readily recognized by the G.E. people; and, in fact, many of the software subroutines in both the micro-processor and the host computer are exactly as received from G.E.

In August the control system was shipped to PDTS-ETS; and, as work on the concentrator itself progressed, various control functions were activated. Basic slew motion was used in September, offset track was accomplished in October, and coarse or ephemeris controlled sun track was demonstrated in November after a water cooled calorimeter was installed at the focus. On November 29 auto track using the sun sensors was achieved.

From a controls point of view this initial operational checkout was performed without significant difficulties. For example, the EPROMs (erasable-programmable-read-only-memory) in the micro-processor shipped from Pasadena to ETS in August are still in use. Admittedly, there are several changes that will now be made, but these are not in the basic control function. There are problems in low temperature start-up and clock operation that need to be understood; and some modifications will be required. Again, in the basic control function area, the control system seems to work very, very well. There are mechanical problems in the azimuth axis that are related most probably to overloaded wheel bearings.

There are three basic characteristics of this PDC-1 control system. The motion is elevation-over-azimuth; the motions are, of course, completely separate. Now, first, the motion is on-off or start-stop in nature. The system remains off until an appropriate deadband error value is reached. It then moves at an appropriate speed until a proper hysteresis error value is reached. Motion then is stopped and the system remains off until the error builds up to start another cycle. This description obviously applies to tracking motion. However, the slew-to-a-position motion is accomplished with the same (software and hardware) mechanization; if outside an appropriate deadband, move at an appropriate speed, etc. etc. The second item is that there are two motion speeds. The tracking speed is about 0.15 degree per second; the slewing speed is about 1.5 degree per second. The absolute value of neither of these is critical. The tracking speed is much larger than the average sun rate of 15 degrees per hour or about 0.004 degrees per second. The resulting azimuth and elevation motions are completely unsyncronized sawtooth motions of quite short duty cycles (perhaps no longer than 1:10 and as short as 1:200) depending on the time of day. The slew motion is fast enough to minimize the time the sun's image is on the faceplate of a receiver and is used to "slew" on and off the sun as well as to move to and from a fixed coordinate position. The third item is that there are two sun sensing modes. For coarse track the position of the sun is "sensed" from an ephemeris calculation using Julian date and time of day, etc. Slewing on sun is accomplished by commanding coarse track, and the control system reverts to coarse track when clouds obscure the sun. For auto track, a photoresistive sun sensor (manufactured by Mann Russell) is used. After coarse track has been achieved, the system may be commanded to auto track during which the sun tracker does the controlling with a nominal 0.1 degree deadband giving a 0.1 degree peak-to-peak sawtooth motion. The nominal deadband value for the coarse or ephemeris controlled motion is 0.3 degree.

Figure 1 is a block diagram of the control system. There are two manual control modes. Local manual control uses the local push-button stations on the azimuth platform, the motor control units and the DC motors only; it is fully open loop, i.e., push, hold, and observe - and walk if there is azimuth motion. The remote manual station in the trailer provides essentially the same open-loop control capability implemented through relays in the CCU that are also used in the computer controlled motions.

There are two closed loop control modes. These utilize the 8080 type mirco-processor and must be used to provide tracking motions. For coarse track (on sun at calculated ephemeris values of azimuth and elevation) and offset track (at fixed angles from the sun, typically down and east), the loop consists of the syncro measurement, comparison with the desired position in the micro-processor, relay outputs to the motor control unit and finally the motor and mechanically coupled syncro. After coarse track is achieved and control is transferred to the sun sensor, the closed control loop consists of the sun sensors directly driving the CCU relays, the motor control unit and motor. In this latter auto track

mode, the measured position from the syncro is still periodically compared with the calculated sun position ; when a difference exceeds limit values, control is transferred back to the ephemeris mode or, in the case of a larger error, an emergency detrack signal is generated.

The command list for computer controlled motion is given in Table 1. These commands are entered at the keyboard of a conventional CRT operator's terminal. Except for the much longer initialization message, the host computer, a DEC LSI-11, generates a five byte command message, two sync bytes, message length byte, command byte and check sum byte and sends it to the CCU micro-processor. At the CCU after this message is received, a fixed length 20 byte status and data message is generated and returned to the remote host computer. When check sums don't check or time out circuits are not properly reset, the message cycle is repeated or eventually emergency action is taken.

In Table 2, commands 2, 3, and 4 are the tracking commands and 5, 6, and 7 are the "go to" a coordinate position commands. All these have been previously identified. CMD 10, Detrack, is an emergency action which commands the dish to move at slew speed, down in elevation and east (CCW looking down) in azimuth, for a period of about ten seconds. The presumption is that the dish has been tracking the sun, that something has gone wrong, and the desired action is to move about 15 degrees off the sun in both axes as rapidly as possible. As a matter of fact, the normal operation of going off-sun, i.e., from coarse or auto track to offset track, is physically done in the same manner. CMD 1, Detrack Reset, is the recovery process from Detrack. The enable and disable commands need no explanation. The second digit in the command, shown as all 1's in the table, is a holdover from the original capability of command of three dishes from one CRT terminal and host computer.

The 60 byte initialization message must be sent at system start up and whenever a change in system performance is desired. It contains time, day number, latitude and longitude, the azimuth and elevation values for the fixed coordinate positions, syncro zero or bias values, offset track angles, and the several hysteresis and deadband angles. Nominal values for the parameters are stored in the host computer memory (time and day number are computed each time). Normally these memory values are sent to he CCU; however, they may be changed by keyboard entry if this is desired. The last command, CMD 14, is a dummy command; it causes the CCU to return the data and status message with no other action.

The last exhibit, Table 2, is meant to convey a brief, very top level description of how the control algorithm works. The same action takes place for both the azimuth and elevation axes using in many cases the same software routines not only for both axes, but also for the several tracking and slewing modes. The tracking subroutine is driven by time interrupts every 0.1 second. First, syncro measurements are digitized and positions, A1, and offset positions, A2, are calculated. There are four B values available, the three fixed coordinate positions and the sun position whose very slowly changing value is updated every second in a

separate subroutine. Next position errors (and also their absolute values) are computed using the A and B parameters for the desired operating mode. When an error remains within the applicable deadband, no action is taken. When outside, the proper speed and direction of motion are commanded (started or allowed to continue). When the error is reduced to the hysteresis value, the motion is stopped, actually allowed to decelerate at the proper rate.

In closing, let me repeat that the control system for the PDC-1 concentrator has worked very, very well in this initial installation and first operational checks. Several very ordinary problems typical of first operation were readily solved; none of these involved intrinsic functional operation. There are some low temperature, start up problems that must be resolved. There are modifications, perhaps more properly stated as additional features, to be implemented as the requirements for operation at ETS evolve. Subsequent to the symposium presentation in early December, it has been verified that that the azimuth wheel bearings have seriously deteriorated; one has effectively destroyed itself. When this is corrected and the mechanical motions and forces become more repeatable, the control system will be more finely tuned and its actual performance be observed and documented.

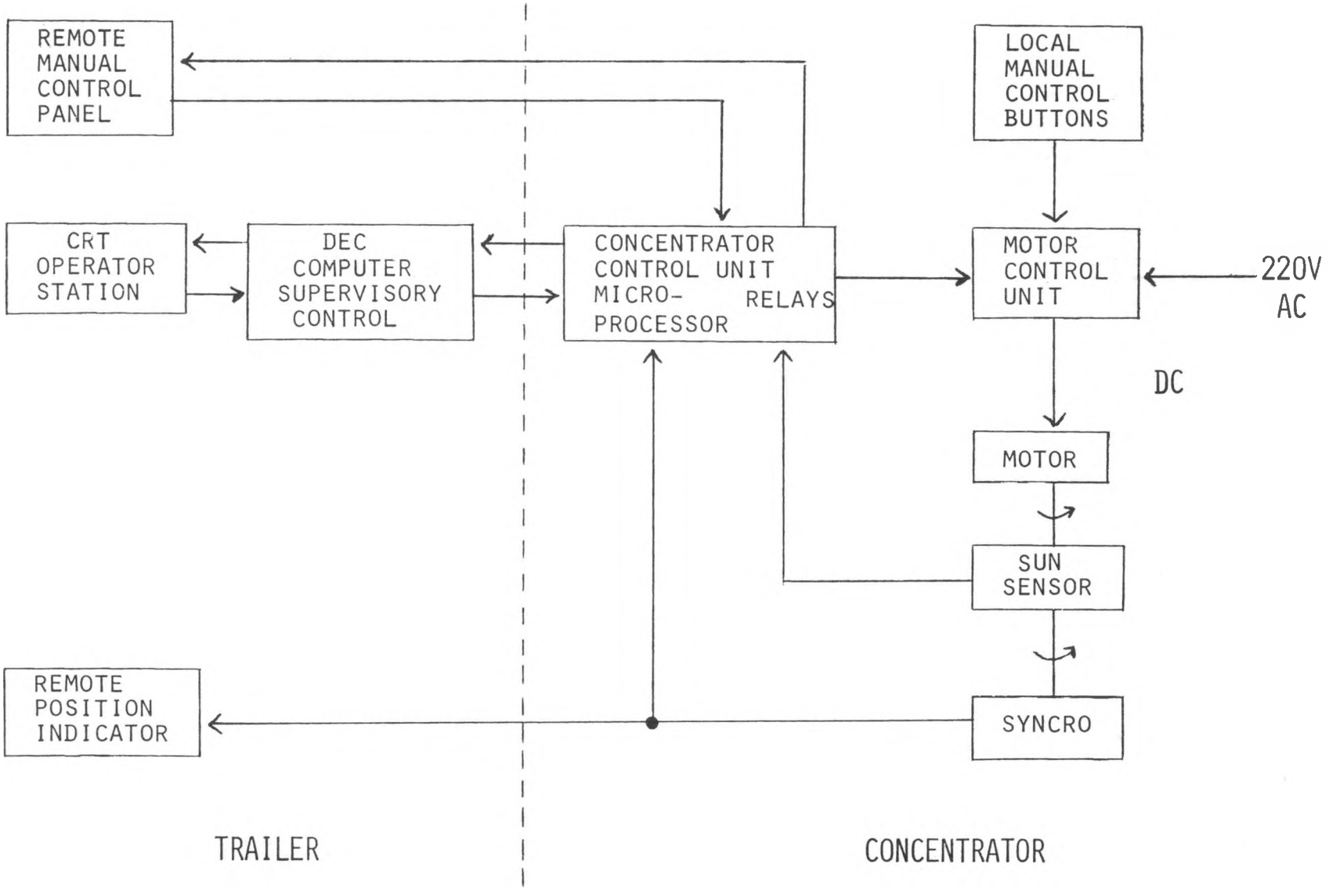

Figure 1. PDC-1 Control System Block Diagram

Table 1. PDC-1 CONTROL SYSTEM
COMMANDS FOR COMPUTER CONTROLLED MOTION

CMD 1, 1	DETRACK RESET.
CMD 2, 1	OFFSET TRACK.
CMD 3, 1	COARSE TRACK (COMPUTED SUN).
CMD 4, 1	AUTO TRACK (SUN TRACKER).
CMD 5, 1	COORD # 1.
CMD 6, 1	COORD # 2.
CMD 7, 1	COORD # 3.
CMD 10, 1	DETRACK.
CMD 11, 1	INITIALIZE MICROPROCESSOR.
CMD 12, 1	ENABLE.
CMD 13, 1	DISABLE.
CMD 14, 1	DATA/STATUS REQUEST.

Table 2. PDC-1 CONTROL SYSTEM

MICROPROCESSOR COMPUTED POSITION ERROR

A1	AZPOS = AZ SYNCRO - AZ BIAS	0.1 SEC.
A2	AZOFFPOS = AZPOS - AZOFF BIAS	0.1 SEC.
B1	AZCOORD1 = STOW POSITION	CONSTANT
B2	AZCOORD2 = 2ND POSITION	CONSTANT
B3	AZCOORD3 = 3RD POSITION	CONSTANT
B4	AZSUN = CALCULATED SUN	1.0 SEC.
	AZ POSITION ERROR = $A_N - B_M$	0.1 SEC.
	MOTION CONTROL:	0.1 SEC.
	SLEW/TRACK DEADBAND.	
	SLEW/TRACK SPEED AND DIRECTION.	
	SLEW/TRACK HYSTERESIS.	

PDC-1 OPTICAL TESTING

Edwin W. Dennison/Maurice J. Argoud
Jet Propulsion Laboratory
Pasadena, CA

ABSTRACT

During the development of the first JPL parabolic dish concentrator (PDC-1), an optical test program was used to determine the image forming characteristics of the reflecting panels and provide data for estimating the concentrator thermal performance. The first optical tests of the prototype panels were made in the JPL 25 ft. space simulator during the summer of 1981. Twelve of the final concentrator panels were tested outside of the panel storage building at night during the spring of 1982. The final tests were made on the fully assembled concentrator at the JPL Parabolic Dish test site in October-November 1982.

All of the performance tests were based on measurements of the optical imaging characteristics of reflecting panels illuminated by a real or virtual point source of light. Two diagnostic optical techniques were used to determine the relationship between the image quality and the mechanical properties of the reflecting surface.

These optical tests were effective for evaluating the performance characteristics of the PDC-1 panels and also proved to be of great value in the development of a successful panel installation procedure.

A cold water cavity calorimeter will be used for the final evaluation of the concentrator. However, all of the data now available indicates that the PDC-1 will have satisfactory imaging characteristics.

INTRODUCTION

One useful description of the performance characteristics of a solar concentrator is the tabulation of the thermal power focused into a receiver aperture as a function of the aperture diameter. If a concentrator is to be used with a specific receiver, the description can be given as a single number instead of a table or graph. These numbers (kilowatts) are normalized to a direct normal insulation of one kilowatt per square meter. The fixed parameters that affect concentrator performance are the mechanical design, the component materials and the methods of manufacture and installation. During operation, the variable parameters are temperature, wind, orientation with respect to gravity, pointing accuracy, and deterioration resulting from environmental exposure.

The performance description has two essentially independent

components. One is the total or absolute value of the power content of the focal plane image and is determined by the total concentrator area less the structure blockage and the reflectance or transmittance of the image-forming elements. The second component is the relative optical performance and is determined by the optical surface irregularities and the shape or position of these optical surfaces. The product of these two components is the total power passing into a receiver aperture.

This report covers the progress that has been made toward measuring the relative optical performance of the Parabolic Dish Concentrator No. 1 (PDC-1) which is being tested by the Jet Propulsion Laboratory (JPL) at the Parabolic Dish Test Site, Edwards AFB, California.

TEST APPROACH

The approach to the optical performance measurement by JPL has been to use a test configuration in which a perfect reflecting panel would form a point image from a point source of light.

For a spherical surface this configuration occurs with the source and image at the center of curvature of the mirror. This method was successfully used for testing the JPL test bed concentrator mirrors. Parabolic surfaces only satisfy the ideal configuration requirement when the source is on the optical axis at infinity and the image is in the nominal focal plane. In practice the source can be finite in size and the distance close enough for practical measurement.

For example a perfect paraboloid with the PDC-1 dimensions will form an image with a maximum diameter of 4.12 cm (1.6 in.) from a source of 32 cm (12.6 in.) diameter at a distance of 400 m (1,310 ft) in a focal plane that is displaced 13 cm (5.1 in.) from the nominal focal plane. This test setup gives comparable results to those which would be obtained if a point source at infinity were used.

The point-source configuration was chosen because it provides unambigious data about the reflecting surfaces. With point-source data it is possible to predict, with acceptable accuracy, the intensity distribution of a concentrator when it is pointed at the sun. However, the image formed from an extended source, such as the sun, cannot be easily used to determine the point-source image intensity distribution.

The measured data was reduced to a mathematical expression based on two Gausian distribution terms. These equations represent the measured data with a root means square (RMS) error of less than 1 percent. This mathematical form is also easy to use for calculating the image intensity distribution, intercept factor distribution, and fraction of the focal plane power that passes through any specified receiver aperture.

MEASUREMENTS

The first measurements of the PDC-1 optical performance were made

in the JPL 25 foot space simulator during the summer of 1981 because it was believed that the simulator would produce a collimated beam of light over one full concentrator gore (a 30° segment of the concentrator consisting of three panels). This work has been described in detail elsewhere (1). The tests were performed on the first article prototype panels manufactured by Design Evolution 4 (DE-4) under a subcontract to the General Electric Company.

In addition to the direct image photographs, the intercept factor distribution was determined from a raster scan of the image with a photo-detector. Image diagnostic photographs were made from a panel image by a lens located behind a focal plane aperture mask (Figure 1). The reduced data indicated that the PDC-1 design concept would give acceptable performance, and construction of the prototype concentrator was initiated. During the Spring of 1982, DE-4 manufactured the PDC-1 panels and shipped them to JPL for testing. The space simulator was not available for solar panel testing at that time; therefore, an alternate test configuration was needed. The configuration used is shown in Figure 2. The direct image and the diagnostic photographs were taken using the same technique as had been used in the space simulator. The intercept factor distribution was determined by measuring the amount of light passing through an aperture mask. The data indicated that the production panels formed a higher quality image than the prototype panels, particularly for apertures larger than 7 inches in diameter.

The PDC-1 testing started during the early fall of 1982. The direct images were photographed through a telescope located at the vertex of the concentrator. All of the direct images are shown in Figure 3. The same telescope was used with a photo-detector to measure the intercept factor distribution. The aperture masks were white and the photo-cell measured the amount of light that did not pass through the aperture. This technique was used because the large rim angle (52°) of the concentrator precluded the possibility of using any practical optical system behind the focal plane.

The unexpectedly large size of the focal plane image necessitated the use of a diagnostic technique to determine the source of the image errors. Because the optical panels had shown good imaging characteristics during the earlier tests, it appeared that the source of the problem must be the concentrator structure or the method of panel installation. The large rim angle also eliminated the possibility of any practical diagnostic optical system behind the focal plane. The most successful technique was to view a target of colored patterns mounted at the focal plane (Figure 4) from a distance of 600 to 900m(2,000 to 3,000 ft) through a small telescope. Pictures were also taken through this telescope (Figure 5). The observed color of each part of the reflecting panels indicated the area on the target that would be illuminated by a distant point source reflected from the panels.

The diagnostic pictures demonstrated that the panels were distorted by excessive tension, that this tension could be removed, and that the image quality of the concentrator was very substantially improved by reinstalling the panels[2]. These pictures also indicated that the

basic concentrator structure is very rigid and shows no significant deformation by gravity. This diagnostic procedure also demonstrated that the concentrator was less temperature-sensitive after the panels were reinstalled.

CONCLUSION

The final concentrator performance evaluation will come from the cold- water cavity calorimeter measurements. However, the point-source optical testing techniques have proven effective for determining the performance chacteristics of a solar concentrator during the initial development and production as well as being a valuable tool for diagnosing optical problems. The diagnostic pictures and the intercept factor distribution (Figure 6) indicate that the PDC-1 will give satisfactory performance with the organic Rankine cycle power conversion unit. Future improvements in the panel construction and installation techniques may permit the use of this concentrator with the higher temperature power conversion systems.

REFERENCES

(1) E. W. Dennison and M. J. Argoud, Solar Concentrator Panel and Gore Testing in the JPL 25 Foot Space Simulator, AIAA 2nd Terrestrial Energy Systems Conference, (AIAA-81-2534), December 1-3, 1981 (Colorado Springs, CO).

(2) I. F. Sobczak and T. Thostesen, Progress Report on the Development of the PDC-1 Concentrator, Fourth Parabolic Dish Solar Thermal Power Program Review, November 30-December 2, 1982 (Pasadena, CA).

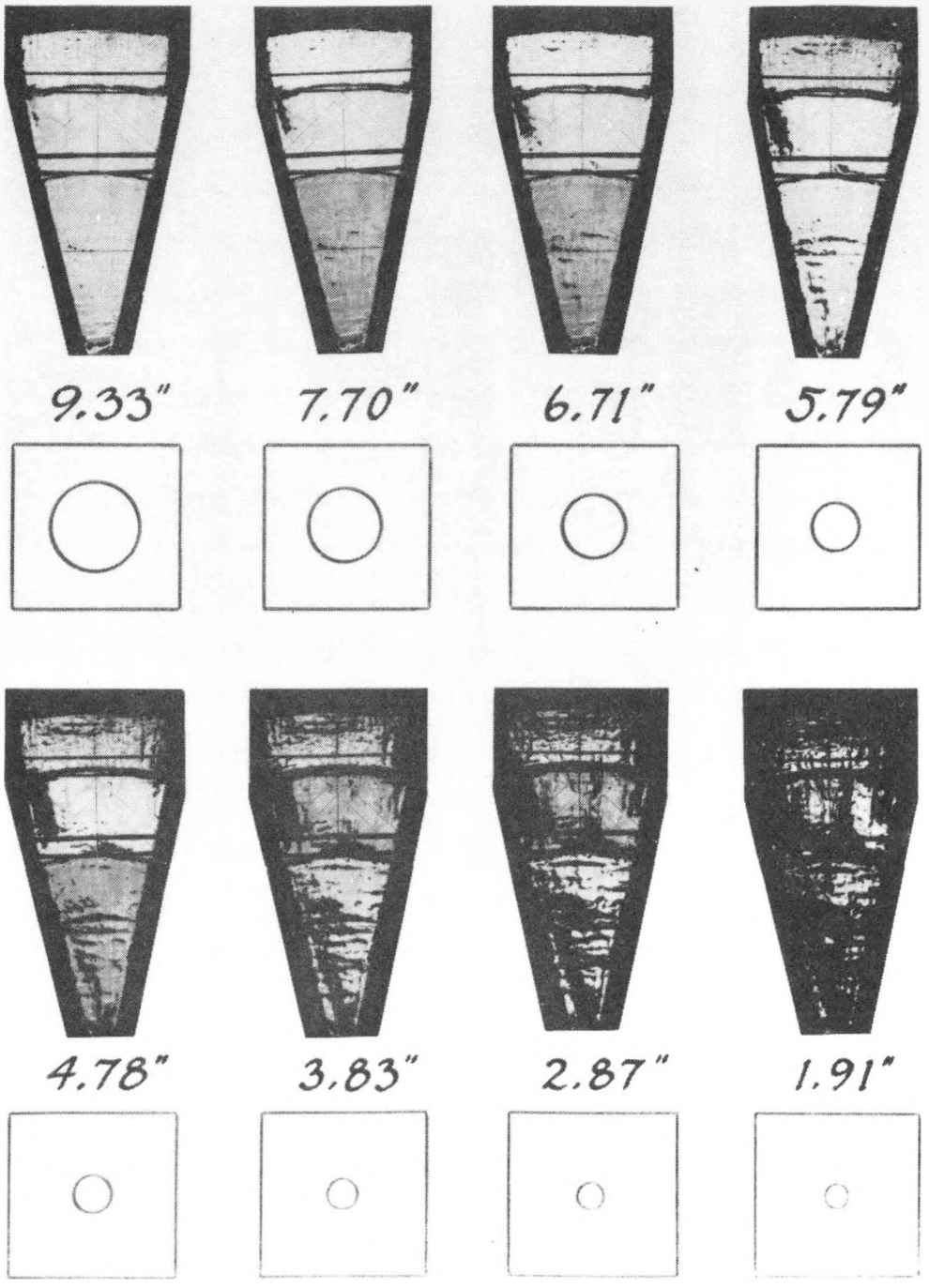

Fig. 1. Diagnostic Images of the Prototype Panels Made in JPL's 25-Ft Space Simulator. The bright part of each image indicates an area of the reflecting panel that forms an image smaller than the indicated aperture diameter.

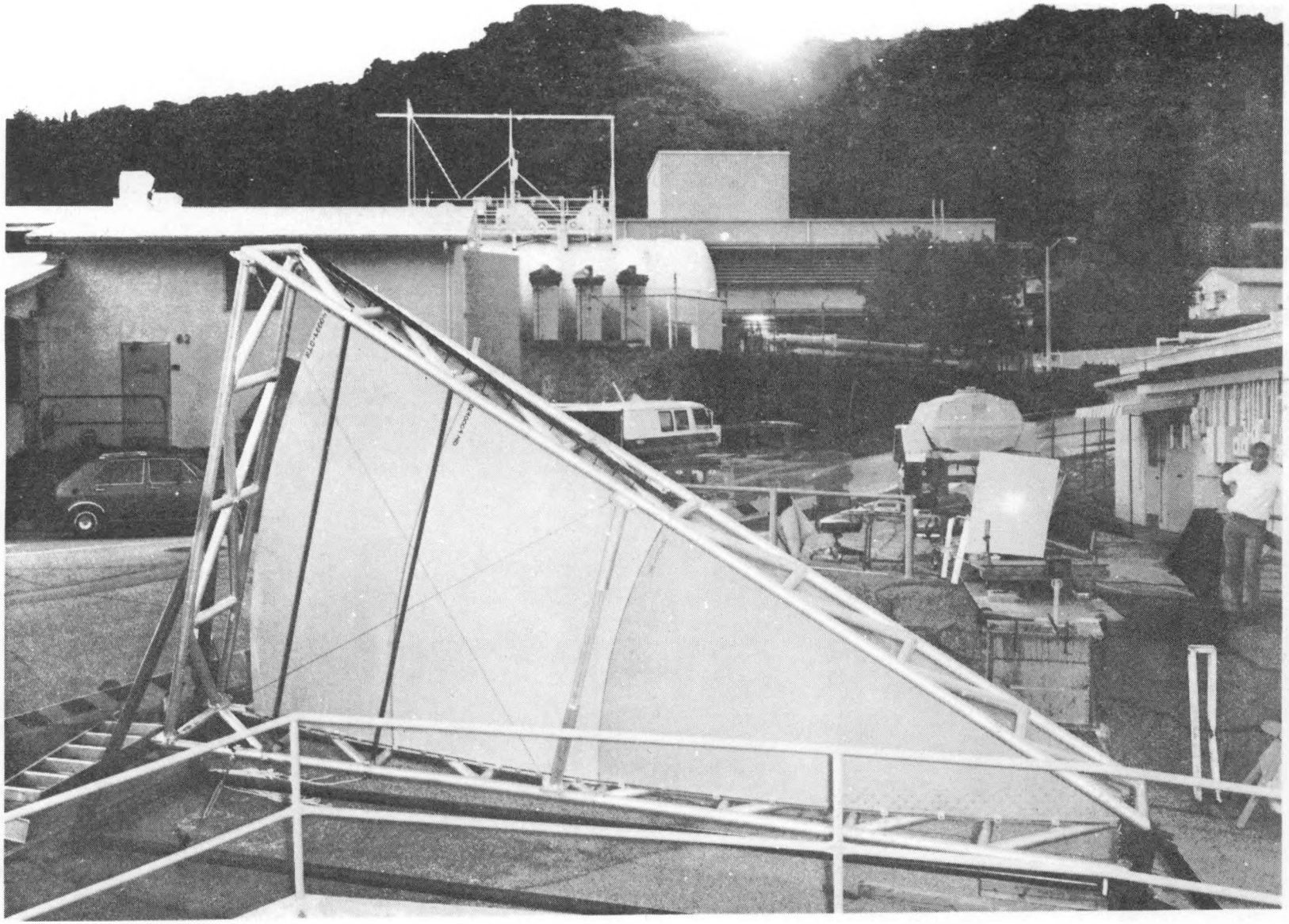

Fig. 2. Configuration Used to Measure the Production Panels. The point light source is located on the mesa (center background) at a distance of 430 m (1400 ft). The 3 panels (1 gore) are mounted in a supporting fixture that simulates the PDC-1 structure (left center). Image (right center) is formed on the focal plane target.

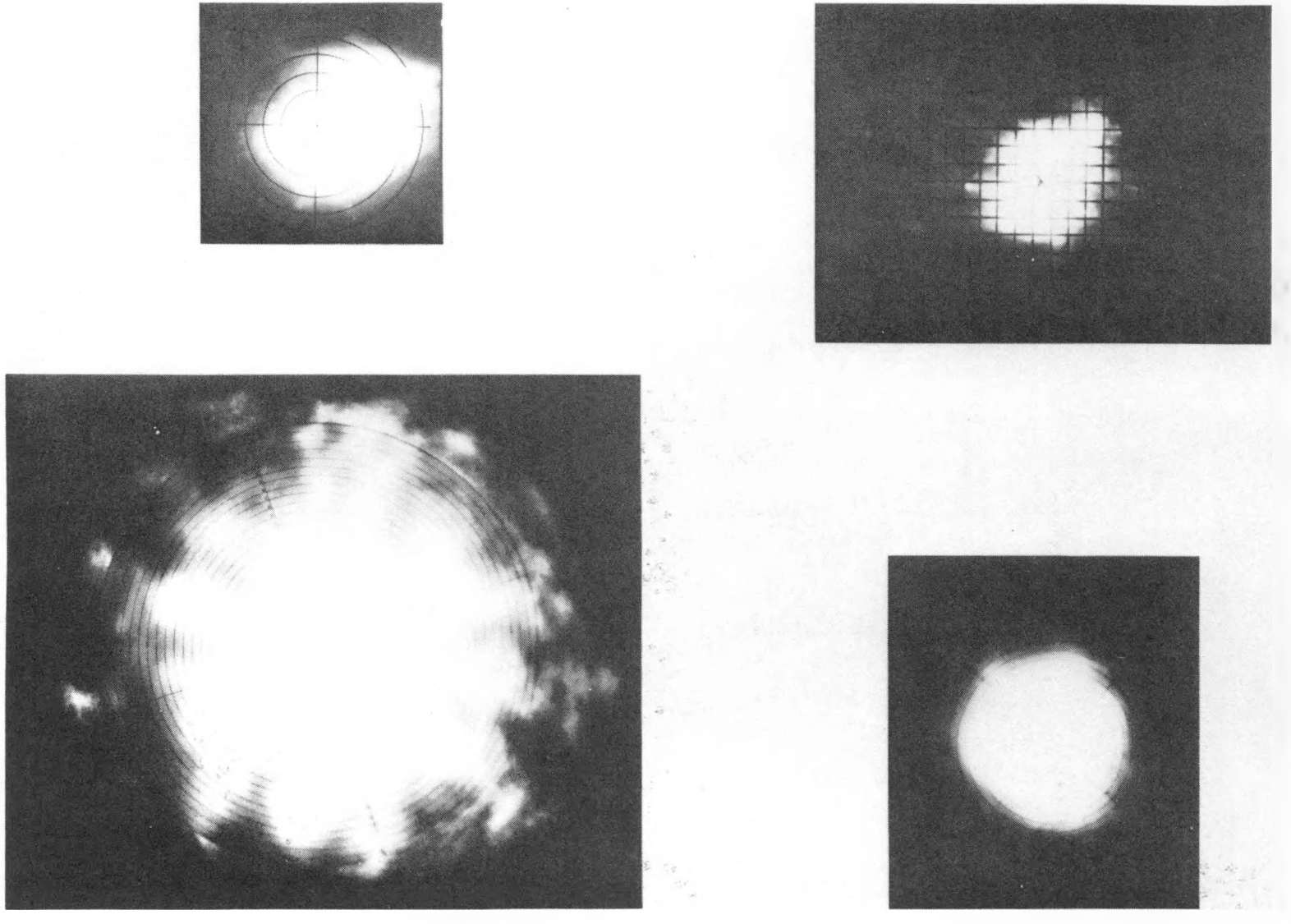

Fig. 3. Direct Images of a Point Source Formed by the PDC-1 Paraboloidal Reflecting Panels. The upper left image is from the prototype panels; the upper right image is from the production panels. The lower images are from the assembled concentrator before (left) and after (right) re-installation of the panels.

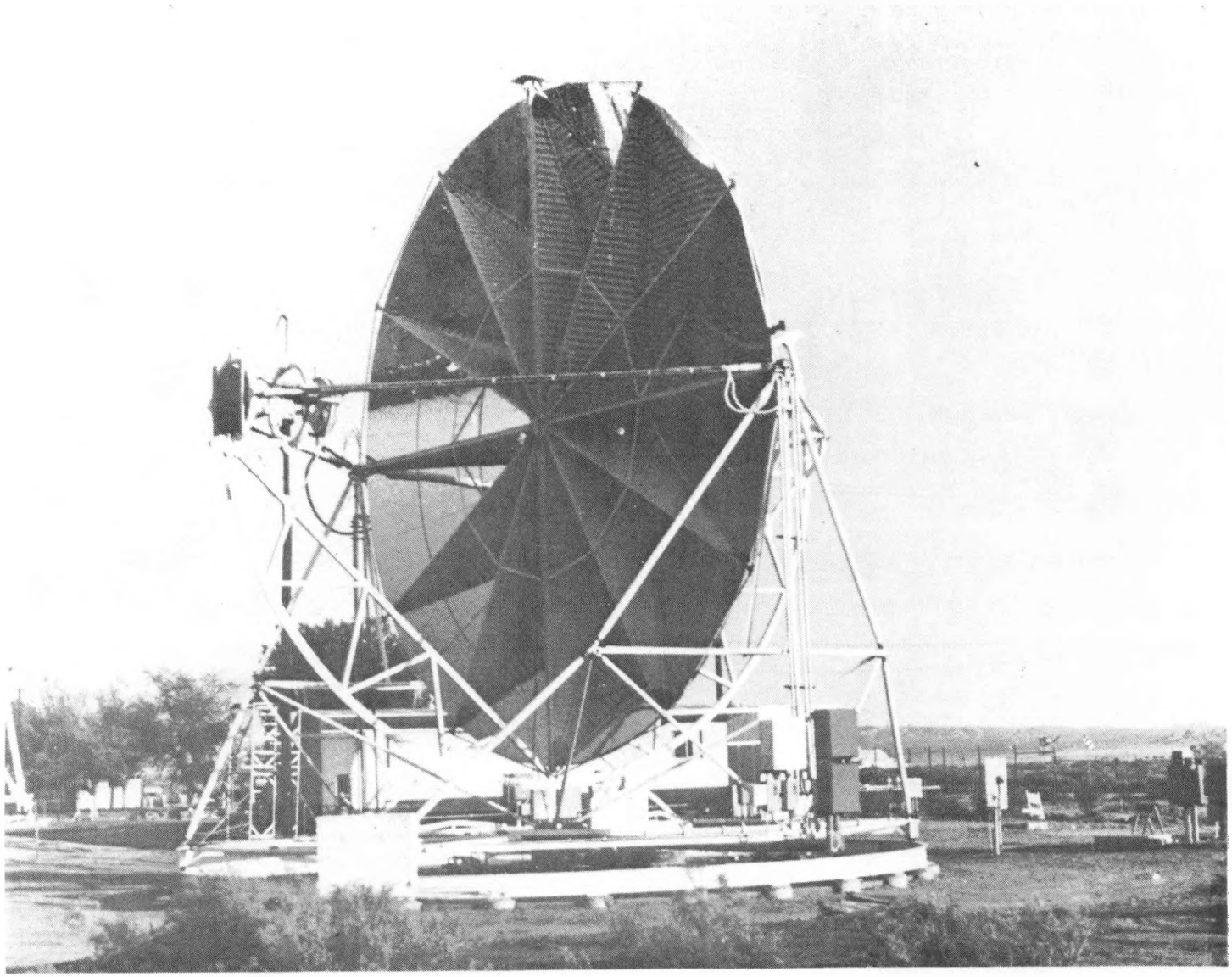

Fig. 4. PDC-1 Assembled Concentrator Located at the JPL Parabolic Dish Test Site. The colored targets were mounted in the focal plane (left) and a flood light for nighttime photographs is mounted near the vertex.

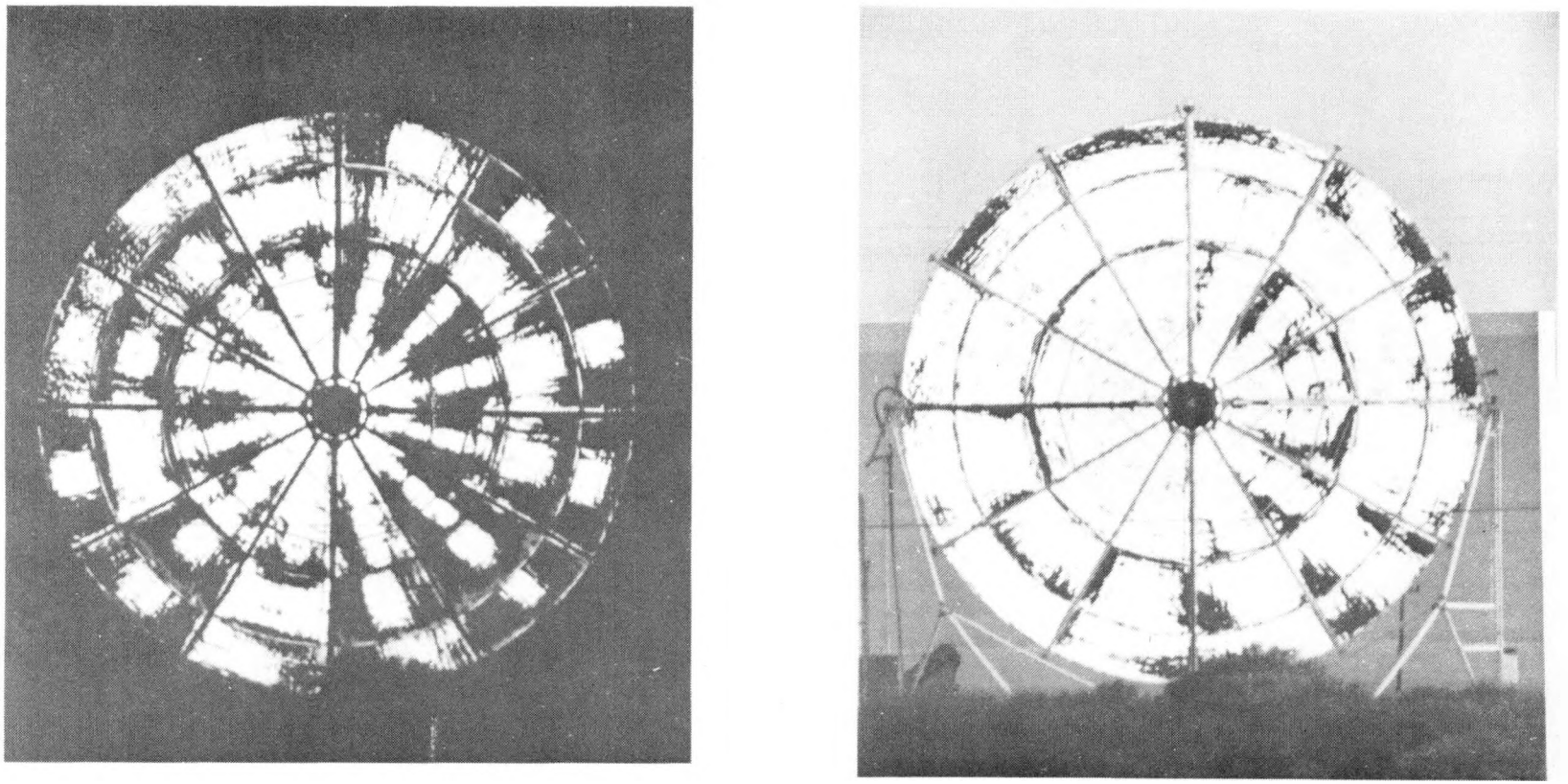

Fig. 5. Diagnostic Photographs Taken of the Assembled Concentrator. The left image is at an ambient temperature of 1.67°C (35°F) and the right image at 18.3°C (65°F). The white areas indicate regions of the reflecting panels forming an image smaller than 15 cm (6 in.) in diameter. The dark areas indicate panel areas forming images up to 38 cm (15 in.) in diameter from the colored parts of the focal plane target.

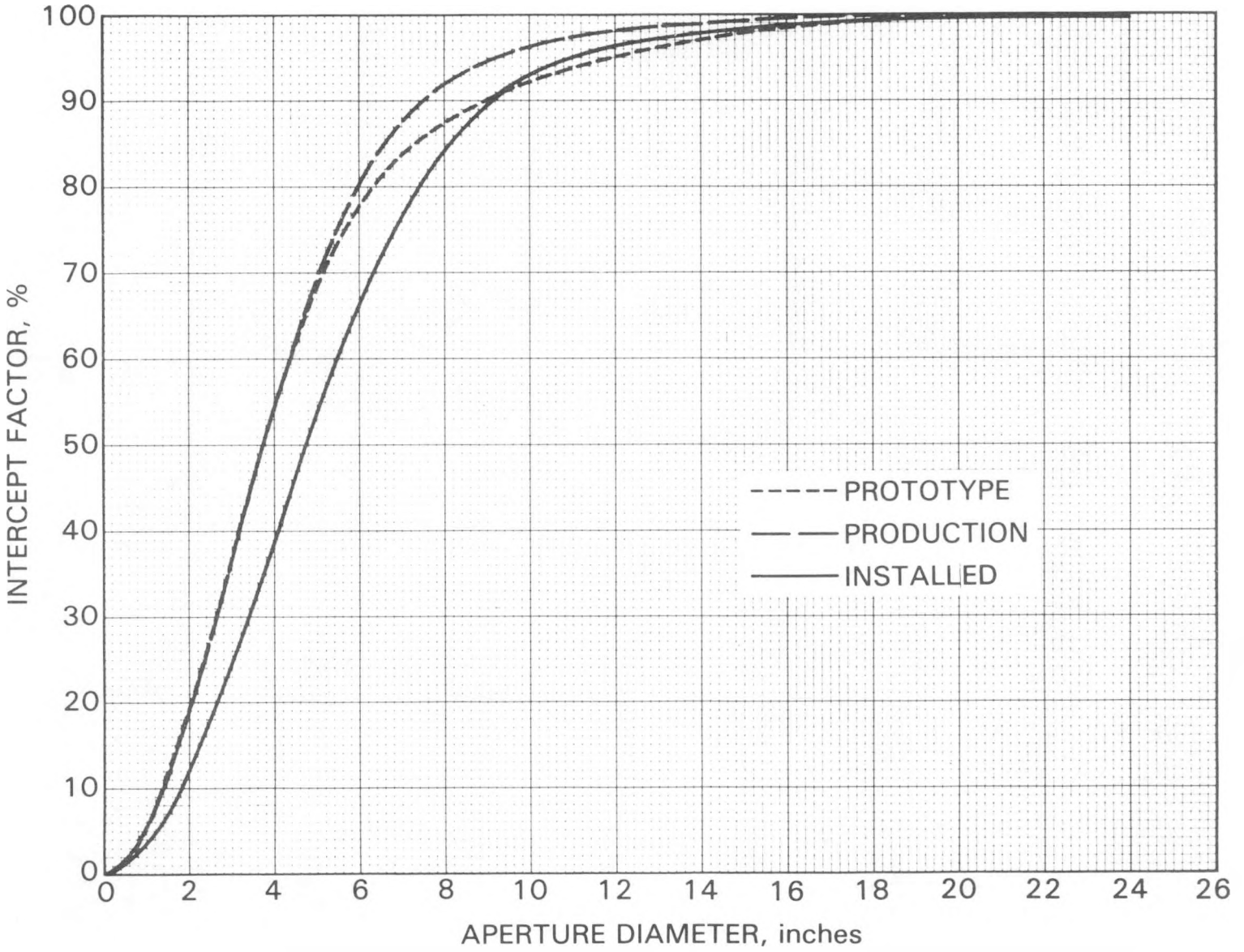

Fig. 6. The Intercept Factor Distribution Curves from the Prototype, Production, and Assembled Concentrator (After Re-Installation)

Commercialization of Solar Energy Resources

William R. Gould
Chairman and Chief Executive Officer
Southern California Edison

Since the announcement of our alternatives and renewables program in 1980, initial skepticism from our utility brethren has yielded to widening and deepening support.

Faced with rising fuel, construction and capital costs, all of which contribute to higher electric rates, utilities, regulatory bodies and consumers have become increasingly interested in the potential of alternative and renewable resources.

We at Edison continue to be optimistic about our program to accelerate development of solar and other renewable and alternative resources for generating electricity. In fact, we now expect more than one-third of our added firm capacity in the next decade to come from co-generation and renewable resources, compared with a pre-1980 estimate of only 14 percent.

Our dedication of the Solar One generating station in the high desert near Barstow on November 1 symbolized the fact that electric utilities are performing a fundamental and aggressive role in pulling the solar technologies toward commercialization.

Each day the world becomes a little more familiar with the enormous implications of these alternative and renewable resources for ensuring reliable power and reducing dependence upon oil and gas. Their characteristics of lesser capital intensity, shorter lead times, broader public acceptance, and greater system planning and construction flexibility formed our 1980 policy rationale and are well on their way to becoming axioms of today's power planning.

Today's electric utility executives evaluate these resources as part of their stewardship for both customer and shareholder. We are caught between a regulatory command to provide as much reliable, "least cost" electricity as customers want, and a fiduciary responsibility to stockholders demanding a reasonable return on investment.

In the final analysis, many expectations are competing. Utility executives want to meet growth; stockholders want a fair return on their investments; customers want reliable service and lower rates; and special interest groups want their favored forms of generation developed, often at the expense of others.

Furthermore, customers cannot always be expected to master the complexities and subtleties of our highly technical industry. They measure our performance by the reliability of service and the amount of their electric bills.

At this moment, our industry is being criticized by customers for high electric bills, primarily because of our high costs of fuel, capital and general inflation. It's one of the most important and difficult issues we've faced. More than ever before, corporate decisions must be measured against this test: what is the impact upon the customer?

In this climate of uncertainty, my company hopes to avoid locking itself into any long-term, expensive power plant project during this decade, focusing instead on smaller facilities to reduce the risk of miscalculation and to protect our ratepayers and shareholders.

The outlook for alternative and renewable resources continues to be encouraging, and, overall, we are ahead of expectations.

Nearly half (1,100 firm megawatts) of our goal of 2,150 megawatts of alternate/renewable resources by 1992 are on-line, under construction, or represent signed contracts or letters of intent. This includes 263 megawatts (66 MW firm) from wind, 36 megawatts from solar, 103 megawatts from geothermal and 864 megawatts from cogeneration, small power producers and hydroelectric. We now use eight primary energy resources to generate electricity - oil, natural gas, coal, water, nuclear, wind, geothermal and solar - more, we believe, than any other electric utility in the world.

Edison also is participating in the construction of the nation's largest integrated coal gasification project, scheduled to become operational in 1984. If this project meets expectations, we could realize a valuable source of clean-burning, medium BTU gas for existing plant boilers that are currently limited to natural gas and imported fuel oil. Also, we could demonstrate a new base load concept for the utilization of coal.

Cogeneration has emerged as a major source of electric power generation. The sequential production of electricity and thermal energy in the form of process heat or steam offers substantial improvements in fuel use efficiency and will reduce our nation's fossil fuel consumption. In addition, it is based on proven technologies with off-the-shelf components offering additional flexibility and reliability to the electric system. Edison is actively pursuing cogeneration contracts with large commercial and industrial customers and expects that cogeneration will provide more than 750 MW of firm capacity to the Edison grid by 1992.

In addition, we're supporting fuel cell research and, in October, we helped dedicate a local biogas system plant that is pioneering the use of landfill methane gas to generate electricity for Edison customers.

Current Edison solar research and development projects cover a broad spectrum, ranging from dendritic web and multi-layer solar cells to a 100-megawatt solar central receiver plant. Other solar projects include advanced concentrators, salt ponds, wind turbines and biomass.

I might add that JPL's parabolic dish test site, located at Edwards Air Force Base, fortuitously provides Edison with a fourth kind of solar electricity for its system in addition to central receiver, photovoltaic and parabolic trough facilities.

Our program, then, is diverse by design. Stability is important to a resource strategy, and the diversity offered by a variety of resources stabilizes a system.

Diversity is strategic for several reasons, particularly with renewables. First, in the initial stages of a technology's development, it is often unclear just which features will lead to the greatest efficiencies, assuming that O&M costs are not so high that efficiency ceases to be a major criterion.

It is noteworthy here today that such considerations have guided development of various types of solar concentrators as well as the choice of engine cycles to produce electric power from parabolic dishes.

Another reason that diversity is important to resource strategy is that location may affect the desirability of a resource. Environmental concerns, such as land use, land subsidence, aesthetics, water consumption, socioeconomic and cultural issues and contamination of both water and air, must not be overlooked when evaluating a site for electricity generation from renewable resources.

Solar plant sites, for instance, are likely to be sited in desert areas, posing conflicts with desert landowners, recreational facilities and other competing interests. Also, as with conventional fuels, transportation can be a factor in choosing a location for generation with renewables.

A third reason that stability through diversity is important is that resources and technologies must match system load characteristics and varying climatic conditions. In that sense, Edison is fortunate, because its system summer peak coincides with solar availability.

Thus, while yielding individually small increments to system load, we hope renewable resources will complement each other so that, together, they provide a significant and reliable source of supply.

But, many considerations influence the development of new technologies, and for that reason, I believe in keeping things in perspective. While the long-term outlook for renewable and alternative technologies is encouraging, and the potential contribution to the country is substantial, the development of the more exotic of these resources is not without risk.

Near-term costs, which include research and development and manufacturing facilities, may not compare favorably with the cost of proven, conventional technologies. Operating characteristics and technical performance of many of these technologies are not well defined.

That is why Edison, other utilities, entrepreneurs, government agencies and national laboratories will play growing and critical roles in the commercial deployment of these technologies. And, a belief that entrepreneur ownership of this emerging technology will play an important role in meeting future needs of Edison customers is integral to our role in the process.

Accordingly, Edison is actively negotiating with entrepreneurs to develop cogeneration and renewable energy projects. We offer an approach that is beneficial to all. We are willing to provide entrepreneurs with sufficient incentives to develop these resources, but the incentives must be balanced against our concern for the long-range impact on electric rates and service to our customers.

We are concerned about cost. We believe that utilities should be allowed freedom to negotiate with third parties the price of electricity sold to Edison. Cost should depend on

circumstances of individual projects. To that end, we believe that negotiating contracts meets the financial needs of both entrepreneur and ratepayer. Our company acts, in effect, as an intermediary for the ratepayer's benefit.

The contracts and agreements we have signed demonstrate dramatically that negotiation is accelerating successfully the commercialization of these new technologies. Negotiation is creating competition among entrepreneurs, thereby improving efficiency and reducing costs to ratepayers. Embracing the spirit of the Public Utilities Regulatory Policies Act, Edison will continue to provide appropriate incentives for entrepreneurs to finance and install qualifying facilities.

Today, for technologies such as cogeneration that are near or at commmercial maturity, Edison provides entrepreneurs with feasibility analysis, technical consultation and other services. For emerging technologies, we believe that sharing some of the risks (and potential rewards) is the best encouragement that we can offer entrepreneurs.

Accordingly, whenever possible we offer joint project arrangements to develop these emerging technologies. For example, our 1980 Wind Project Opportunity Announcement, a national first, solicited joint venture participation by entrepreneurs to develop wind parks.

We will, under certain conditions, participate in a wind park project by providing items such as land, interconnection, technical consultation, siting and permit support, price guarantee, wind resource insurance, project management, financial analysis and other services.

Another example was our Solar Project Opportunity Announcement this year for "Solar 100," an advanced, 100-megawatt solar generating station, which would be the nation's first large-scale commercial solar central receiver. Our announcement attracted four responses from private industry in September.

We have found that entrepreneurs are willing to sell electricity to us at a rate based upon a percentage of our incremental cost in exchange for our participation and assumption of certain risks. They have been receptive to our balanced approach.

Our participation may reduce capital requirements, interest rates, risks and exposures for an entrepreneur. It also may increase the probability of success and, in certain cases,

ensure a more uniform cash flow. We also can provide technical and managerial expertise to bring facilities on line in a timely manner.

Our aggressive efforts have resulted in cost-effective, cost-justified, market-competitive arrangements with responsible private entrepreneurs. We will have more than met our resource requirements through 1985, when all of these committed projects go into operation.

On November 18, we had executed contracts or signed letters of intent with 21 different parties for geothermal, wind and solar projects totaling 402 megawatts (205 MW firm). That does not include our own projects, or the more than 700 megawatts in wind and solar projects as well as over 1000 megawatts of cogeneration projects currently in the contract negotiation stage. Moreover, we have been able to meet our goals at less than avoided cost, which over the lives of these contracts, will save our customers millions of dollars.

I have tried to communicate the reasons why we are encouraged with our alternatives and renewables program, despite the risks presented by commercialization of these resources.

In conclusion, despite the recent economic downturn, which has made all our jobs more difficult, there is good news. Our goals and our negotiation policies are helping to ensure a market for new, viable technologies. We look forward to the beginning of economic recovery, which will be good news for investors.

And, I want to emphasize that our original motivations remain. Renewables will replace costly oil and natural gas as a generating resource; construction modularity provides flexibility to meet today's uncertain demand growth; retirements of older, existing plants are scheduled and necessary, regardless of the rate of demand growth.

In order to further improve the business environment to attract private sector investment in alternative and renewable technologies, we expect regulators and legislators to continue playing critical roles. Regulators are in a position to provide signals to both federal and state legislators to extend tax incentives for the entrepreneur. They also are in a position to coordinate the streamlining of the approval and permitting process.

I believe that our principal challenge is to see that we maintain, with the aid of proper regulations, a balance between consumer and utility stockholder interests. It's a problem that can be solved only by consensus and is more perplexing than the technological mountains climbed by our industry in the past.

Any consensus on power will be attained only by solving a communications problem. All of us--utility, consumer, legislator, suppplier, regulator, special interest group--must be convinced that the objective of reliable, reasonably-priced power is generic and one we have tried hard to attain through years of skyrocketing fuel costs and double-digit inflation.

A giant step in reaching our mututal goal will be bringing the renewable and alternative energy resources of our nation into play as quickly and efficiently as possible.

In closing, I am reminded that the incentive that drove our company toward the use of alternate and renewable resources was grounded in optimism, hope and confidence in mastering new technologies to serve the world.

I sense the spirit of that incentive motivating and encouraging us today as we review the potential of parabolic dish solar thermal technology in our efforts to achieve a higher degree of energy independence.

STIRLING MODULE CONCENTRATOR

(VANGUARD I)

TERRY HAGEN

ADVANCO CORPORATION

"This paper is based on work sponsored in part by the Department of Energy under cooperative Agreement No. DE-FC04-82AL16333."

CONCENTRATOR SUMMARY

- CONCEPTUAL MODEL
- DESIGN IMPROVEMENTS
- MIRROR LAYOUT
- OPTICAL ANALYSIS/DESIGN
- RACK/NODE DESIGN
- TRUSS STRUCTURAL ANALYSIS/DESIGN
- DESIGN LOADS
- EXOCENTRIC GIMBAL DESIGN
- PEDESTAL/FOOTING DESIGN
- TRACKING SYSTEM
- TEST SITE

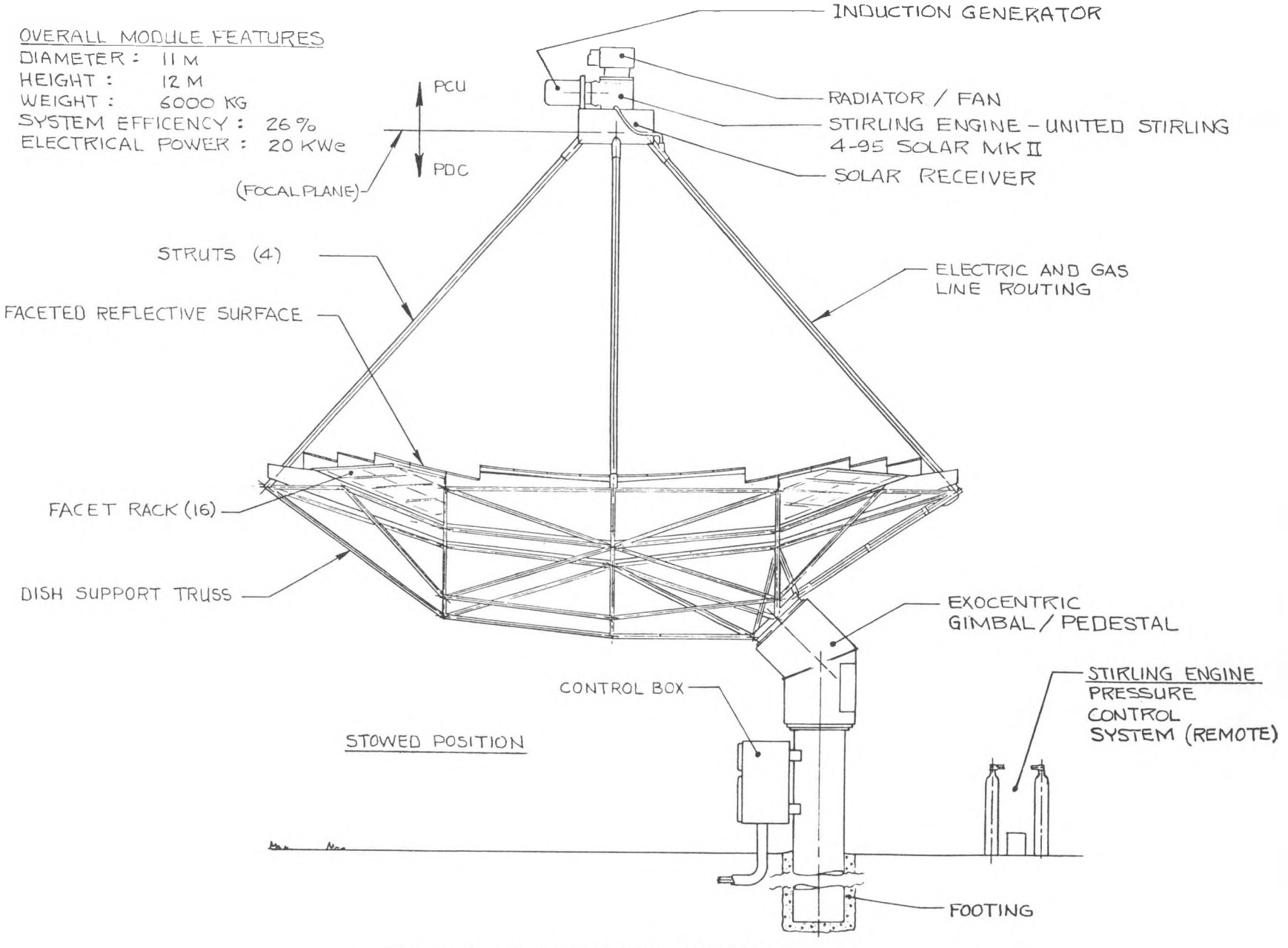

Figure 9. Vanguard Dish-Stirling Module

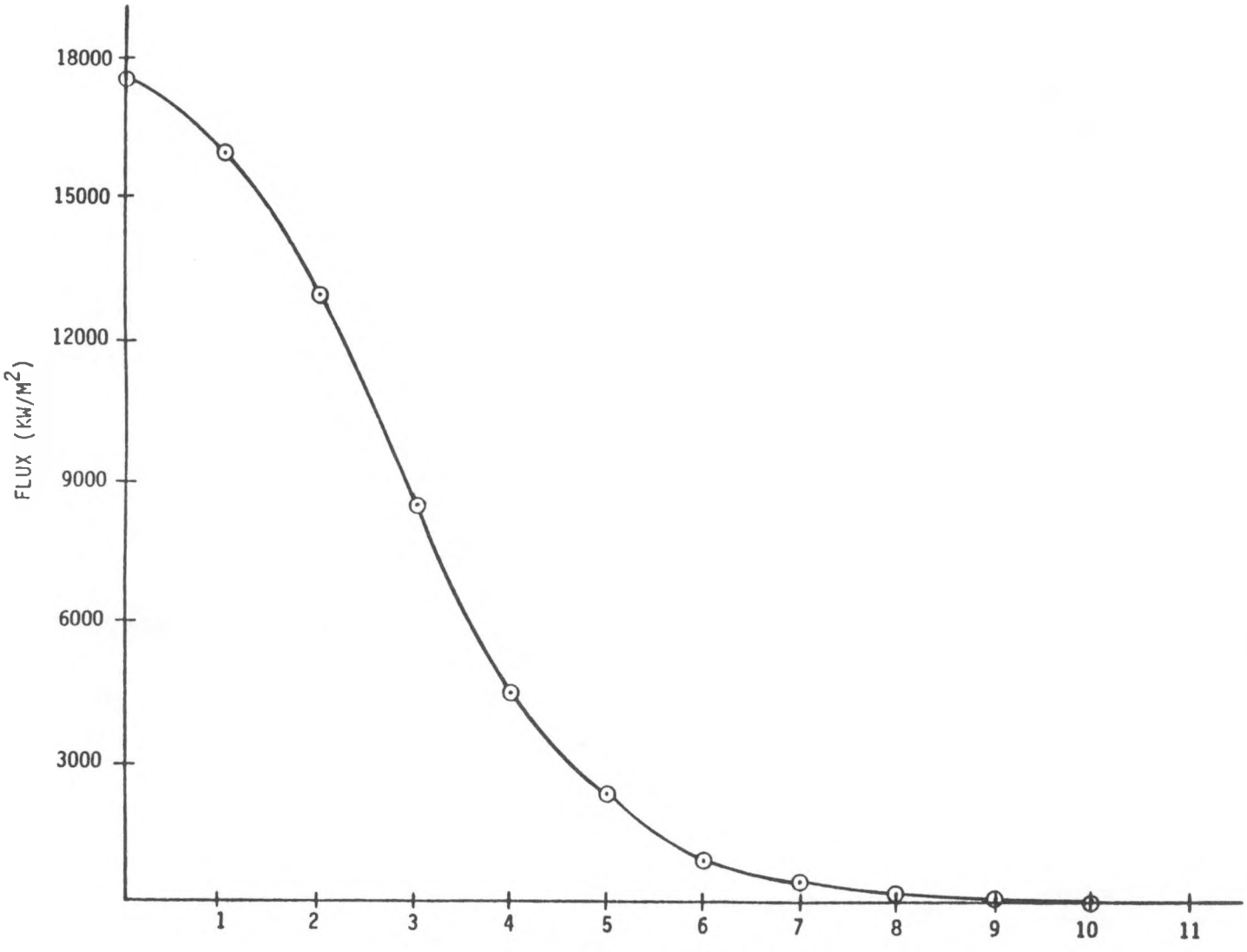

Focal Plane Flux No Re-aiming of Mirrors

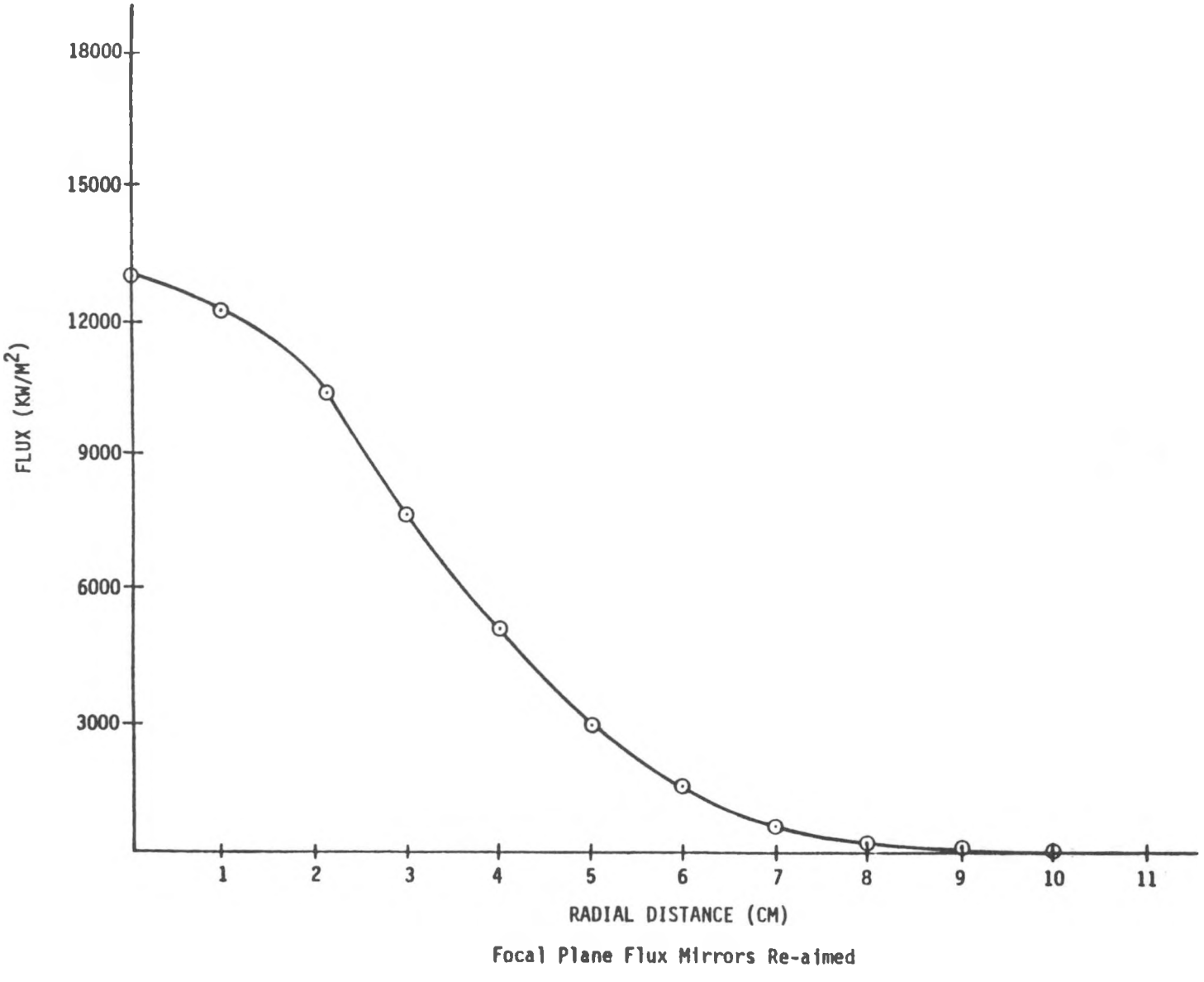

Focal Plane Flux Mirrors Re-aimed

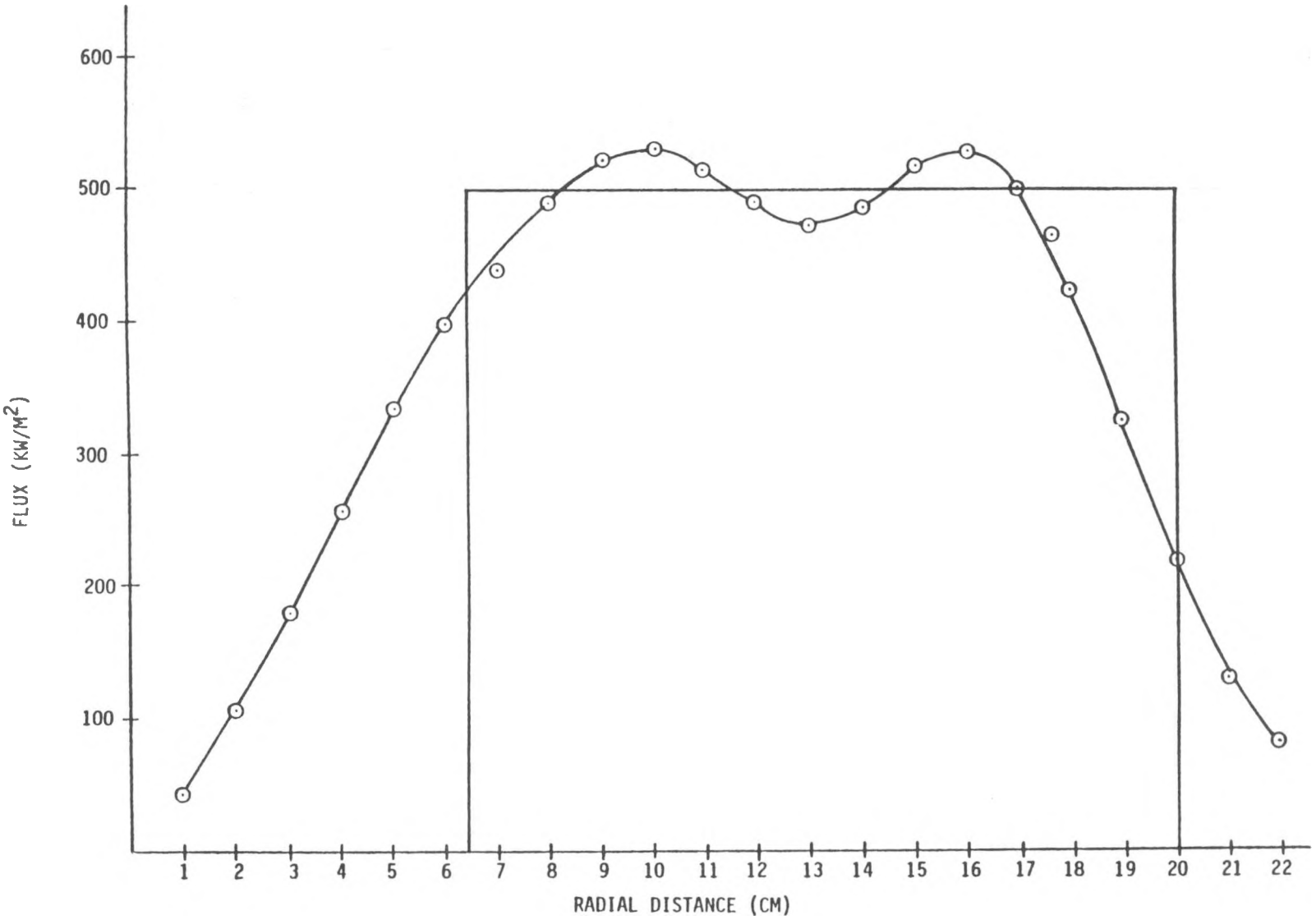

Cone Flux No Re-aiming of Mirrors Cone Vertex 273 mm From Focal Plane

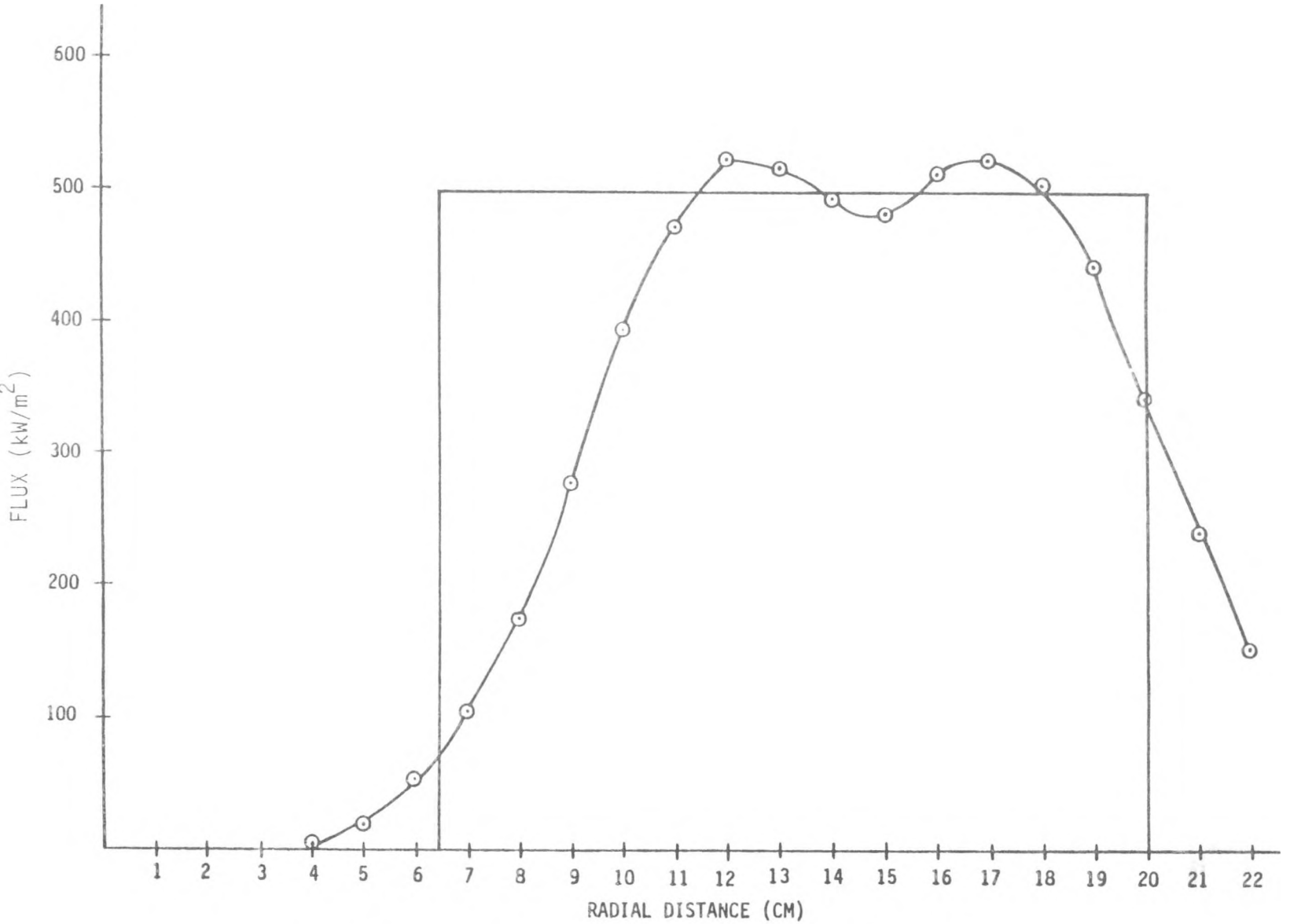

Cone Flux Mirrors Re-aimed Cone Vertex 293 mm from Focal Plane

DESIGN WIND LOAD REQUIREMENT AT DIFFERENT OPERATING CONDITIONS

(MINIMUM PER JPL SPECIFICATIONS/GUIDLINES)

OPERATING CONDITIONS	WIND SPEED (MPH)
1. OPERATING STEADY STATE	15
2. OPERATING WITH 20% GUSTS	30
3. SLEW TO STOW	50
4. SURVIVAL IN STOW	90
5. SURVIVAL UNSTOWED	50

MIRROR LAYOUT CONCEPT

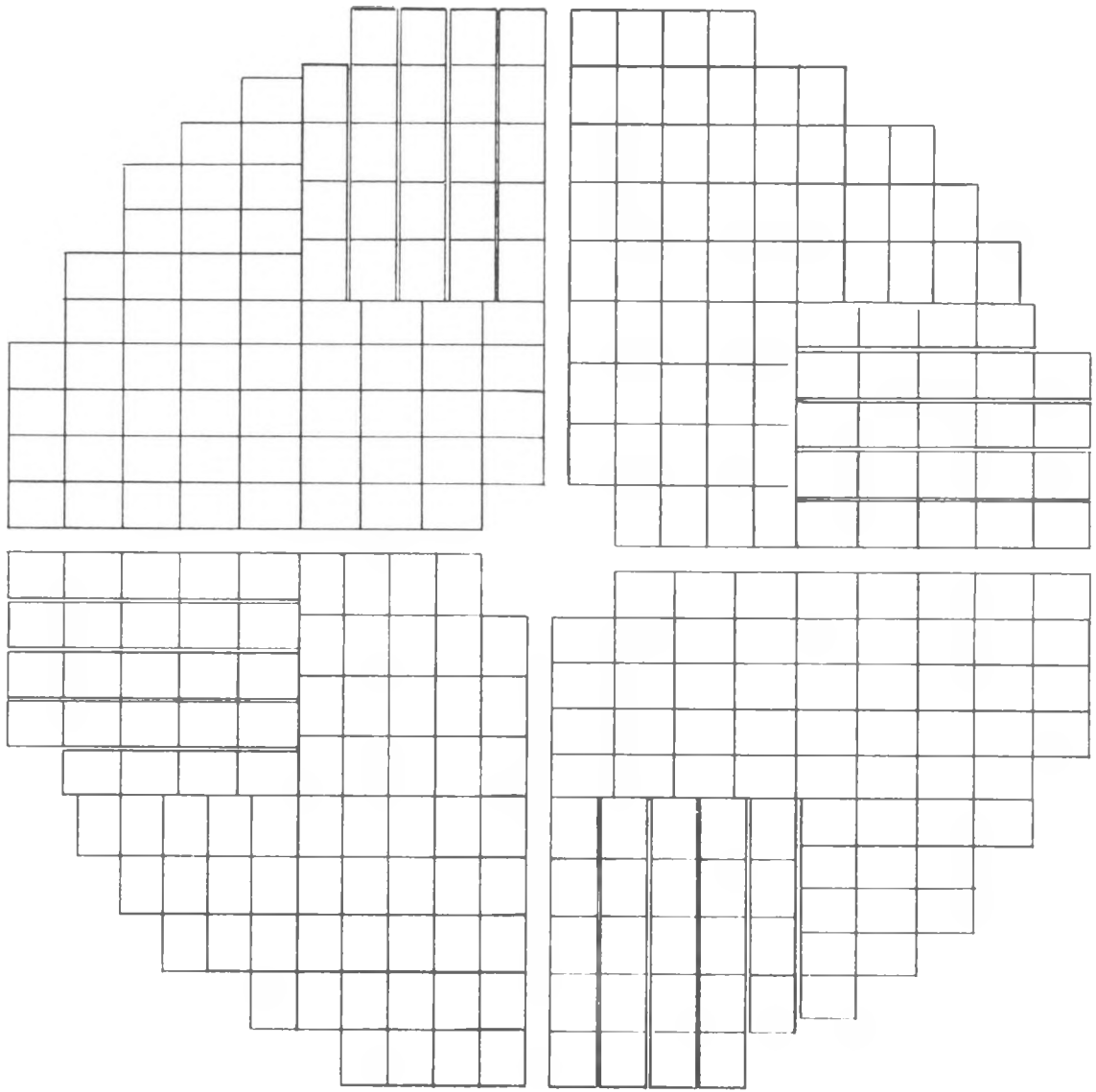

TYPES OF FOOTINGS

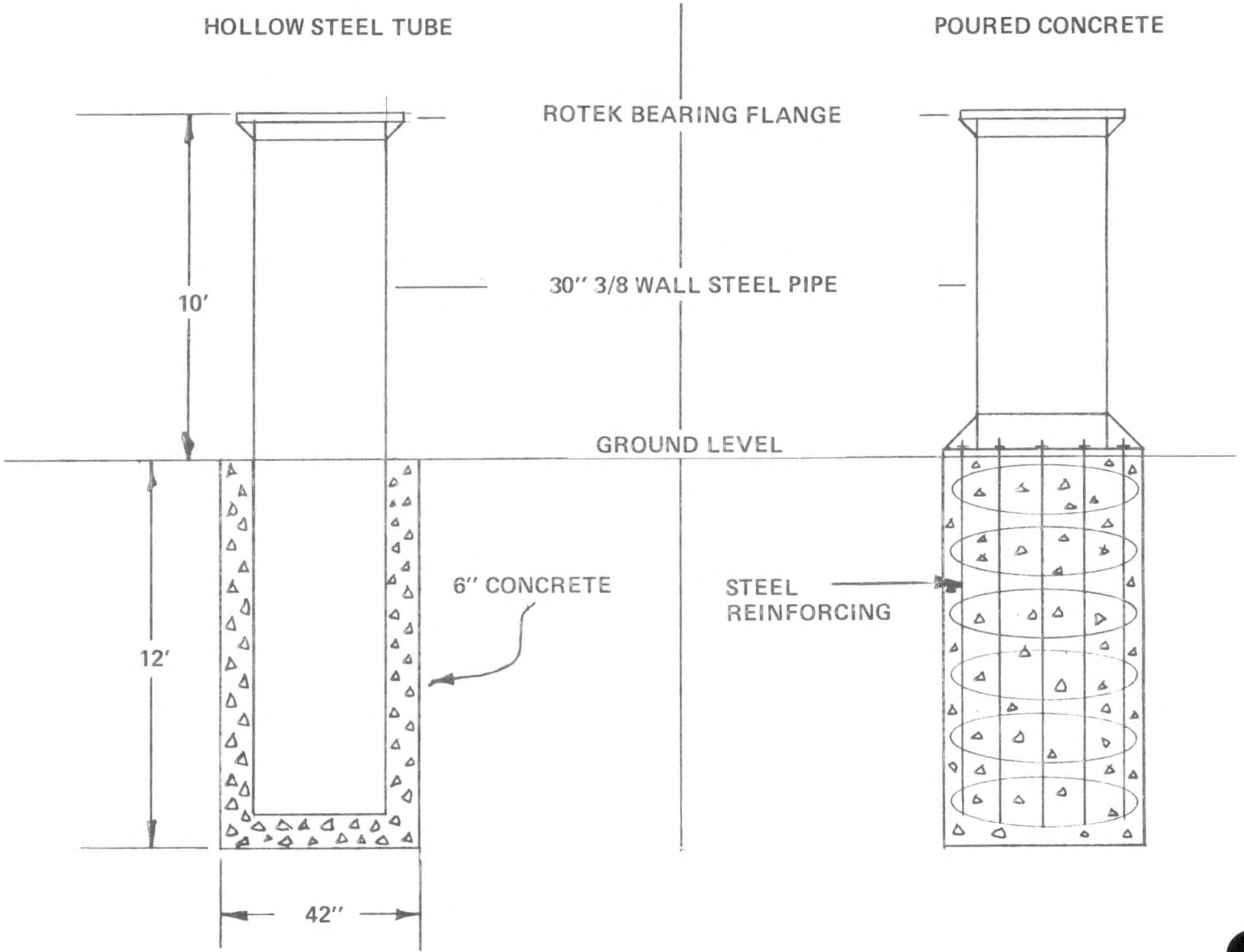

RELIABILITY OF LEVEL AND METHOD OF "WALK-OFF" PROTECTION

PROTECTION LEVEL	DETRACKING METHOD				"WALK-OFF" PROBABILITY PER MODULE YEAR
	1	2	3	4	
	GRID ENERGIZED AZIMUTH AND ELEVATION DRIVE MOTORS	GASOLINE GENERATOR ENERGIZED ELEVATION DRIVE MOTOR	BATTERY (CHARGER) ENERGIZED D.C. ELEVATION DRIVE POWER MOTOR	GRAVITY DRIVEN GIMBAL	
0	√				0.424
1	√	√			5.65×10^{-3}
1	√		√		1.55×10^{-3}
1	√			√	4.17×10^{-4}
2	√	√	√		4.22×10^{-4}
2	√	√		√	1.06×10^{-5}
2	√		√	√	2.06×10^{-6}
3	√	√	√	√	1.21×10^{-6}

TRACKING SYSTEM CONCENTRATOR CONTROL UNIT

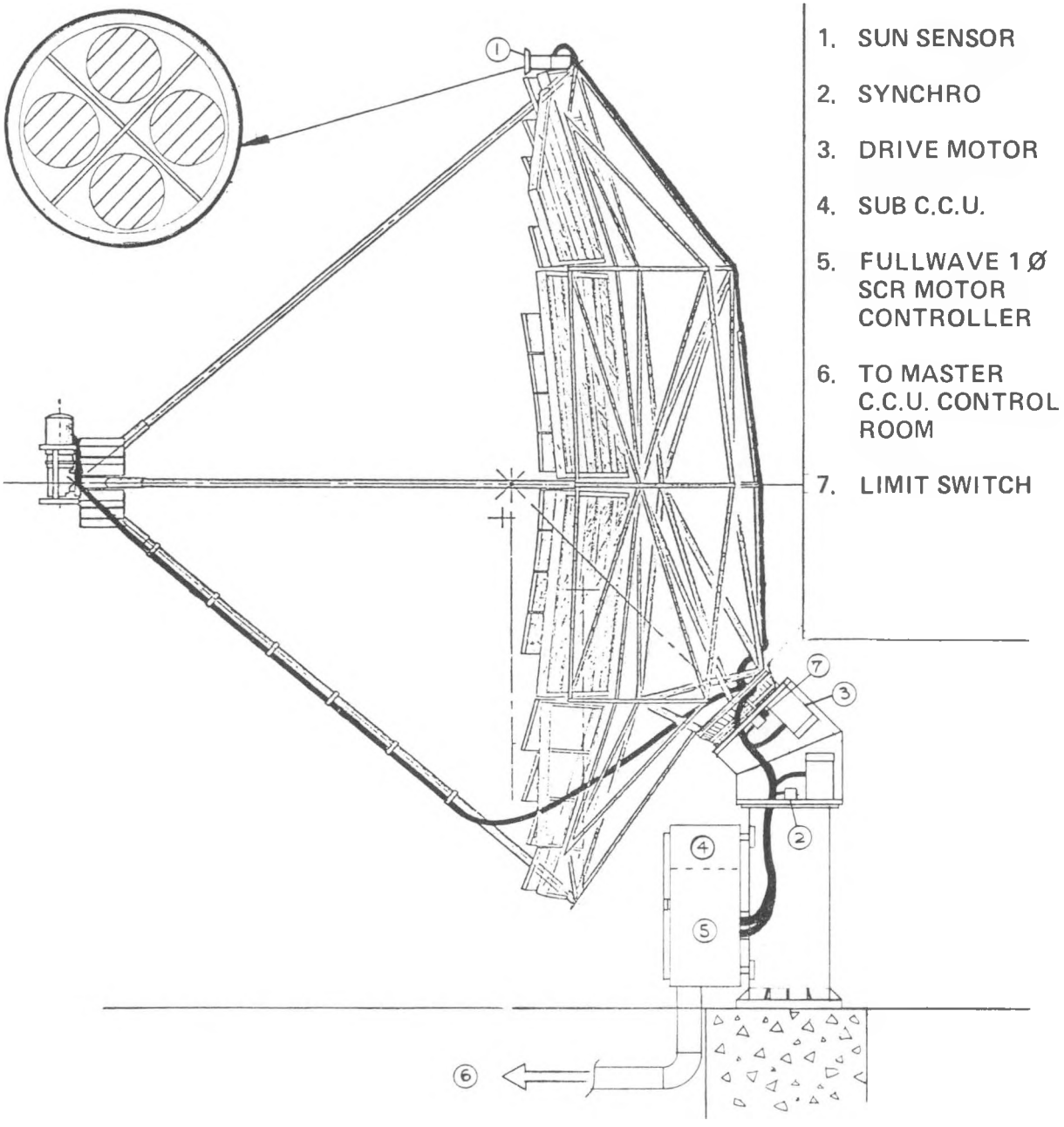

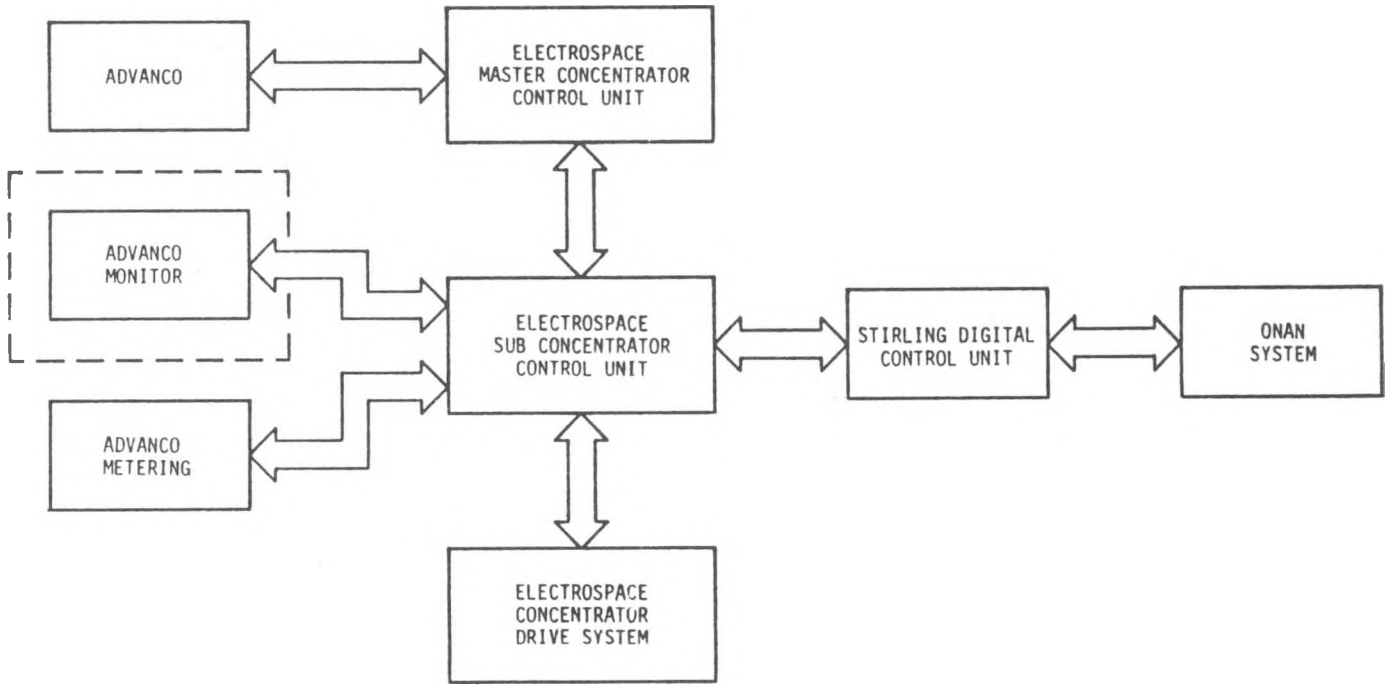

Supervisory Controls Block Diagram

Blank Page

A Transmittance-Optimized, Point Focus Fresnel Lens Solar Concentrator

M.J. O'Neill, V.R. Goldberg, D.B. Muzzy

E-Systems, Inc.

Energy Technology Center

P.O. Box 226118

Dallas, Texas 75266

INTRODUCTION

E-Systems is currently developing a point-focus Fresnel lens solar concentrator for high-temperature solar thermal energy system applications. The concentrator utilizes a transmittance-optimized, short-focal-length, dome-shaped refractive Fresnel lens as the optical element. This unique, patented (Ref. 1) concentrator combines both excellent optical performance and a large tolerance for manufacturing, deflection, and tracking errors.

Under Jet Propulsion Laboratory (JPL) funding, E-Systems has completed the conceptual design of an 11-meter diameter concentrator which should provide an overall collector efficiency of about 70% at an 815°C (1500°F) receiver operating temperature and a 1500X geometric concentration ratio (lens aperture area/receiver aperture area).

In the following paragraphs, a review of the Fresnel concentrator development program will be presented, including a description of the concentrator, a summary of its expected performance, the key features of the lens, a parquet approach to lens manufacturing, a description of a prototype lens panel, and a discussion of the ongoing prototype test program.

CONCENTRATOR DESCRIPTION

The point-focus lens concentrator is shown in Figure 1 and described in Table 1. The optical element is a convex, dome-shaped, acrylic Fresnel lens. The dome consists of ten conical-segment rings, which are each flat in the radial direction and curved in the circumferential direction. The rim angle of the lens (from optical axis to outermost prism) is 45 degrees. Each of the conical-segment rings is about 61 cm wide, with a smooth outer surface and a prismatic inner surface. The lens is made of uv-stabilized acrylic plastic, about 2.4 mm thick. Steel space-frame structure is employed for both the basic concentrator and the pedestal. Reinforced concrete is used for the foundation. The tracking system provides full two-axis sun-tracking and inverted (lens-down) stowage. The Fresnel concentrator will be adaptable to a wide variety of receivers currently under development by JPL and others. The air volume between lens and receiver is enclosed with a thin aluminum conical shroud to minimize dirt and moisture accumulation on the inner surface of the lens. A slight pressurization of

this air volume may be desirable for dust infiltration prevention. The total concentrator weight is about 13,000 pounds (13 pounds per square foot of aperture).

CONCENTRATOR PERFORMANCE SUMMARY

The point-focus Fresnel concentrator performance is summarized in Table 2 for two cases of practical importance. The first case corresponds to a high-temperature receiver which would be required for a Brayton or Stirling engine application. For this case, a 1500X geometric concentration ratio is utilized (corresponding to a receiver aperture diameter of 0.28 meter). After treating reflection/absorption losses in the acrylic lens, 90% of the sunlight is transmitted. Of this transmitted sunlight, about 92% is contained within the limited 0.28 meter receiver aperture circle; i.e., 92% is the receiver intercept factor. About 6% of the lens aperture is blocked by structure; thus the blocking/shading factor is 94%. After all of these loss mechanisms are considered, the overall optical efficiency is 78%. Still considering Case I, this 78% optical efficiency for an 11-meter diameter concentrator (aperture area = 95 m^2) corresponds to a black-body receiver energy absorption rate of 59 kw (thermal) under a direct insolation of 800 w/m^2. Assuming an 815°C receiver temperature, the black body thermal radiation loss will be 5 kw (thermal). Thus, the net collector output will be 54 kw (thermal), corresponding to a 71% overall collector efficiency.

For the second case in Table 2, a lower temperature receiver is assumed, corresponding to a Rankine engine application. For this lower temperature, a lower geometric concentration ratio (500X) provides better overall collector performance. After considering the same loss factors described above, the concentrator optical efficiency is 83%, this higher value being attributable to a better receiver intercept factor for the larger receiver aperture diameter (0.49 meter). After subtracting the 2 kw (thermal) black-body radiation loss corresponding to a receiver temperature of 371°C, the net collector output will be 61 kw (thermal), equivalent to an overall collector efficiency of 80%.

KEY LENS FEATURES

The patented E-Systems concentrator is a dome-shaped Fresnel lens with a smooth outer surface and a prismatic inner surface. The lens is a convex, non-spherical-contour lens, in which each prism transmits direct solar rays with equal angles of incidence and excidence, as shown in Figure 2. This incidence/excidence symmetry (also called the minimum deviation condition) provides each prism with the lowest possible reflection losses, and thereby the highest possible transmittance, for that prism's light deviation (turning) angle, as proven rigorously in Reference 1. In addition to maximal transmittance, this minimum-deviation-prism lens also provides a maximal tolerance for lens contour errors (slope errors), an

improved tolerance for lens manufacturing errors (prism angular errors and rounded prism peaks), and a smaller solar image size (including finite solar disk angular diameter and chromatic aberration effects), when compared to previous flat and spherical contour lenses. The optical performance superiority of the new lens is fully described in References 2 and 3. Perhaps the most important attribute of the new transmittance-optimized lens is its high slope error tolerance, which allows a substantial relaxation of the support structure stiffness requirements, and thus a significant reduction in weight and cost of the concentrator. Compared to a reflective concentrator (e.g., a 45 degree rim angle parabolic dish), the Fresnel lens concentrator is more than 100 times more tolerant of radial slope errors, as dramatically illustrated in Figure 3.

PARQUET LENS MANUFACTURING APPROACH

One potentially low-cost manufacturing approach for the point-focus lens is the parquet approach of Figure 4. The dome consists of conical segments which are curved in the circumferential direction and straight in the radial direction. This approach allows the acrylic plastic lens material to be made in flat form and mechanically held in the conical geometry in the completed concentrator. The unfolded flat conical segments can be subdivided into a number of identical lens panels. While these panels would ideally utilize prims running circumferentially along concentric circles, current manufacturing approaches for prismatic sheet can not achieve these non-linear prisms. Fortunately, low-cost manufacturing approaches are available for making linear prismatic sheet. Thus, the lens panel of Figure 4 is configured to approximate the ideal curved-prism geometry by utilizing a parquet of linear prism elements. The two key variables of this parquet lens approach are the element width (w) and the gap width (g) between elements, since the element width causes a focal-plane image enlargment and since the gap width causes transmittance losses. Prototype fabrication efforts have proven that the gap width can be maintained at about 0.5 mm. Element width selection is based on optical analyses discussed below.

Optical analyses of the parquet lens concentrator have been completed. These analyses are based upon cone optics; i.e, the theoretical mapping of the conical bundles of radiation which originate at the solar disk, which are incident upon the lens outer surface, and which form elliptical images in the focal plane, as shown in Figure 5. Because of dispersion (chromatic aberration), the solar images of different wavelengths are spread across the focal plane, as shown in Figure 5. For any fixed receiver aperture diameter and any particular prism in the lens, the design wavelength can be selected to minimize the energy missing the receiver aperture, and thus to maximize the intercept factor. The current lens has been tailored for a 1500X design concentration ratio by properly varying the design wavelength for the various prisms comprising the lens.

For the parquet lens approach, the effect of the parquet element on lens focussing is the formation of a linear solar image in the transverse direction of Figure 5, with the total image transverse length being equal to the parquet element width (w) plus the solar disk image width. The computer model treats this parquet element effect and calculates the radiant flux profile in the focal plane by integrating over all contributing portions of the lens (treating the local lens transmittance), and over all contributing wavelengths, to define the total radiant flux concentration at each point in the focal plane. Results of such a flux profile calculation for several parquet element widths are shown in Figure 6. The radiant flux is normalized by the one-sun direct solar flux incident on the lens, while the radial position in the focal plane is normalized by the lens aperture radius, for the results shown in Figure 6. As expected, the larger the parquet element width, the more spread out the image becomes. However, the image spreading effect is small for element widths of 5 inches and less, when one notes that a 1500X geometric concentration ratio corresponds to a receiver normalized radius (ρ/R) of 26×10^{-3} in Figure 6. The flux profile labeled W=0 represents the ideal lens with non-linear prisms.

The flux profiles of Figure 6 can be integrated over various size receiver circles to define the overall energy interception rate for various geometric concentration ratios. The results of such an integration are shown in Figure 7, wherein the intercepted energy rate has been normalized by the energy rate incident on the lens outer surface; thus the effective transmittance (optical efficiency) is shown as a function of geometric concentration ratio for lenses with various parquet element widths. (The results of Figure 7 do not include absorption losses within the thin acrylic lens, which are expected to be 1-2%, based upon measurements for similar acrylic Fresnel lenses. Also, the results in Figure 7 do not include structural blocking/shading losses, although this 6% loss was included in Table 2.) Note that wide parquet element widths work well for low geometric concentration ratios, but not well for high geometric concentration ratios, due to the image spreading effect of the parquet width. Note also that there exists an optimal element width for each value of geometric concentration ratio, this optimum corresponding to the best tradeoff of image spreading losses (which increase with element width) and gap losses (which decrease with element width since g/w represents the lost gap area fraction). For 1500X geometric concentration ratio, element widths of 2, 3, and 4 inches provide essentially equal performance. To minimize lens complexity, the 4-inch element width has been selected for prototype fabrication, as discussed below.

PROTOTYPE LENS PANEL

A prototype lens panel, using the parquet lens manufacturing approach, has been fabricated for optical testing. This panel is described in Table 3. The panel represents one part of the conical ring located between 27.9° and 32.1° of local rim angle, measured from the lens optical axis. This

segment was selected for prototype fabrication because its optical performance is typical of the full dome lens performance. A nominal 2 foot by 4 foot panel size was selected for prototype fabrication, using 12 linear prismatic parquet elements of 4 inch average element width (w) to form the 4 foot curved dimension of the panel. The linear prismatic elements were made by 3M Corporation to E-Systems specification, using 3M's low-cost lensfilm process. The twelve elements were solvent-bonded to a single piece of extruded acrylic sheet to form the final panel. The entire laminated panel thickness is about 0.1 inch.

TEST PROGRAM

Testing of the prototype lens panel is just underway. As outlined in Table 4, two basic test approaches are being employed to measure the optical performance of the lens panel. The first test, which has been completed, is a simple laser/silicon photovoltaic cell transmittance test. The cell was placed at various distances from the lens to intercept transmitted laser light within various total acceptance angles. A beam expander was used with the laser to intercept several prisms with the transmitted beam. The transmittance was measured as the ratio of the cell short-circuit current with the cell intercepting transmitted light divided by the cell short-circuit current with the light directly incident on the cell (no lens between laser and cell). For an acceptance angle corresponding to 1500X geometric concentration ratio, the typical measured transmittance values were 85-86%.

The second test planned for the prototype lens panel involves actual outdoor testing of the lens, with focal plane flux scans using a row of silicon cells as the sensors. Initial outdoor testing has been plagued with several problems, and meaningful data has not yet been obtained. However, the visible image produced by the lens panel has the proper size, shape and color variation predicted by the computer analysis. Good transmittance versus geometric concentration ratio data should be obtained within the next few weeks. Pending successful completion of in-house testing, the prototype lens panel will be delivered to JPL for further independent testing.

REFERENCES

1. O'Neill, M.J., "Solar Concentrator and Energy Collection System," U.S. Patent No. 4,069,812, 24 January 1978.

2. O'Neill, M.J., "A Unique New Fresnel Lens Solar Concentrator," Silver Jubilee Congress of the International Solar Energy Society, Atlanta, Georgia, May 1979.

3. O'Neill, M.J. and R.A. Waller, "Analytical/Experimental Study of the Optical Performance of a Transmittance-Optimized Linear Fresnel Lens Solar Concentrator," Annual Meeting of the International Solar Energy Society, Phoenix, Arizona, June 1980.

FIGURES AND TABLES

Figures and tables are located on the following pages.

FIGURE 1

E-SYSTEMS
Energy Technology Center

POINT FOCUS
FRESNEL LENS CONCENTRATOR

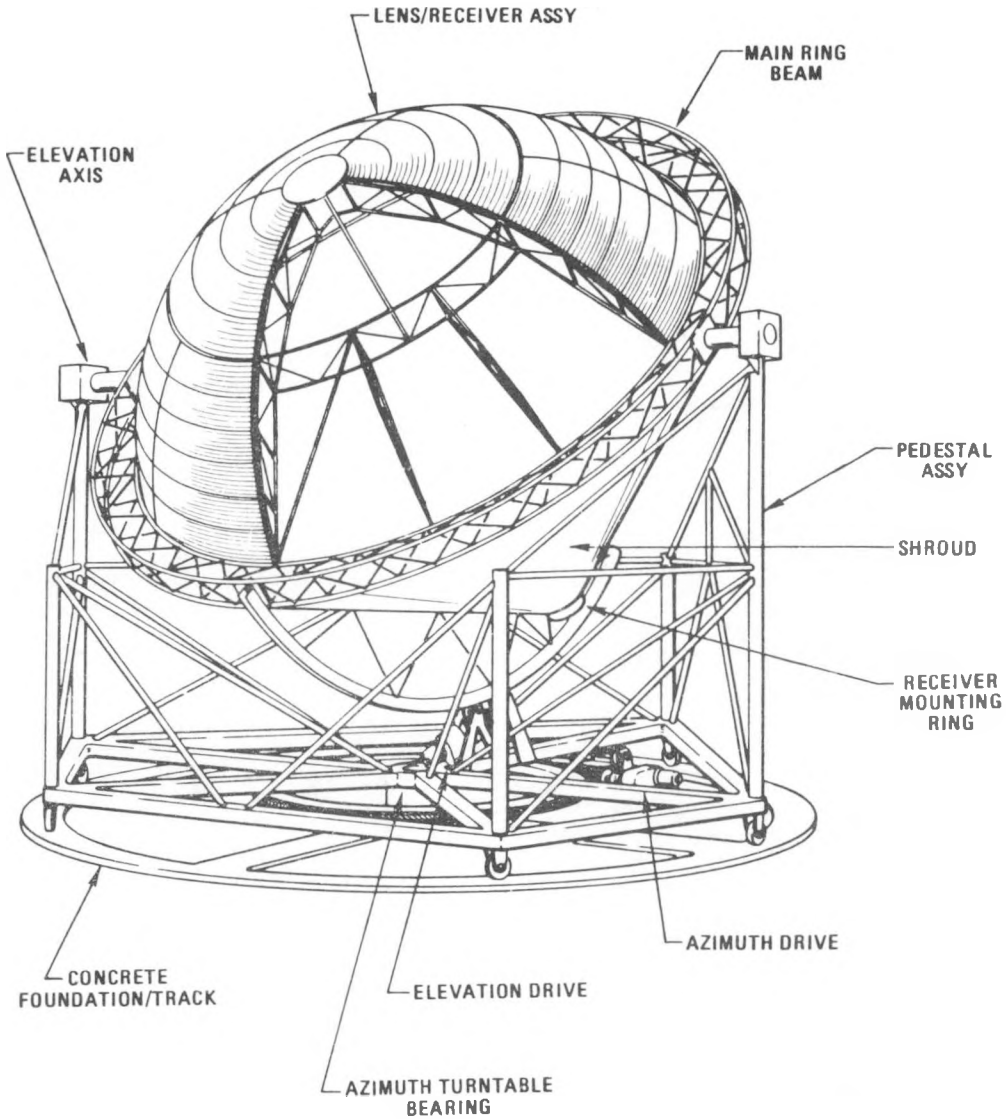

FIGURE 2 -

E-SYSTEMS
Energy Technology Center

PRISM FACE OVER-EXTENSION TO MINIMIZE OPTICAL LOSSES

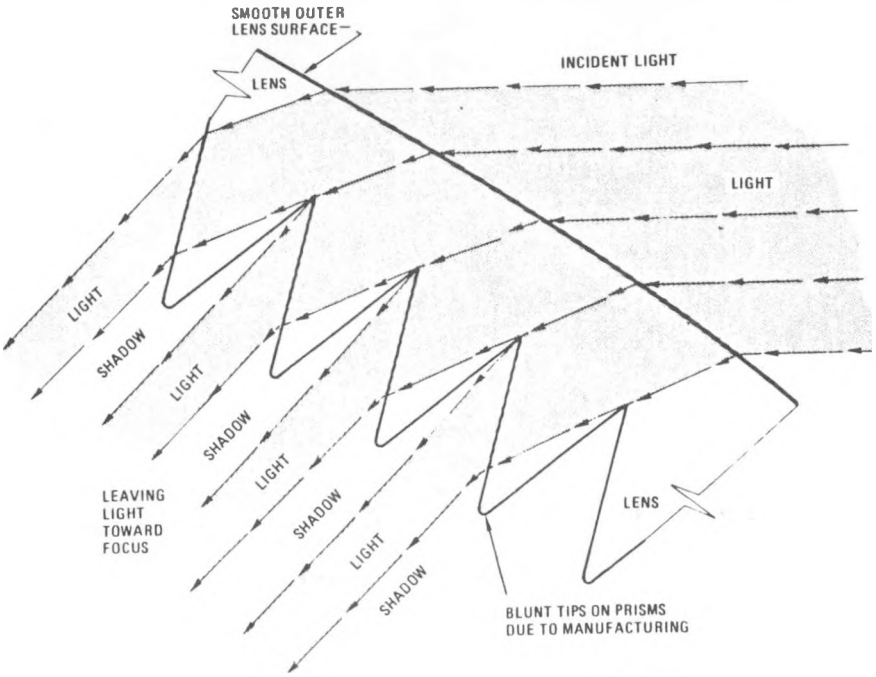

FIGURE 3 -

E-SYSTEMS
Energy Technology Center

SLOPE ERROR EFFECT ON IMAGE DISPLACEMENT FOR FRESNEL CONCENTRATOR vs PARABOLIC DISH

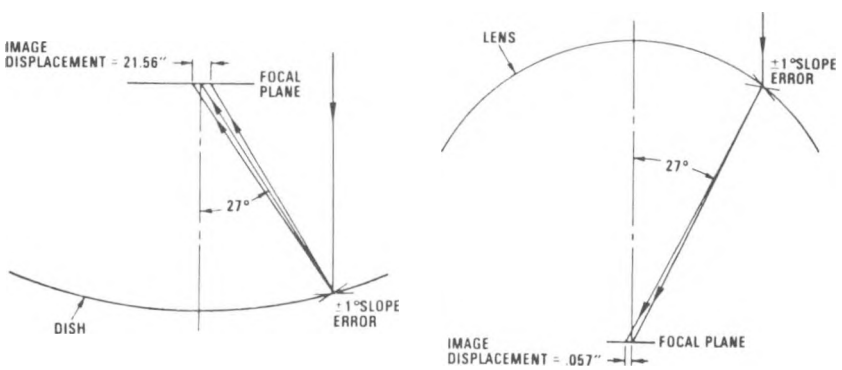

PARABOLIC DISH
- 45° RIM ANGLE
- 36 FOOT APERTURE
- +1° SLOPE ERROR AT 27° LOCAL RIM ANGLE
- PLUS AND MINUS SLOPE ERRORS CAUSE EQUAL DISPLACEMENTS IN OPPOSITE DIRECTIONS

FRESNEL LENS
- 45° RIM ANGLE
- 36 FOOT APERTURE
- ±1° SLOPE ERROR AT 27° LOCAL RIM ANGLE
- PLUS AND MINUS SLOPE ERRORS CAUSE EQUAL DISPLACEMENTS IN SAME DIRECTION

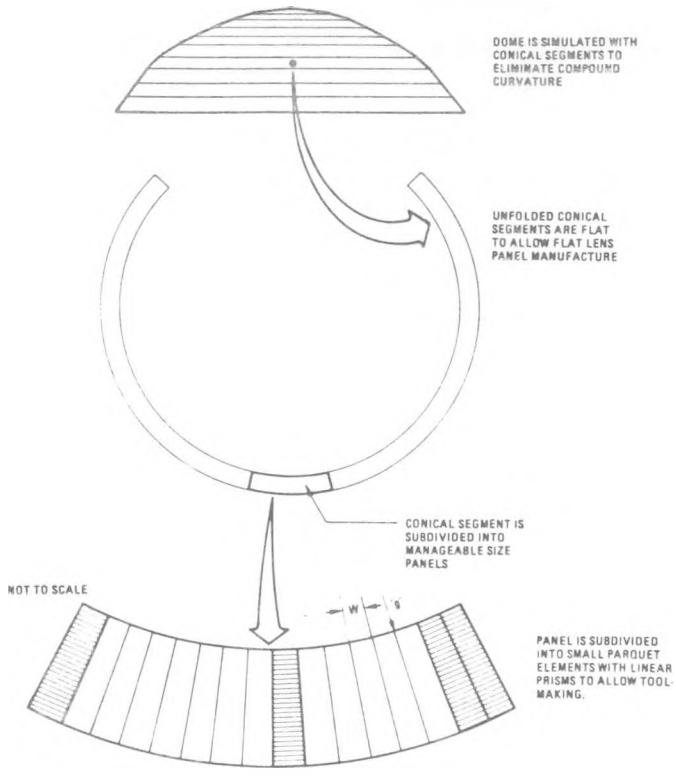

FIGURE 4 - *GEOMETRY INVOLVED IN USING FLAT LINEAR FRESNEL LENS ELEMENTS TO MAKE DOME POINT FOCUS LENS*

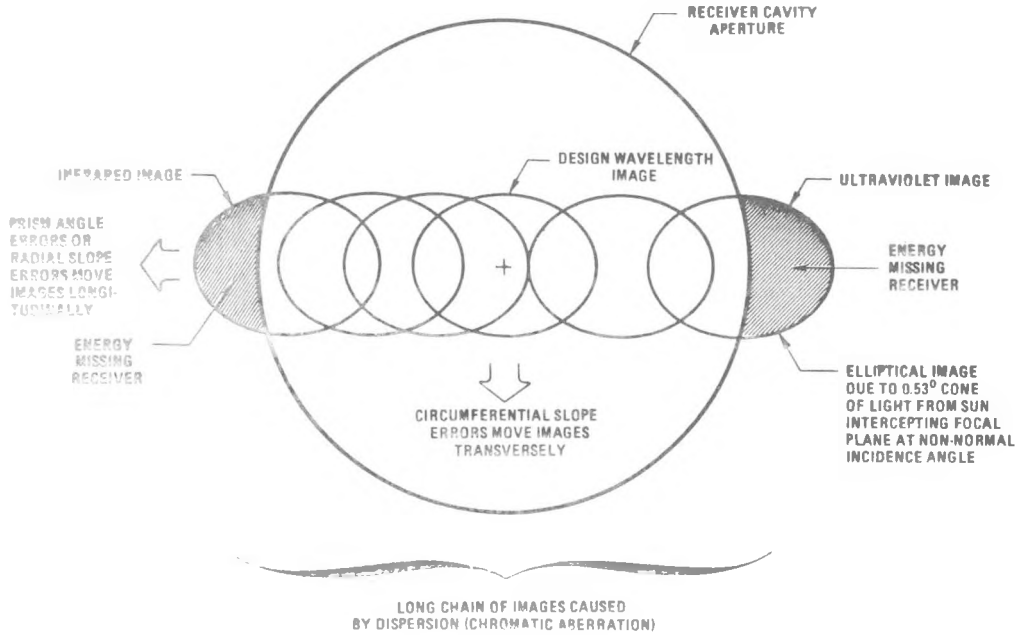

FIGURE 5 - *TYPICAL IMAGE PATTERN PRODUCED BY DIFFERENTIAL ELEMENT OF LENS SHOWING EFFECTS OF DISPERSION AND ERRORS – NOT TO SCALE*

FIGURE 6 - **FLUX PROFILES FOR OPTIMAL 45° RIM ANGLE LENSES**

E-SYSTEMS
Energy Technology Center

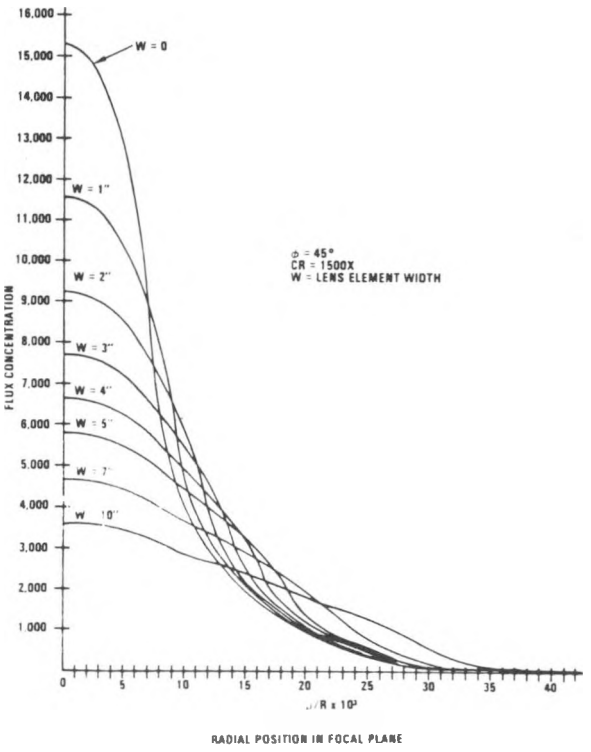

FIGURE 7 - **EFFECTIVE TRANSMITTANCE VERSUS GEOMETRIC CONCENTRATION RATIO FOR SEGMENTED LENS**

E-SYSTEMS
Energy Technology Center

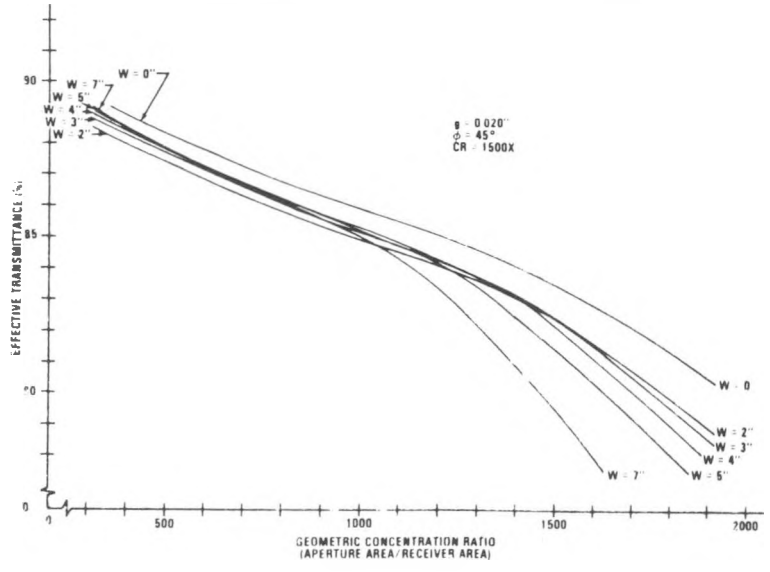

TABLE 1

E-SYSTEMS Energy Technology Center

RECOMMENDED SYSTEM DESCRIPTION

- PHYSICAL
  - CONCENTRATOR APERTURE DIAMETER — 11M (36 FT.)
  - CONCENTRATOR RIM ANGLE — 45 DEGREES
  - OVERALL COLLECTOR WEIGHT — 13,000 POUNDS (EXCLUSIVE OF RECEIVER)
- LENS PANELS
  - REFRACTIVE MATERIAL — ACRYLIC (2.4 MM NOMINAL)
  - PANEL CONSTRUCTION — BONDED CONICAL SEGMENT PANELS
  - DUST PROTECTION — PRESSURIZED INTERIOR (BETWEEN LENS AND SHROUD)
- LENS/RECEIVER ASSEMBLY
  - LENS SUPPORT STRUCTURE — STRUCTURAL STEEL SPACE FRAME WITH MAIN RING BEAM, 12 RADIAL BEAMS, AND INTERMEDIATE SUPPORTS.
  - RECEIVER SUPPORT STRUCTURE — BIPOD AND SWAY BRACES, WITH PRESSURIZED SHROUD
- PEDESTAL (ALIDADE)
  - AXIS CONFIGURATION — EL OVER AZ, WHEEL TRACK
  - CONSTRUCTION — STRUCTRUAL STEEL SPACE FRAME
- FOUNDATION
  - TRACK — CIRCULAR REINFORCED CONCRETE RING
  - AZIMUTH AXIS — CONCRETE PIER FOR AZ BEARING MOUNT, CONCRETE BEAMS INTEGRATING PIER AND RING TOTAL CONCRETE 7CU. YDS.
- DRIVES AND TRACKING
  - AZIMUTH RANGE — ±180 DEGREES
  - AZIMUTH DRIVE — CABLE WINCH, POSITIVE ACTION
  - MAX. AZIMUTH VELOCITY TO STOW — 2,000 DEG./HOUR
  - AZIMUTH MOTOR — AC SYNCHRONOUS STEPPER, 1800 IN-OZ @ 72 RPM
  - ELEVATION RANGE — ±90 DEGREES
  - ELEVATION DRIVE — CABLE WINCH, POSITIVE ACTION
  - MAX. ELEVATION VELOCITY TO STOW — 2,000 DEG./HOUR
  - ELEVATION MOTOR — 1800 IN-OZ @ 72 RPM, AC SYNCHRONOUS STEPPER
- RECEIVER
  - WEIGHT (IPL DEFINED) — 705 POUNDS

TABLE 2

E-SYSTEMS Energy Technology Center

SYSTEM PERFORMANCE SUMMARY

• OPTICAL PERFORMANCE	CASE I	CASE II
GEOMETRIC CONCENTRATION RATIO	1500	500
LENS TRANSMITTANCE	90%	90%
RECEIVER INTERCEPT FACTOR	92%	99%
BLOCKING/SHADING FACTOR	94%	94%
OVERALL OPTICAL EFFICIENCY	78%	83%
• THERMAL PERFORMANCE (@ 800 WATTS/M² INSOLATION)		
RECEIVER CAVITY TEMP	815°C (1500°F)	371°C (700°F)
RECEIVER RADIATION THERMAL LOSS	5 KW (THERMAL)	2KW (THERMAL)
COLLECTOR NET OUTPUT	54 KW (THERMAL)	61 KW (THERMAL)
COLLECTOR OVERALL EFFICIENCY	71%	80%

E-SYSTEMS
Energy Technology Center

TABLE 3 - PROTOTYPE LENS PANEL

LOCATION WITHIN DOME LENS	- CONICAL SEGMENT BOUNDED BY LOCAL RIM ANGLES OF 27.9° AND 32.1°.
PANEL SIZE	- 4 FEET AVERAGE CIRCUMFERENTIAL ARC LENGTH BY 2 FEET STRAIGHT LENGTH.
CONFIGURATION	- 12 LINEAR PRISMATIC ELEMENTS, 4 INCH AVERAGE WIDTH BY 2 FEET LENGTH.
MATERIALS	- LINEAR PRISMATIC ELEMENTS MADE OF 3M ACRYLIC LENS-FILM, SOLVENT-BONDED TO SINGLE PIECE OF EXTRUDED ACRYLIC SHEET - TOTAL PANEL THICKNESS ≈ 0.1 INCH.

E-SYSTEMS
Energy Technology Center

TABLE 4 - PROTOTYPE LENS PANEL TESTING

1. LASER/PHOTOVOLTAIC CELL TRANSMITTANCE TESTING

- o BEAM EXPANDER USED WITH HELIUM-NEON LASER TO INTERCEPT MULTIPLE PRISMS.
- o SILICON CELL USED AS SENSOR, WITH CELL SHORT-CIRCUIT CURRENT LINEAR TO IRRADIANCE.
- o TRANSMITTANCE = $\frac{\text{CELL CURRENT WITH TRANSMITTED BEAM}}{\text{CELL CURRENT WITH DIRECT BEAM}}$
- o CELL-TO-LENS SPACING VARIED TO CHANGE ACCEPTANCE ANGLE.
- o KEY RESULTS - TRANSMITTANCE FOR 1500X ACCEPTANCE ANGLE ≈ 85-86%

2. OUTDOOR FOCAL PLANE FLUX SCANS

- o ROW OF SILICON CELLS TRAVERSES FOCAL PLANE.
- o RECORDER MONITORS CELL CURRENTS DURING TEST.
- o CELLS CALIBRATED VERSUS PYRHELIOMETER.
- o COMPUTER INTEGRATION OF TWO-DIMENSIONAL FLUX PROFILE PROVIDES OPTICAL EFFICIENCY VERSUS GEOMETRIC CONCENTRATION RATIO.
- o PROBLEMS ENCOUNTERED IN RESOLUTION, CALIBRATION, ALIGNMENT, ETC.
- o GOOD DATA NOT YET AVAILABLE.

Blank Page

NON-IMAGING SECONDARY CONCENTRATORS

Roland Winston/Joseph O'Gallagher
University of Chicago
Chicago, IL.

Abstract

Secondary concentrators deployed at the focal plane of a parabolic dish can significantly increase the system concentration ratio or alternatively decrease the tolerance requirement. Several trumpet shaped radiation flow line concentrators were tested with the JPL Test Bed Concentrator at the Parabolic Dish Test Site in the Mojave Desert. Primary flux inside an 8 inch diameter circle was redirected into 5 1/2 inches with an efficiency exceeding 96%. A power gain of 30% was observed.

NONIMAGING SECONDARY CONCENTRATORS

R. WINSTON AND J. O'GALLAGHER

PROGRAM SUPPORTED BY: THE U.S. DOE THROUGH THE ACADEMIC AND UNIVERSITY PROGRAMS BRANCH OF THE SOLAR ENERGY RESEARCH INSTITUTE

AND IN PART BY: THE SOLAR THERMAL TECHNOLOGY GROUP AT JPL

NONIMAGING SECONDARY CONCENTRATORS

- PURPOSE
  - o IN A POINT FOCUS GEOMETRY A GIVEN TOTAL ANGULAR TOLERANCE BUDGET $\pm \theta_I$ (INCLUDING SUNSIZE, SLOPE AND TRACKING ERRORS, ETC.) THE MAXIMUM ALLOWABLE GEOMETRIC CONCENTRATION IS

$$C_{MAX} = \frac{1}{\sin^2 \theta_I}$$

  - o ALL IMAGING SINGLE STAGE CONCENTRATORS (E.G. PARABOLOIDAL DISHES) WILL FALL SHORT OF THIS LIMIT BY A FACTOR OF > 4
  - o A PROPERLY DESIGNED SECOND STAGE ELEMENT PLACED NEAR THE FOCAL PLANE CAN RECOVER MUCH OF THIS SHORT-FALL
  - o CAN EITHER A) INCREASE C BY FACTOR OF $\sim 2\text{-}4$ FOR GIVEN θ_I
    OR B) FOR A GIVEN C INCREASE θ_I BY FACTOR $\sim 1.4\text{-}2$

- SECOND STAGE DESIGNS
  - o COMPOUND ELLIPTICAL CONCENTRATOR OR CEC (VARIANT OF CPC)
  - o FLOW LINE CONCENTRATOR OR TRUMPET (A HYPERBOLA OF REVOLUTION)

$$C_2 = \frac{A}{A'}$$

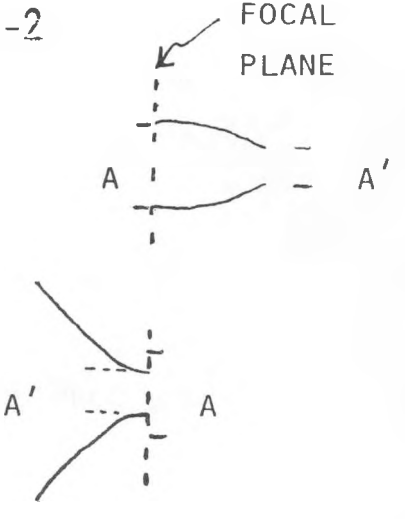

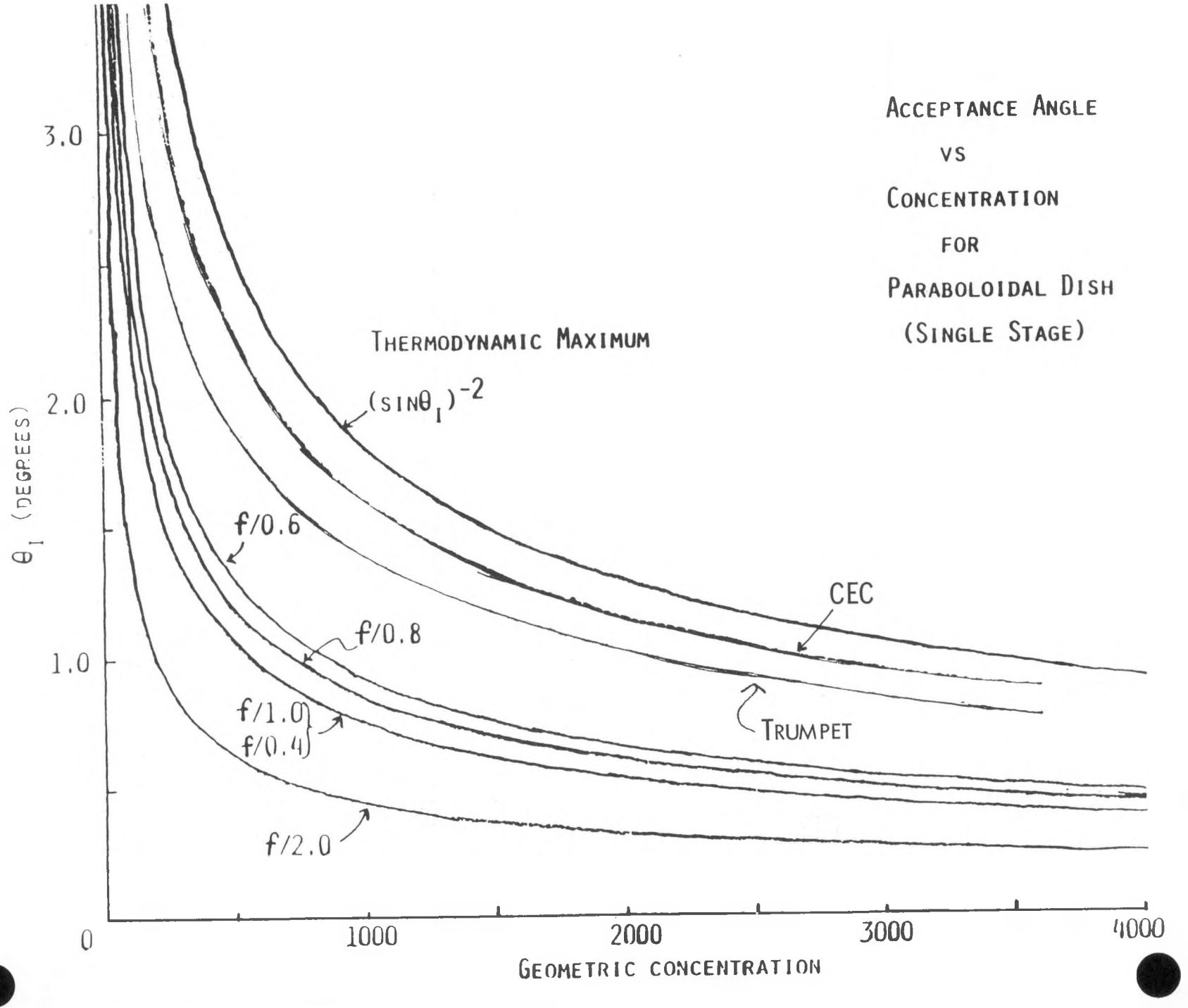
ACCEPTANCE ANGLE
VS
CONCENTRATION
FOR
PARABOLOIDAL DISH
(SINGLE STAGE)
THERMODYNAMIC MAXIMUM
$(\sin\theta_I)^{-2}$
CEC
TRUMPET
f/0.6
f/0.8
f/1.0
f/0.4
f/2.0
θ_I (DEGREES)
3.0
2.0
1.0
0
1000
2000
3000
4000
GEOMETRIC CONCENTRATION

SELECTION OF SECOND STAGE DESIGN

CEC	vs.	TRUMPET
o HIGHER POSSIBLE C_2		o C_2 LIMITED TO ~ 2
o OPERATES ON MOST OF BEAM		o OPERATES ONLY ON EDGES OF BEAM
o RELATIVELY LARGE REFLECTION LOSS		o LOW REFLECTION LOSS
o RELATIVELY LARGE THERMAL ABSORPTION		o LOW THERMAL ABSORPTION
o EXTENDS BEHIND FOCAL PLANE		o EXTENDS IN FRONT OF FOCAL PLANE

TRUMPET OPTIMIZATION

- FOR A GIVEN PRIMARY THERE EXISTS A WHOLE FAMILY OF TRUMPETS OF DIFFERENT C_2, TRUNCATION HEIGHT, h AND INTERCEPT FACTOR γ
- MUST CHOOSE VALUES OF C_2 AND h WHICH MAXIMIZE $C = C_1 \cdot C_2$ AND γ WHILE MINIMIZING SHADING
- TYPICALLY SOLUTION YIELDS $C_2 \sim 2$ AND SHADING LOSS < 0.02 OF PRIMARY APERTURE

FULL SCALE EXPERIMENT

TRUMPET/TESTBED CONCENTRATOR

NOV. 1-5, 1982

JPL/EDWARDS TEST SITE

KEY CONTRIBUTORS

- o Others at Chicago
  - Eli Kritchman
  - Peretz Greenman
- o At JPL
  - Chuck Stein
  - Len Jaffe
  - Ed Dennison
  - Bill Owen
- o At Edwards
  - John Woodbury

EXPERIMENT PARAMETERS

PRIMARY

o DESIGN

- OMNIUM-G PARABOLOIDAL DISH
- 6 METER DIAMETER
- F/0.67
- RIM ANGLE 41.1^0
- FOCAL SPOT DIAMETER ~8 INCHES
- C_1 = 870X

o ACTUAL

- JPL TBC WITH MIRROR FACETS PARTIALLY UNCOVERED TO SIMULATE OMNIUM-G
- ~10 METER EXPOSED DIAMETER
- EFFECTIVE FOCAL RATIO ~ F/0.66
- EXPOSED RIM ANGLE ~40^0
- APPROXIMATE FOCAL SPOT DIAMETER ~ 8 INCHES
- C_{1GEOM}(72 MIRRORS) = 965X
- C_{1GEOM}(176 MIRRORS) = 2360X

SECONDARY

o TRUMPET

- VIRTUAL SOURCE DIAMETER 8.0 INCHES
- TRUNCATED HEIGHT= 30 INCHES
- ENTRANCE APERTURE= 31 INCHES
- EXIT APERTURE= 5.5 INCHES
- C_2 = 2.1X

$C_1 \cdot C_2$(72 MIRRORS) = 2025X
$C_1 \cdot C_2$(176 MIRRORS) = 4960X

SCHEMATIC DIAGRAM OF TBC/TRUMPET EXPERIMENT CONFIGURATION.

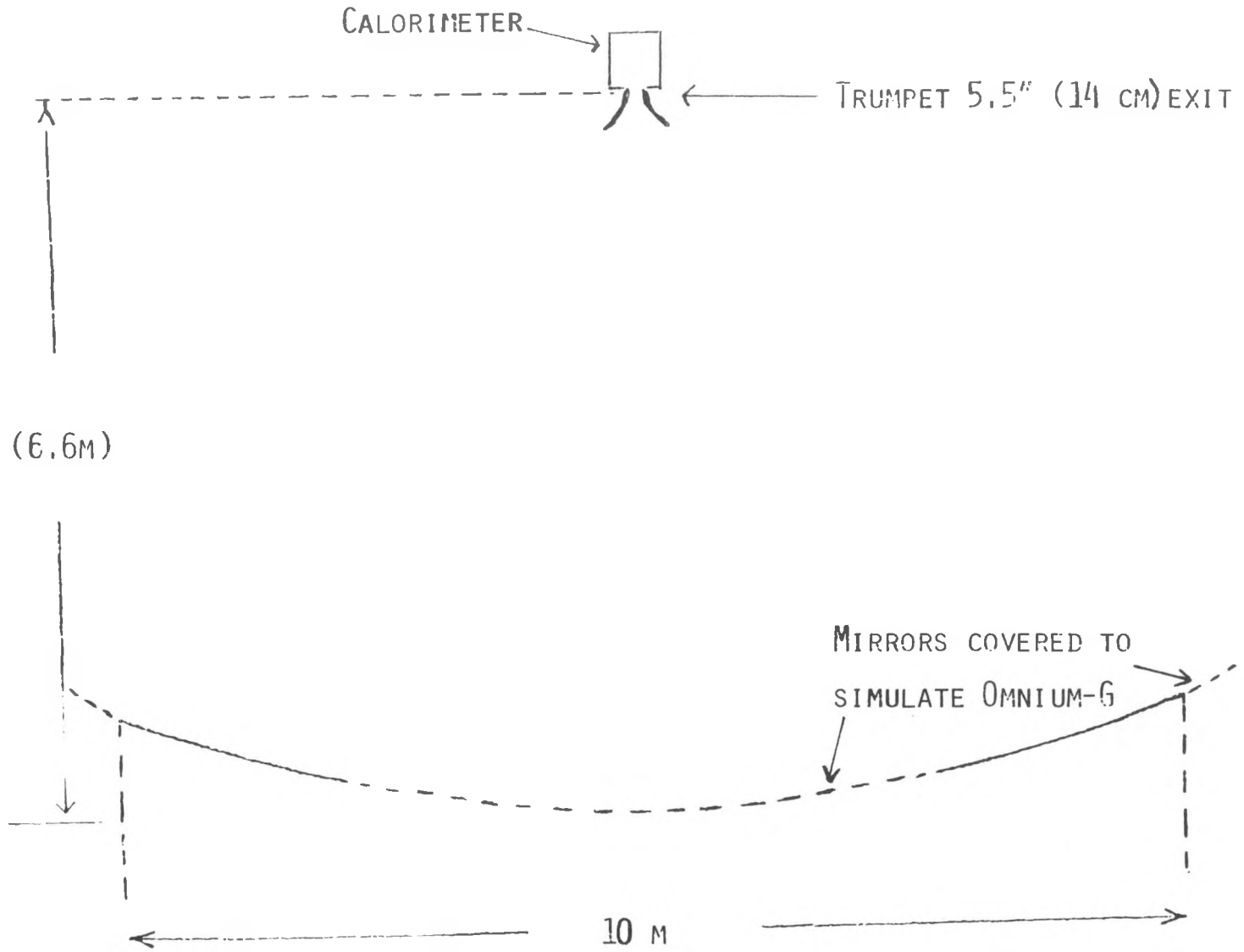

EXPERIMENT PLAN

- OBJECTIVES
  - o TO DETERMINE THE OPTICAL RESPONSE FUNCTIONS OF THE SECOND STAGE ELEMENT AND COMBINED SYSTEM AND COMPARE WITH MODEL PREDICTIONS
  - o TO INVESTIGATE THE THERMAL LOADS PRODUCED BY THE CONCENTRATED RADIATION ABSORBED BY THE 2ND STAGE
  - o TO IDENTIFY ANY PRACTICAL PROBLEMS ASSOCIATED WITH THE FURTHER IMPLEMENTATION OF THE CONCEPT
- TRUMPET TEST MODELS
  - o PASSIVELY COOLED AL SURFACE ON AL SHELL
  - o WATER COOLED AL SURFACE ON AL SHELL
  - o WATER COOLED SILVER PLATE SURFACE ON CU SHELL
- TEST PLAN
  - o MEASURE TOTAL SYSTEM ENERGY THROUGHPUT WITH AND WITHOUT TRUMPET
  - o MAP FLUX DISTRIBUTION IN FOCAL PLANE WITH AND WITHOUT TRUMPET
  - o MEASURE SYSTEM ANGULAR RESPONSE FUNCTION WITH AND WITHOUT TRUMPET
  - o MEASURE TEMPERATURE DISTRIBUTION ON TRUMPET MODELS WHEN ALIGNED AND MISALIGNED

EXPERIMENTAL RESULTS

TRUMPET/TBC PERFORMANCE MEASUREMENTS

RAW DATA

	NO TRUMPET	WITH TRUMPET (5.5" EXIT)
5.5" RECEIVER	17.9± 0.2 KW	23.2± 0.3 KW (ALUMINUM)
8.0" RECEIVER	24.9± 0.2 KW	23.8± 0.1 KW (SILVER)

PERFORMANCE SUMMARY

	TRUMPET EFFICIENCY	GAIN IN INTERCEPT
ALUMINUM	93± 1.5%	+29± 2 %
SILVER	96± 1 %	+33± 2 %
PREDICTED (AL FOR OMNIUM-G)	91 %	+34 %

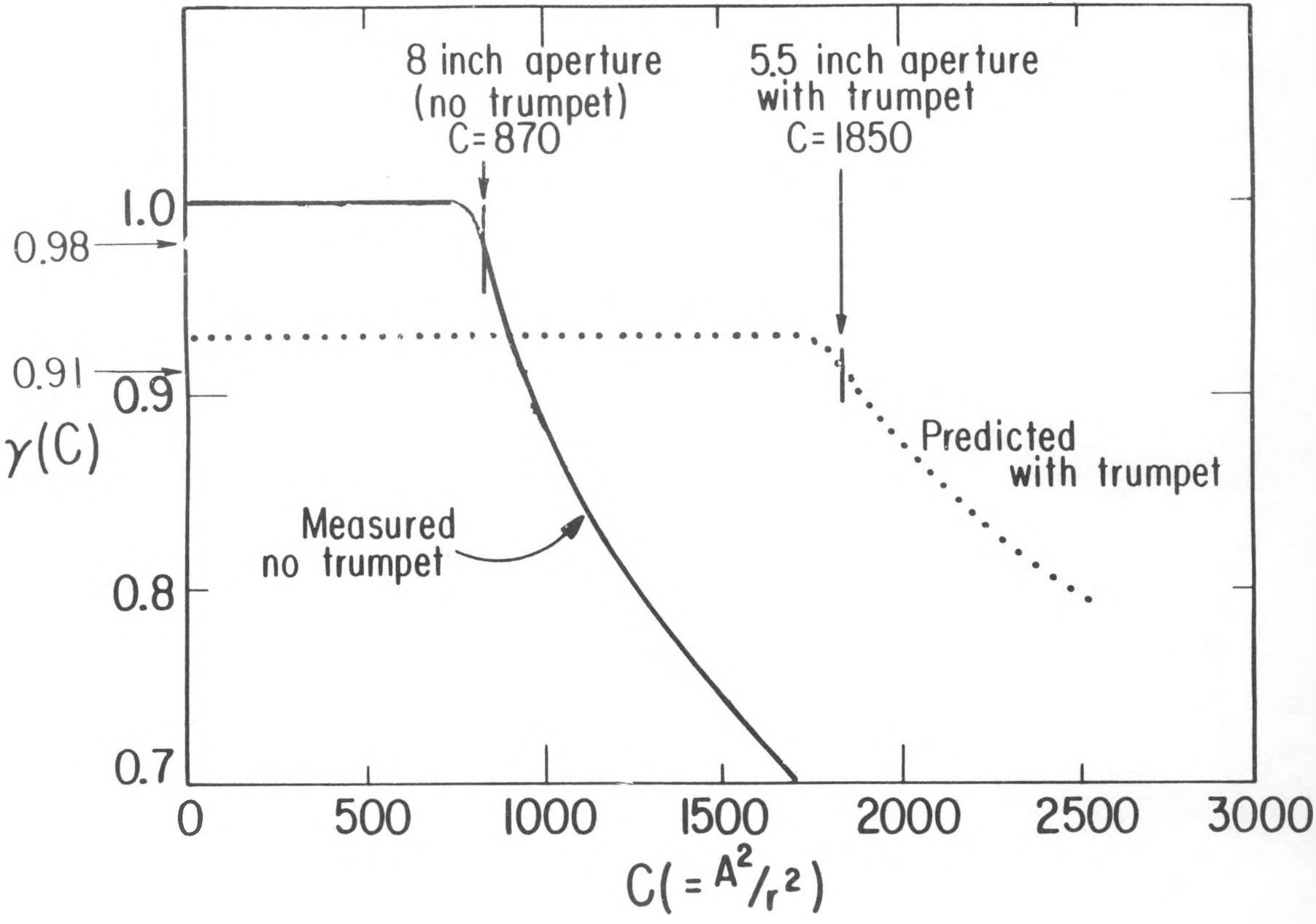
8 inch aperture
(no trumpet)
C=870
5.5 inch aperture
with trumpet
C=1850
1.0
0.98
0.91
0.9
0.8
0.7
γ(C)
Measured
no trumpet
Predicted
with trumpet
0
500
1000
1500
2000
2500
3000
C(=A²/r²)

THERMAL LOADS

- Approximately 4% - 8% of total power absorbed by trumpet
- Silver Trumpet with cooling coils brazed to outside worked perfectly
  - Measured temperatures at throat did not exceed 30°C (8° above ambient)
- Al Trumpet with no cooling
  - Measured temperatures near throat > 350°C
  - Local Melting at "hot spots"
- Al Trumpet with wrap-around cooling
  - Operated satisfactorily when centered on sun
  - Throat temperatures ~100 - 150° C
  - Local melting when deliberately misaligned.

SUMMARY

- o NONIMAGING SECOND STAGE CONCENTRATORS HAVE POTENTIAL TO RELAX TOLERANCES AND/OR INCREASE ACHIEVABLE CONCENTRATION OF EXISTING SYSTEMS
- o TRUMPET DESIGNS HAVE FAVORABLE REFLECTION LOSS
- o EXPERIMENT ACHIEVED:
  - FACTOR OF 2 GAIN IN NET FLUX CONCENTRATION
  - 30% GAIN IN INTERCEPT
  - AGREES WITH MODEL PREDICTIONS
- o MANY POSSIBLE APPLICATIONS
  - ULTRA HIGH CONCENTRATION SYSTEMS
  - LOW COST PRIMARIES
  - PARTICULARLY USEFUL FOR SPHEROIDAL OR LONG FOCAL LENGTH SYSTEMS
- o WITH CAREFUL DESIGN THE OPTIMIZED TWO STAGE SYSTEM SHOULD ALWAYS ACHIEVE SUBSTANTIAL PERFORMANCE IMPROVEMENT AT RELATIVELY SMALL COST INCREMENTS

Blank Page

SOLAR THERMAL TECHNOLOGY: POTENTIAL IMPACTS ON ENVIRONMENTAL QUALITY AND PETROLEUM IMPORTS*

W. R. Gates**
Jet Propulsion Laboratory, California Institute of Technology

This paper describes work conducted at the Jet Propulsion Laboratory (JPL) during 1982 in support of the Department of Energy's (DOE) Solar Thermal Technology Program. The work was sponsored by Sandia National Laboratory, Livermore (SNLL), who serves as the technical program integrator for the Solar Thermal Technology Program. Under an agreement with SNLL, JPL had responsibility for assessing the benefits and impacts associated with the successful development of cost-competitive solar thermal electric systems.

This paper begins with a brief overview of the benefit assessment methodology. Following this overview, results are presented for three of the potential impacts associated with an expanding, cost-competitive solar thermal electric industry: energy cost savings, environmental impacts, and petroleum import impacts. The paper concludes by discussing the implications these results have regarding federal participation in the development of Solar Thermal Technologies (STT). Particular emphasis is given to the role of the Federal Business Energy Tax Credit and Federal funding for Research and Development.***

STT Benefits Assessment Overview

The Solar Thermal Technology Program includes a variety of technologies serving a range of applications. Solar thermal technologies can generally be divided into two categories: concentrating systems and non-concentrating systems. Concentrating systems reflect solar radiation to a simple axis or

---

*The methodology and results presented here are the collaborative effort of a number of individuals. In addition to the author, E. S. Davis, Robert Gershman, Michael Guth, Dr. Hamid Habib-agahi, and Dr. Katsuaki Terasawa, from the Jet Propulsion Laboratory (JPL), and Michael Davisson, under contract to JPL, all made substantial contributions. Any remaining errors or omissions, of course, are the responsibility of the author.

The research described in this paper was carried out by the Jet Propulsion Laboratory, California Institute of Technology, for the U.S. Department of Energy through an agreement with the National Aeronautics and Space Administration.

**Economist, Solar Thermal Power Systems Project.

***For a more complete description of the methodology and results presented here, see W. R. Gates, et al., "Solar Thermal Technologies Benefits Assessment: Objectives, Methodologies, and Results for 1982," Jet Propulsion Laboratory, California Institute of Technology: Pasadena, CA. Forthcoming.

point. Central receivers, parabolic dishes, and troughs are examples of concentrating systems. Non-concentrating systems, such as solar ponds, utilize solar radiation in its diffuse state. Concentrating and non-concentrating systems can both be operated either during hours when solar radiation is available (without storage) or on demand throughout the day and night (storage-coupled). Thus, solar thermal power systems can assume a variety of technological configurations.

Similarly, solar thermal technologies provide a source of energy capable of generating either thermal or electric power. Therefore, STT can be employed in a variety of applications, including: electric utilities, industries requiring thermal power, and as total energy systems capable of providing both electric and thermal power. In the future, STT may be used to provide transportable fuels and chemical feedstocks. This flexibility enables STT to satisfy many categories of energy demand.

Finally, each solar thermal technology/application combination provides a variety of potential benefits and impacts. A partial listing of the potential impacts would include: energy cost savings, environmental impacts, national security implications, impacts on oil imports, employment effects, tax revenue impacts, creation of an STT export market, increased competition in the energy sector, and improvements in the U.S. technology base. Due to variations in fuel prices, insolation levels, and energy demands, these benefits will be region and time specific.

To accurately assess the benefits of the Federal STT program, all potential benefits, both quantitative and qualitative, must be evaluated for each solar thermal technology, in every potential application. However, this analysis has been restricted to concentrating solar thermal technologies (central receivers and parabolic dishes), without storage, in electric utility applications. Only three impacts have been considered: energy cost savings, environmental impacts, and impacts on oil imports. The analysis has been further restricted to the Southwest and Southcentral regions of the United States, and to the 1990s time frame.

Benefits Assessment: Methodology

The value of the benefits realized from STT in electric utility applications depends critically on the installed capacity of STT. The capacity of economically justified STT installations is determined by two factors: the cost of producing STT (STT supply side) and the value of STT to electric utilities (STT demand side).

On the supply side, STT production costs will be influenced by the success of the R&D effort, the production volume, the STT storage capacity, and such regional considerations as labor and materials costs. Because estimating STT production costs is beyond the scope of this report, benefits were assessed assuming three alternative STT system costs. The range of costs reflects variations in STT production volume and R&D success, and was selected to include the STT cost goal established by the Solar Thermal Cost Goal Committee for solar thermal installations in 1990 with no storage capacity. Regional variations in STT costs were not considered.

On the demand side, the value of STT to electric utilities was determined through utility simulation. A generic STT system was used to represent both central receivers and parabolic dishes. The value of STT depends on a variety of considerations: some, including insolation levels and fuel prices, will vary across geographic regions; others, such as the demand for electricity, electric utility generating capacity and financial parameters, and the STT storage capacity will vary across both utilities and solar thermal systems. To simplify the required analysis, two hypothetical electric utilities were examined: one represents the Southwestern states, while the other represents the Southcentral and Southeastern states. The financial parameters selected for this analysis characterize an investor-owned utility. Three insolation levels were selected to reflect regional variations in solar radiation. The fuel price assumptions for the Southwestern states differed from those used for the Southcentral and Southeastern states, reflecting regional variations in fuel prices. High, medium, and low fuel price scenarios were used for each region to reflect uncertainty over future fuel prices. Only one time horizon was considered, 1990 STT installations. The STT system examined in this report has no storage capacity.

Using these simplifying assumptions, the value of STT (demand) and STT costs (supply) were estimated for increasing levels of STT installations. Comparisons of STT costs and values indicate the economically justified market potential of STT in 1990. The utility simulation also indicates the type and quantity of fuel displaced as STT penetration increases. This information was used to assess the potential value of the benefits accruing from the installation of cost-competitive STT systems, under alternative assumptions regarding future fuel prices and STT system costs.

1990 Market Potential for Cost-Competitive Solar Thermal Electric Systems

Once a range of values has been estimated for both STT supply and demand, the estimates can be combined to determine the economic market potential for STT in the year being analyzed, and the corresponding energy cost savings (see Figure 1). The demand curves represent the price that potential consumers would be willing to pay for each quantity of STT capacity. The supply curve indicates the quantity of STT capacity manufacturers would provide for alternative STT price levels. Thus, the intersection of the supply curve and the demand curve will determine the total capacity for which STT provides a cost-effective alternative in 1990. The area bounded by the demand curve, the supply curve, and the left-hand vertical axis provides a measure of the after-tax energy cost savings.

Figure 1 illustrates that the size of the market strongly depends on achieving the STT cost targets and is sensitive to future fuel prices. The prices that utilities would willingly pay for STT are higher at lower levels of STT usage corresponding to applications using the highest priced fuels in areas with the best insolation. Values decrease as the level of STT usage increases since STT must displace lower priced fuels in regions with less desirable insolation levels. The rate of decrease is rapid at first, becoming more gradual as penetration increases. In the medium oil price scenario, for example, utilities would pay $2000/kWe (1981 dollars) for the first 500 MWe of STT capacity. To achieve a market penetration of 2000 MWe, STT system costs would have to fall to $1100/kWe (1981 dollars).

The economic market potential for STT at a particular time is likely to exceed the actual level of STT purchases and installations. Consumers may be constrained by capital market imperfections or imperfect information, while suppliers in growing industries frequently face bottlenecks in establishing the required industry infrastructure, especially in industries experiencing a relatively rapid rate of technological change. For these and other reasons, actual purchases of STT may be less than the total projected demand for that period. Cumulative installations during the 1990s, however, will approach the total capacity for which STT is cost-competitive. This suggests a dynamic approach to projecting futue STT deployment decisions. Since a dynamic formulation is beyond the scope of this analysis, static estimates of total potential demand have been used.

Total Energy Cost Savings of Solar Thermal Electric Systems

Table 1 summarizes the net energy cost savings for three oil price scenarios and three levels of STT costs. If STT systems cost $2200/kWe, installations will be cost-effective only in the high energy price scenario. However, at a cost of $1,300/kWe, STT would be preferred in the utility sector under all three oil price scenarios. The net energy cost savings in the $2200/kWe case range from zero to $1 billion; at $1300/kWe, benefits vary from zero to $10 billion.*

The patterns of the values in Figure 1 and Table 1 are more important to note than the actual values themselves. In particular, under some plausible scenarios for future fuel prices and STT system costs, the 1990 economic market potential and corresponding energy cost savings are zero. Under other plausible scenarios, the values become significant. This pattern has important implications for federal participation which will be discussed later in this paper.

Results of Utility Simulation

Figure 1 indicated that the 1990s STT economic market potential is limited except under optimistic assumptions regarding future fuel prices and STT system costs. However, the incremental value of STT, as estimated in this analysis, reflects the value to the average utility in each region, assuming an aggressive transition from oil and natural gas capacity to coal-fired power plants. Taken together, the high percentage of coal-fired capacity in the

---

*The values reported in Table 1 and Figure 1 are 1990 values (in 1981 dollars). In order to derive the present value of the net energy cost savings, the values must be discounted to the current period. Using the real federal discount rate of 7 percent per year, the minimum value suggested by the Office of Management and Budget, the values reported here would be reduced by approximately 60 percent when discounted to 1982. When comparing the net energy cost savings with the future required federal investment in R&D, both cash flows must be expressed in dollars for equivalent years.

FIGURE 1

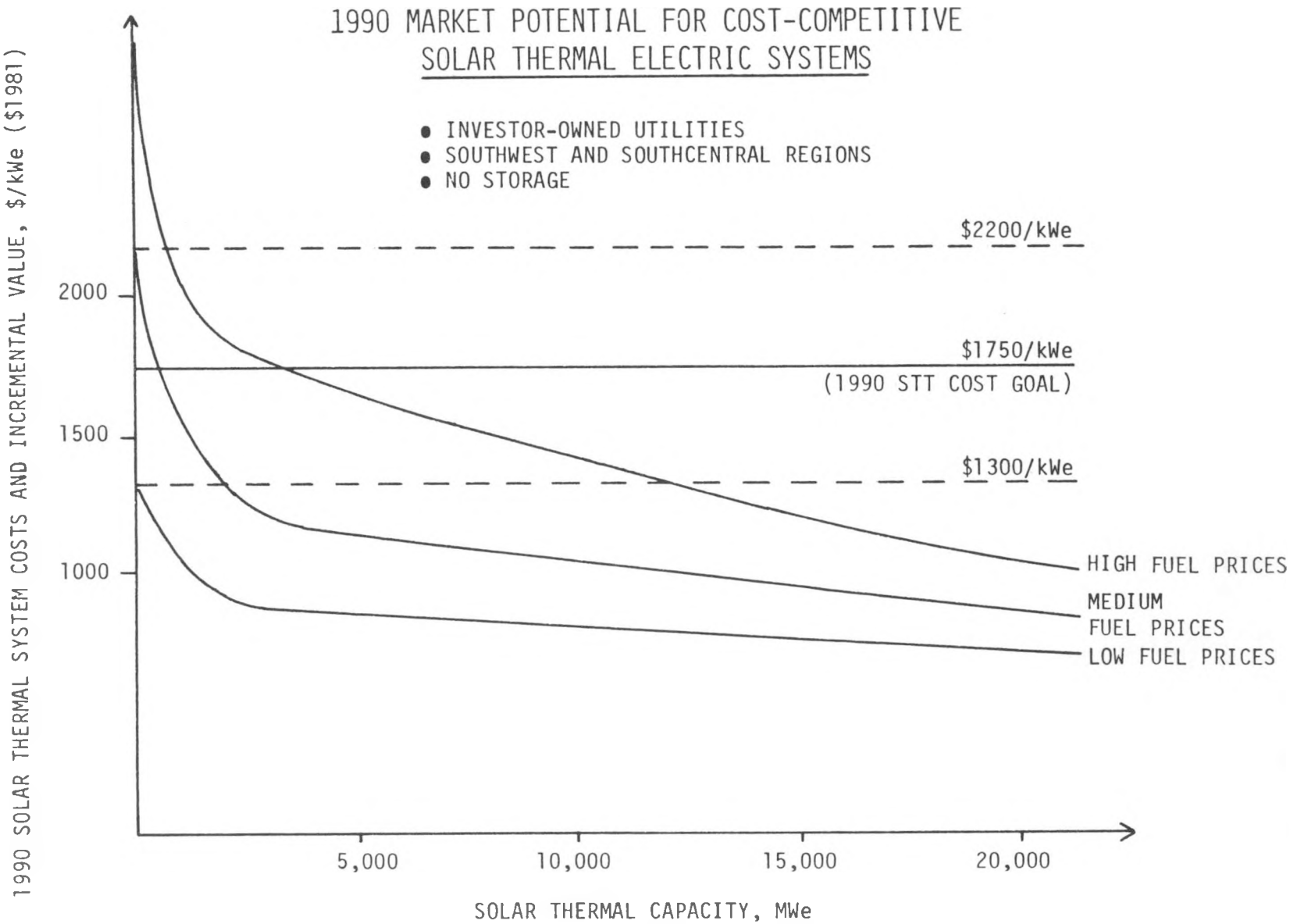
1990 MARKET POTENTIAL FOR COST-COMPETITIVE
SOLAR THERMAL ELECTRIC SYSTEMS
• INVESTOR-OWNED UTILITIES
• SOUTHWEST AND SOUTHCENTRAL REGIONS
• NO STORAGE
$2200/kWe
$1750/kWe
(1990 STT COST GOAL)
$1300/kWe
HIGH FUEL PRICES
MEDIUM
FUEL PRICES
LOW FUEL PRICES
2000
1500
1000
5,000
10,000
15,000
20,000
1990 SOLAR THERMAL SYSTEM COSTS AND INCREMENTAL VALUE, $/kWe ($1981)
SOLAR THERMAL CAPACITY, MWe

TABLE 1

TOTAL NET ENERGY COST SAVINGS OF SOLAR THERMAL ELECTRIC SYSTEMS

(1990 VALUES IN BILLIONS OF 1981 DOLLARS)

STT SYSTEM COSTS**	NEP-III ENERGY PRICE SCENARIO*		
	LOW	MEDIUM	HIGH***
$2,200/kWe	0	0	1
$1,750/kWe	0	****	3
$1,300/kWe	****	2	10

*LOW, MEDIUM, HIGH REFER TO THE NEP-III ENERGY SCENARIOS BASED UPON THE 1990 IMPORTED OIL PRICE OF 44, 52, 68 (1981 $/BARREL).

**LOW, MEDIUM, AND HIGH SYSTEM COSTS REFLECT VARYING PRODUCTION VOLUMES AND LEVELS OF R&D SUCCESS.

***ASSUMES THAT CONVENTIONAL GENERATING CAPACITY REPRESENTS THE BEST ALTERNATIVE TECHNOLOGY. THIS ASSUMPTION MAY PROVE UNREALISTIC, ESPECIALLY IN THE HIGH OIL PRICE SCENARIO.

****POSITIVE VALUES WHICH BECOME ZERO AFTER ROUNDING TO NEAREST BILLION.

utility's generation mix and the poor correspondence between peak insolation and peak electricity demand for the utilities used in the simulation, create a situation which is relatively unfavorable for solar thermal electric systems without storage. STT competes primarily with coal-fired generating capacity (coal represents more than 60 percent of the fuel displaced for the first one percent of STT penetration). Despite the high coal displacement, STT without storage can compete, on a limited basis, in utilities which exhibit these average characteristics.

In actuality, initial STT installations during the late 1980s and early 1990s will occur in utilities where the value of STT is relatively high. This will include those utilities which continue to use a significant quantity of oil and natural gas, utilities which have a close correspondence between peak electricity demand and peak insolation, as well as remote sites and non-grid connected applications (island utilities, stripper oil wells, agricultural irrigations, etc.). Stimulated by both the Federal Business Energy Tax Credit and Federal accelerated depreciation, and augmented in some states by additional energy tax credits and accelerated depreciation, third party investors offer an alternative means through which STT can penetrate the electric utility and remote site markets.

These early, high-valued applications are expected to provide markets for the early, high-cost STT systems, facilitating the transition from a high-cost small-scale STT industry to an industry using mass production techniques. Considering these favorable markets, the values indicated in Figure 1 and Table 1 should be considered as lower bounds on the actual 1990s STT economic market potential and energy cost savings.

Environmental Impacts: California's South Coast Air Basin

Environmentally, STT provides important benefits by reducing the use of fossil and nuclear fuels in electrical power generation. Reducing the use of nuclear fuels will help alleviate the problems associated with nuclear waste disposal; reducing the use of fossil-fired fuels will alleviate air pollution emissions (including SO_x, NO_x and CO_2 build-up).

From the utility simulation used to derive the demand cuves depicted in Figure 1, information is available regarding the quantity of each fuel type displaced by STT for each point on the demand curve. Considering the proposed 1990 air pollution standards, this data can be used to determine the reductions in air pollution attributable to STT for each fuel price and STT system cost combination.

California's South Coast Air Basin has significant air pollution problems. A substantial amount of the emissions creating air pollution in the South Coast Air Basin originate from oil-fired power plants. Approximately 30 percent of the sulfur oxides and 10 percent of the nitrogen oxides, two important components of air pollution in Southern California, can be attributed to emissions from oil-fired power plants. The major electric utility in the area, Southern California Edison, has a high percentage of relatively new oil-fired plants. The high dependence on oil as a fuel source for electricity generation in Southern California, and the related air pollution problems are not expected to change dramatically before 1990.

STT penetration in Southern California can have significant environmental impacts. STT installations would reduce the capital expenditures associated with improved emissions control technology, an impact estimated to add an additional 50 to 150 dollars per kilowatt of installed capacity to the 1990 value of STT.* STT would also eliminate power plant emissions that were not controlled by the proposed 1990 power plant emissions standards. This would create health benefits, reduce crop damage, and provide salable pollution offsets. The regional environmental impacts can be significant for Southern California and other specific air basins in high insolation regions where electric power plant emissions create air pollution problems.

Environmental Impacts: Conclusions

Compared to the quantity of fossil fuels consumed nationally in the electric utility, transportation, industrial, commercial, and residential sectors, the potential STT fuel displacement is relatively insignificant. Correspondingly, the impact of STT on the national air pollution problem will also be limited.

Regionally, however, the environmental impact of STT can be significant. Electric power plants account for a substantial percent of the pollutants in many regional air basins. STT penetration in these air basins would reduce the capital expenditures associated with emission control technology. This could add up to $150/kWe to the value of STT estimated earlier in Figure 1. At $1750/kWe, this represents almost 10 percent of the initial system cost. STT would also eliminate power plants emissions that were not controlled by emissions standards. These additional reductions in air pollution provide health benefits and reduce crop damage. Finally, STT installations would provide salable pollution offsets. Industrial growth is frequently constrained in air basins where pollution exceeds federal standards. The creation of salable offsets through STT installations would provide the opportunity for further industrial growth. The regional environmental impacts of STT are potentially significant.

STT Impact on Oil Imports

Fuel displacement data can also be used to discuss the potential impact of STT on U.S. petroleum imports. Because imported oil is the highest cost source of oil in the United States, reductions in oil consumption are typically expected to translate directly into import reductions. Furthermore, due to substitution opportunities between petroleum and natural gas, a portion of any natural gas displaced is frequently expected to further reduce oil imports. Oil import reductions will have both national security and balance of payments implications.

---

*Based on the avoided capital expenditures for improved pollution control technology as required to meet the shorter proposed emission controls standards for 1990.

Refining a barrel of crude oil produces a range of products including gasoline, distillate oil (diesel fuel), and residual oil. As the relative prices of refined products change, there is flexibility in the mix of products produced during the refining process. This flexibility, however, is limited in the short-run, until refineries can respond by changing the technology embodied in their refining capacity.

Utilities primarily consume two types of oil: residual oil is used to satisfy intermediate load electricity demands, while distillate oil is used to satisfy peak-load demands. In the short-run, little substitution occurs between residual and distillate oil in electricity generation. In the Southwest, there is currently a glut of residual oil available from refining domestic crude oil. Crude oil is imported into the Southwest in order to satisfy the transportation demand for oil (diesel fuel and gasoline). A similar situation exists in the Southcentral U.S. Residual oil consumption exceeds the supply from domestic crude on the East Coast. To use the excess supply of Southcentral and West Coast residual oil to satisfy the excess demand for residual on the East Coast would require the oil be both transported and further refined to lower the sulfur content. These costs make this reallocation economically prohibitive in most cases. Residual oil shipments from the Gulf Coast to the East Coast are limited. Excess residual oil in the West is exported to Japan and the Far East.

Since early STT installations are expected to occur in the Southwest and Southcentral states, the residual oil displaced by STT will not reduce oil imports in the short run. Distillate oil consumption exceeds the supply from domestic crude throughout the United States, however, so any distillate oil displacement will have an impact on oil imports.

As Figure 2a indicates, STT without storage displaces primarily residual oil. Distillate oil consumption actually increases. Correspondingly, the direct impact of STT on oil imports in the short run is expected to be small. With storage, the STT fuel displacement potential increases, reducing the consumption of both residual and distillate oil (see Figure 2b). Reduced distillate consumption can lead directly to reduced demand for imported oil. However, this impact would be small relative to the total demand for imported oil in the United States projected to equal three million barrels per day in 1990).

In conclusion, STT can reduce oil consumption in the electric utility sector. The oil displacement potential increases with the addition of storage capacity. However, the direct impact of STT on oil imports in the short-run is expected to be small. The tendency for STT without storage to displace residual oil, the current glut of residual oil in the West and Southcentral United States, the prohibitive costs of reallocating excess residual to the East Coast, and the limited short-run substitution between types of oil in both refining and electricity generation, all serve to minimize the short-run impact of STT on oil imports.

In the long-run, competitive industries characteristically demonstrate substantial flexibility. Refinery and utility generating capacity can be expected to change in response to the glut of residual oil. Substitution will occur both between types of oil and between oil and other fuels. Alternative uses will be found for residual oil, some of which may reduce the demand for

FIGURE 2

AVERAGE ANNUAL STT OIL DISPLACEMENT BY TYPE

(MEDIUM FUEL PRICE SCENARIO)

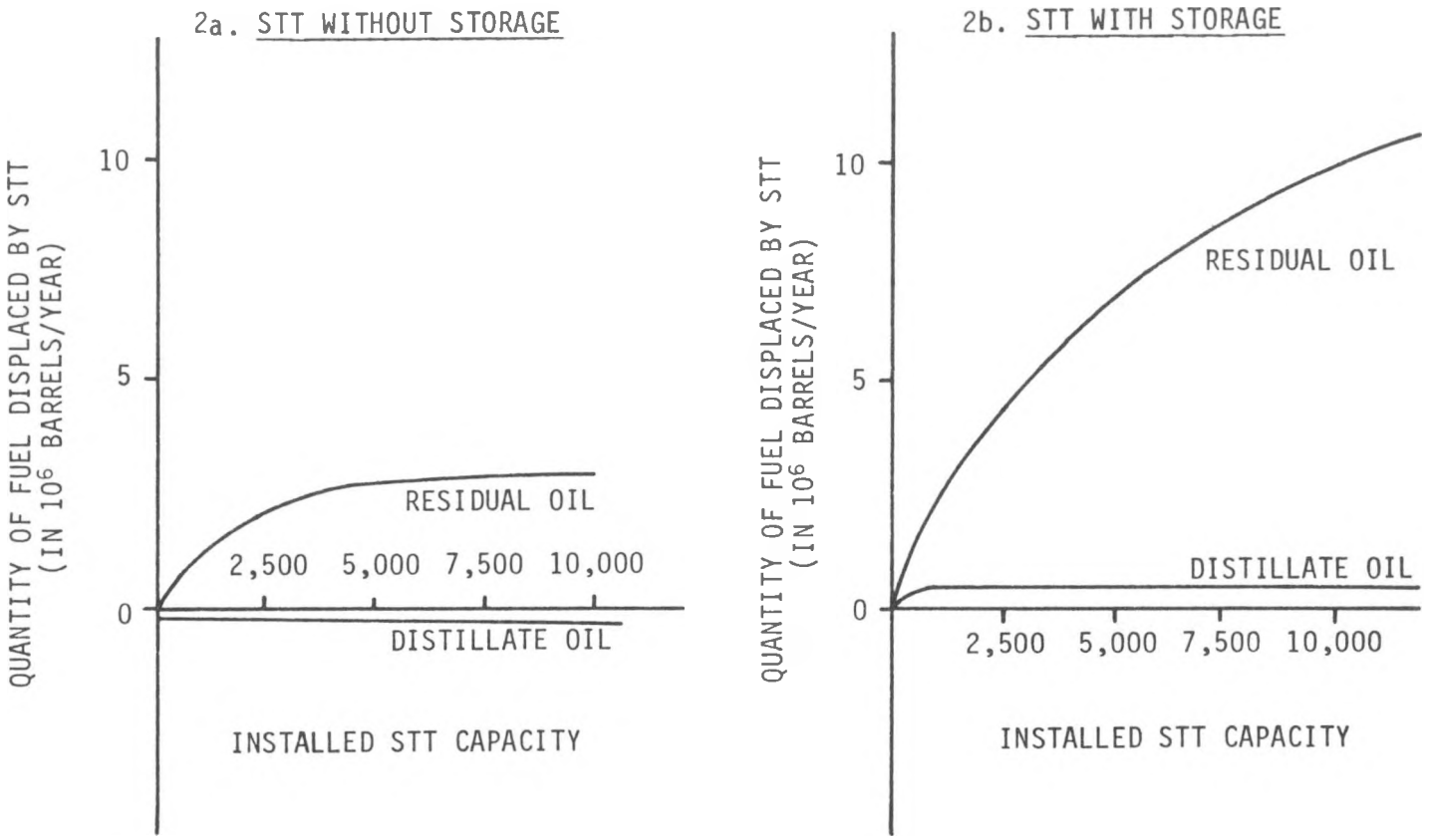

other types of oil. Since imported crude is the highest cost source of oil in the U.S., these changes should reduce oil imports. As a result, the direct and indirect long-run impacts of STT on imported crude oil can be significant. In this case, STT would reduce oil imports, increase national security, and improve the U.S. balance of payments.

Conclusions

This analysis has estimated the 1990 economic market potential and corresponding energy cost savings associated with cost-competitive installations of STT in electric utility applications under a range of future fuel price scenarios and STT system cost. This analysis concludes that the potential benefits from solar thermal technology R&D can be expected to vary widely depending both on the STT system cost and the relevant fuel price scenario (recall Figure 1 and Table 1). As with most technology development projects, the outcome of the R&D effort is quite uncertain, as reflected by the range of plausible STT system costs. In the STT R&D program, however, this uncertainty is compounded by the extreme variability in expectations regarding future fuel prices. World oil prices are largely determined through the price-setting policies of the OPEC cartel, which can lower oil prices and undercut the price of developing technologies. After the 1978-79 Iranian oil embargo, fuel prices were generally expected to fall within the medium or high fuel price scenario. Since the oil glut early in 1982, the low oil price scenario appears most probable. Because of the past fluctuations in oil prices and the perceived threat of OPEC price cuts, there is a greater-than-average uncertainty regarding the benefits from STT R&D. To private industry, STT R&D represents a risky investment; private STT R&D initiatives are unlikely in the absence of federal participation.

The Federal Government, however, has a variety of concerns, including minimizing the impact of energy market imperfections, protecting the economy from the disruptive influence of rapidly escalating fuel prices, and limiting the environmental consequences of oil, coal, and nuclear facilities. Due to the energy market imperfections introduced by the OPEC cartel, private industry is unlikely to independently finance STT R&D. Expenditures on STT R&D could result in significant energy cost savings, limit the impact of oil price increases, and reduce environmental degradation associated with conventional energy technologies. These social benefits would far exceed the costs of the federal R&D program. Therefore, federal participation to capure these significant national benefits is justified.

To provide the incentives to stimulate the establishment of a cost-competitive STT industry, the Federal Government can follow two complementary approaches. If extended, the Federal Business Energy Tax Credit will encourage third party investments in solar thermal power systems. These early purchases will encourage volume production resulting in STT cost reductions. Simultaneously, federal R&D programs can be used to further refine the technology base leading to STT systems capable of meeting and surpassing the 1990s cost target. This combination of federal incentives can facilitate the creation of a self-sustaining private STT industry. In return, the STT industry provides the economy with potential economic and social benefits, including: savings in energy costs; improvements in environmental quality; and, in the long-run, possible reductions in oil imports.

Blank Page

Hamid Habib-agahi
Jet Propulsion Laboratory
Pasadena, California

IMPACT OF THE FEDERAL ENERGY TAX CREDIT ON THE SOLAR THERMAL INDUSTRY AND GOVERNMENT REVENUE

INTRODUCTION

This analysis of the impact of the Federal energy tax credit on the solar thermal industry and Federal income tax revenues indicates that extending the federal energy tax credit beyond 1985 is necessary for the establishment of a viable solar thermal electric industry. The analysis is of the investment in solar thermal technologies by limited partnerships as this type of ownership can make the most use of existing tax laws.

The results of this study show that during the early stages of industry development, when system costs are still at high levels, assumed to be about $4,000/kWe, there will be no investment without the energy tax credit. With the extension of the energy tax credit, investment begins to look attractive to owners requiring a return of 18% or greater on their investment at a debt to total investment ratio of 36% or more. The less equity required of an owner, the more attractive the investment looks, assuming debt financing would be available. However, repayment assurances such as coverage ratios required by conventional lenders make it unlikely that a debt fraction higher than 50% should ever be reasonably considered. As the industry matures and capital costs drop to $2,200/kWe, an investor requiring a 20% return may be persuaded to invest at debt fractions as low as 25%. The return becomes greater both with an increase in the debt fraction and the extension of the energy tax credit, assuming no variation in the interest rate. The calculation of increased rate of return to equity with higher debt fractions assumes that the interest rate on debt is not sensitive to the size of the loan. As the debt fraction increases, however, the interest rate may also increase to the point where increased interest expenses actually decrease the return to equity.

The next focus of the analysis is the impact of the energy tax credit on government revenues. The study indicates that, in general, the energy tax credit is essential to the establishment of the industry, but can be dropped as the industry matures. The effect on government revenues is then the present value of revenues lost due to the energy tax credit, and revenues gained due to income taxes from the industry. At a $4,000/kWe system cost and 15% energy tax credit, the present value of all government revenues discounted at 13% nominal is negative. As the system cost comes down and the investors begin to pay more taxes, Federal receipts increase. Once the industry is established with the aid of the energy tax credit, the costs have decreased, and the energy tax credit dropped, the flows to the Federal government will be positive.

OVERVIEW

The objective of this analysis is to examine whether or not the Federal energy tax credit is an effective instrument for stimulating the solar thermal electric industry. The question of the cost of the energy tax credit to the Federal government must also be examined.

There are several scenarios in which a solar thermal electric industry might operate that need to be examined.

System costs can vary from $4,000/kWe in 1985 dollars for the infant industry to $2,200/kWe in 1985 dollars for the relatively mature industry. In either case, the impact on return to the owner needs to be examined both with and without the Federal energy tax credit. The type of ownership considered in this study is the limited partnership. A limited partnership is able to take the full tax loss against income generated from other sources at the maximum tax rate while the solar thermal system is operating at a loss.

If an investor is evaluating a solar thermal system for maximum return on his equity, then his option would be for as high a debt fraction as possible, at reasonable debt cost. However, a lender may not be willing to assume a large share of the risk. The return to equity was therefore evaluated at debt fractions of 25% to 75%. Naturally, the less equity an investor was required to put in, the greater his rate of return and the more willing he would be to invest.

To evaluate the financial return of a solar thermal system, a cash flow model was devised. The model calculates the income from the sale of electricity to a utility minus expenses as pretax net income. State-specific adjustments are made to calculate state income tax. In this case, California was modeled. Federal taxable income is then calculated, and the federal tax is computed. When the net income is negative, the federal revenues are negative for that year for the solar thermal project, assuming that the owners can apply the losses to income generated from other sources. To calculate return, appropriate adjustments are made for depreciation, payment of the loan principal, and tax credits. The model then calculates the internal rate of return for the thirty year system life. Conclusions can then be drawn about the likelihood of investment. The net system lifetime present value of government revenues, tax receipts minus the energy tax credit, are calculated using a real discount rate of 7%. A complete description of the model follows.

MODEL

The cash flow analysis model is defined in the following manner.

$$I_t = P_t \cdot Q$$

$$P_t = P_0 \cdot \prod^{t-1} (1+g_{e_t})$$

where

I_t = Income in Year t

P_t = Price in \$/kWh in Year t

P_0 = Initial Electricity Price in \$/kWh

g_{e_t} = Escalation Rate of Electricity in Year t

Q = Annual Electricity Output in kWh

$$PNI_t = I_t - (M_t + PI + INS + F_t + MISC_t)$$

where

PNI_t = Pre-tax Net Income in Year t

M_t = Operations and Maintenance in Year t

$$M_t = (\%\ CI) \cdot \prod^{t-1} (1+g_{O\&M_t})$$

CI = Capital Investment in \$

$g_{O\&M_t}$ = Escalation Rate of O&M Expenses in Year t

$$PI = \frac{i}{1-(1+i)^{-n}} \cdot D$$

where

PI = Principal and Interest Mortgage Payment

i = Loan Interest Rate

D = Initial Amount of Debt in \$

$D = \alpha_D \cdot CI$

α_D = Debt Fraction

n = Loan Lifetime

INS = Insurance Expenses as a Percent of the Initial Capital Investment

F_t = Fuel Cost at Time t

$$F_t = F_0 \cdot \prod^{t-1} (1+g_{f_t})$$

F_0 = Initial Fuel Cost

g_{f_t} = Escalation Rate of Fuel Costs in Year t

$MISC_t$ = Miscellaneous Expenses in Year t

State taxes are calculated next as pre-tax income adjusted by the principal repayment on the loan and allowable state depreciation.

$$STI_t = PNI_t + A_t - SD_t$$

where

STI_t = State Taxable Income in Year t

A_t = Amount of Principal in the Mortgage Repayment in Year t

$A_t = PI - i \cdot D_{t-1}$

D_{t-1} = Outstanding Balance on the Loan

SD_t = Depreciation Allowed by the State in Year t

State taxes are then

$$ST_t = \tau_s \cdot STI_t$$

τ_s = State Tax Rate

Federal taxable income is then the State taxable income with appropriate adjustments:

$$FTI_t = STI_t - ST_t + STC_t + SD_t - FD_t$$

where

FTI_t = Federal Taxable Income in Year t

STC_t = State Tax Credit in Year t

FD_t = Depreciation Allowed by the Federal Government in Year t

$FD_t = (CI - [.5 \cdot FTC_0]) \cdot FDR_t$

FTC_0 = Initial Federal Allowable Tax Credits, the Sum of the Energy Tax Credit and the Investment Tax Credit

FDR_t = Federal Depreciation Rate in Year t

Federal taxes are then:

$$FT_t = \tau_f \cdot FTI_t$$

τ_f = Federal Tax Rate

The income to the limited partnership is the Federal taxable income with the following adjustments:

$$R_t = FTI_t - FT_t + FTC_t - A_t + FD_t$$

where

R_t = Return to the Limited Partnership in Year t

FTC_t = Federal Energy Tax Credit in Year t

The internal rate of return (IRR) to equity can then be calculated as the discount rate at which the sum of the discounted returns to the owner equals his equity investment, or the rate that satisfies the following equation:

$$CI \cdot (1 - \alpha_D) = \sum_{t=1}^{T} \frac{R_t}{(1+IRR)^t}$$

where

T = System Lifetime

ASSUMPTION

1. All figures are in nominal terms.
2. Price of electricity = net avoided cost
   + capacity credit
   + O&M credit
   11.8¢/kWh in 1985*

*Based on 100% oil displacement and the methodology developed in Gates, W. R., et al., "Solar Thermal Technologies Benefits Assessment: Objectives, Methodologies, and Results for 1982," Jet Propulsion Laboratory, Pasadena, CA. February 1983.

3. Quantity of energy produced

= 100 MW * 8760 hr./yr. * .25 capacity credit

= 220 * 10^6 kWh/yr.

4. Expense terms and Escalation Rates

O&M Costs = 2% of the initial capital investment, escalated at the O&M rate of escalation in subsequent years

Cost of debt = 13.5%

Insurance and Miscellaneous = 2% of the initial capital cost, annually

Capital Cost = $4000/kW in 1985 and $2200/kW in 1990, both in 1985 dollars. The 1990 cost in 1990 dollars is $2900.

Federal Depreciation = ACRS, 5 year schedule; the applicable percentages for 5-year property are 15, 22, 21, 21, 21, with the basis reduced by 1/2 the allowable Federal tax credit according to the provisions in the Tax Equity and Fiscal Responsibility Act of 1982 (TEFRA).

State Depreciation = Straight line depreciation, 3 year schedule, with the basis for depreciation reduced by the amount of the state tax credit according to California law.

State Tax Rate = 10.5%

Federal Tax Rate = 50%, the maximum marginal rate for individuals and partnerships.

State Tax Credit = 25% through 1990, and allowed to expire after that

Federal Tax Credit = 10% investment tax credit, evaluated with and without the additional 15% energy tax credit

Salvage Value = 0

System Lifetime = 30 Years

Loan Lifetime = 20 Years

Debt Fraction = Evaluated for a range of debt fraction, from 25% through 75%

General Inflation = 6%

Electricity Price Escalation = 9%

O&M Escalation = 7%

Fuel Costs = 0

ANALYSIS

Figure 1 illustrates the analysis for a system installed with a capital cost of $4000/kWe in 1985 dollars. Assuming a limited partnership would require an internal rate of return to equity of approximately 18-20% or better, no limited partnership would invest in a solar thermal project without the Energy Tax Credit. With the Energy Tax Credit, investment begins to be attractive with an 18% return at debt financing of greater than 35%. While the return to equity continues to increase with increasing debt fractions, in this case with the interest rate on debt held at 13.5% nominal for all debt fractions, the probability of obtaining debt financing decreases with the larger sizes of the loan requests. Lending institutions will typically look at debt coverage ratios as assurances of the ability of the borrower to repay the loan. The debt coverage ratio used here was defined as the net operating income (revenues minus O&M, insurance, fuel, and miscellaneous variable costs) divided by debt service (principal plus interest payment). A cash reserve account was set up using the energy tax credit, to be drawn down to meet debt coverage ratios as needed. The coverage ratio cut-off minimum of 1.2 was used as this is typically the minimum of acceptable ratios defined in bond agreements of municipal utilities. Using this as the limiting factor of available debt financing, the analysis showed that 46% is the maximum achievable debt ratio. Figure 1 then indicates that if a limited partnership is to invest in

Figure 1. Solar Thermal System Return

$4000/kWe Capital Cost

(in 1985 Dollars)

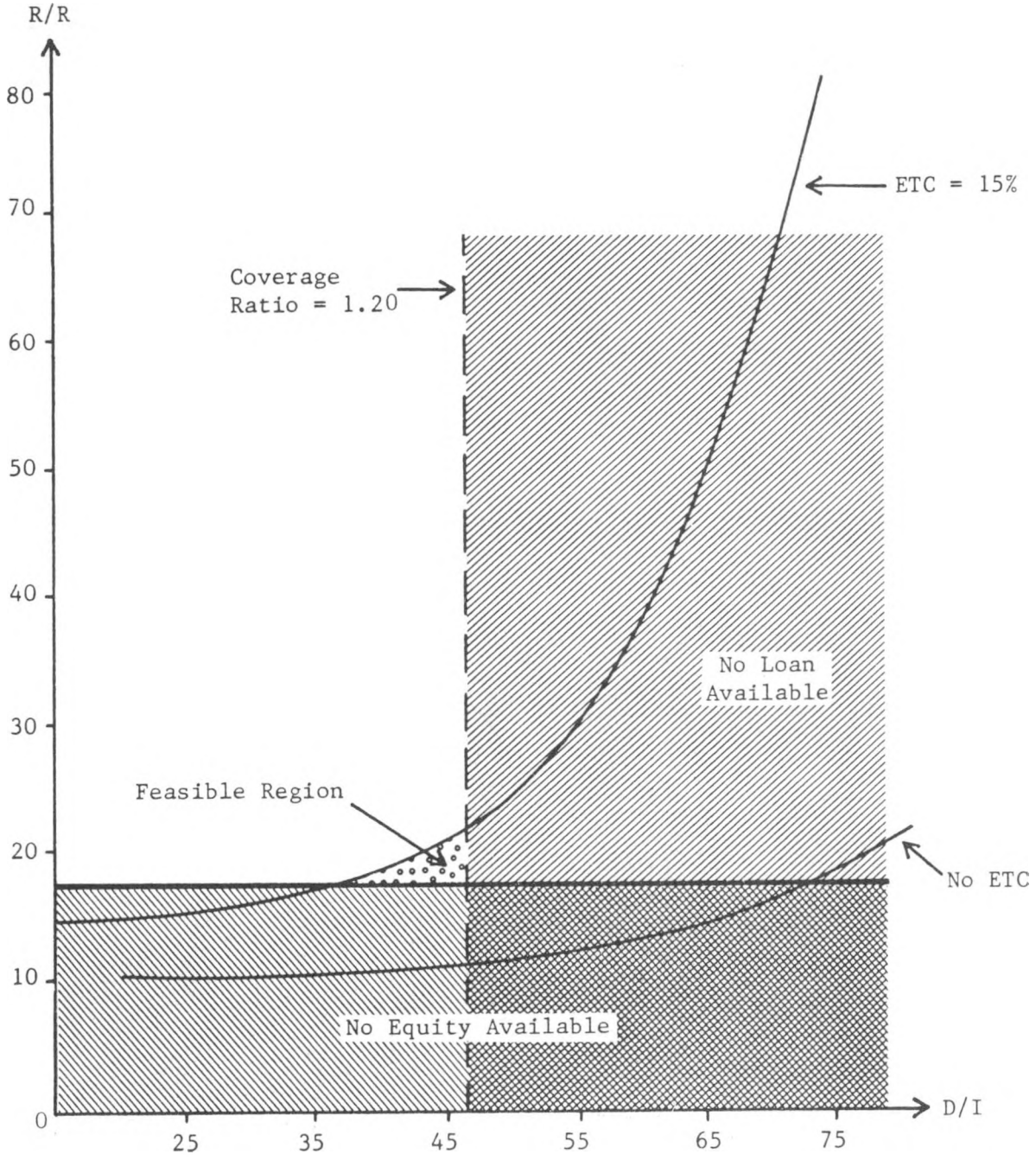

solar thermal systems of the initial high cost technology, the investment scenario will allow debt financing of between 36% and 46%, with an internal rate of return to equity of between 18% and 23%.

The calculations of return to equity may be affected by two factors, both tending to reduce the estimate of return. First, as the debt fraction increases from 36% to 46%, the interest rate may increase, thus reducing the return. Secondly, and perhaps more importantly is the consideration of the cash reserve account. The cash from the tax credits was taken into account in the calculation of the investors' return to equity. If the tax credit amount is spread over several years to reduce losses rather than received in the first year, the internal rate of return will be reduced from that shown in Figure 1.

Once the industry is well established and costs drop to more competitive levels, both the attractiveness of investment in terms of return to equity and the ability to obtain debt financing improve. Figure 2 illustrates the analysis for the case of solar thermal investment of $2200/kWe in 1985 dollars, assumed to take place in 1990 at $2900/kWe in 1990 dollars. In this case, investment will be attractive either with or without the Energy Tax Credit. With the ETC, the return to owners' equity is greater than 22% at all levels of debt financing. The return again increases as the debt fraction increases if the interest rate is held constant. With no ETC, the internal rate of return is lower, but still above 19% at debt financing of 25% or greater. Debt availability also increases over the 1985 case of high capital cost. Capital costs have dropped so that less investment is required to generate revenue. With no ETC, the coverage ratio of 1.2 is satisfied with debt financing of 55% or less. This coverage was estimated without using the cash generated by the 10% investment tax credit. If this cash were put into a

Figure 2. Solar Thermal System Return

$2200/kWe Capital Cost

(in 1985 Dollars)

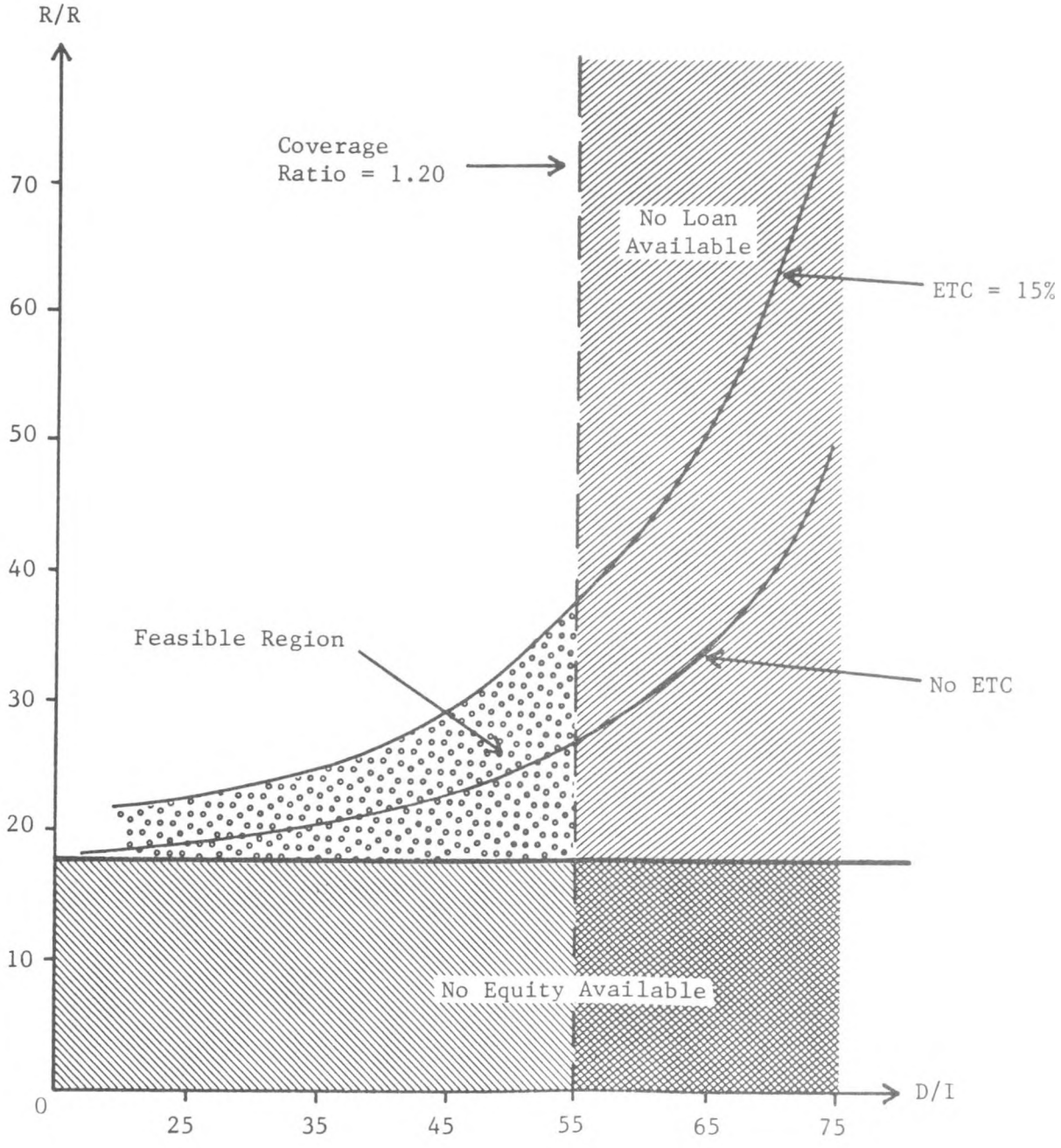

reserve account as was done with the analysis of the earlier period, slightly more debt financing would appear to be available. In the 1990 case with the energy tax credit of 15% extended, debt financing would appear to be available at all levels analyzed, that is through 75%, using the reserve account method.

The second reason for performing this study was to investigate the net effect on government revenues of investment by limited partnerships in solar thermal technologies. Initial investment in 1985 is assumed to take place only with the Energy Tax Credit. At 36% to 46% debt financing, the probable investment scenario, the government loss in revenues is between 90 and 100 million dollars in 1985$. The $90 to $100 million is the present value of the stream of government revenues calculated over the system lifetime at a real government discount rate of 7%. The government will regain some of this loss when the capital cost drops to $2200 in 1985$, in 1990. However, to match the initial $100 million loss generated by a 100 MW plant in 1985, investment in 200 MW of generating capacity is required. See Figure 3.

Table 1 gives a summary of all calculations analyzed by the case flow model.

A caveat which needs to be added to the picture of investment potential is a word about market size. The solar thermal system is without storage. The revenue calculations of net avoided cost apply only when the solar thermal system is operating to replace an oil-fired peaking plant. This will take place only when peak demand matches peak insolation. The number of oil-fired power plants which can actually be replaced in the South and Southwest is limited by a mismatch of demand and insolation peaks. Thus, solar thermal technologies may require storage, a shift in demand peaks, or some other major scenario change to realize full market potential.

Figure 3. Lifetime Net Government Revenues Per 100 MW's Installed

(in 1985 Dollars)

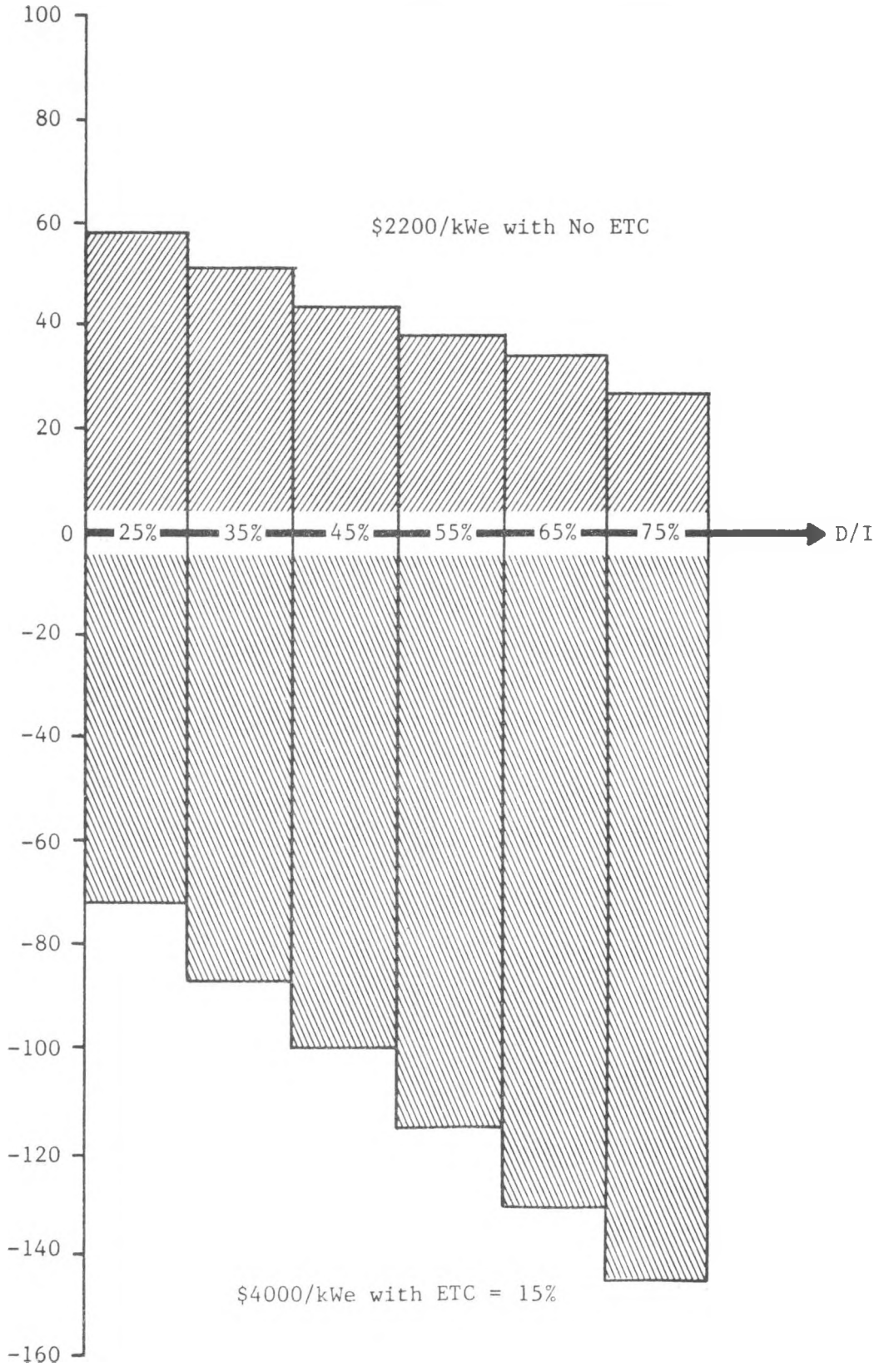

Table 1. Investment Scenario For 100 MW Solar Thermal System

a. 1985 Capital Investment = $4000/kWe, ETC = 15%

Debt/Investment (%)	Rate of Return (%)	Federal Taxes ($ x 10^6)	Tax Credits ($ x 10^6)	Government Revenue ($ x 10^6)
25	14.8	15.8	-88.5	- 72.7
35	17.0	1.3	-88.5	- 87.2
45	20.8	-13.3	-88.5	-101.8
55	29.6	-27.9	-88.5	-116.4
65	49.3	-42.4	-88.5	-130.9
75	89.5	-57.1	-88.5	-145.6

b. 1985 Capital Investment = $4000/kWe, ETC = 0

Debt/Investment (%)	Rate of Return (%)	Federal Taxes ($ x 10^6)	Tax Credits ($ x 10^6)	Government Revenue ($ x 10^6)
25	10.0	- 34.6	-35.4	- 70.0
35	10.6	- 49.2	-35.4	- 84.6
45	11.3	- 63.8	-35.4	- 99.2
55	12.4	- 78.4	-35.4	-113.8
65	14.2	- 96.6	-35.4	-132.0
75	19.4	-107.6	-35.4	-143.0

All Figures are in 1985 dollars.

Table 1 (Continued)

c. 1990 Capital Investment = $2900/kWe in $1990, ETC = 15%

Debt/Investment	Rate of Return	Federal Taxes	Tax Credits	Government Revenues	
(%)	(%)	($ x 10^6)*	($ x 10^6)*	(x10^6$)*	(x10^6$)**
25	22.2	138.4	-64.2	74.2	40.3
35	25.0	127.8	-64.2	63.6	34.5
45	29.2	117.3	-64.2	53.1	28.8
55	36.5	106.7	-64.2	42.5	23.1
65	50.0	96.2	-64.2	32.0	17.4
75	79.0	85.5	-64.2	21.3	11.6

d. 1990 Capital Investment = $2900/kWe in $1990, ETC = 0

Debt/Investment	Rate of Return	Federal Taxes	Tax Credits	Government Revenues	
(%)	(%)	($ x 10^6)*	($ x 10^6)*	(x10^6$)*	(x10^6$)**
25	19.2	130.9	-25.6	105.3	57.0
35	20.9	120.3	-25.6	94.7	51.4
45	23.4	109.8	-25.6	84.2	45.7
55	27.3	99.2	-25.6	73.6	40.0
65	34.4	88.6	-25.6	63.0	34.2
75	49.4	78.0	-25.6	52.4	28.5

*Figures in 1990 dollars.
**Figures in 1985 dollars.

CONCLUSION

If the Federal Energy Tax Credit is allowed to expire in 1985, near-term private investment in solar thermal electric power systems is unlikely. The expected return to third party owners of a 100 MW solar thermal power plant, assuming 65% debt financing, would be less than 15% (nominal), and the expected return would fall for lower debt fractions. With the extension of the ETC, there does exist a potential financial framework for investment to occur with $4000/kWe capital costs. Debt financing appears to be available for up to 45% of the system cost. Third party owners using 35% to 45% debt financing can anticipate a return to their investment of 18%-22%, respectively. With these rates of return, the markets provided by third party owners may be sufficient to enable the solar thermal systems industry to employ mass production techniques, bringing system costs to more competitive levels. If solar thermal capital costs drop to $2900/kWe in the 1990 time frame (1990 dollars), investment will be attractive even without the ETC. Third party investors can expect a 20% to 30% return and debt availability to 55% of the system costs.

The cost of the ETC to the Federal Government in lost tax revenues is between $90 and $100 million (1985$) for each 100 MW solar power plant. This is the amount of revenue lost through the ETC in 1985, and through "negative" taxes to the 100 MW solar thermal project. By 1990, when the Energy Tax Credit is no longer necessary to stimulate investment, the government revenue stream will be positive. However, using a government nominal discount rate of 13% (7% real) to calculate present value, it will take twice as many power plants in 1990 as were put in in 1985 to make up for lost government revenues.

It should be noted that the revenue stream was calculated on a net avoided cost basis. However, fuel costs have been one of the more volatile factors in recent economic periods, both increasing and decreasing rapidly. If fuel

costs drop, anticipated revenues from solar thermal electric systems will also drop. Private investments in both solar thermal systems and production facilities will become less attractive. In order to stimulate the private investment required to create a self-sustaining private solar thermal industry, federal incentives such as extension of the energy tax credit are needed.

Blank Page

ADVANTAGES OF LARGE PARABOLIC DISH SYSTEMS FOR POWER GENERATION*

A.G. Sutsch

Institute for Computer-assisted Research in Astronomy, CH-1715 Alterswil, Switzerland

ABSTRACT

The advantages of the Large Parabolic Dish System-LPDS over other competing solar thermal power plants are discussed: absence of all cosine losses resulting in higher net power output (annual kWh) throughout the year, even heat flux distribution in the important component, the receiver; proven technology transfer into solar receivers stemming from 25 years experience in high temperature material behaviour using the Bammert-Criteria for design parameters; multi-purpose, 24 hour continuous electricity production via a thermal storage unit; industrial process heat utilization either at high temperature (950°C) or as waste heat from the turbine exhaust (100-300°C); communication benefits using the dish as an antenna during non-sunshine hours for telephone, telex, etc. as an earth station or direct line communication; high plant efficiency due to high process temperature (950°C) resulting from high concentration ratios in the focal plane area of the parabolic dish. These advantages make the LPDS a desirable system choice for the isolated load market and developing countries.

KEY WORDS

Solar energy; thermal power conversion systems; solar energy conversion into electrical and mechanical power; small industrial gas turbines; parabolic dish; high temperature energy storage; communication.

INTRODUCTION

Solar energy can provide an answer for the energy problems especially in remote locations for the isolated load market and developing countries where conventional fuels are very costly to transport and an electric grid is too expensive to maintain. In countries with adequate insolation (generally 45° North and South latitude),

* From the Proceedings of the International Solar Energy Society Congress (Brighton, England; August 23-28, 1981), printed by Pergamon Press.

i.e. sufficient sunshine hours throughout the year, solar thermal power plants find a vast and expansive market if they can fulfill general user requirements, such as: reasonable cost for installation and maintenance, amortisation time within present day industrial schemes (typically 10-15 years) taking into account zero primary energy costs during the life of the plant, high availability with continuous electric and/or industrial process heat production, depending on user requirements.

It is this last factor where all present day solar thermal power plants fail: they deliver electric/ industrial process heat - energy during sunshine hours only; for an industry or utility this is a completely inadequate situation. Major emphasis, therefore, has to be placed on energy storage, either thermal, electric, or chemical to provide 24 hours of continuous energy production with net power output at a reduced level during non-sunshine hours being permissible, maintaining a base load only.

It is misleading and counterproductive to the development of solar thermal power plants if a "design point" (maximum energy production level) is quoted, as is the case in almost all present day solar thermal power plant installations. The user is interested in kilowatt hours output per year on a continuous basis and cost per kilowatt hour; only if this philosophy can be adopted and systems working under such conditions presented does solar energy become a competitive and viable source of energy production on an electric or industrial process heat level.

The LPDS represents a solution to these problems and this paper lists some of the advantages over other competing solar energy systems in the same power range.

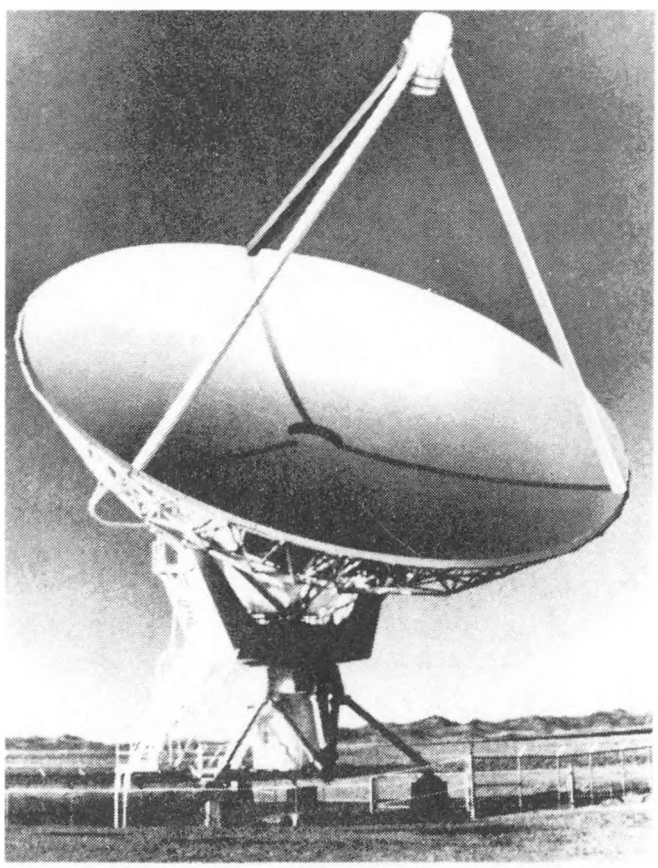

Fig. 1. Large Parabolic Dish System.

COSINE FACTOR

Figure 1 shows an artist's concept of the LPDS, consisting of a large parabolic dish as used in radio-astronomy as collector with a reflective coating on the aluminium panels; the receiver and turbo-converter are placed at the focal area of the dish, held in place by four supporting struts.

By its configuration, a high process temperature and thus high conversion efficiency is achieved with a parabolic collector. The parabolic dish, mounted on an altazimuth or equatorial mount tracks the sun from sunrise to sunset, accounting for one of its outstanding differences with other solar power plants: the absence of all cosine losses due to constant two-axis tracking, holding the incoming solar radiation always parallel to the optical axis of the dish. This major feature accounts for a yearly increase in power delivered in excess of 30% over other competing solar thermal power plants due to two phenomena: 1. daily cosine losses and 2. cosine losses within one solar year.

Design points in power output for solar thermal power plants are usually given for site noon at the summer solstice (June 21, 12:00) resulting in reduced power output throughout the rest of the year and providing misleading figures for average power delivered (thermal and electric). The LPDS reaches its maximum (equal to constant)power output on any day throughout the year at any time with the sun a certain angle (typically 7-10°) above the horizon; reduced insolation energy right after sunrise and shortly before sunset is due to radiation absorption within the earth's atmosphere for low elevation angles because of dust, humidity, etc.

A heliostat-tower system exhibits a strong cosine loss factor in the morning after sunrise and evening before sunset with the sun only grazing the heliostats (low angle of incidence=low angle of reflection) to reflect the sunlight onto the receiver (tower) thus resulting in a greatly reduced power profile for the morning delivering up to 40% less in thermal power than at noon of the design point. This cosine loss factor (the daily cosine loss factor) is symmetrical for a symmetrical heliostat field and applies as well for the afternoon hours before sunset.

The LPDS awaits the sun at sunrise with the optical axis of the dish pointing to the solar disc center, and constantly tracks it throughout the entire day with radio-astronomical precision (typically $\pm$ 10 arcsec). In this way, delivered power is only dependent on the transparency of the atmosphere, i.e. radiation received on a surface normal to the sun's radiation direction, and maximum power is equal to constant power output - the "design point" of the LPDS.

RECEIVER DESIGN CONSIDERATIONS

The most critical component of a solar thermal power plant working at high temperatures is the receiver. Basically, the receiver is a heat exchanger transferring the heat absorbed from solar radiation to a working fluid flowing in passages or tubes. The receiver design concept is one of the most decisive questions for high plant efficiency and cost effectiveness. Receiver technology and its optimization will play an important role in the development of future solar thermal power plants.

Closely related to the already mentioned cosine loss factor in a heliostat-tower system is the varying load factor on the receiver tubes due to an uneven irradiation profile throughout the day. This results in only partial load on some parts of the receiver with possible overloading of other parts; this again has two effects:

1. the receiver has to be larger than optimally necessary since it only receives part of the load some of the time (morning and afternoon); the size is determined by the design point, the maximum radiation received at noon on the summer solstice. Therefore, the receiver becomes more expensive considering the very costly INCOLOY 800H or similar as a guideline for high temperature applications,
2. overlaoding of certain receiver areas is possible due to uncertain tracking of heliostats; the heliostat being a mass-produced item exhibits higher tracking errors than its LPDS counterpart, the large parabolic dish. This shows even more, the farther away a heliostat is from the receiver; gear backlash and pointing inaccuracy result in larger spillage or radiation intensity profile uncertainty for greater distances since the errors occur within the drive mechanism and increase in dimension with distance; this effect is amplified when wind is present.
Receiver overload leads to shorter life time of the expensive receiver tubes (ruptures) before the designed tube service life.

A major factor for choosing a parabolic dish collector tracking the sun continuously from morning to evening is the uniform energy distribution profile in the focal area (heat flux distribution) throughout the day. When the dish follows the sun from sunrise to sunset only the amplitude of the focal plane intensity profile changes due to varying insolation values (morning, noon, evening) but the heat flux distribution over the focal area remains constant throughout the day since the sun is always held on the optical axis of the dish and tracked with arcseconds accuracy. This most important consideration for the construction of efficient receiver designs cannot be fulfilled by the heliostat-tower concept.

RECEIVER TECHNOLOGY

For the 250 kWe demonstration plant a conventional metal tube receiver (Incoloy 800H) is being considered (Fig.2). This technology has been employed successfully for years in gas-, oil-, and coal-fired heaters of open- and closed-cycle gas turbines. In the past 25 years extensive theoretical (1) and experimental work has been done for the development of conventionally fired heaters. We have running experience with several plants in Germany (2) with a lifetime for each plant in excess of 100,000 hours. This running experience warrants the use of this high-temperature technology to be transferred into receiver designs of solar power plants. The radiation part of such heaters corresponds to the receiver; the place of the burner (coal, gas, oil) is taken by solar radiation.
Figure 2 shows a diagrammatic sketch of a first generation steel alloy receiver with heater tubes aligned in a circle around the receiver wall, a window for radiation entrance, the radiation distribution cone of ceramic material with cooling tubes, inlet and

outlet headers within the insulation.
Future generation receivers would be of ceramic material throughout to allow higher process temperatures (up to 1,300°C) and increase overall plant efficiency even further ($\eta_{plant} \geq 26\%$).

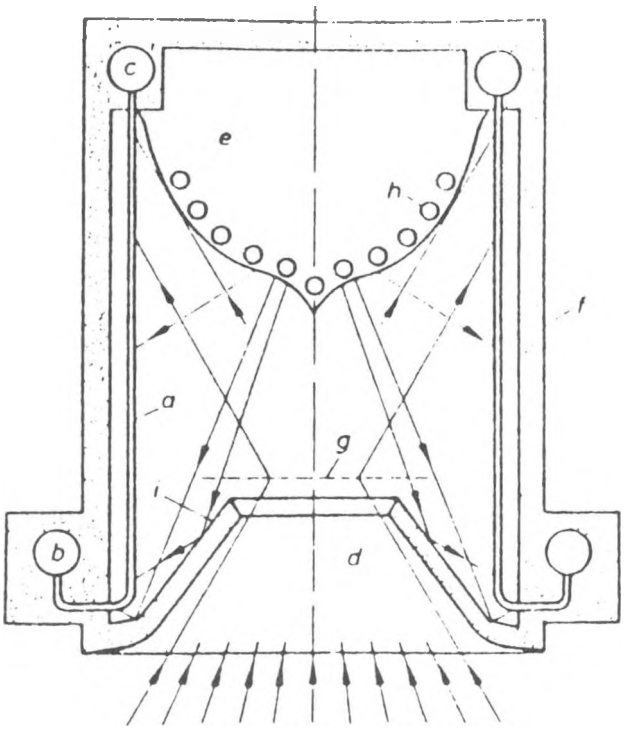

a	receiver tubing	e	radiation distribution cone
b	inlet header	f	receiver cage with insulation
c	outlet header	g	focal plane area
d	window	h	cooling tubes
		i	reflective wall

Fig. 2. Receiver.

MULTI-PURPOSE SYSTEM

One of the unique features of the LPDS is its multi-purpose use for production of electricity and industrial process heat on a 24 hour continuous basis. A major drawback of all solar thermal power plants to date is their operation only part of a 24 h day and only during sunny periods. Cloud passages cause instability, interruption, or total loss of electric power production - a situation unacceptable to an industry or utility. The LPDS overcomes these important drawbacks by feeding thermal energy from the receiver to a storage unit of MgO_2 brick (or similar) in a closed cycle system; heat exchanger tubing within the storage unit provides the necessary turbine inlet temperature of up to 950°C (typically 800°C for the prototype unit). For varying ambient air intake temperatures into the compressor of the gas turbine due to changing air temperature during the day and electric load conditions on the generator, a by-pass regulating valve on the

return cool gas line to the storage unit (Fig.3) feeds directly into the hot gas line in order to keep the turbine inlet temperature at a constant value, mixing the required cool gas with hot gas from the storage unit to insure a constant or variable load depending on user requirement.
Taking thermal energy for the turbine always from the storage unit also disregards cloud passages and insures stable operating conditions throughout the day and night.
Electricity production at night is provided via the gas turbine drawing thermal energy from the storage unit; night time electricity consumption is on a reduced level to typically 40% of consumption during the day, dependent on user profile, as most industries go off the line. Although the gas turbine will run at a reduced load, plant efficiency remains nearly constant with the ambient air at the compressor intake dropping to the much lower night temperature, resulting in higher compressor efficiency.

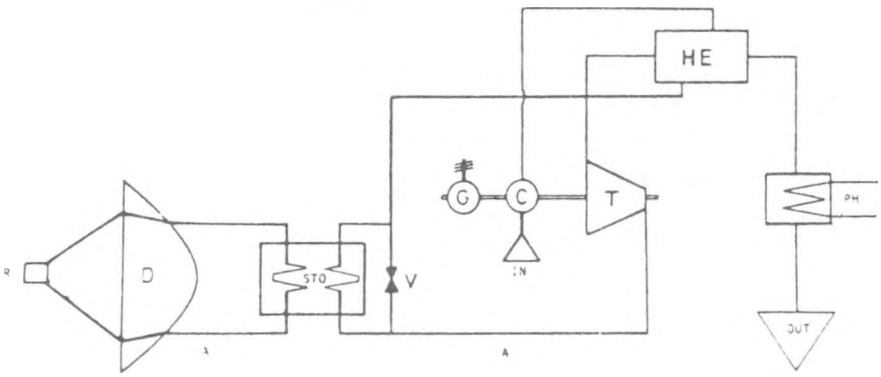

A	working medium tubes	PH	process heat (waste heat)
C	compressor	R	receiver
D	dish collector	STO	storage
G	generator	T	turbine
HE	heat exchanger	V	valve

Fig. 3. Schematic cycle diagram for L. P. D. S.

Waste heat from the gas turbine can be exploited further for desalination, absorption cooling, direct heating, or low power steam production, or any type of process heat requiring temperatures between 100-300°C, thus making use of the total thermally available entropy spectrum. Employing both electricity and industrial process heat production results in total plant effectiveness of up to 80%. If desired, industrial process heat at high temperature (up to 950°C) can be utilized directly out of the storage unit via a heat exchanger.

Communication Benefits

The multi-purpose role of the LPDS is further enhanced by the fact that during non-sunshine hours the LPDS can be converted to a powerful communication station for either transmission and reception in direct line or satellite communication work as an earth station for telephone, telex, radio, television, data transmission, etc. -

the original role the dish was taken from. Conversion to transmission/reception is achieved by inserting a Cassegrainian subreflector in front of the receiver cage, with communication equipment mounted permanently in the vertex of the dish; this changeover requires app. 20 minutes with the dish in horizon position as shown in Fig. 4.

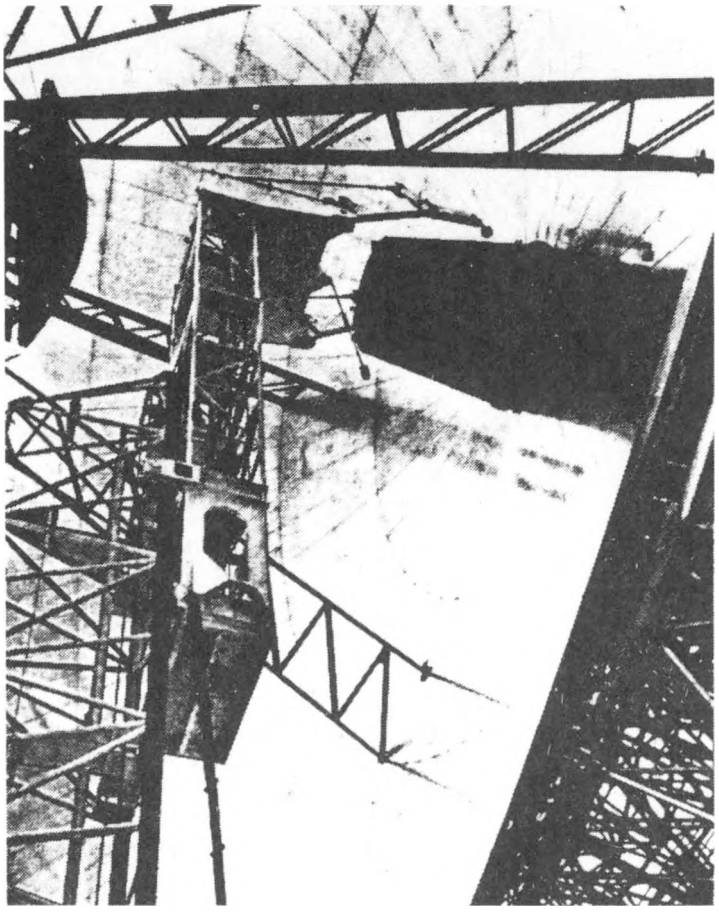

Fig. 4. Feed change with "cherry picker" - crane.

This multi-purpose application greatly reduces installation cost and accelerates repayment time, making far better use of the equipment than if it were purely used for power generation. INTELSAT earth stations today (over 100 participating countries) amortize in app. 5 years; this also applies in developing countries where the LPDS would preferably see its field of active service. A cost comparison study (3) has shown that the LPDS on its merits as a power station alone (not taking into account the communication benefits) can draw even in power production cost with a Diesel generating station in the I.L.M. (Isolated Load Market) within app. 8 years based on 1981 Diesel fuel costs in the ILM; considering communication benefits, this time is even further reduced in favour of the LPDS.

PROVEN TECHNOLOGY APPLICATIONS

There are over 300 parabolic dish antennas in use today in communication (INTELSAT network, TELCOMSAT, etc.); large fully steerable dishes with diameters of 50 m to 100 m with very exacting specifications have been in service in radio-astronomy for several decades.
Tracking accuracy represents no challenge to today's electronics and has been used successfully in radio-astronomy within arcseconds. Accordingly, power ranges for single LPDS stations up to 2,000 kWe (7,900 kWth) with a 100 m dish are possible using existing technology. Larger systems would consist of several dishes connected electrically, each with its own turbo-conversion system.
Small gas turbines are readily available within the mentioned power ranges (200-2,000 kWe); their operation on hot air allows increased turbine inlet temperatures due to lack of corrosive or erosive materials, such as oil and gas fuels.
Receiver technology has been described earlier (ibid.)

HIGH PLANT EFFICIENCY

Parabolic dishes by their design feature high concentration ratios from $C = 3{,}000$ to 10,000 suns, yielding very high process temperatures $T \geq 2{,}000°C$ within the focal area. This high process temperature (air at $T \geq 950°C$) for the demonstration power plant, increasing to $T \geq 1{,}300°C$ with the advent of ceramic receivers provides a very high conversion efficiency $\eta = 40\%$ thermal to electric, thus increasing overall plant efficiency $\eta_{(plant)}$ to levels that cannot be attained by other solar thermal power plants; the LPDS is seen to reach 21% overall plant efficiency with steel-alloy receivers and more than 30% with ceramic receivers; a heliostat-tower system for the same power range achieves 15% efficiency for a steam process and 18% with a gas process (4).

CONCLUSION

The advantages of the Large Parabolic Dish System-LPDS over competing solar thermal power plants have been described. A listing in brief form follows:

1. 30% higher annual net power output than competing systems due to absence of cosine losses as a result of constant two-axis tracking.
2. Even heat flux distribution in focal area throughout the day allowing receiver optimization for steel alloy and ceramic receivers.
3. Multi-purpose system for 24 h continuous electric power and process heat production out of thermal storage unit. Industrial process heat from turbine exhaust heat at app. 100-300°C for absorption cooling, desalination, direct heating, etc.
4. Communication benefits during non-sunshine hours for direct line or as a satellite earth station.
5. High concentration ratio and high process temperature yield high conversion efficiency and high plant efficiency.
6. Transfer of proven technology insures viability, high availability, low maintenance cost.

7. Electricity, process heat utilization, and communication combined render the LPDS a 100% effective system.
8. LPDS systems can be linked electrically in multiple units for higher electric power output (maximum single unit dish size 100m diameter for 2,000 kWe output).

These advantages reduce system installation cost, accelerate repayment time, and make the LPDS a highly desirable system for the isolated load market and in developing countries.

REFERENCES

Sutsch,A.G.(1979). Solar Energy Power Plant. Institute for Computer-Assisted Research in Astronomy, Alterswil, Switzerland

(4) Bammert, K., Sutsch, A.G., Simon, M., Mobarak, A. (1980). Small Gas Turbine with Large Parabolic Dish Collectors. ASME 81-GT-201.

Sutsch, A. G. (1980). Comparison between heliostat-tower concept and large parabolic dish collectors for solar thermal power plants. Institute for Computer-Assisted Research in Astronomy, Alterswil, Switzerland.

Bammert, K. (1979). Studies of Solar Gas Turbine Modules. Comm. of the European Communities, Centro Euratom, Ispra, Italy, Research Project No. 879-78 SISP D.

Bammert, K., Simon,M.,Sutsch,A.G. (1981). Large parabolic dish collectors with gas turbines. Atomenergie-Kerntechnik Bd.38 (1981)Lfg.4, 257-267.

(2) Bammert, K. (1981).Long-term experience with coal fired heaters in German closed-cycle air turbine plants. Atomenergie-Kern technik Bd.38(1981)Lfg.4, 241-256.

(1) Bammert, K., Seifert, P. (1981).Tube Stresses in the Radiation Part of Solar Receivers and of Conventionally Fired Heaters. ASME 81-GT-200.

(3) Sutsch, A. G. (1980). Cost Comparison Study Large Parabolic Dish System Versus Diesel Power Plant for the Isolated Load Market in Developing Countries. Institute for Computer-Assisted Research in Astronomy, Alterswil, Switzerland.

Blank Page

DEVELOPMENT OF LIGHTWEIGHT DISH CONCENTRATORS IN COMBINATION WITH FREE PISTON STIRLING ENGINES

J. Kleinwächter

Bomin Solar

Lörrach, F.R.G.

At least since the first oil-crisis in the year 1973 it was realized on international level that solar power stations for decentral production of electric, mechanic and thermal energy are representing a big and interesting potential, especially in the world's sunny regions.

Today, in the year 1982, several test-installations with an output of 1 $MW_{elec.}$ as a maximum, proved that it is possible to build such solar power plants with a reasonable efficiency. However, compared to conventional power plants (oil, gas, nuclear power), they are still much too expensive, and as a result of generally practised method of construction (power tower, solar farm) no cost reduction for mass production is to be expected.

Having carefully analyzed the reasons leading to these high investment costs for solar power plants, BOMIN-SOLAR developed a real new solar power plant conception. The determining factor for a more low-priced power station is an extreme light-weight construction of the systems collecting the sunlight. Center piece of the BOMIN-SOLAR power station are large foil-membrane mirrors, getting their parabolic shape by an under- overpressure. These extremely light-weight mirrors are protected against wind and weather by transparent protective domes or -tunnels, and are concentrating sunlight on a novel type of Stirling hot air generator, transforming the concentrated sunlight directly into electric alternating current.

This unique BOMIN-SOLAR conception allows to keep the building material necessary for installation of one electric power unit ten times lower compared to those of conventional solar power plants. Thus, the BOMIN-SOLAR concept meets the technical as well as the economical requirements to guarantee a successful mass-marketing.

Heliostates for power-towers and large dish solar concentrators are weighing $\geqq 500$ kg/m². This leads to a high weight per unit of power and is therefore a limiting factor for the putting on the market of solar power stations. It is shown that with a new type of air-deformed membrane concentrator under transparent protection domes the needed material input/kW_{el}-output can be substantially diminuished.

1. Principle of function

As shown in **Fig. 1** the energy density on a receiver in the focus of a concentrator mirror can be enhanced by the factor of over 1000 by using two-dimensional optical concentration. Such high concentration factors allow the transformation of radiant energy into high level thermal energy of 873 K (600°C) with an efficiency of about 70%. Temperatures around 600°C are the process temperatures of classical power plants (oil, coal, gas, nuclear energy) and are used in modern industry for high value energy transformations, like electric power, mechanical power and for chemical and metallurgical processes.

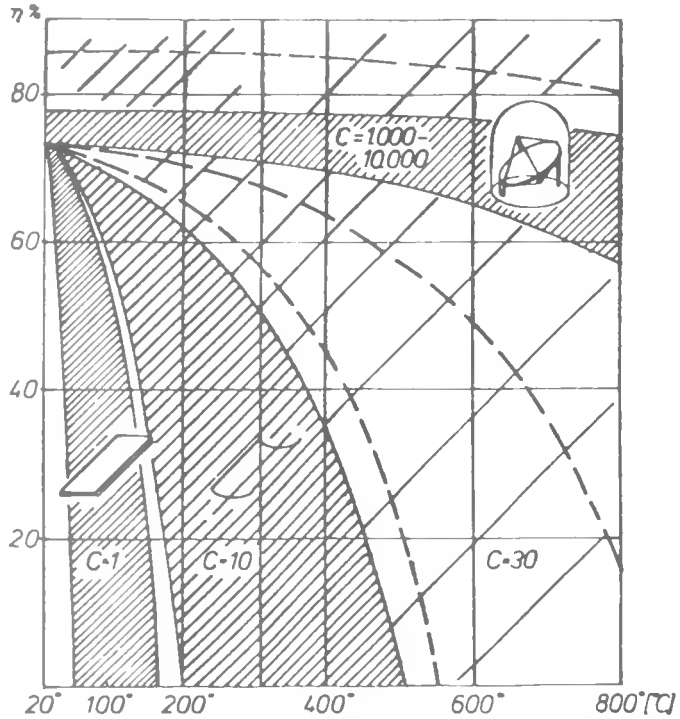

Fig. 1 Efficiencies of transformation from solar radiant energy into thermal energy as a function of the temperature and of the optical concentration

Therefore the basic principle of a thermal solar power station is the substitution of the classical steam generating part of a power station by a solar concentrator under preservation of the other subsystems (e.g. turbine and generator).

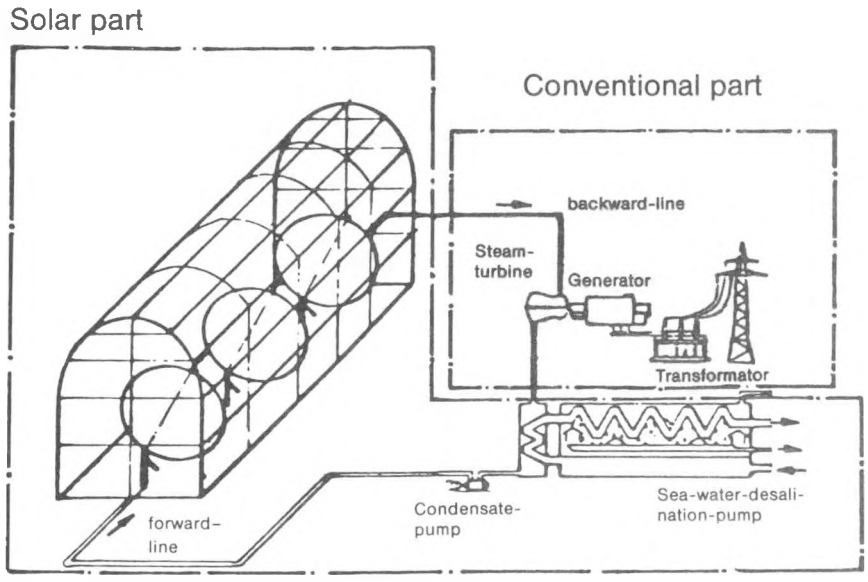

Fig. 2 Thermal solar power station

As for the conventional power plant only very big, centralized units (bigger than some hundred MW) are giving economic sense, **for solar power stations small and medium units (some 10 to some 100 kW, in modular construction) are the ideally adapted size.** For this reason solar power stations with their stand point near the customer are suitable to utilize the big amount of waste heat in second and third processes. This represents a substantial advantage of solar power stations compared with conventional power stations. **Fig. 2** shows e.g. the utilization of the power station's waste heat for a sea water desalination plant. This principle leads **to multiple-purpose solar power stations.** While conventional power plants are using the high level thermal energy only with an amount of 30% for the electric transformation and are wasting 70% of the input energy **decentral solar power stations with multi-purpose utilization can reach between 60% and 80% of overall efficiency.** Therefore they are working more economically and efficiently.

The technical realization of such power plants represents two main difficulties:

- 1. Exact rotational paraboloid mirrors with high concentration values are expensive and complicated to build.
- 2. As the energy density of the incoming solar radiation is about 1 kW/m² big captation surfaces are needed. They must be heavy and stable in order to guarantee even under the influence of strong wind forces a good focalisation of the solar rays.
  This leads to the actually main critic against solar power stations:
- **Over 5.000 kg of material is needed to install 1 kW of electric energy. (1).**

Conventional power plants need material amounts only in the range of 500 kg/installed kW_{el}. As the weight of the installed material influences strongly a power station's installation price it is obvious that the high „weight per unit of power" of solar power stations represents a great difficulty when putting on the market.

However, the reason for this is not a natural limit but the negative effect of combining two functions: the optical and the mechanical one. The optical function of a solar mirror is to reflect the incoming sun rays to a target. Solar energy as high frequency electro-magnetic wave is underlying the skin effect when trapped by a metallic surface. The needed thickness Δ for reflecting more than 90% of the incoming light is calculated as follows:

$$\Delta = \frac{1}{\sqrt{\varkappa \cdot f \cdot \mu}} \approx 100\ \mathring{A} = 10^{-8}\,m \quad \ldots\ldots\ldots\ldots\ldots\ldots\ldots\ [1]$$

f = light frequency $\quad$ $\varkappa$ = electric conductibility $\quad$ μ = magnetic permeability

In case of an aluminium reflector the transmission and reflection as a function of the metal thickness is given in Fig. 3.

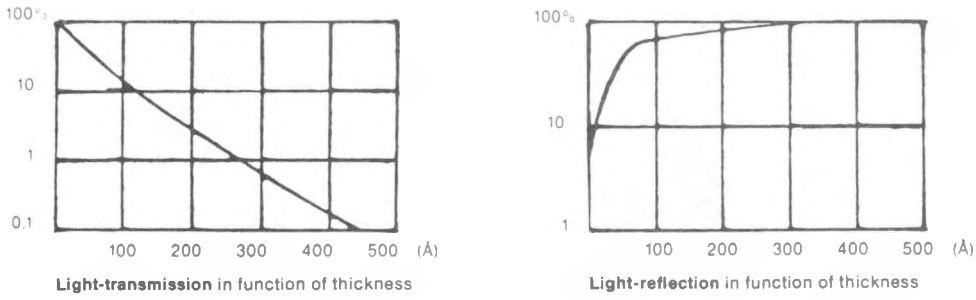

Fig. 3 Light-transmission and reflection in function of the Al-mirror thickness

Therefore, the optical function may be realized by very thin metallized films, having only the weight of some fractions of a gram/m². The reason why heliostates for power tower stations or large dishes for solar farms are weighing ≧ 500 kg/m² is the fact, that their large surfaces must resist to strong wind forces, without changing their optical precision. This mechanical function implicates heavy-weight constructions. In the year 1976 BOEING presented a new conception of a light-weight heliostate mirror for power tower stations. This firm utilized metallized plastic foils, stretched over a metallic skeleton in order to produce a plane, circular mirror of 5,5 m in diameter. This circular mirror, satisfying the optical function was protected under a transparent Tedlar dome, satisfying the mechanical function. This separation of the two functions creates a new type of light weight solar system. (2).

Since 1972 our company is developing rotation paraboloid mirrors by stretching plane mirror foils over hollow, drum-shaped bodies. Production of a slight over- or underpressure inside the hollow body creates an enough good approximation to an exakt parabolic dish (Fig. 4).

Fig. 4 Underpressure mirror **Overpressure mirror**

With such mirrors concentration ratios C ≧ 1000 can be obtained (Fig. 5).

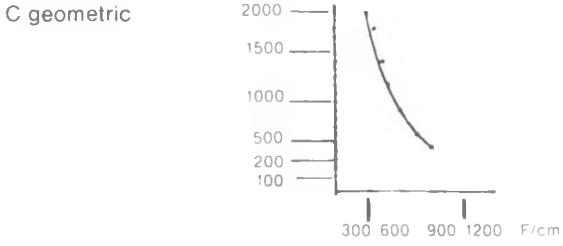

Fig. 5 Concentration ratio of a 3 m underpressure mirror as a function of the focal length F.

By protecting these dishes under transparent domes, a new type of modular, light-weight solar power station is realized (Fig. 6): The SKK = Solar Kuppel Kraftwerk

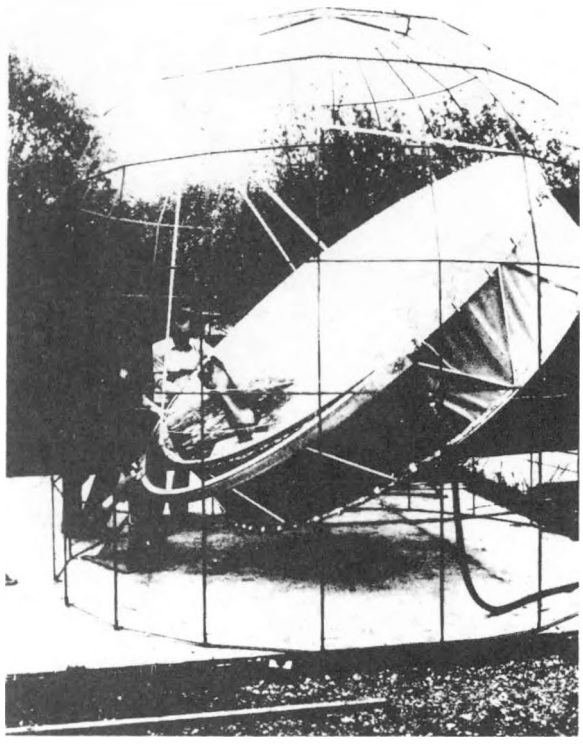

Fig. 6 BOMIN-SOLAR experimental SKK

2. Membrane Technology

Pneumatic solar concentrators are produced by elastic deformation of thin, mirrored plastic, metal, or glass-plates, which are fixed to a surrounding rigid structure. Under neglecting the stiffness, the thickness and the weight of such membranes and assuming that the radial forces S are uniformly distributed around the circumference (Fig. 7).

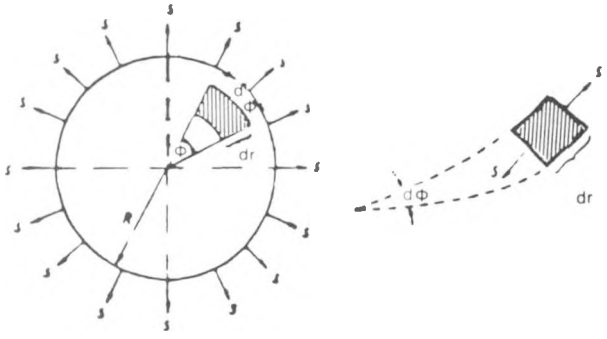

Fig. 7 Air pressure forces on the mirror membrane

It can be shown that the membrane's equilibrium shape (Fig. 8) obtained by solving the differential equation [2] representing the vertical equilibrium of forces in the membrane

$$\frac{d^2w}{dr^2} + \frac{1}{r} \cdot \frac{dw}{dr} = \frac{P}{S} \quad \ldots\ldots\ldots\ldots\ldots\ldots\ldots\ldots \quad [2]$$

is a paraboloid one. Shapes obtained under realistic conditions are slightly differing from the paraboloid, but are sufficient for solar applications (Fig. 8).

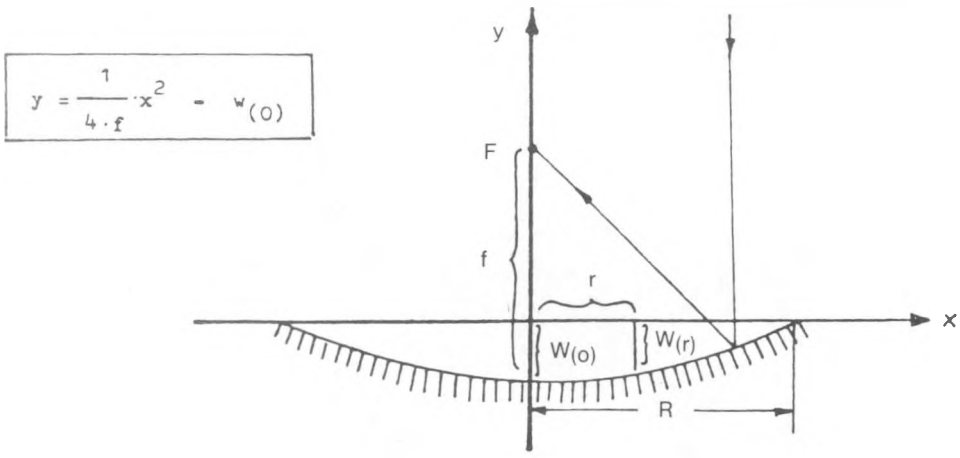

Fig. 8 Elastic deformation shape of the membrane

For the SKK-concept the choice of qualified foils is of extreme importance. Not only the firm Boeing, developing foil-heliostates under protection domes since 1974, (M. Berry, H. Dursch, R. Gilette), but also our firm working on similar problems since 1973 decided that only foils made of fluorine synthetical are coming up to the requirements because of their versatile qualities and excellent long-duration characteristics. Among the numerous foils, the HOSTAFLON-ET, introduced to solar technology by Justi seems to own the most fascinating characteristics.

Resistance of the HOSTAFLON-ET-Foil to atmospheric conditions:

- 5 years of outdoor tests were showing no essential changes of mechanic and optic values.
- Accelerated exposure suggests a life-duration of more than 10 years by a decrease of the mechanical and optical qualities smaller 5%.

Some physical data of the foil

Thermal operation:	– 190°C to 150°C
Melting range:	265°C to 278°C
Transparency (100 µm foil):	95% of global radiation
Tensile strength (at 23°C):	52 N/mm²
Yield stress (at 23°C):	30 N/mm²
Breaking extension (at 23°C):	300%
Tear strength (at 23°C):	500 N/mm

The foil is weldable and metallizable. Therefore it is used not only for the dome-covering but also for the foil mirror.

The exceptional mechanical properties of HOSTAFLON-ET-Foil enabled us to develope a simple sewing-method for the assembly of large membranes.

The BOMIN-SOLAR power station principle has three main advantages against other solar power station conceptions:

- 1. A significant smaller weight per unit of power

  $\frac{\text{(kg of needed material)}}{\text{produced electric kW}} \ll 5.000 \text{ kg/kW}_{el}$
- 2. Simple, economic and precise production of the concentrator mirror
- 3. Protection of the mirror optic against sand, dust and storm.

We developed two modular sizes of 3 m and 10 m in diameter (Fig. 9).

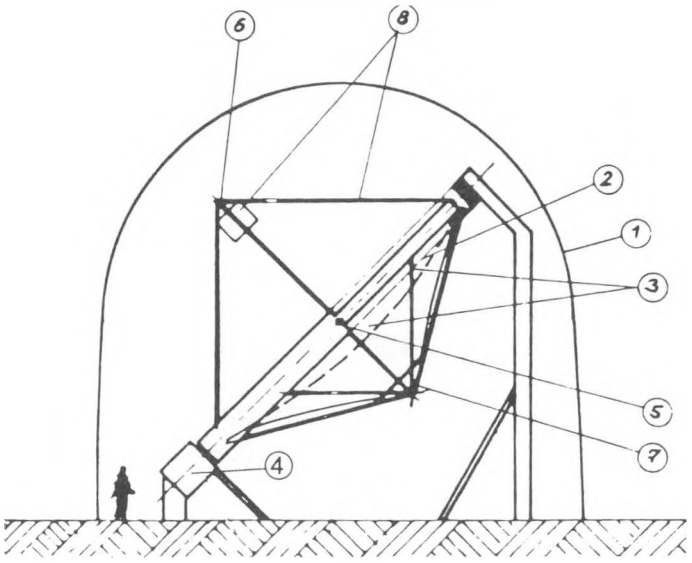

Fig. 9 Profile through the SKK

① transparent dome
② mirror foil
③ underpressure hollow body
④ daily tracking axis
⑤ seasonally tracking axis
⑥ tracking electronic
⑦ underpressure sensor
⑧ receiver and attachement

The system's optical performance is given in Fig. 10.

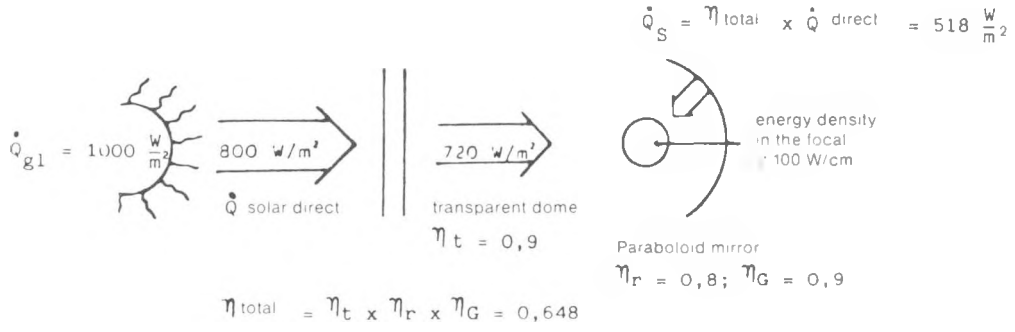

Fig. 10 Optical flow diagram

Technical performance of both systems

diameter of the mirror	3 m	10 m
surface of the mirror	7,06 m²	78,5 m²
weight of the mirror	approx. 200 kg	approx. 2000 kg
weight of the protective dome	approx. 200 kg	approx. 2000 kg
material of mirror and cover	HOSTAFLON-ET	HOSTAFLON-ET
focal length F: variable	1,5 m	5 m
concentration factor C	≦ 2000	≦ 2000
transparency t of protection cover	0,9	0,9
reflectivity r of the mirror membrane	0,8	0,8
performance factor G of the concentrator mirror	0,9	0,9
optical efficiency of the mirror r x G	0,72	0,72
thermal power in the hot spot (with 800 W/m² direct insolation)	3,7 kW	40,7 kW
efficiency ratio of the receiver	0,8	0,8
efficiency ratio of the Stirling generator	0,3	0,3
electric output of the Stirling engine	0,9 kW, AC	10 kW, AC
thermal output (100°C) of the Stirling engine	1,75 kW	20 kW
kg material installed/kW_{el} output	approx. 450 kg	approx. 400 kg
kg material installed/$kW_{el.}$ + kW_{therm} output	approx. 150 kg	approx. 140 kg

Both mirror types can be assembled to SKK-farms (Fig. 11)

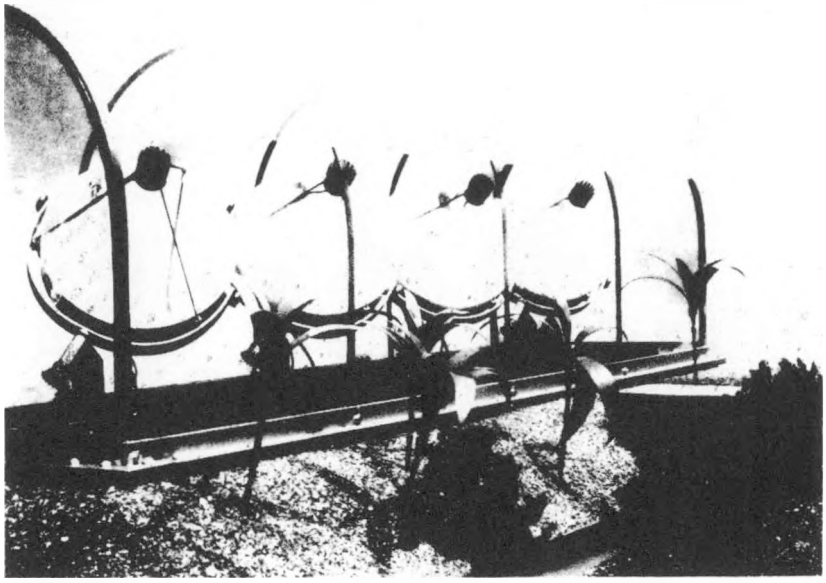

Fig. 11 SKK-farm

In cooperation with Sunpower U.S.A., we developed free piston Stirling generators for the 3 m and 10 m mirror (Fig. 12)

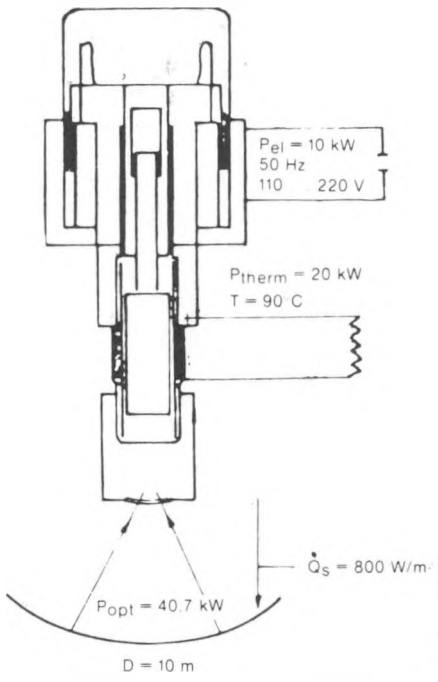

Fig. 12 Stirling-Generator

References

(1) Internal Report, 1979 Seri, 1617 Cole Boulevard, Golden, Colorado 80401

(2) **R. B. Gilette,** Development and Test of Heliostates and Control System for Thermal Power Plants. BOEING Company, Seattle, Internal Report

(3) **H. Fitz,** Hoechst Werke Gendorf, Foils made of Fluorine-Synthetic-Materials. Information paper: Kunststoffe, 70. edition 1980, published by Carl Hauser, Munich 86

(4) **H. and J. Kleinwächter,** Economically Working Big Scale Solar Power Station, Comples Conference, Milano 1979

(5) **J. and H. Kleinwächter,** Solar World Forum, Brighton, England 23-28 August 1981

DESIGN AND CONSTRUCTION OF A 3 kW SEALED STIRLING ENGINE TEST MODEL

AUTEURS : M. DANCETTE, G. WINTREBERT

SOCIÉTÉ BERTIN & CIE

B.P. 3

78373 PLAISIR CÉDEX, FRANCE

Summary

This paper presents the Stirling engine test model that Bertin & Cie has designed and constructed, in collaboration with Creusot-Loire, and with the financial help of the CEC.

The basic principles of a Stirling engine are briefly described and the present technological difficulties which are encountered in the development of these machines are pointed out (gas leakage on the dynamic seals, and pollution of the regenerator exchangers). Then are presented the basic technological alternatives chosen by Bertin to overcome these difficulties (sealed machine, electrical power output instead of mechanical free pistons with dry bearings, and linear generators controlled by an electronic system).The primary aim of the Stirling test model constructed by Bertin is to validate these technological options.

Then the general conception and the estimated power balance of this engine are presented, with the first test results of the various components. These tests have already shown a satisfactory mechanical behaviour, and very encouraging heat exchangers performances.

1. Introduction

The Stirling engine was invented in 1816 by Robert Stirling. Throughout the nineteenth century, many of such "hot air" engines were made. They were reliable, rather safe, but not very efficient. At the beginning of the century these engines were gradually superseded by internal combustion engines. The rebirth of the Stirling engine is due to Philips in Eindhoven in the 1930s, which begun new developments, mainly for refrigerating Stirling engines. During the 1970s, with the depletion of oil supply, a lot of studies have been carried out on Stirling engines, and a few prototypes have been tested. In spite of its numerous advantages, in comparison with the internal combustion engine, the Stirling engine has not yet succeeded in competing with it, because of the severe technological difficulties encountered, as soon as high efficiency is required.

Bertin & Cie has based its development program upon a new basic conception of the Stirling engine to overcome these difficulties, and has made a 3 kW engine test model in order to validate these choices.

The design and the construction of this test modelhave been carried out with the help of the CEC and in collaboration with Creusot-Loire. The DGRST, in France, has also financed part of the engine heat exchangers tests.

The study and the design of the engine have been made from November 80 to September 81. It has been constructed from November 81 to May 82. Then the various components have been tested, and the tests of the whole engine are now just starting.

After describing the Stirling engine principles and the technological choices made by Bertin, the design, the construction and the tests of the components are presented and finally the conclusion of this work is given.

2. Basic principles of a Stirling engine

2.1. Stirling cycle

The theoretical Stirling cycle is a thermodynamical gas cycle, which is composed of two constant volume, and two isothermal processes as shown on diagram I.

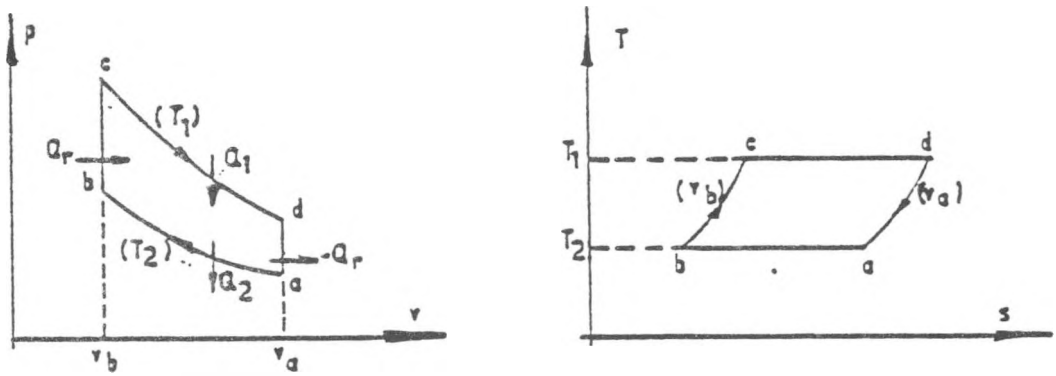

Diagram I : (pressure, volume) and (temperature, entropy) curves of the Stirling cycle

It is a regenerative cycle : the heat Q_r extracted from the gas during the transformation d ⟶ a can be stored in a regenerator matrix, and given back to the gas during the transformation b ⟶ c.

If the regenerator efficiency is equal to 1. , the cycle efficiency is that of Carnot and the mechanical work produced by gas mass unit during a cycle is :

$$W = - r (T_1 - T_2) \log \frac{v_a}{v_b}$$

2.2. Ideal Stirling engine

The ideal Stirling engine is a volumetric external combustion engine, which operates on a Stirling cycle. Such an engine requires a hot exchanger and a cold exchanger to keep the expansion and compression volumes isothermal, and in addition a regenerator, as mentioned in the preceding paragraph.

Diagram II shows the two basic kinds of Stirling engines :

- two pistons engine, with one piston for compression of the cold volume, and one piston for expansion of the hot volume, both of them being used to circulate the gas through the regenerator, between hot and cold side.

- piston and displacer engine, in which the piston is used for both compression and expansion, and the displacer for heating or cooling the gas through the regenerator.

The first kind is called "α-type", and the second "β-type" or "γ" if the piston and the displacer are in two separate cylinders connected with a pipe.

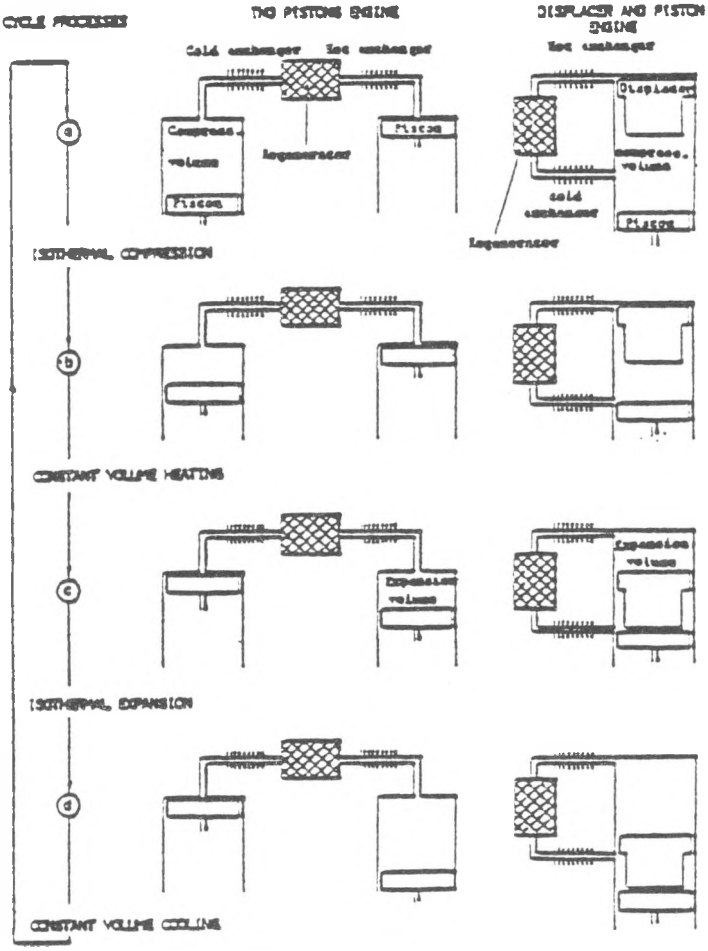

Diagram II - Piston and displacer motions in ideal Stirling engines

2.3. Real Stirling engine

The main differences between a real Stirling engine and the ideal Stirling engine are the following ones :

- piston and displacer dynamics : in the ideal engine, each of the successive displacements of the pistons and the displacer corresponds to a given thermodynamic transformation. In a real Stirling engine, the two bodies move simultaneously (according to linear oscillating almost sinusoidal motions, with a phase angle near 90°, as it is shown on diagram III). As a consequance, the (p, V) curve of the thermodynamic cycle is made round, and the power output for a given machine is lowered, although the efficiency is still that of Carnot.
- dead volumes : in the ideal engine, only the volumes swept by the pistons and the displacer are considered. In a real engine, the "dead volumes" (heat exchangers, pipes, etc...) represent more than 50 % of the total gas volume, which lower the compression ratio and the power output.
- adiabatic volumes : in the ideal engine, it is assumed that the volumes are isothermal. This is nearly true for the heat exchangers volumes, whereas the swept volumes of the moving bodies rather behave like adiabatic volumes. This causes the mixture of gases at different temperatures, which reduces the overall efficiency.
- thermal and mechanical losses : also occuring in a real engine, the following phenomena result in reducing the efficiency :

. heat exchangers and regenerator lack of efficiency
. heat loss with surroundings
. heat conduction between the hot and the cold parts

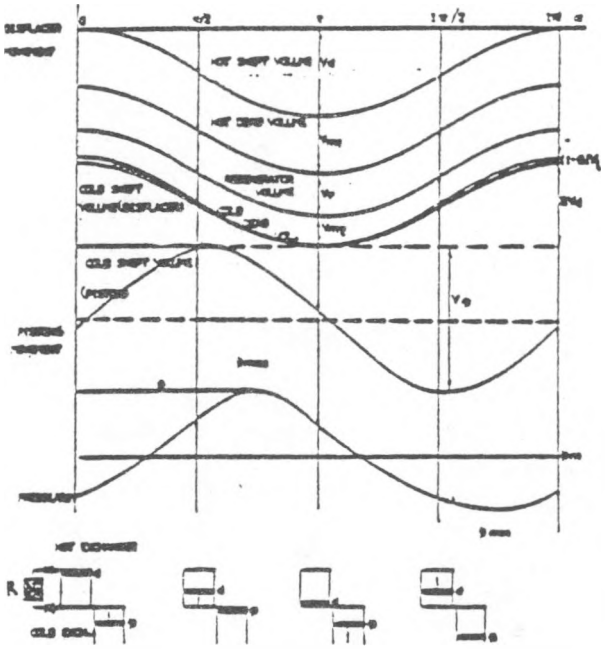

Diagram III : Piston and displacer motions and pressure variation in a real γ-type Stirling engine

. pressure drop in the exchangers, the regenerator and the pipes
. gas leakage through the piston and the displacer seals
. mechanical friction losses

3. Stirling technological difficulties and Bertin's basic conception

The two main technological obstacles to the development of reliable Stirling engines are the following ones :

a) in order to reach high heat exchangers efficiency, it is necessary to use a high thermal conductivity gas, helium or hydrogen, as a working fluid. This gas must be pressurized (30 to 100 bar) to get reasonable specific power. The piston seal must prevent leakage of this gas from the engine. The problem of the reliability of such a dynamic seal is not yet satisfactorily solved.

b) Stirling engines use a regenerator heat exchanger, which must be very efficiant (between 98 and 99 %), as the energy stored in this exchanger is five to ten times greater than the energy transferred by the hot exchanger on a cycle. A large exchange area within a small volume is required for this regenerator which is made of a woven-screen matrix of very small hydraulic diameter (≈ 100 µ).

Classical mechanical arrangements (swashplate or crank driven engines) require a lubricating system, which induces accumulation of oil particles in the regenerator, inhibiting the gas-flow.

The Bertin & Cie Stirling engine research program is based on three basic alternatives, which were made to overcome the two difficulties mentioned above :

1) the power output is electrical, instead of mechanical, and the whole machine is sealed and filled with the working fluid. Nothing but a static seal is required for the power lead to pass through the crankcase, which is well known and reliable.

2) to prevent pollution of the regenerators, oil must be suppressed, and, consequently, all complicated mechanisms. So it was chosen to use a free displacer and free pistons associated with rectilinear alternators. The low radial strength allows the use of dry bearings.

3) dynamic control of the displacer and pistons motion is no more insured by connecting rods, but by an electrical coupling.

In order to validate these three basic technological options, Bertin has designed, constructed and started testing a 3 kW Stirling engine test model which is described hereafter.

4. Conception and design of the Stirling engine test model

4.1. General conception

The general conception of Bertin's engine test modal results from both technological analysis and theoretical models describing the thermodynamical, thermal, mechanical and electrical processes occuring inside the machine. The main characteristics of the engine are given hereafter, before presenting briefly the particular studies which were carried out, in order to validate the final design.

4.1.1. Thermodynamical cycle

The working gas is helium. Its pressure varies from 37 to 55 bar. The nominal temperatures are 590°C for the expansion volume, and 70°C for the compression volume.

4.1.2. Mechanical arrangement

The test model is a γ-type engine, with one displacer and two power pistons in opposition, in separate cylinders, the axis of which are perpendicular. The displacer is driven by a rod moved by an electric motor. It is

intended to replace it by a rectilinear electric motor in the future. The displacer is guided by the rod, on two dry bearings. The two power pistons in opposition are associated with two rectilinear generators, developed by MM. JARRET. The oscillation of the pistons is controlled by the gas spring of the working fluid itself. Only a small mechanical spring is required to center the pistons motion. When the displacer is moved at the resonance frequency of the pistons, it can be shown that the pistons stroke and the mechanical power are maximum, and the phase lag of the pistons relative to the displacer is about 90° , The pistons are guided by two dry bearings, one on the piston itself, and one at the end of the piston rod.

The nominal frequency is 50Hz which is a compromise between the heat exchanger efficiency and the generator electrical efficiency. Nominal strokes are 25 mm for the displacer and 42 mm for the pistons.

Pressure tightness on the pistons and the displacer rod is simply insured by the very small bearing clearance (1 to 2/100mm). Pressure tightness on the displacer cylinder itself is insured by a row of labyrinths.

4.1.3. Dry bearings

The nominal operating conditions of the dry bearings of the pistons and the displacer rod are :

- diameter : 20 and 66 mm
- maximum speed : 4.2 m/s and 6.7 m/s
- maximum load : about 1 bar
- clearance : 1 to 2/100 mm
- friction coefficient : $\leq$ 0.1

Experience is very poor in that field of dry friction at low load and high speed. So it was decided to start a large test program, in order to select the couples of materials which can operate in such conditions. This program is carried out in collaboration with CREUSOT-LOIRE and with the help of the CEC, and its interest widely exceeds the field of Stirling engines (applications to dry compressors and internal combustion engines are considered). Presently, a few materials have already been tested and the two best adapted that we have selected are the following ones :

a) pistons coated with Molybdenum, and cylinders in nitrided stainless steel,

b) pistons and cylinders coated with a ceramic layer, called "Hexaplasma".

The first couple of materials has been chosen for the Stirling engine, for it is presently better known by industrial manufecturers.

4.1.4. Heat exchangers

The hot exchanger is composed of 24 pipes drilled in a flat plate. It has been designed either to be put at the focussing point of a parabolic dish, or to use a gas burner as the hot source.

The mean nominal temperature of the plate is about 670°C. It is made of refractory steel. The cold exchangers are 12 water cooled exchangers, each composed of 5 tubes in which helium is circulated. The regenerators are made of 12 woven-screen matrices, with a porosity of 70 %, a nominal thermal efficiency of 98.6 % and a maximum pressure drop of about 0.4bar.

4.1.5. Electric generator

The electrical power output is insured by a rectilinear generator, which has been developed by MM. JARRET for their internal combustion free piston engine. These generators have been designed for an operating frequency of 100 Hz but presently we use them only at 50 Hz. These generators are driven by an electronic control and connected to an electrical battery (72 V).

4.1.6. Control and regulating systems

The three main regulating systems are :

- regulation of the hot exchanger temperature controlled by the hot

source power,

- regulation of the displacer frequency, controlled by the electric motor potential,
- regulation of the electrical battery potential.

In addition, the piston stroke is controlled by excitation of the generator coils.

4.2. Final design

4.2.1. Second order model

In order to design the engine, Bertin & Cie has made a theoretical model, including all the thermodynamical, thermal and mechanical irreversibilities which are calculated independently and successively (a so-called "second order model").

The "first order model" is that of an ideal Stirling engine, taking account of dead volumes and sinusoidal motions for pistons and displacer. With that model, it can be shown that the mechanical power output of the engine is :

$$W = \frac{\pi}{4} f p \frac{V_d V_p}{V_o} \sin \varphi \left(1 - \frac{T2}{T1}\right)$$

With :

f	frequency
p	mean pressure of the cycle
T_1	hot volume temperature
T_2	cold volume temperature
V_o	total working fluid volume, referred to the cold temperature
V_d, V_p	volumes swept by the displacer and by the two pistons
φ	phase angle between displacer and pistons

From this first order model, the various losses are then calculated, in order to set up the net power balance of the engine (see Fig.IV).

4.2.2. Power balance of the engine (calculated)

With the final design of the engine, the power balance is the following one (in Watts) :

- Hot source power	q_{n1}	= 10,000
- thermal loss to surroundings	q''	= 400
- thermal loss inside the engine	q'	= 2,030
- useful hot thermal power (first order model)	q_1	= 7,570
- total mechanical power to the pistons (first order model)	W_p	= 4,010
- total mechanical power to the displacer (first order model)	W_d	= 530
- pistons mechanical losses	W'_p	= 410
- displacer mechanical losses	W'_d	= 740

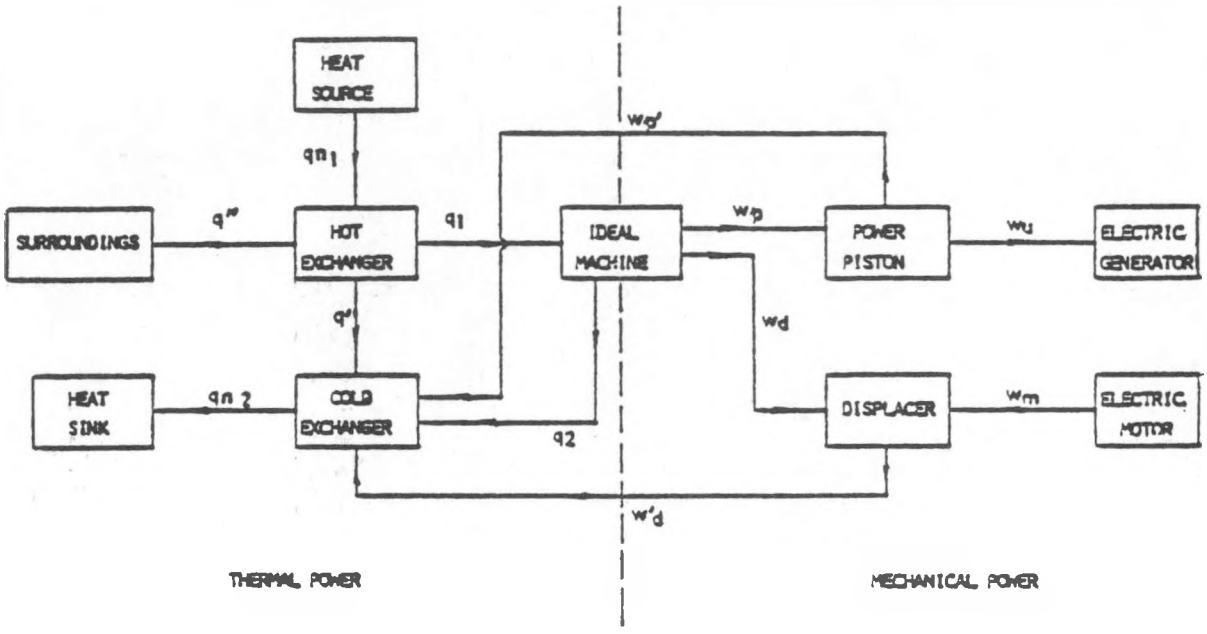

Diagram IV - Power balance of a Stirling engine (second order model)

- net mechanical power required by the displacer	W_m	= 210
- net mechanical power of the pistons (available)	W_u	= 3,600
- thermal power extracted by the cold exchangers	q_{n2}	= 6,200

5. Construction of the test model

After the final design of the machine, detailed plan were drawn and the various components were fabricated and checked before being assembled.

Fig. V shows a general schematic view of the thermodynamical part of the engine. Photographs VI, VII, VIII and IX show some of the most important pieces, and photograph X the heat exchangers assembled.

6. First experimental results on the engine test model

During a step by step assembly of the engine, tests were made on isolated components of the test model, in order to verify the good behaviour of mechanical parts and to measure the thermal performance of the heat exchange components.

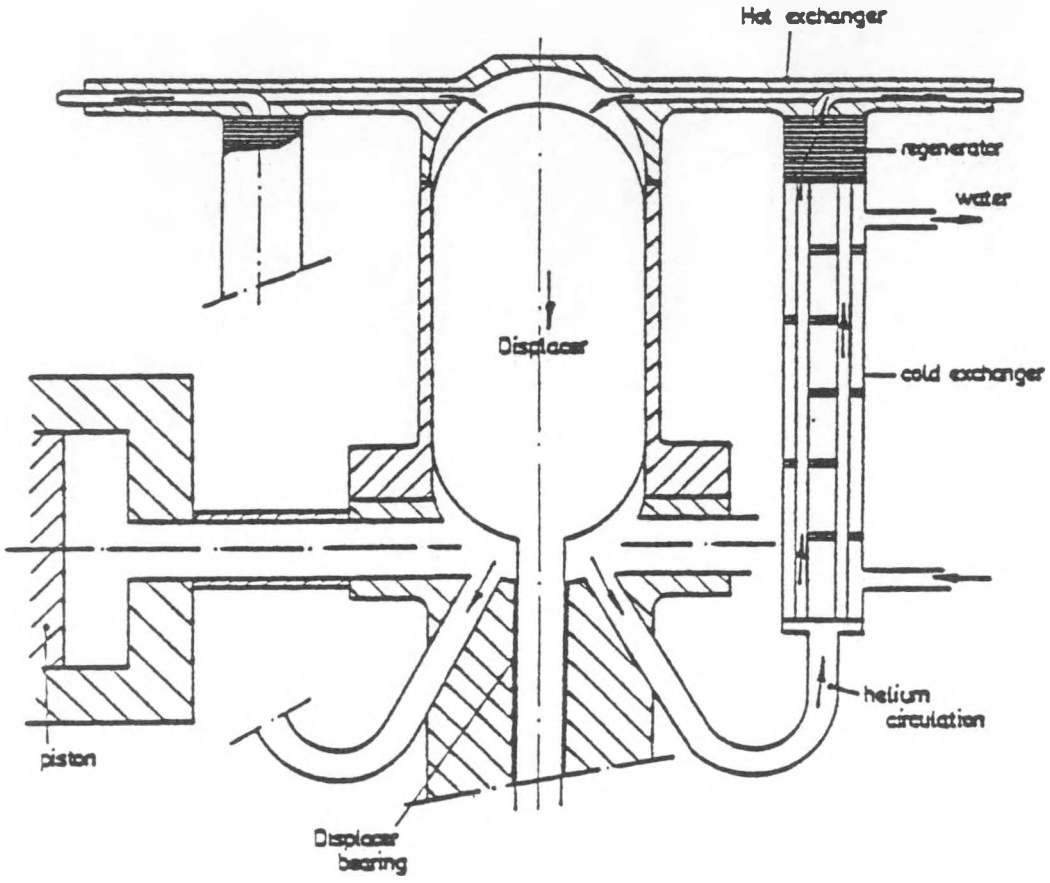

Diagram V - General schematic view of the Stirling engine test model

First, the displacer driven by the auxiliary motor were tested separately to check the reliability of the dry bearings. The mechanical friction was satisfactory and almost no abrasion could be seen after more than 50 hours testing.

Then, the heat exchangers were assembled and the crankcase was pressurized, allowing to make measurements of the pumping loss and the thermal losses with periodic flow conditions very similar to the actual engine conditions. A complete instrumentation of the test model was used to make a first energy balance with no power output.
Good agreement was found between the experimental results and the calculations of the theoretical model, and thus the overall expected performance of the engine is confirmed. We give results for a typical case hereafter.

frequency	: 42.5 Hz
hot temperature	: 320°C
cold temperature	: 35°C

	Measurements (W)	Model (w)
Thermal losses (altogether)	1,000	1,100
Regenerator thermal loss	550	600
Pumping loss	300	230
Mechanical friction loss	100	90

The measured thermal losses, perfectly significant of the Stirling engine losses, show less than 20 % discrepancy with the estimated value.

A particular study of regenerator effectiveness was made, and allowed to validate our theoretical model based on quasi-steady assumptions for heat transfer phenomena. In the case above, we assessed a very good efficiency of 98.5 %.

We also paid particular attention to the flow friction losses, measuring the pressure drop through the heat exchangers and the resulting pumping loss. All results are reported on diagram XI and compared to the calculated values. The quasi-steady evaluation was found to under-estimate the maximum pressure drop by 60 % at the highest frequency, and the pumping loss by 30 %. The discrepancy increasing with higher frequency is probably due to non stationary phenomena associated with periodic flow conditions.

During those tests, we observed a satisfactory behaviour of this part of the engine regarding pressure tightness of dry bearings, loss vibrations of the machine, and small deformations due to thermal stresses (at 350°C).

So far, those first results are promising for the overall performance of the engine test model.

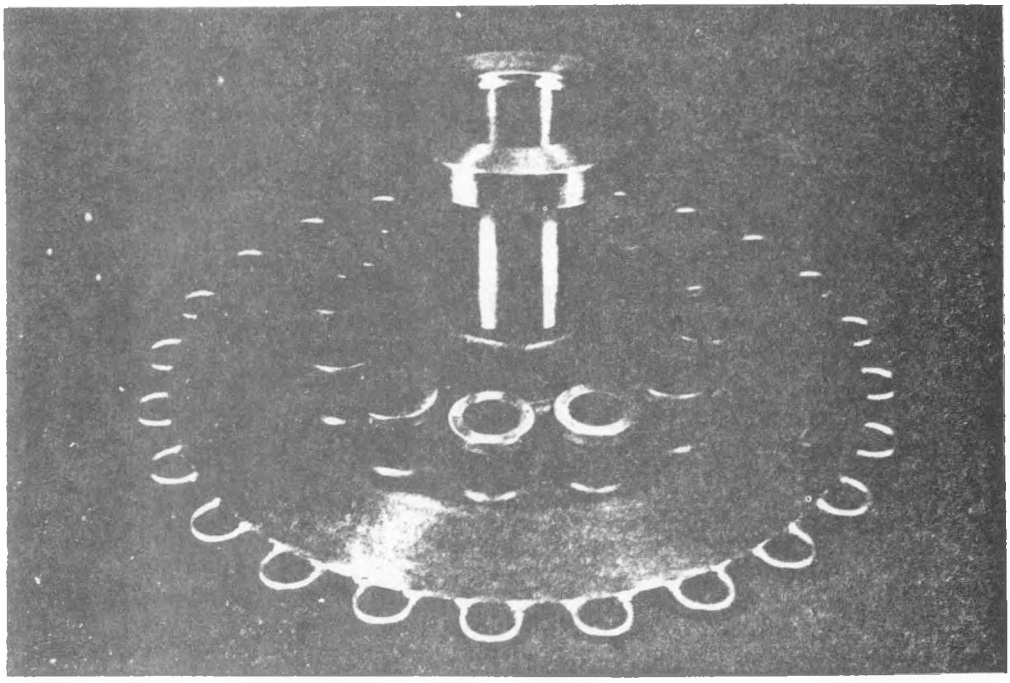

Fig. VI - Hot exchanger

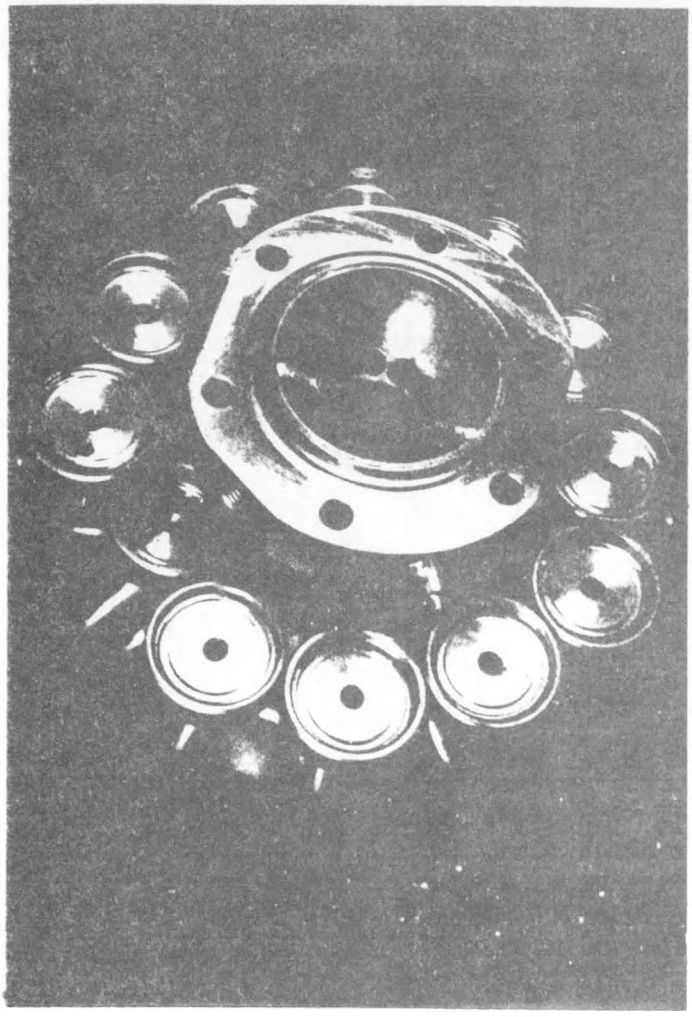

Fig. VII - Displacer cylinder lower part

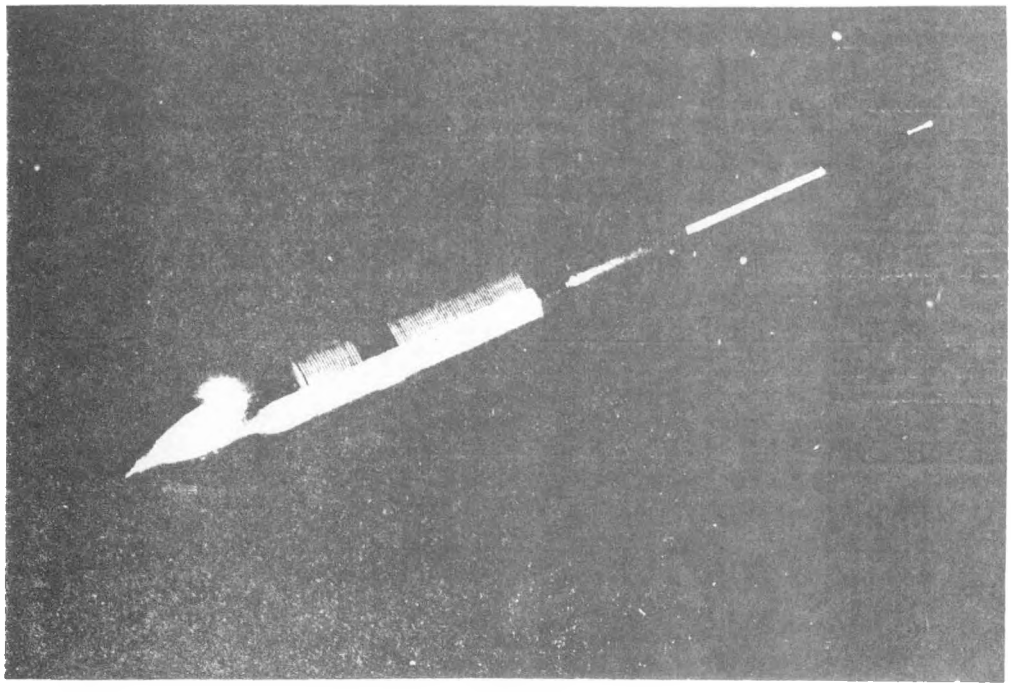

Fig. VIII - Displacer

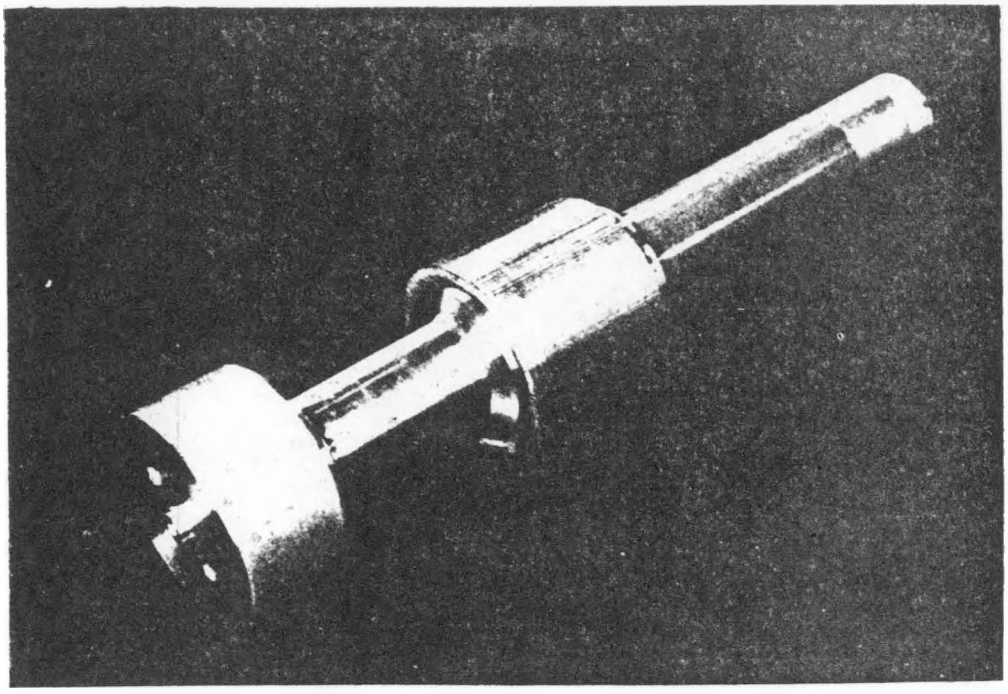

Fig. IX - Power piston and generator rotor

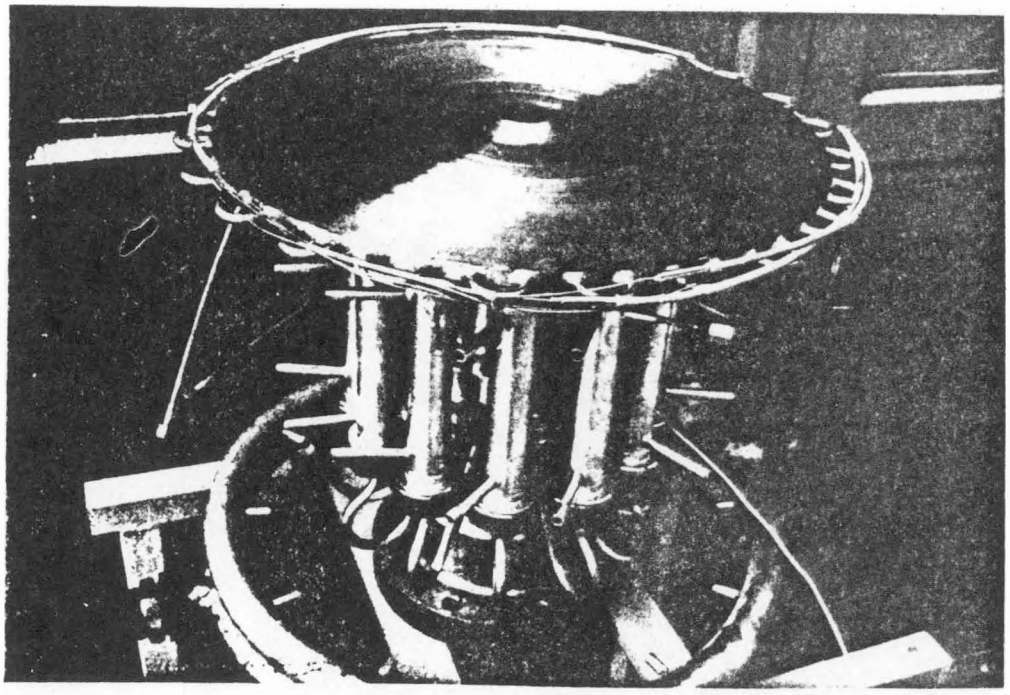

Fig. X - Heat exchanger assembled

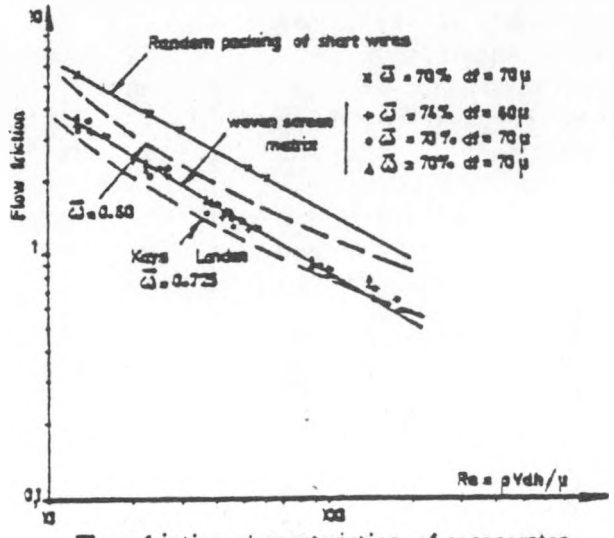

Flow friction characteristics of regenerator matrices (static flow)

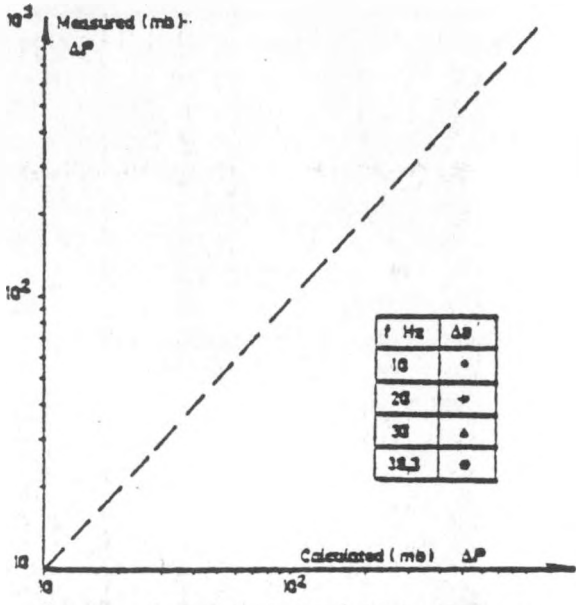

Pressure drop through the heat exchangers with periodic flow conditions (for maximum instantaneous mass flow)

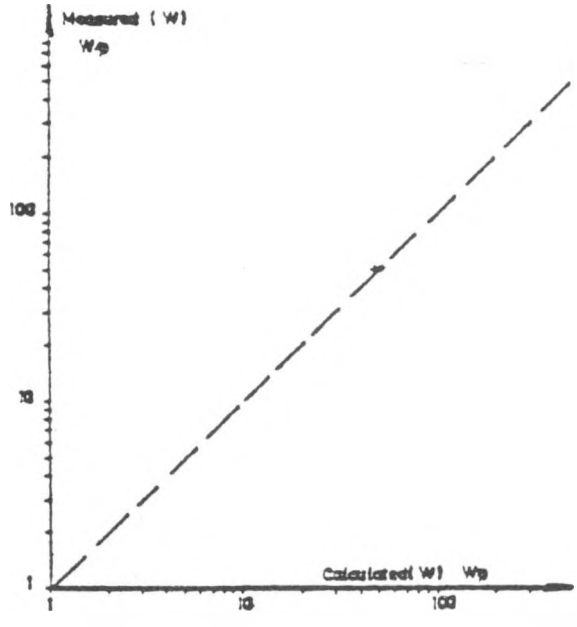

Pumping loss through the heat exchangers with periodic flow conditions

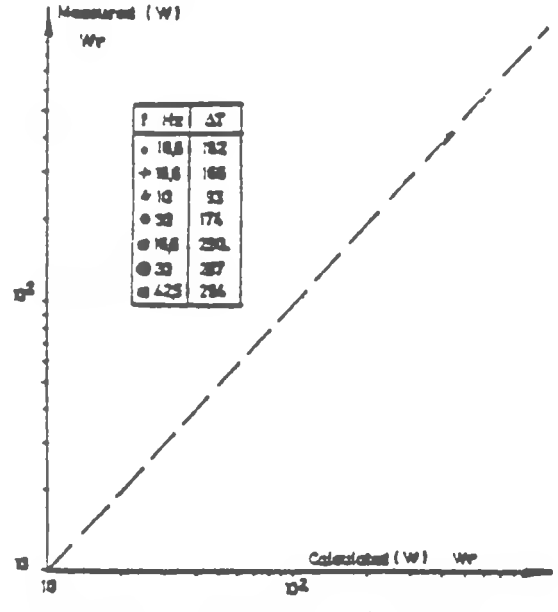

Regenerator thermal loss with periodic flow conditions

Diagram XI - The measured values are results from tests on the Stirling test modal (the power pistons being isolated)

7. Conclusions

Bertin & Cie has designed and constructed a Stirling engine test model in order to validate basic technological alternatives to face the present difficulties encountered in the development of such machines.

The tests of the various components have shown satisfactory mechanical behaviour, and very encouraging performances of the heat exchangers. Dry bearings of the displacer rod have been tested more than 50 hours without any friction or abrasion problems. The tests of the whole engine are just starting at the end of October 1982.

It is now intended to carry out a large test program of the engine model, during 18 months, in order to validate the three basic options made by Bertin & Cie, to test all the technologies used in that engine and to measure the characteristics of the various components and of the whole test model.

Then, Bertin & Cie will be in position to start the design and the construction of Stirling engine prototypes for precise applications and well identified markets.

SOLAR POWER FOR ISRAEL

Aharon Roy and Michel Izygon
Ben Gurion University of the Negev
Beer Sheva, Israel

and

Sidney Hoffman
President
Energy Projects Corporation
Jerusalem, Israel

Israel has no oil, gas or coal of its own. All energy needs are supplied through the purchase of fossil fuel from other countries, many of which are far away overseas. Consequently, energy is expensive here. The cost of electricity is 8(USA) cents per kWh and is on the rise.

Israel is blessed with sunshine and industrious manpower. Solar insolation, 2000kWh/year/m² direct normal radiation; in some areas, even more. No wonder that solar flat-plate collectors for water heating are widely used here. In relative terms, solar heating is used here more than in any other country in the world. However, the fuel replaced here by solar hot water is just 1-2% of the national energy bill. Extending the usage of solar energy to more applications, in particular steam and electricity, is required.

It is of great interest to note some characterizing features of the flat-plate collector industry here. Production scale is of the order of 100,000m² a year. Several dozens factories or shops produce them. Installation is done by trained workers. You should see how quickly they transport, assemble and install a unit on a house. The parts come in a modular form and it is a simple matter to put them together. The final installed system is cheap, around 100-150 dollars per aquare meter collector. This includes everything, including also a hot water storage tank with an electrical element (for backup), thermostat, switches, lines, etc. The installed system is much cheaper than in many other countries, and this is despite the fact that Israel has to import most of the materials of which the system is made. The reason for the resultant cost-competitiveness of the installed system is the cheap labour involved, the adequate scale of production and the simplicity of the design. It seems that a major factor in this simplicity is the moderate size and weight of the units that can be handled by a small crew of 2-3 people without resort to a crane and other expensive tools.

We think we can apply this commerciallization philosophy also to the development of the parabolic dish thermal power in Israel. We are planning the design of relatively small dishes, e.g., 3-4m(dia) (around 10m² net) to be constructed from locally available materials and by simple production methods. Five to ten such dishes in a N-S row should not require extensive piping and such a row may replace one of the more customary, large dishes (7-11m.dia). It will be designed for easy maintenance, and probably also with capabilities for periodic alignment or replacement of mirrors.

We plan to compare the cost-competitiveness of the system based on this concept with others by techno-economic models in which the annual (life-cycle) cost plus maintenance, and the efficiency (losses, parasites, etc.) for each subsystem, are

functionally defined[1] and verified. This will help identify the priorities for R & D work. For instance, we may find that we have to divert research efforts towards minimizing piping losses.

In Israel hot water costs 6-8 cents/kWh(even for solar heated water). Commercialli-zation of the dish technology may be enhanced by co-generation of electricity and hot water. System costs of even 300-400$/m² (dish-area) may become cost competitive near customers for hot water. This will justify sizeable production rate and then production-type tooling (and various improvements), thereby decreasing costs and opening new markets. We thus may develop a parabolic dish industry, a challenge which is facing us all for quite a while. Putting it in more general terms: based on the successful solar experience in Israel we suggest a particular interaction with our end-users and our local labour and production capabilities. This should strongly affect integration optimization, and the final system design.

We feel that Israel is a very good place for a very near-term large scale commer-cialization of the dish technology. If this can be accomplished, it should help boost and extend viability and advanced R & D in this field. We shall be glad to tie links of cooperation with researchers and developers in this area, and get suggestions from potential vendors for subsystems, components and materials. We may also wish to hear of potential people of experience for hire for Israel.

References

1. Aharon S. Roy, "Economic Methodology for Solar Power-Generating Systems", Proc. 13th IECEC (San Diego), 20-24 August 1978, Vol.3, pp.2175 - 2179.

THE WHITE CLIFFS SOLAR POWER STATION

Stephen Kaneff
Australian National University, Canberra, Australia

We have had an interest in concentrating collectors for some 10 years, stemming from the need for high temperatures in our long term project on solar thermochemical power systems, the advantages of such systems residing in the potential for storage, both short and long term and the relatively lossless transport of energy from a collector field to a central plant, coupled with the long term prospects for using such systems to produce various energy rich products in a relatively benign manner.

Accordingly various concepts have been explored over the years (for example the thin metal shell paraboloids of a colleague Dr. P.O. Carden and the development of various relationships whereby manufacturing imperfections of the elements of an array can be more economically compensated by computer control than by more precise manufacture, as studied by Dr. B.P. Edwards), but beyond producing single prototype units, little was done prior to 1979.

In July 1979 a Grant was obtained from the New South Wales State Government who perceived the need to supply remote and inland communities with power from sources independent of oil based units. A proof of concept system was specified, employing high temperature technology based on steam and a simple uniflow steam engine as this was seen to be more appropriate as regards maintenance on the spot by those versed in motor vehicle repairs and servicing, the steam engine being realised from converting a diesel to steam operation, thereby again facilitating maintenance and the availability of spare parts. A power output of 25 kWe was chosen as being not too small to be considered a toy and not too large as to be potentially too expensive as a starting point. No storage was to be provided in the first instance but this was

intended, along with a facility to use waste heat from the station for water desalination, as a second stage of the project.

However, when White Cliffs* was eventually selected for the site for the station some 6 months after the project had commenced, the need arose for a stand alone system since there was no existing town supply. Battery storage for overnight operation was selected as being readily realisable together with diesel back up in case of cloudy weather. A flash boiler was also part of the system to enable testing of the steam engine and to act as an emergency supply in case of diesel unavailability. Subsequently the station was also required to run automatically and unattended in line with the remoteness of the site and the difficulty of availability of suitable maintenance personnel, apart from day to day routine checks.

Component development was carried on until August 1980, after which engineering designs and manufacture were commenced. The dishes were completed by February 1981, installed in June and tracking in August. Station hardware was completed in December 1981. Commissioning tests were commenced in January 1982 and specifications were met (after a number of minor changes and optimising of operating strategies) in early June. Other changes have subsequently been made, notably to the absorbers (single turn coils instead of double turn) and generally efforts designed to improve reliability to match that normally expected of commercial fossil fuel systems as viewed by the consumer.

---

* White Cliffs is a small (40-50 townspeople) opal mining community some 1100 km west of Sydney. Only the town is connected, not the surrounding mines with their sometimes hundreds of transient miners, who generally live underground.

1. The Collector Array

Fourteen 5 metre diameter paraboloidal dishes, each arranged to track in an altitude/azimuth mode are set in two diverging rows away from the plant, away to the south (a better from the viewpoint of length of steam pipe arrangement would have been to site all collectors on a north-south line with the plant in the centre of the array). As is evident from the photograph of one arm of the array, each dish is supported at the rim by a steel frame which pivots horizontally and is carried by a pedestal around which it rotates. The pedestal is simply a pipe 30 cm. diameter set in a 60 cm. diameter hole in the ground, 3 metres deep. A shadow disk sensor provides signals to each drive motor (printed circuit motors drawing a total current which averages some 20 watts in the absence of wind) driving through cyclodrive gearboxes then a lead screw in the case of the elevation actuator and a 2 metre diameter ring in the case of the azimuth drive (providing a 30:1 reduction). To allow slewing from the same units, the tracking is intermittent with a mark space ratio of about 60:1. An inhibit signal is provided after each axis has brought the sensor signal to zero in the tracking mode, thus preventing very effectively any oscillations which might otherwise occur in buffetting winds as a result of the resilience in frames and supports while at the same time maintaining tracking accuracy. The sensors are mounted at the top of the dish rims.

The dishes themselves are constructed as a fibreglass substrate moulded around the supporting ring and lined with some 2300 glass mirrors shaped to match the paraboloid (plane mirror segments glued with RTV adhesive). The dish rim angle is 70^{o} which allows the absorber to be mounted from the centre of the dish with little trouble. The units have been designed to maintain operation at wind speeds up to 80 km/hour and then to park in the vertically facing position if wind velocities

increase beyond this figure, which in fact has not been recorded during three years of records - although speeds near this value have occurred several times and successful operation has been confirmed. See Figure 1(a).

In the environment of White Cliffs we have determined an operating strategy as regards dish cleanliness as follows: Normal parking involves facing horizontally to the south, the horizontal facing position gathering the least dust and dew. Operation over most of 1982 has required cleaning less often than every two weeks with a notable recent exception in November when ten days after a previous cleaning and in the presence of fine dust in the atmosphere for several days, followed by some rain, the dishes were found to have dropped their output by 20% ! This fortunately is not a regular occurrence but denonstrates the need for continual vigilance. Our cleaning procedures are quite simple - an implement made from a broom covered with foam plastic to provide resilience and ready accommodation to the dish contours is covered with a lambswool pad and held in a suitable manner on the end of a long pole (a 2" diameter PVC pipe) which allows a firm but flexible movement over the dish surface - dry - when the dish is tracking in the early morning or late afternoon. Depending on whether the dish is simply dusted with very fine particles or caked, so cleaning time per dish varies from less than 10 minutes to some 20 minutes. Fortunately there is no grime.

The collector array has given very few problems and has been retained in the as designed and installed form without change. We consider it successful.

2. The Steam System

Many considerations led to use of steam as an energy transport medium, not the least being the large amount of conventional wisdom accumulated over the years and, as it turned out, a

Figure 1(a). Paraboloidal Dishes at White Cliffs Solar Power Station, Australia

misplaced understanding that a working high performance steam engine could be obtained as a custom built purchase from experienced organizations. Steam car enthusiasts have been developing high performance engines for a long time but have apparently not produced units which can be considered to be reliable on a commercial basis. Having obtained an engine which isbased on a simple and elegant concept, we had to spend the major part of the effort on the project in turning this into an acceptable unit for power station operation.

Associated with the plane mirror segmented reflecting surface is a semi-cavity absorber (a true cavity being not practicable) designed to have good performance. A feature of the mirror segmented design is the fact that energy densities are less stringent than in units with 'perfect' optics, thereby allowing the absorbers to be subjected to less thermal stress, especially under transient conditions of motion or of solar variation. Figure 1(b)shows the arrangement of each absorber which receives feedwater at pressures up to 70 atmospheres (1000 p.s.i.), equality of flow in each unit being assisted by water flow equalizers which drop the pressure some 10 atmospheres (150 p.s.i.) at rated flow of 3.71 ml/s. per absorber. The water flows through azimuth and elevation rotary joints then to the absorber preheater and main absorber where steam is generated at temperatures of up to 550^{o}C and pressures of 70 atmospheres (1000^{o}F, 1000 p.s.i.).

The steam gets its final degree of superheat in the cavity section of the absorber (insulated by a stainless steel cap lined with kaowool (calcium silicate) insulation), then flows through the rotating joints to the steam line which takes it to the engineroom. All steam ducts where practicable are lined with microtherm insulation. Table I indicates the various design specifications and parameters for the absorber and Table II indicates performance. It may be noted that efficiency of conversion from direct component of solar energy varies from about 74% for steam at 250^{o}C and 7 atmospheres pressure

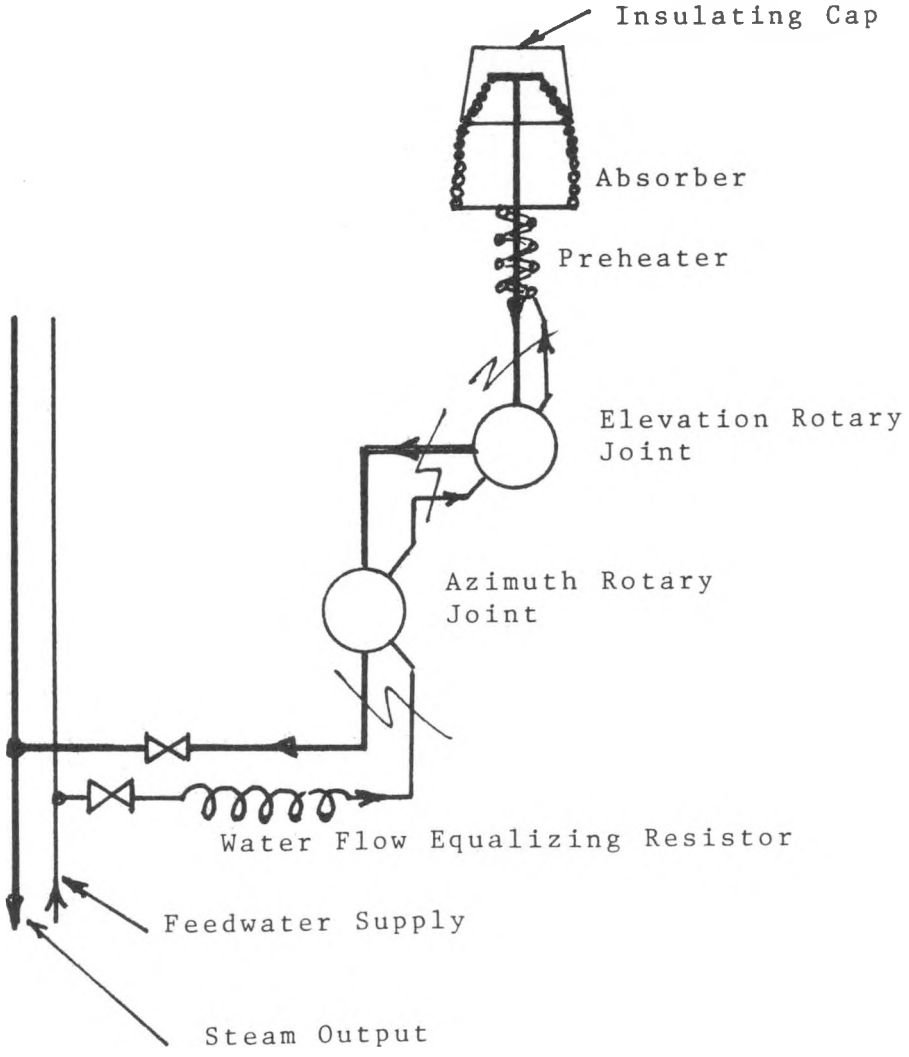

Figure 1(b). Collector Fluid Circuit

TABLE I

WHITE CLIFFS ABSORBER SPECIFICATION (ANU 5 metre dish)

Dish Specifications

Diameter	:	5.06 m
Aperture	:	20 m^2
Facet Size	:	100 mm square
Rim Angle	:	70^o

Absorber Materials

Single tube spiral	:	0.375" x 22 SWG 321 SS
Feedwater Tubes	:	0.25" x 22 SWG 321 SS
Exit Steam Tube	:	0.375" x 20 SWG 321 SS
Steam Tube Focal Protection	:	Stainless steel outer tube
Manifolds	:	316 SS
Absorber Cap	:	
Intermediate Insulation Former	:	2" x 16 SWG 316 SS
Lower Absorber Post	:	Galvanised Steel - 4" Rectangular Section
Absorber Surface	:	Pyromark Black Paint
Steam Tube Insulation	:	Microtherm Block

Input and Losses (estimates)

Design Insolation at Dish	:	1.0 kW/m^2
Design Reflectivity	:	0.80
Fractional Interception	:	0.95
Absorbtivity	:	0.95
Convection Loss	:	100 W
Reradiation Loss	:	200 W
Conduction Loss from Steam Tube	:	100 W
Conduction Loss from Cap	:	50 W

Fluid Flow and Heat Transfer

System Pressure	:	6.9 MPa (1000 psi)
Absorber Pressure Drop	:	6.8 kPa (1 psi)
Steam Exit Temperature	:	550^oC
Maximum Wall Temperature	:	600^oC
Typical Heat Transfer Coefficient	:	0.2 W cm^{-2} $^oK^{-1}$

Stresses

Absorber Tube Wall Stress	:	4000 psi
Steam Tube Wall Stress	:	4800 psi
600^oC Allowable 0.2% Yield Stress	:	15300 psi
600^oC Allowable Creep Rupture Stress	:	8400 psi
100,000 hrs 650^oC Creep Rupture Stress	:	6800 psi
10,000 hrs 700^oC Creep Rupture Stress	:	7000 psi

Approx. only (figures refer to earlier design

Dish Focal Measurements (by Moon Shots)

95% Capture Focal Diameter	:	400 mm
95% Aperture Concentration Ratio	:	160
Flux Concentration Ratio	:	410

(Flux Concentration Ratio is relevant to the absorber design)

Output

Absorber Design Efficiency	:	0.88
Design Output Power	:	14.0 kWt (at 1 kW/m^2 insolation)

TABLE II

Test Results from ANU 5 metre dish

Location of Test: White Cliffs N.S.W.
Date: 7 April, 1982

Description of test:

An individual collector tracked the sun while fed with feedwater from a 3 cylinder reciprocating pump whose back pressure can be adjusted. Flow of feedwater was measured from calibrations of the pump and array system taking into account back pressure. Readings of insolation were taken from a pyrheliometer at the station. Temperature was measured at two points, the absorber coils on the side away from the sun (under the insulating top cap) and in the steam line between the two rotating joints respectively conveying steam and feedwater via the azimuth and elevation axes. J-type thermocouples whose voltage was read by high impedence meters were employed for temperature measurement. Enthalpy was obtained from steam tables.

Average reflectivity of morror glass was ascertained at 0.84, using a pyrheliometer measuring the direct and reflected beams.

time	Insolation W/m^2	Input Power kW	Feed water back press. p.s.i.	Steam Press. p.s.i.	Feed water flow ml/s	Added Enthalpy kJ/kg	Absorb. Temp. ^oC	Steam Temp. ^oC	Output kW	Efficiency %	Output at Insolation of 1 kW/m^2
3.33	860	17.05	150	100	4.4	2856	348	254	12.6	74	14.6
3.48	853	16.91	250	200	4.45	2806	337	243	12.5	74	14.7
3.53	849	16.83	380	330	4.1	2990	368	334	12.3	73	14.5
3.56	847	16.79	500	460	4.1	2993	372	343	12.25	73	14.5
4.00	842	16.69	640	600	3.87	3141	466	413	12.2	72.5	14.4
4.04	837	16.59	780	740	3.74	3186	507	439	11.9	72	14.2
4.07	833	16.51	900	860	3.56	3294	587	482	11.7	71	14.0

Input Power = Nett aperture area x incolation = 19.82 x insolation
$19.82\ m^2$

Cold water calorimetry gave values of 75% efficiency, or 14.8 kW output at an insolation level of 1 kW/m^2

The values in the last column in the table are projected for an insolation level of 1 kW/m^2 on the reasonable assumption that the efficiency will not change very much in moving to this output.

(100 p.s.i.) to 71% for steam at 480°C and 59 atmospheres pressure, corresponding respectively to outputs of 14.6 kW and 14.0 kW respectively in the steam. In the latter case the steam entering the engineroom from all 14 collectors is some 160 kW thermal.

The steam system is illustrated in Figure 2, the path followed by the steam after entering the engineroom being as follows: If the steam conditions are such that the pressure and temperature are inadequate, a motor-driven bypass valve diverts the steam to the condenser. When operating temperature and pressures are attained, the bypass valve closes automatically, the throttle opens, the engine is turned over and starts and the drain valve closes, all automatically. A vacuum pump allows extra energy to be extracted from the steam which is exhausted into a vortex chamber for primary oil removal (due to engine lubrication requirements, some oil mixes with the steam and must be removed thoroughly otherwise the absorbers can be affected by cracked oil) the steam passing through the condenser then flowing as condensate to the condensate tank. Occasionally the condensate (together with residual oil and oil pumped from time to time from the primary oil separator) is pumped to a compartment of the feedwater tank where surface oil is skimmed off, together with some water, the mixture being centrifuged and the products returned respectively to the engine oil tank and feedwater tank. Because some of the oil forms an emulsion with the water, further filtering is necessary before delivery to the feedwater pump. An excellent degree of filtering has been achieved, providing crystal clear feedwater to the feedwater pump.

The system operating strategy is arranged to permit all available solar energy to be utilized. This is facilitated through an energy balance system shown diagramatically in Figure 3. The steam engine may run or not, depending on the amount of insolation - a ratchet coupling allows the engine

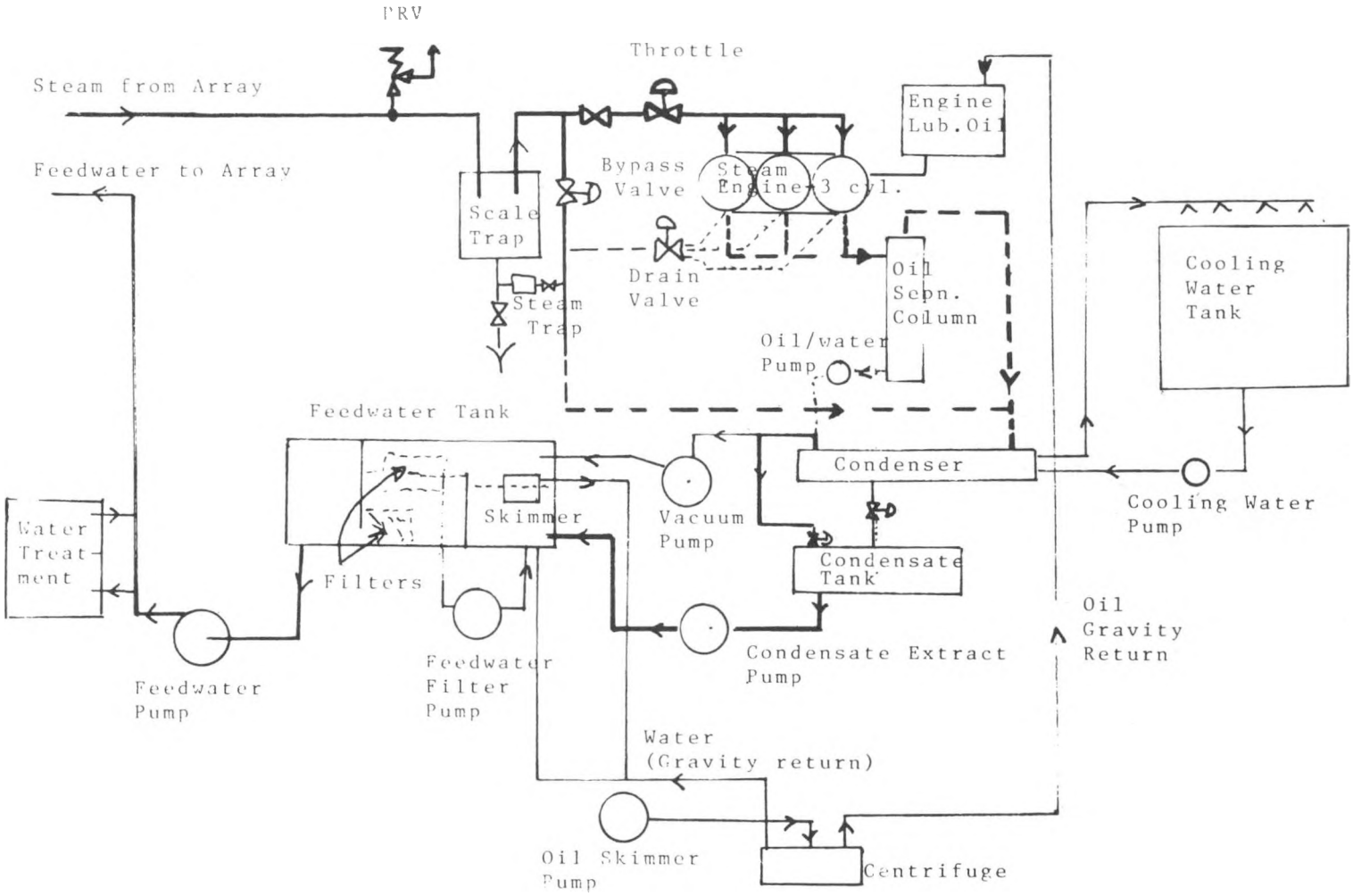

Figure 2. Steam/Water System

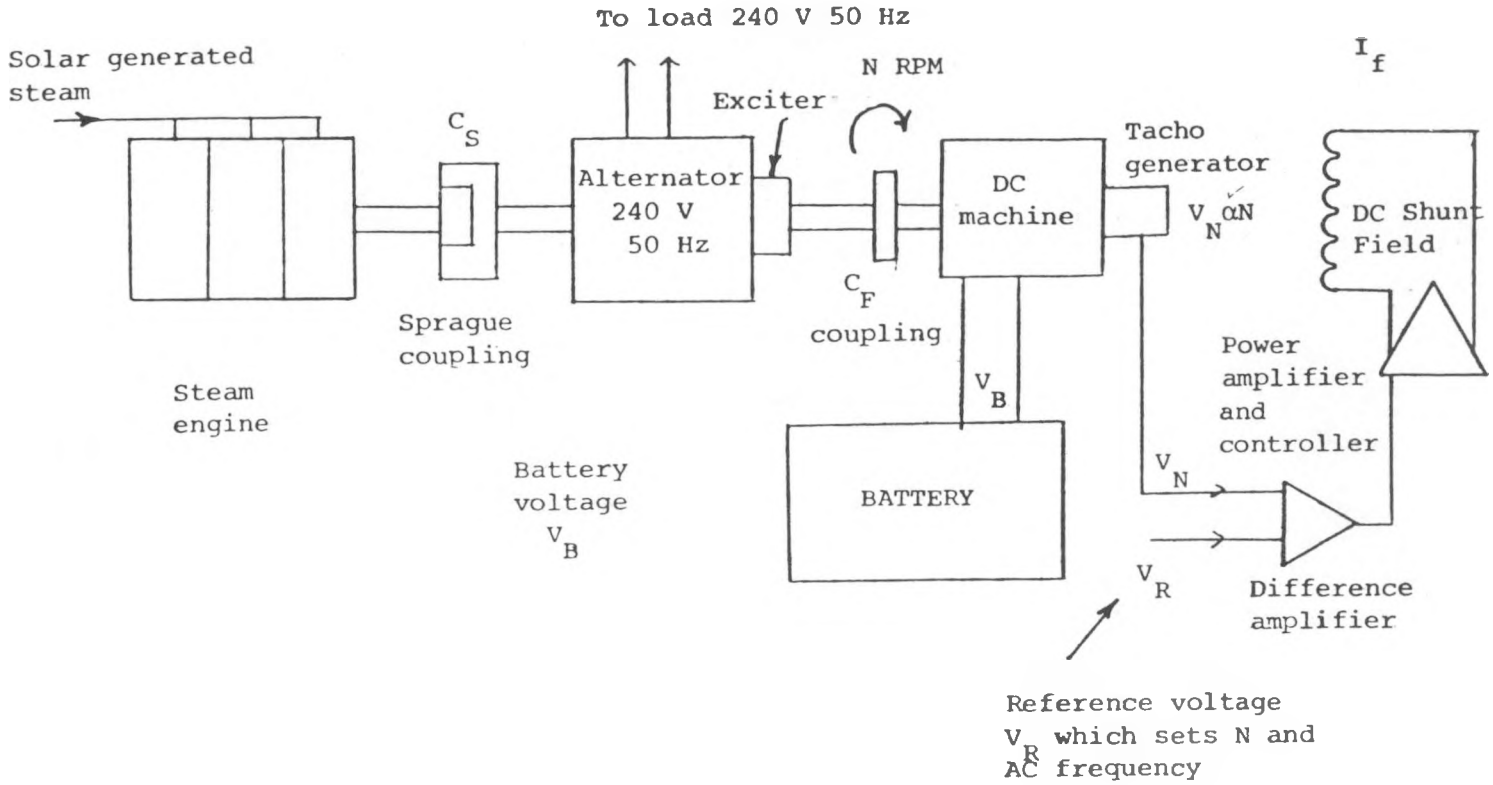

Figure 3. Machine/Battery (dc) Storage System

to be stationary, to drive or to coast. When the alternator load is less than the engine output, the shaft speed increases, causing the dc machine field to cause this machine to generate and charge the battery store with the excess energy, maintaining the shaft speed of the three machines near 1500 r.p.m. (50 Hz). On the other hand if the alternator load is greater than the engine output, the shaft speed drops below rated, the dc field is controlled to make this unit motor and assist the engine. In the absence of solar energy, the dc machine drives the alternator until the battery store is depleted, when the diesel back up unit comes on line automatically. The ac/dc set runs continuously. Storage is designed to be adequate for overnight operation on a midsummer sunny day.

The system starts just after sunrise each day in response to a clock setting which first switches on the feedwater and cooling water pumps, then raises the dishes from a horizontally facing position to face vertically for 4 minutes to ensure that the absorbers are filled with water and have no trapped air. The array then moves towards the east and down, in about 3 minutes acquiring the sun (or on cloudy days being moved in an approximate track by timed pulses which are always over-ridden by the sun sensors). In the presence of intermittent cloud during the day the engine continues to operate, sometimes stopping sometimes coasting on stored energy in the heat transport system, sometimes providing useful power. At the end of each day, in response to a clock pulse, the array parks in a south position facing horizontally and the steam system stops, the ac/dc set continuing on battery energy.

The next stage involving use of waste heat for water desalination is proposed to take advantage not only of the low quality heat from the cooling system but also the heat in the early morning and late afternoon which does not produce useful nett output, i.e.,for about one half hour after sunrise and one half hour before sunset.

3. The Steam Engine

For reasons already indicated, this unit employs a diesel engine converted to steam operation. The particular unit employed, a Lister 3 cylinder engine is used in its thousands in Australia and has the advantage that each cylinder and head is removable. By replacing only the cylinder walls and head whith new components and using commercial truck pistons and liners, the conversion to steam is readily effected. The major problems involve the valve mechanism and the feedwater treatment for oil removal.

The valve mechanism is conceptually simple - each piston carries 3 pins which, in approaching top dead centre (TDC) lift 3 balls which otherwise seat to prevent steam from entering from a chamber above the cylinder. The balls having lifted, allow steam to fill the space above the piston; subsequently as the piston moves away from TDC the valves close off the steam which then expands and is exhausted with vacuum assistance. A power stroke is obtained from each cylinder each revolution. To achieve reliable operation over significant periods without maintenance, required much attention to the valve mechanism as regards exact geometric configuration and dimensions, proper valve constraints and especially a satisfactory materials and hardness matching between all the appropriate components.

The other substantial problem concerned, as already noted, the acheivement of a satisfactory oil removal from the condensate. Both problems have been solved satisfactorily and a relatively robust engine has been developed.

Engine performance is indicated in Table III. Typical exhaust temperatures are 68-73^{o}C. Efficiency rises above 22% at higher quality steam. With compounding, efficiencies of 27% are expected.

TABLE III

Engine Performance

(Tests 6 June, 1982)

Feedwater Flow ml/s	Engine Input Steam Pressure p.s.i.	Steam Temp. °C	Total Added Heat kW	Engine Exhaust Pressure kPa	Engine Output Mech. kW	Engine Efficiency %
50.4	480	240	135	-85	22.3	16.5
50.4	500	248	135	-85	24.6	18.2
50.4	510	273	140	-83	26.0	18.6
50.4	540	302	143	-83	27.8	19.4
50.4	590	369	152	-82	31.4	20.6
50.4	600	415	157	-82	34.4	21.9

50.4 ml/s is rated flow for the system

4. Overall System Performance

The station electrical output as a function of insolation is indicated in Figure 4. Nett output is some 2.8 kW less than the values shown as this is the normal energy required to run the system (pumps, array tracking, centrifuge) but can occasionally exceed this value by 1 kW or more when condensate pumps and vacuum pumps are energised for short periods.
It may be noted that system output can differ significantly at similar insolations due to different steam conditions.
It is worth optimising feedwater flow to optimise output and microprocessor control is envisaged as a further development.

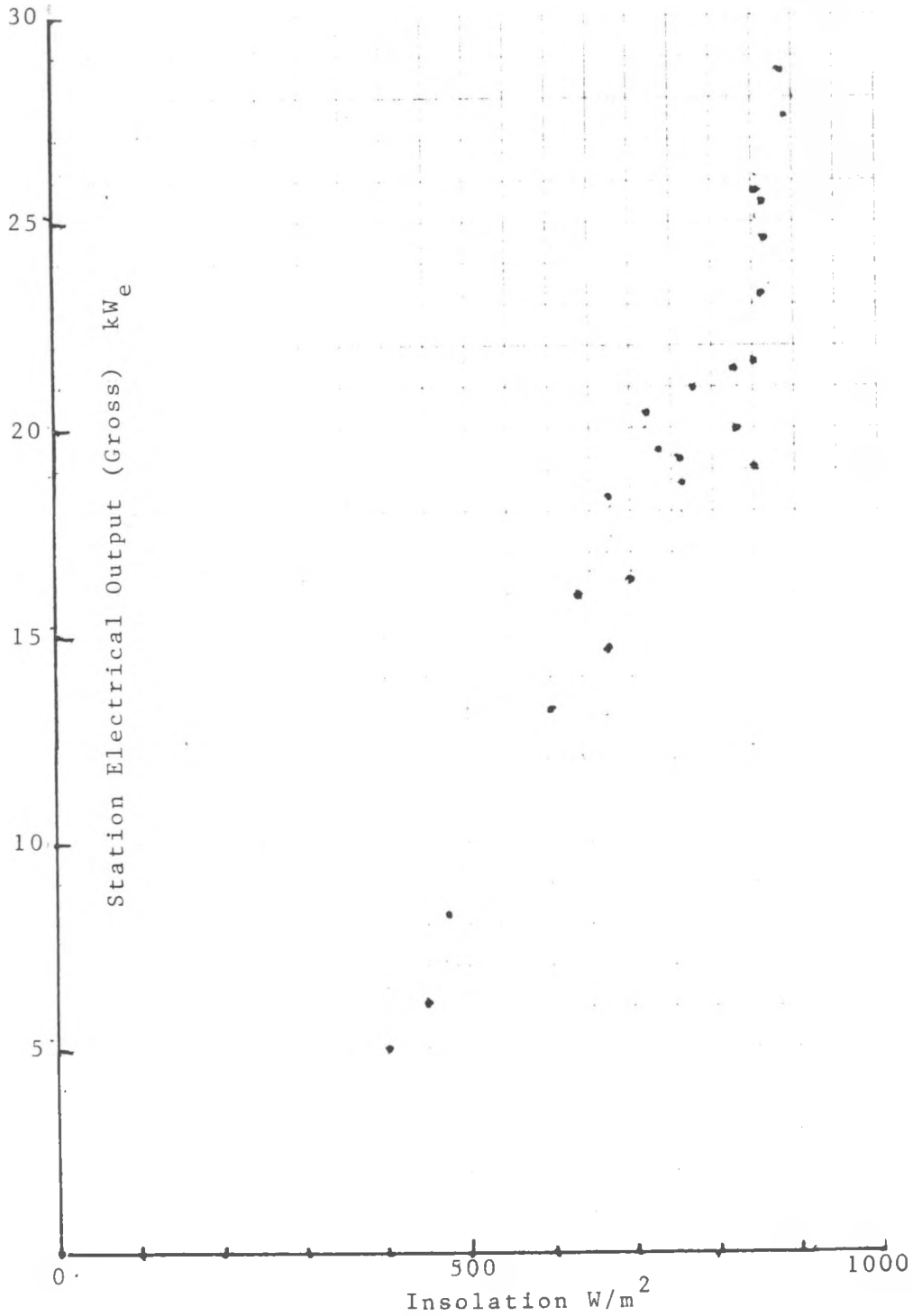

Figure 4. System Output versus Insolation

5. System Costs

Hardware costs on site have comprised the following:

14 dishes, incl. absorbers, actuators and drives with electronic controls etc.	$A 99,000
Steam system, including pipes, insulation, installation, valves , co-nectors etc.	77,000
Engine, feedwater treatment and cooling system	35,000
Electrical system, alternator, dc machine, energy balance	$ 28,000
Energy store (battery) and control	27,000
Insolation and wind monitoring	8,000
Buildings, fences	16,000
Transport	12,000
Total	$A 302,000

Comment: some of the above costs could be avoided through not being essential, or by changing designs and details in minor ways. In the light of experience, dishes could be produced 10 metres in diameter rather than 5 metres, thereby reducing the number of dish units to 4 and the costs of the dish system by an expected factor of about 2. Plumbing, wiring and general equipment arrangement can be modified to achieve further economies, as can the buildings. The current cost corresponds to a cost of $12,000 per installed kW. This might be reduced to half if the next generation designs can come to fruition. An obvious first step involves the use of fewer larger collectors (not implemented in the first instance due to various environmental uncertainties and the general drive to ensure that the first system is successful).

Apart from capital costs it is necessary to identify the true running costs - it is expected that these can be revealed with some confidence by the end of 1983.

6. Relevance to Other Applications

The solar array seems to hold potential for industrial process heat in the medium to high temperature range. The steam engine appears attractive, with its flash boiler suitably modified, for applications which can take advantage of waste combustible materials and crops; we consider it to be an attractive alternative to using such materials for ethanol production. In some applications direct burning to produce steam has a distinct advantage over the production of ethanol and its use in an internal combustion engine. The general simplicity and robustness of the steam engine, even in its high performance mode, might well find application in many areas where small power supplies can take advantage of indigenous combustible materials.

In the longer term, we look forward to the first solar thermochemical system using paraboloidal collectors and producing not only electricity but also various energy rich products such as fuels and fertilizers.

In Conclusion, the White Cliffs solar power station is viewed as a vehicle for ascertaining the feasibility of employing high temperature technology to supply inland and remote areas with electrical energy and water with acceptable economics. The first system has already been superceeded in our minds with simpler more economical technology which deserves to be explored and exploited. If the promise of other heat engines is realised in due course, even better economies would be achieved, particularly for larger systems. This will not necessarily rule out the use of high performance simple steam engines for certain applications. In any event the future of solar thermal power seems assured.

Acknowledgements

In a project of this nature many individuals have made contributions. Special thanks are due to Dr. E.K. Inall for work on the steam and water treatment system, to Commander G.J. Vagg for advice and assistance on the steam system, to Dr. P.O. Carden in the early stages of the project, to Messrs.H.P. Cantor,R. Whelan, K. Thomas,to the Workshop Staff of the Research School of Physical Sciences and the Technical Staff of the Department of Engineering Physics. A substantial Grant for the project from the New South Wales State Government is gratefully acknowledged and we acknowledge also the assistance and co-operation received from the New South Wales Energy Authority. Finally we thank the Australian National University for the provision of support for the project through ANUTECH and the Research School of Physical Sciences and to Environ Mechanical Services for assistance with planning, costing and scheduling.

APPPENDIX

ATTENDEES

Blank Page

FOURTH PARABOLIC DISH SOLAR THERMAL POWER PROGRAM REVIEW

Pasadena, California

November 30 - December 2, 1982

PARTICIPANTS

AL NEMER, Mousa M. (816) 753-7600 x 249
Proj.Mgr., Solar Energy Desalination
Midwest Research Institute
425 Volker Blvd.
Kansas City, MO 64110

ALPER, Marshall (213) 577-9325
Manager of Solar Energy Programs
Jet Propulsion Laboratory
4800 Oak Grove Drive MS 502/306
Pasadena, CA 91109

ANDERSON, Mark

Sacramento Municipal Utility Dist.
PO Box 15830
Sacramento, CA 95813

ANGELSBERGER, Mario (037) 441889
Software Development
Institute/Computer Assisted Resrch
in Astronomy Observatory
Alterswil, CH-1715 SWITZERLAND

ANSON, Bruce (602) 267-7904
Development Engineer
Garrett Turbine Engine Co.
111 S. 34th St., PO Box 5217
Phoenix, AZ 85010

ATKINSON, John (714) 635-5591
Technical Director
Advanced Solar Power Co.
2201-A E. Winston Road
Anaheim, CA 92806

BABBE, Robert (714) 720-6255
Activity Manager
Ford Aerospace Co.
Ford Road
Newport Beach, CA 92663

BARBIERI, Rosalyn (619) 756-5249

Barbieri Energy Assoc.
P.O. Box 1797
Rancho Santa Fe, CA 92067

BEALE, William T. (614) 594-2221
President
Sunpower Inc.
6 Byard Street
Athens, OH 45701

BIGGER, John (415) 855-2178
Project Manager
Electric Power Research Institute
PO Box 10412
Palo Alto, CA 94303

BLUM, Edward H. (202) 822-3650
VP & Exec.Dir., Alt.Energy Financing
Merrill Lynch White Weld Cptl Mkts
1828 L St., NW, Suite 906
Washington, DC 20036

BODA, F. (714) 720-6416
Engineer
Ford Aerospace Co.
Ford Road
Newport Beach, CA 92660

BRATT, Christer 40-100950

United Stirling AB (Sweden)
Box 856
S20180, Malmoe, SWEDEN

CARLEY, William J. (213) 577-9384
Group Supervisor
Jet Propulsion Laboratory
4800 Oak Grove Dr., M.S. 510/200
Pasadena, CA 91109

CEDILLO, Raymond (213) 572-1505
Project Director
Southern California Edison
2244 Walnut Grove
Rosemead, CA 91770

CHINGARI, Gastone (202) 296-1610
Mgr., International Programs
IIT Research Institute
1825 K St., NW, Suite 310
Washington, DC 20006

CHUKA, John (213) 640-2429

Advanco Corporation
999 N. Sepulveda Blvd.
El Segundo, CA 90245

DAHL, Michael, M. (303) 234-2718
General Engineer
Bureau of Reclamation
PO Box 25007 D.F.C.
Denver, CO 80225

DANCETTE, Michel (3) 056.25.00
Ingenieur
Societe Bertin & Cie
BP No.3
Plaisir, Cedex, 78373 FRANCE

DENNISON, Edwin W. (213) 577-9228
Member Technical Staff
Jet Propulsion Laboratory
4800 Oak Grove Dr., M.S. 510/200
Pasadena, CA 91109

DRUMHELLER, Kirk (504) 375-2323

Battelle Northwest
Box 999
Richland, WA 99352

EASON, Ernie (415) 321-6350
Engineer
Failure Analysis Associates
2225 E. Bayshore Dr.
Palo Alto, CA

ELFE, Thomas B. (404) 894-3650
Senior Research Scientist
Georgia Institute of Technology
Engineering Experiment Station
Atlanta, GA 30332

FALLER, Richard J. (714) 968-1890
Engineer
McDonnell Douglas
5301 Bolsa Avenue
Huntington Beach, CA 92646

FELLOWS, Merrilee (213) 572-6597
Research Scientist
Southern California Edison
PO Box 800
Rosemead, CA 91770

FOX, Richard (213) 956-7722
Director, Research & Development
WED Enterprises
1401 Flower Street
Glendale, CA 91201

FRANKEL, Eugene (415) 368-8197
Science Consultant (temporary)
House Subcommittee/Energy Dev&Appl
B-374 Rayburn Bldg.
Washington, DC 20003

FULTON, D. G. (714) 720-6762

Ford Aerospace & Communications
Ford Road
Newport Beach, CA 92660

GATES, Bill (213) 577-9393

Jet Propulsion Laboratory
4800 Oak Grove Dr., M.S.
Pasadena, CA 91109

GOLDBERG, Vernon R. (214) 272-0515
Mgr., Energy Programs
E-Systems, Inc.

Garland, TX

GOODWIN, Lee Martin (202) 429-9618

Goodwin & Schwartzstein
2010 Massachusetts Ave., NW
Washington, DC 20037

GOULD, William
Chairman of the Board
Southern California Edison Co.
PO Box
Rosemead, CA

GRIGSBY, Carl E. (714) 544-7415
Consultant
CG Research Associates
17531 Chatham Drive
Tustin, CA 92680

HABIB-AGAHI, Hamid (213) 577-9543

Jet Propulsion Laboratory
4800 Oak Grove Dr., M.S.
Pasadena, CA 91109

HAGEN, Terry (213) 640-2429
Sr. Project Engineer
Advanco Corp.
999 N. Sepulveda
El Segundo,CA 90245

HALBERT, David D. (915) 698-8800
Director of Marketing
LaJet Energy Co.
PO Box 3599
Abilene, TX 79604

HALLARE, Bengt G. (703) 549-7174
President
United Stirling, Inc.
211 The Strand
Alexandria, VA 22314

HANSON, John (505) 846-5223
AF Energy Technology Liaison Officer
DOE-Air Force Engg & Services Cntr
PO Box 5400
Albuquerque, NM 87115

HAUGER, James Scott (703) 459-4404
President
Applied Concepts Corp.
109K N. Main Street
Woodstock, VA 22666

HLINAK, Anthony J. (312) 399-8285
Project Manager
Gas Research Institute
8600 W. Bryn Mawr Avenue
Chicago, IL 60631

HOBGOOD, John (714) 635-5591
Project Manager
Advanced Solar Power Co.
2201-A E. Winston Road
Anaheim, CA 92806

HOLBECK, Herbert (213) 577-9294
Task Mgr., Brayton Module Develpmnt
Jet Propulsion Laboratory
4800 Oak Grove Dr., M.S. 510/200
Pasadena, CA 91109

HOFMANN, Helmut 004989-60005521
Dipl.Ing., Propulsion/Energy Tech.
MBB-Space Division
Postfach 801169
8000 Munchen 80, GERMANY

HUANG, Louis (805) 982-4675
Project Engineer
U.S. Navy
Naval Civil Engineering Lab-L63
Port Hueneme, CA 93043

HUTCHISON, Gus (214) 721-1070
President
Solar Kinetics, Inc.
3300 Century Circle
Irving, TX 75060

HUYCK, Philip (212) 909-2633
Consultant
The First Boston Corp.
Park Avenue Plaza
New York, NY 10055

IZYGON, Michel (203) 333-3118

National Energy Reserves, Inc.
10 Middle St., Suite 735
Bridgeport, CT 06604

JAFFE, Leonard (213) 577-9312
Project Systems Engineer
Jet Propulsion Laboratory
4800 Oak Grove Dr. M.S. 506/418
Pasadena, CA 91109

KANEFF, Stephen (062) 492462
Professor
Head, Dept. of Engg. Physics
Australian National University
Canberra, A.C.T. 2600 AUSTRALIA

KEARNEY, David W. (213) 680-3273
Vice President
Insights West, Inc.
900 Wilshire Blvd, Ste 1100
Los Angeles, CA 90017

KENDALL, James (213) 354-2708
Research Affliate
Jet Propulsion Laboratory
4800 Oak Grove Drive MS 82-110
Pasadena, CA 91109

KICENIUK, Taras (213) 577-9419
Experiment Mgr.
Jet Propulsion Laboratory
4800 Oak Grove Dr., M.S. 510/200
Pasadena, CA 91109

KLACHKIN, Eli (203) 333-3118

National Energy Reserves Inc.
P. O. Box 1700
Bridgeport, CT 06601

KLEINWACHTER, Jurgen (07621) 5093
Technical Director
Bonin-Solar
D-7850 Lorracy Industriestry
Lorracy, WEST GERMANY

KOSTRZEWA, Lawrence (312) 399-8238
Project Engineer
Gas Research Institute
8600 W. Bryn Mawr Ave.
Chicago, IL 60631

KREPCHIN, Ira P. (617) 890-3200
Project Engineer
Foster-Miller
350 Second Avenue
Waltham, MA 02154

LANE, Jack (613) 993-2371
Sr. Research Officer
National Research Council
Bldg M-17, Montreal Road
Ottawa, Ontario, K1A0R6, CANADA

LEONARD, James A. (505) 844-8508

Sandia Labs
PO Box 5800
Albuquerque, NM 87185

LIVINGSTON, Floyd (213) 577-9416
Task Leader
Jet Propulsion Laboratory
4800 Oak Grove Dr., M.S. 510/200
Pasadena, CA 91109

LUCAS, John W. (213) 577-9368
Mgr., Technical Development
Jet Propulsion Laboratory
4800 Oak Grove Dr., M.S. 502/419
Pasadena, CA 91109

LUDTKE, Norman F. (313) 755-4400
Vice President
Pioneer Engineering & Mfg. Co.
2500 E. Nine Mile Road
Warren, MI 48091

MACIAS, Manuel (91) 2708901
Dr. Phisic
Asinel-Projecto-Gast
Po Castellana 143
Madrid, 20, SPAIN

MACKIN, Robert (213) 577-9586
Mgr., Fossil Energy Program
Jet Propulsion Laboratory
4800 Oak Grove Dr.,M.S. 502-317
Pasadena, CA 91109

MARRIOTT, Alan T. (213) 577-9366
Mgr, Module/Systems Development
Jet Propulsion Laboratory
4800 Oak Grove Dr., M.S. 502/419
Pasadena, CA 91109

MARTIN, David E. (913) 864-4078
Acting Director, Applied Energy Rsch
University of Kansas Cntr for Rsch
2291 Irving Hill Drive
Lawrence, KS 66045

MARTIN, Robert L. (816) 753-7600
Project Mgr.
Midwest Research Institute
425 Volker Blvd.
Kansas City, MO 64110

MAYR, Guenter (0711) 818275
Ing. Grad.
Schlaich & Partner
Feuerbacherweg 142
D-7000 Stuttgart 1, GERMANY

MECKLER, Milton (213) 995-7672
President
California Solar Technology
17525 Ventura Blvd. #307
Encino, CA 91316

MOE, George (714) 896-4557
Program Mgr.
McDonnell Douglas
5301 Bolsa Avenue
Huntington Beach, CA 92647

MORSE, Howard L. (415) 964-3200
Vice President & Manager, Sys. Dev.
Acurex Solar Corporation
485 Clyde Avenue
Mountain View, CA 94042

MOUSTAFA, Safwat (00965) 816007

Kuwait Instit.for Scientific Resch
PO Box 1741, Safat
Kuwait City, KUWAIT

MUNOZ-TORRALBO, Antonio (1) 2-157256
Head, Research Division
Centro De Estudios De La Energia
Augustin De Foxa 29-1A
Madrid, 33, SPAIN

MURPHY, Lawrence M. (303) 231-1050
Group Mgr.
Solar Energy Research Institute
1617 Cole Blvd.
Golden, CO 80401

McCAUGHEY, Owen J. (714) 838-1980
Chief Executive Office
McCaughey & Smith Energy Assoc,Inc
130 Centennial Way, Ste C
Tustin, CA 92680

McLANE, Pat (213) 577-9413
Conferences Coordinator
Jet Propulsion Laboratory
4800 Oak Grove Dr., M.S. 502/404
Pasadena, CA 91109

NELVING, Hans Goran 40-100950

United Stirling AB (Sweden)
Box 856
S20180, Malmoe, SWEDEN

NUSSDORFER, Ted (603) 885-3102
Engineer
Sanders Associates
95 Canal Street
Nashua, NH 03061

O'GALLAGHER, Joseph (312) 962-7757

University of Chicago
5640 Ellis Avenue
Chicago, IL 60637

O'NEILL, Mark (214) 272-0515
Dir., Fresnel Collector Programs
E-Systems, Inc., Energy Tech Center
PO Box 226118
Dallas, TX 75266

ORTABASI, Ugur (07) 37723157
Dir., Solar Energy Research Centre
University of Queensland
Serc, University of Queensland
Brisbane, Queensland, AUSTRALIA

OVERLY, Peter (415) 964-3200
Project Manager
Acurex Corp.
485 Clyde Avenue
Mountain View, CA 94042

OWEN, William (213) 577-9315

Jet Propulsion Laboratory
4800 Oak Grove Dr., M.S. 510/200
Pasadena, CA 91109

PAPPAS, George (505) 846-5205

DOE, Albuquerque Operations Office
PO Box 5400
Albuquerque, NM 87115

PAYNE, Larry (915) 698-8800
Director of Engineering
LaJet Energy Corp.
PO Box 3599
Abilene, TX 79604

PERCIVAL, Worth H. (703) 549-7174
Technical Director
United Stirling Inc.
211 The Strand
Alexandria, VA 22314

POND, Stanley L. (303) 444-5105
Vice President for Engineering
Applied Concepts Corp.
2501 So. Co. Rd. 21
Berthond, CO 80513

PONS, Robert (714) 720-6544
Mgr., Mech. Engineering Dept.
Ford Aerospace Co.
Ford Road
Newport Beach, CA 92663

POTTHOFF, Robert
Sr. Engineer
San Diego Gas & Electric
Box 1831
San Diego, CA 92112

RANNELS, James (202) 252-1623
Program Mgr.
DOE Headquarters
1000 Independence Ave.
Washington, DC 20585

RICE, Mark (518) 271-7743
President
Power Kinetics, Inc.
1223 Peoples Avenue
Troy, NY 12180

ROBILLARD, Geoffrey (213) 577-9135
Assistant Laboratory Director
Jet Propulsion Laboratory
4800 Oak Grove Dr., M.S. 502/317
Pasadena, CA 91109

ROSE, Thomas K. (612) 574-5404
Mgr., Developmental Programs
Onan Corporation
1400 73rd Avenue, NE
Minneapolis, MN 55431

ROSS, Darrell L. (213) 577-9317
Group Spvr, Terrestrial Solar En.Eng
Jet Propulsion Laboratory
4800 Oak Grove Dr., M.S. 507/228
Pasadena, CA 91109

ROUSSEAU, J. (213) 512-4598

Garrett AiResearch Co.
2525 W. 190th St.
Torrance, CA 90509

ROY, Aaron (203) 333-3118

National Energy Reserves, Inc.
10 Middle St., Suite 735
Bridgeport, CT 06604

SEARS, Dana A. (612) 561-6973
Staff Engineer
Onan Corporation
1400 73rd Avenue
Minneapolis, MN 55432

SHINE, Dan (603) 885-2970
Business Dev. Mgr., Energy Sys Cntr.
Sanders Associates
95 Canal Street
Nashua, NH 03061

SHOJI, James (213) 710-2319
Manager, Adv. Sys. Analyses
Rocketdyne Div. of Rockwell Intl.
6633 Canoga Avenue
Canoga Park, CA 91304

SIMON, Michael M. (089) 811-6309
Dipl.-Ing.
ISET
Melssheimer Str. 5
D-8 Munich 60, GERMANY

SNOW, Edward (303) 333-3118
Vice President
National Energy Reserves, Inc.
10 Middle Street
Bridgeport, CT 06604

SOBCZAK, Isidore F. (714) 720-6212
Supervisor
Ford Aerospace & Communications
Ford Road
Newport Beach, CA 92660

SOUVA, Eugene C. (213) 417-6875
Sr. Sales Engineer
Garrett Corporation
9851 Sepulveda Blvd.
Los Angeles, CA 90009

STALLKAMP, John (213) 577-9073

Jet Propulsion Laboratory
4800 Oak Grove Dr., M.S. 502/119
Pasadena, CA 91109

STEIN, Charles K. (213) 577-9417
Review General Chairman
Jet Propulsion Laboratory
4800 Oak Grove Dr., M.S. 507/228
Pasadena, CA 91109

STEITZ, Peter (816) 333-4375
Chief, Power Supply Section
Burns & McDonnell Engg. Co., Inc.
PO Box 173
Kansas City, MO 64141

STINE, William (213) 799-4717
Professor
Cal Polytechnic State Univ.
1230 Grace Drive
Pasadena, CA 91105

STOLPE, John (213) 572-1556
Supervising Research Engineer
Southern California Edison
2244 Walnut Grove Ave.
Rosemead, CA 91770

STRAIN, Ed E. (602) 267-2797
Program Mgr.
Garrett Corp.

Phoenix, AZ

STRAUGHAN, Ian R. (213) 572-1556
Mgr., Geo Science
Southern California Edison
2244 Walnut Grove Avenue
Rosemead, CA 91770

SUTSCH, Arthur G. (037) 441889
Director
Institute/Computer Assisted Resrch
in Astronomy Observatory
Alterswil, CH-1715 SWITZERLAND

TERASAWA, Katchen

Jet Propulsion Laboratory
4800 Oak Grove Dr., M.S.
Pasadena, CA 91109

TRUSCELLO, Vincent (213) 577-9367
Mgr., Thermal Power Systems Project
Jet Propulsion Laboratory
4800 Oak Grove Dr., M.S. 502/419
Pasadena, CA 91109

UNDERWOOD, Arthur F. (619) 328-8248
Consulting Engineer

74 Lakeview Dr.
Palm Springs, CA 92264

VAN GRIETHUYSEN, Valerie J. (513) 255-6235
Mechanical Engineer
AF Aero Propulsion Laboratory
AFWAL/POOC
Wright-Patterson AFB, OH 45433

WASHOM, Byron (213) 640-2429
President
Advanco Corporation
999 N. Sepulveda Blvd.
El Segundo, CA 90245

WATIKER, Jeffrey A. (703) 998-0922
Systems Analyst
Meridian Corp.
5201 Leesburg Pike, Suite 400
Falls Church, VA 22041

WEISIGER, Joe (505) 846-5207
Senior Program Coordinator
DOE, Albuquerque Operations Office
PO Box 5400
Albuquerque, NM 87115

WELLS, David N. (703) 549-7174
Systems Integrator
United Stirling, Inc.
211 The Strand
Alexandria, VA 22314

WILLCOX, William W. (213) 700-4310
Member of Technical Staff
Rockwell International
8900 DeSoto Avenue
Canoga Park, CA 91304

WILLIAMS, Carl (915) 698-8800
President
LaJet Energy Co.
P. O. Box 3599
Abilene, TX 79604

WILSON, John W. (202) 822-9157
Executive Director
Renewable Energy Institute
2010 Massachusetts Ave., NW
Washington, DC 20036

WINSTON, Roland (312) 962-7756
Professor of Physics
University of Chicago
5630 W. Ellis Avenue
Chicago, IL 60637

WOOD, Douglas E. (206) 627-1627
Director of Research
Solar Steam Inc.
625 Commerce St. Suite 400
Tacoma, WA 98402

ZELLER, John J. (213) 572-1864
Sr. Engineer
Southern California Edison
2131 Walnut Grove Avenue
Rosemead, CA 91770

ZEWEN, Helmut 004989-60006196
Dipl.Ing, N.Sc.,Propulsion/Engy Tech
MBB-Space Division
Postfach 801169
8000 Munchen 80, GERMANY

☆ U.S GOVERNMENT PRINTING OFFICE 1983-646-069 755